Optimal energy utilization in conventional, electric and hybrid vehicles and its application to eco-driving

Felicitas Mensing

UNIVERSITY OF LYON

DOCTORAL SCHOOL E.E.A.

P H D T H E S I S

to obtain the title of

PhD of Science

of the Institut National des Sciences Appliquées de Lyon - INSA Lyon

Speciality : Energy and Systems

defended by

Felicitas Mensing

Optimal Energy Utilization in Conventional, Electric and Hybrid Vehicles and its Application to Eco Driving

Thesis Advisor: Eric Bideaux and Rochdi Trigui

prepared at

Laboratoire AMPÈRE (UMR CNRS 5005)

and LTE IFSTTAR

September 2013

Jury :

Reviewers :	Xavier Roboam	-	Université de Toulouse (LAPLACE)
	Michel Basset	-	Université de Haute Alsace (MIPS)
	Roger FotsuNgwompo	-	University of Bath
Examinators :	Bo Egardt	-	Chalmers University of Technology
	Xavier Moreau	-	Université de Bordeaux (IMS)
	Sebastien Delprat	-	Université de Valenciennes et du Hainaut-Cambrésis
	Helene Tattegrain	-	IFSTTAR
Invited :	Maxime Pasquer	-	ADEME
Advisor :	Eric Bideaux	-	INSA de Lyon (AMPÈRE)
	Rochdi Trigui	-	IFSTTAR (LTE)

Abstract

The transportation sector has been identified as one of many sources of today's energetic and environmental problems. With constantly increasing numbers of vehicles on the road, non-renewable fossil fuels are becoming scarce and expensive. In addition, due to the pollutant emissions of internal combustion engines, the transportation sector is a major producer of greenhouse gas emissions. To resolve these problems researcher are looking for technological solutions, such as more efficient components and alternative drive train technologies, on one hand. On the other hand, work is being done to ensure the most efficient utilization of available technological resources. Eco driving is one way to immediately reduce a driver's energy consumption.

In this thesis the potential gains of eco driving for passenger vehicles will be discussed. The main objective of this work is to, first, identify and compare drive train specific, optimal vehicle operation. Secondly, the effect of real-life constraints on potential gains of eco driving is evaluated. In addition, an approach to integrate mathematical optimization algorithms in an advanced driver assist system for eco driving is proposed.

Physical vehicle models are developed for three representative vehicles: the conventional, electric and power-split hybrid vehicle. Using real-life and standard drive cycles a baseline mission is defined by specifying trip and road constraint. Applying the dynamic programming algorithms the trajectory optimization problem is solved, minimizing energy consumption for the trip. The effect of traffic on potential gains of eco driving is discussed, considering a vehicle following situation. Integrating emission constraints in the optimization algorithm the environmental advantages of eco driving are discussed. Finally, the developed algorithms were integrated in a driver assist system. Experimental tests on a driving simulator were used to verify the effectiveness of the system, as well as driver acceptance.

Keywords: Eco Driving, Energetic Trajectory Optimization, Dynamic Programming, Emissions, Electric Vehicle, Hybrid Vehicle, Advanced Driver Assist System (ADAS)

Résumé

Pour résoudre les problèmes environnementaux et énergétiques liés au nombre croissant de véhicules en circulation, deux approches sont envisageables : l'une est technologique et vise à améliorer les composants du véhicule ou son architecture, l'autre est comportementale et cherche à changer la manière d'utiliser les véhicules. Dans ce contexte, l'éco-conduite représente une méthode, applicable immédiatement, permettant à chaque conducteur de réduire sa consommation.

L'objectif de cette thèse est donc l'analyse des gains potentiels de l'éco-conduite pour les différents types de véhicules existant : thermique, électrique et hybride. Ainsi, la première partie de ce travail se focalise sur une étude théorique visant à calculer les gains potentiels et à déterminer les règles d'éco-conduite, avant d'aborder dans un second temps une mise en situation plus réaliste et une intégration des algorithmes dans un système d'assistance pour le conducteur.

En s'appuyant sur une modélisation énergétique des différents types de véhicules, la détermination et la comparaison du fonctionnement optimal se base sur l'optimisation du profil de vitesse pour des trajets connus. La programmation dynamique a été mise enoeuvre pour calculer la trajectoire optimale énergétique en tenant compte de la contrainte temporelle afin de ne pas pénaliser l'intérêt d'une conduite économe. Evidemment, l'intégration de l'éco-conduite doit, d'une part, tenir compte du trafic à proximité du véhicule et d'autre part, ne pas aboutir à une augmentation des émissions de polluants. Ainsi, en nous appuyant sur des modèles de suivi de véhicules (trafic), nous avons montré que les principes d'éco-conduite restent valables et conduisent de toute façon à des gains énergétiques. Concernant les contraintes d'émissions, des résultats expérimentaux nous ont conduit à adapter nos algorithmes pour répondre simultanément aux aspects écologiques et économiques. Enfin, les connaissances acquises ont été appliquées à la conception d'un système d'assistance testé sur un simulateur de conduite.

Mots-clés: Eco conduite, Optimisation énergétique, Programmation dynamique, Emissions, Véhicule électrique, Véhicule hybride, Système d'assistance

Acknowledgements

At the end this PhD I want to use this space to thank everyone that made this thesis possible and the last years a memorable experience.

First I want to thank my advisors, Eric Bideaux and Rochdi Trigui for their continuous advice and guidance throughout this thesis. I am glad I had the opportunity to benefit from your experiences and knowledge. Thank you for making time in your busy schedules for numerous discussions about bond-graph modeling, EMR, wheel inertias and sometimes eco-driving.

I also want to express my gratitude to my entire jury for willing to examine and comment on my research work. Thank you for your comments and for making time to attend my thesis defense.

I want to thank the LTE laboratory at IFSTTAR for their warm welcome and particularly the VEH group for their constant support and advice. I specifically want to thank the engineers and technician of the LTE laboratory for their help with the experimental tests on the engine dynamometer and chassis test bench. Without the availability of the experimental equipment and human resources this thesis would certainly not have been possible. Particular thanks goes to Pascal Gastineau for never denying to have a coffee break. Once I leave he will finally get to do some work.

In addition I would like to express my gratitude to Helene Tattegrain and Daniel Ndiaye of the LESCOT and LEPSIS laboratory for their advice, help and encouragement on the implementation part of my work. Thank you for your time investment, which made it possible for me to benefit from your knowledge and experience in your respective fields of study.

I want to thank the AMPERE laboratory at INSA Lyon for their overall guidance throughout these last years. A special thanks goes to my PhD colleague Ramon Naiff Da Fonseca with whom I shared some good and bad thesis experiences. I appreciate your spiritual support and our discussions about the abilities of Paint, Inkscape and Power Point will not be forgotten.

I also want to take this opportunity to thank my family and friends. Thank you to my boyfriend for enduring me throughout some phases of non-existent social

life. A big thank you also goes to a little group of runners that kept me sane throughout the rough times by making me run laps around the track.

Last but not least I want to acknowledge and thank ADEME for their financial support of this research work.

Contents

List of Figures

List of Tables

Symbols

symbol	name	unit
a	vehicle acceleration	m/s^2
a_{minx}	maximum deceleration test vehicle	m/s^2
a_{miny}	maximum deceleration preceding vehicle	m/s^2
A	vehicle's frontal surface	m^2
C_{ah}	nominal capacity of battery	Ah
C_d	vehicle's drag coefficient	
C_r	coefficient of rolling resistance	
d	vehicle distance	m
d_0	initial vehicle distance	m
d_f	final vehicle distance	m
d_{safebr}	safe braking distance	m
d_{trav}	traveled distance	m
d_{TIV}	safe following distance computed with TIV rule	m
d_{TTC}	safe following distance specified by TTC	m
d_x	distance of test vehicle	m
d_y	distance of preceding vehicle	m
f_{error}	error function, defines error between desired trip time and computed trip final time	s
F_{aero}	aerodynamic drag force	N
$F_{decelmax}$	maximum vehicle deceleration possible with current adherence	N
F_{drive}	drive force propeling the vehicle	N
F_{grade}	grade resistance force	N
F_{res}	resistance forces acting on the vehicle chassis	N
F_{roll}	rolling resistance	N
g	gravitational constant	m/s^2

i_{gear}	selected gear	
I_{batt}	battery current	A
J_{EM}	inertia of electric machine	kgm^2
J_{eng}	engine inertia	kgm^2
J_{tire}	tire inertia	kgm^2
J_{veh}	vehicle inertia, includes vehicle weight and tire inertia	kgm^2
$\dot{m}_{fuel}$	instantaneous fuel flow	g/s
M_{veh}	vehicle mass (drive train components, chassis,...)	kg
M_{veh_x}	lumped vehicle mass, includes tire inertia	kg
P_{aux}	auxiliary power	W
P_{batt}	battery power used	W
$P_{battout}$	battery output power	W
P_{dembat}	power demanded by the battery management system	W
P_{loss}	total power loss in a drive train	W
P_{lossEM}	power loss in electric machine	W
$P_{lossEM1}$	power loss in electric machine EM1	W
$P_{lossEM2}$	power loss in electric machine EM2	W
P_{out}	drive train output power	W
P_{reqeng}	required engine power for some vehicle operation in Prius	W
R	battery resistance	Ω
R_{FD}	final drive ratio	
R_g	ratio parameter of planetary gear set	
R_G	gear ratio	
R_{tire}	tire radius	
SOC	battery state-of-charge	%
t	time	s
t_f	final time	s
t_{fdes}	desired final trip time	s
Δt_x	time test vehicle needs to decelerate	s
Δt_y	time preceding vehicle needs to decelerate	s
T	specified trip time	s
T_{aux}	torque on engine shaft due to auxiliaries	Nm
$T_{brakemech}$	mechanical brake torque	Nm
T_{drive}	drive torque propeling the vehicle	Nm
$T_{drive_{EM}}$	drive torque at electric machine output shaft	Nm

$T_{drive_{eng}}$	drive torque at engine output shaft	Nm
T_{EM}	electric motor output torque	Nm
T_{EM1}	torque of electric motor EM1 in Prius	Nm
T_{EM2}	torque of electric motor EM2 in Prius	Nm
T_{eng}	engine torque	Nm
T_{engmax}	maximum engine output torque	Nm
T_f	final time of a computed speed profil	s
TIV	time inter vehicular	s
T_{planet}	static torque at planet gear of planetary gear set	Nm
T_{react}	driver reaction time	Nm
T_{ring}	static torque at ring gear of planetary gear set	Nm
T_R	teeth on ring gear of planetary gear set	
TTC	time to collision	s
T_{sun}	static torque at sun gear of planetary gear set	Nm
T_S	teeth on sun gear of planetary gear set	
U_{batt}	battery output voltage	V
v	vehicle speed	m/s
v_0	initial vehicle speed	m/s
v_f	final vehicle speed	m/s
v_{max}	maximum speed limit	m/s
$v_{vehmaxelec}$	maximum speed up to which vehicle can be operated in electric mode	m/s
v_x	speed of test vehicle	m/s
Δv_{xy}	relative speed between vehicle x and y	m/s
v_y	speed of preceding vehicle	m/s
V_{OCV}	battery open circuit voltage	V
X_{glob}	x coordinate of vehicle position in the global plane	m
Y_{glob}	y coordinate of vehicle position in the global plane	m
α_{road}	road grade	rad
α	weighting factor on between fuel consumption and battery use in Prius optimization	
β	weighting factor between fuel/electricity and trip time	
γ_{veh}	vehicle cost, instantaneous optimization objective	
Γ_i	objective function for optimization	
η_{far}	faradaic efficiency	
η_{FD}	final drive efficiency	

η_G	gear efficiency	
λ	weighting factor between fuel and emissions	
μ	adherence coefficient	
ρ	air density	kg/m^3
ω_{EM}	rotational speed of electric machine	rad/s
$\dot{\omega}_{EM}$	rotational acceleration of electric machine	rad/s^2
ω_{EM1}	rotational speed of electric motor EM1 in Prius	rad/s
ω_{EM2}	rotational speed of electric motor EM2 in Prius	rad/s
ω_{eng}	engine rotational speed	rad/s
$\omega_{eng-idle}$	engine idle speed	rad/s
$\omega_{gearmax}$	upper limit of engine speed when using dynamic gear changing	rad/s
$\omega_{gearmin}$	lower limit of engine speed when using dynamic gear changing	rad/s
ω_{planet}	rotational speed of planetary gear on planetary gear set	rad/s
ω_{ring}	rotational speed of ring gear on planetary gear set	rad/s
ω_{sun}	rotational speed of sun gear on planetary gear set	rad/s
ω_{wheel}	wheel rotational speed	rad/s
$\dot{\omega}_{wheel}$	wheel rotational acceleration	rad/s^2

Chapter 1

Introduction

Contents

In this introduction the energetic and environmental problems of the transportation sector today is outlined. An overview on existing advances to solve these problems will be given. With this background the objective and contributions of this thesis work will be defined. Finally, we will present an overview of the thesis content.

1.1 Background

The first passenger vehicle, powered by an internal combustion engine, was developed in 1885 by Karl Benz [1]. The, so-called, Motorwagen can be seen in Figure 1.1. After several vehicles, running on steam or electricity, were introduced, Karl Benz was the first to design a vehicle driven only by an internal combustion engine. However, interest and trust of people in the vehicle came only after Bertha Benz demonstrated the operation of the vehicle with a first long distance trip.

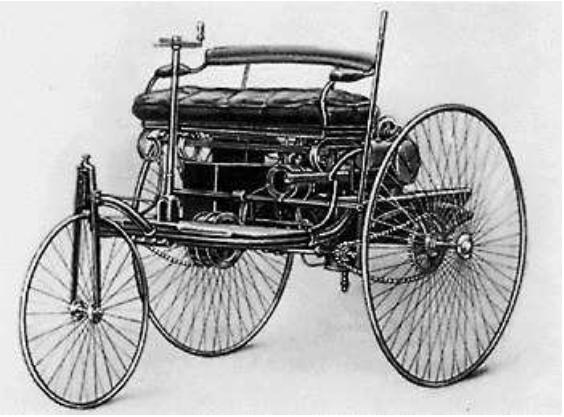

FIGURE 1.1: The Motorwagen designed by Karl Benz [1]

Since the construction of the first conventional automobile, the number of vehicles on the roads has been growing steadily. Around 1900 the number of vehicles on the road is estimated to around 8000 worldwide. This value increased to about 200,000,000 in 1970 and about 500,000,000 in 1990. Projections for the year 2030 predict that this number will keep growing to reach 1,200,000,000 [17].

Initially the automobile vehicle was built in order to transport goods or customers. Today, people often see the private passenger vehicle as a necessary standard to ensure their freedom and independence. In developed countries, such as western Europe and the United States, the number of vehicles per 1000 people lies at around 500 or more [18]. For fast developing countries, such as China and India, these numbers are still lower. However, projections show that car ownership rates will be exponentially increasing in these changing countries [19].

Although the automobile vehicle comes with numerous advantages for the user, it can also be identified as the source of many problems that the transportation sector faces today. Problems in the transportation sector can be classified in two categories. First, there are the energetic problems that are due to the scarcity of non-renewable fossil fuels. Secondly, the environmental issues have to be considered.

From Figure 1.2 we can see that most of the vehicles on the roads in Europe use gasoline or diesel engines for propulsion. Gasoline and diesel fuels are produced from fossil fuels and are therefore considered non-renewable energy sources. In 2010 the International Energy Agency (IEA) declared that the peak of oil production occurred in 2006 [3]. In Figure 1.3 the liquid fuel production worldwide is presented. It can be seen that the value stagnates after the year 2005 to fluctuate

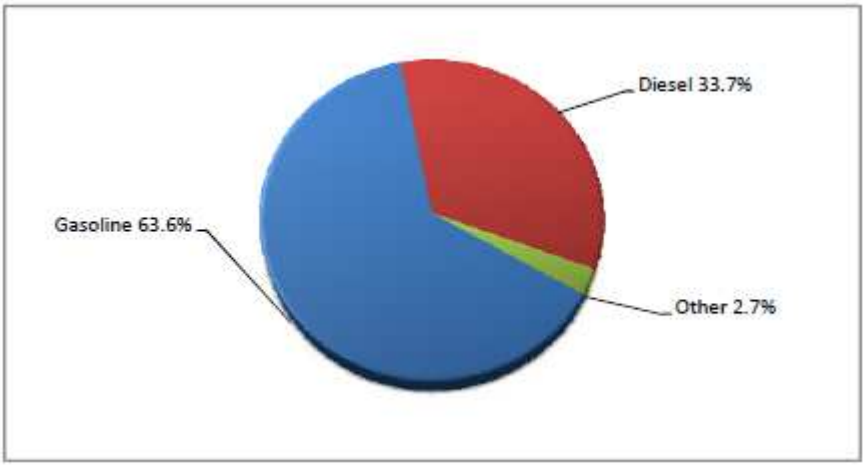

FIGURE 1.2: EU vehicle fleet by fuel type (2008) [2]

around a maximum value. However, although maximum fuel production has been reached, the consumption of fuels worldwide keeps increasing, partially due to the increasing number of passenger vehicles. With the increasing demand and limited supply, gasoline and diesel prices are increasing. Due to these facts we need to ensure the efficient use of the scarce resources while new, alternative energetic solutions are being investigated.

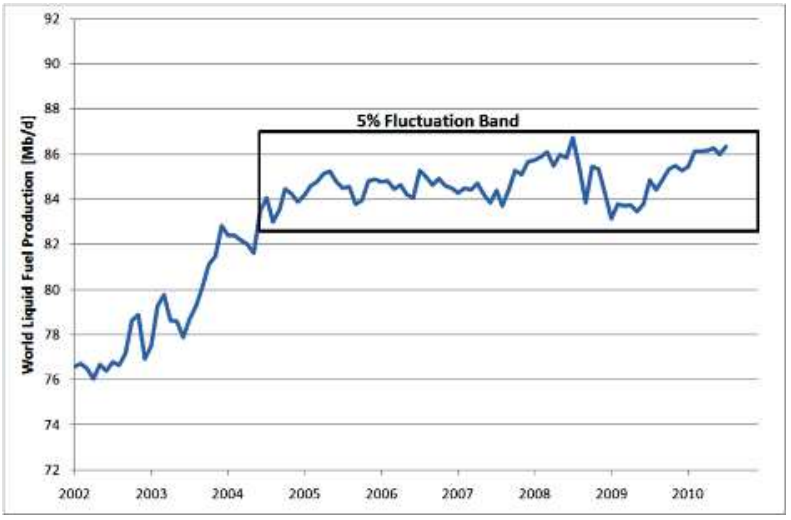

FIGURE 1.3: World liquid fuel production [3]

The transportation sector, being a major consumer of scarce fossil fuels, also contributes significantly to global warming. In the internal combustion engine of conventional vehicles fuels are used in a reaction with air to create energy. As a by-product water vapor, but also pollutants such as particle matter (PM), carbon dioxide (CO2), carbon monoxide (CO), hydro carbons (HC) and nitrogen oxides (NOx), are produced. These are more or less emitted to the environment, where

they lead to air pollution, health problems and contribute to global warming. Figure 1.4 shows greenhouse gas emission per sector in Europe in 2007. We can see that road transportation represents a significant producer of greenhouse gas emissions.

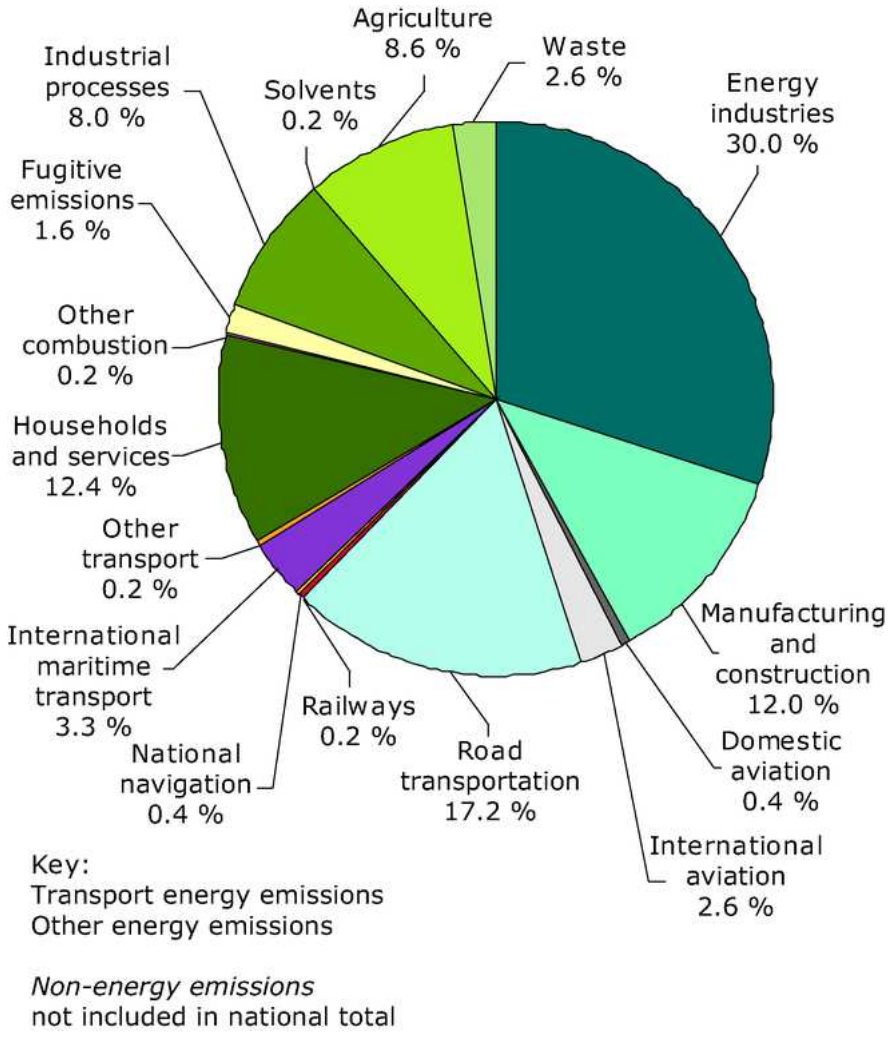

FIGURE 1.4: Greenhouse gas emission per sector in EU-27 (2007) [4]

With these facts in mind it becomes obvious that new fuel efficient solutions need to be identified to make the transportation sector energy efficient and environmentally friendly. In the following we will outline proposed approaches to achieve this.

1.2 Solutions

In the search for solutions to the problems of the transportation sector, researchers are evaluating options in two areas. On one hand, technological solutions are investigated to improve fuel efficiency, consider other energy sources and make vehicle transportation cleaner. A second approach is to develop utilization strategies that ensure the most efficient energy use with existing technological resources.

1.2.1 Technological solutions

Over the last 100 years the basic format of the conventional vehicle drive train has not changed much. But, with technological advances in each drive train component the overall vehicle efficiency has been improved. The engine efficiency has been increased over the last years with the integration of direct injection, valve control and timing, turbo charging and other technological advances. The fuel consumed in modern vehicle drive trains is reduced due to cylinder shut down or by turning off the engine when idling. In addition, progress in the development of advanced transmissions, such as automatic 6 speed transmissions and continuous variable transmissions, allow the engine to operate in more efficient regions [20].

While advanced drive train technologies are developed to increase efficiency and decrease pollutant emissions of the modern conventional vehicle, other approaches investigate the design of alternative drive train architectures. New vehicle architectures starting on the market include the battery electric, fuel cell electric, and hybrid vehicles. Generally, hybrid vehicles are considered more fuel efficient because the drive train allows us to recover kinetic energy when braking. In addition, due to the presence of a second power source, the engine can be turned off or shifted to a more efficient operating point. With electric vehicles the source of energy is flexible. Any energy source can be used to generate the required electricity. This drive train allows us to work with renewable energy sources, such as wind or solar energy.

New alternative drive train technologies are currently rather expensive in comparison with the conventional vehicle. The success of alternative drive trains, such as the hybrid vehicles, is very much related to the development of the fuel price. This can be seen in Figure 1.5, where the US market share of hybrid vehicles is

presented together with monthly gasoline prices. It becomes obvious that environmental reasons do not represent a very strong argument for customers. However, once gasoline prices increase the people are interested in more economic solutions. In addition, regulations and political decisions may have an impact on the market.

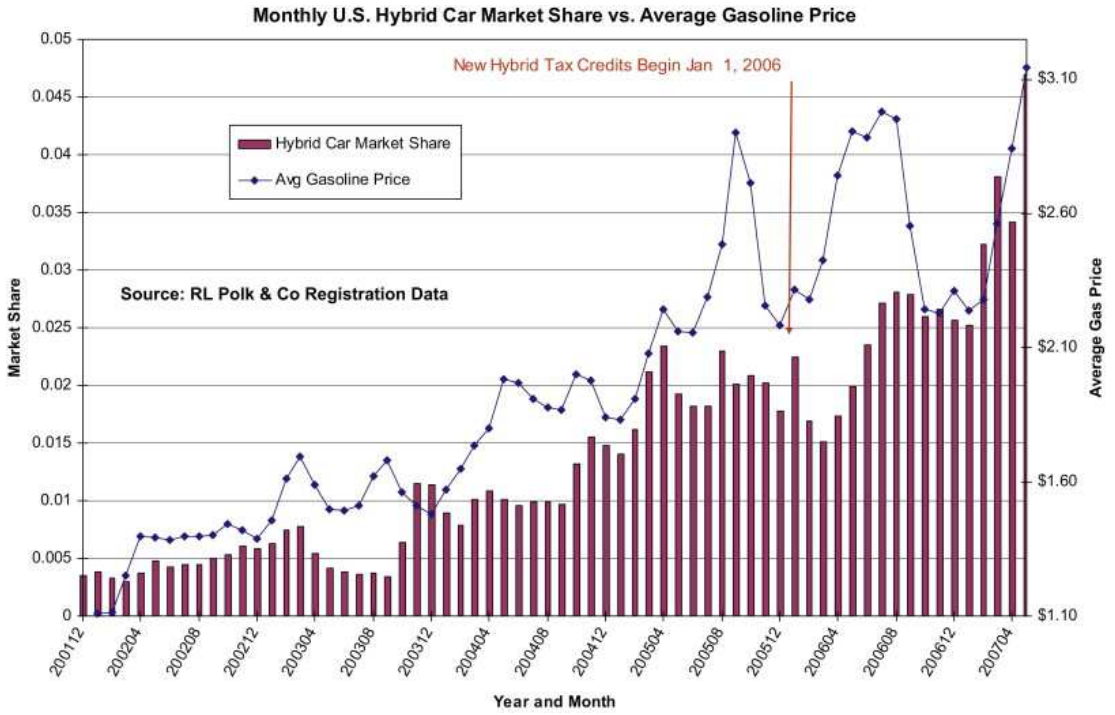

FIGURE 1.5: US hybrid car market share and gasoline prices [5]

To increase the sale of alternative, environmentally friendly, vehicles many governments established incentives on their purchase. With this the initial price for the customer is reduced and the time in which the vehicle becomes profitable decreases. In Figure 1.6 the projected sales numbers of electric and plug-in hybrid vehicles can be seen for several countries. It is expected that we will see more electric vehicles on the roads in the near future. In the meantime the utilization of today's vehicle technology should be optimized.

1.2.2 Energy efficient utilization

While technological developments are on the way, an efficient utilization of existing vehicles on the roads may be a good way to approach the energetic problems. Changing the way current vehicles are used can drastically reduce the global energy consumption and have positive effects on the environment.

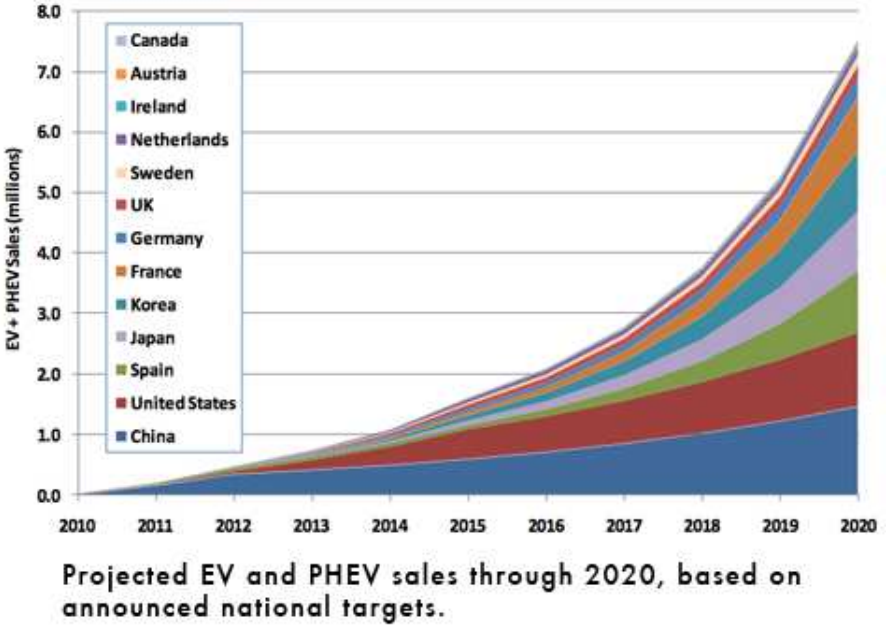

FIGURE 1.6: Projected EV sales [6]

Studies on intelligent vehicle technologies (ITS) are proposing infrastructure-to-vehicle (I2V) and vehicle-to-vehicle (V2V) communication to improve fuel economy [21]. In an urban environment, where fuel consumption is generally high and pollutant emissions should be avoided to increase air quality, frequent start and stops due to traffic lights and traffic congestions lead to non-optimal vehicle operation. Information received from the infrastructure or other vehicles can be used to limit these energetic losses. A representative example of ITS is the travolution project implemented by Audi in the city of Ingolstadt [22]. Audi optimized the traffic light phases in Ingolstadt, but in addition some traffic lights were equipped with communication modules. These modules transmit the time of the next green phase to the Audi test vehicle. The driver can therefore be informed of the appropriate vehicle speed in order to avoid having to stop. V2V communication can serve to transmit information about traffic jams or accidents. Notified drivers can take alternative route choices and traffic congestions can be reduced [23]. This approach leads to improvements in fuel consumption, but also to a reduction in urban pollution due to traffic.

Another, immediately implementable, method to reduce energy consumption of passenger vehicles is to apply, so-called, eco driving strategies. The efficiency of a vehicle is not constant, but changes dependent on vehicle velocity and acceleration. If a driver minimizes his energy consumption due to an appropriate choice of

acceleration rates and vehicle speeds this is referred to as eco driving. The concept of eco driving is immediately implementable without any further technological changes. In order to inform the driver of the best vehicle operation several methods have been investigated. In most countries eco driving courses are offered and it has been shown that drivers succeed to improve their fuel economy by 10-15% [24]. Other approaches use driver assist systems for eco driving to ensure a long term reduction of fuel consumption.

This thesis can be classified in this last category. In this work the maximum potential gains of eco driving strategies are analyzed and applied in the development of an effective driver assist system for eco driving. In the following the objective and contributions of this work will be outlined.

1.3 Thesis contribution

In this work a physical, drive train specific, modeling approach was used in combination with mathematical optimization methods to investigate the maximum potential gains of eco driving. In addition, an approach to implement the developed algorithms in an effective driver assist system for eco driving is presented.

Eco driving rules are often defined very generally and vehicle independent. With complex drive train technologies and alternative drive train vehicles it is important to apply drive train specific operation to achieve maximum gains of eco driving. In this work, detailed models of the vehicle specific drive trains are used to identify best operation. With this approach the here developed algorithms can be applied to simple, mono-source vehicles, such as the conventional or electric vehicle, as well as complex, multi-source drive trains, like the hybrid vehicle. Using drive train specific vehicle models the optimal vehicle functionality can be compared for different vehicle configurations.

While many studies use rule based approaches to identify optimal vehicle operation, we here apply mathematical optimization methods to identify the, theoretical, potential of eco driving. This method serves to establish upper limits of eco driving. In addition optimal vehicle operation can be analyzed and used to derive important factors for maximum fuel efficiency.

Initially a three dimensional dynamic programming method was used to solve the trajectory optimization problem [25]. To reduce the computational effort, a weighting factor was introduced in the cost function in a second approach. In order to satisfy all optimization constraints a nested optimization method, where a two dimensional dynamic programming method is used in combination with advanced root finding methods, was applied [26]. To identify the trade-off between trip time and energy consumption a multi-objective optimization method was implemented to compute the Pareto optimal front [27].

The developed algorithm was applied to several different drive train vehicles. With this we were able to investigate and compare important factors for eco driving for the conventional, electric [28] and hybrid vehicle [29]. The computation of maximum potential gains of eco driving is necessary to identify upper limits for fuel consumption reductions. However, to approach real world energy consumption values traffic constraints have to be taken into account. The developed algorithm was applied to a car following scenario to investigate influences of traffic on potential gains of eco driving [30].

Although most studies only consider energy consumption, eco driving is generally seen as environmentally friendly behavior. In a case study we investigate the economic and ecologic aspects of energetically optimal vehicle operation. The work shows that it is necessary to take into account environmental constraints in order to consider eco driving to be ecologic. In our work we propose a simple strategy to reduce overall pollutant emissions [31].

The theoretical studies enabled us to analyze potential gains of eco driving and to get a deeper understanding of drive train specific, optimal vehicle operation. We were able to identify vehicle specific factors that are important to ensure energy efficient operation. In the final part of this thesis work the developed algorithms were used in the development of an effective driver assist system for eco driving that has been tested on a driving simulator.

1.4 Thesis overview

The thesis content is separated in six chapters with a general conclusion at the end. In Figure 1.7 a schema is presented to visualize the organization of the thesis. In the following an overview of each chapter will be given.

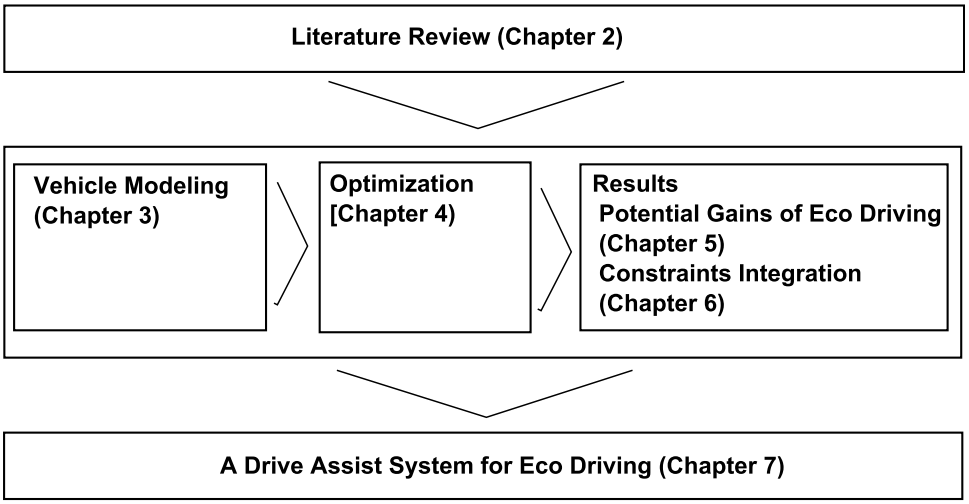

FIGURE 1.7: Thesis overview

Chapter 2 In chapter two an overview of the literature is given. Existing driver assistance systems for eco driving are discussed, listing their advantages and disadvantages. Previous work on trajectory optimization problems for ground transportation is evaluated. With this a general overview of the state of the art in this domain is given.

Chapter 3 Chapter three presents the vehicle modeling. The direct and inverse modeling approach is discussed. Inverse vehicle models for conventional, electric and a representative hybrid vehicle are outlined. In addition the direct vehicle simulation software VEHLIB is introduced.

Chapter 4 In chapter four the optimization algorithms, applied to solve the trajectory optimization problem, are detailed. Due to the complexity of the problem, the dynamic programming optimization method was applied. Initially a three dimensional method was used, that was later reduced to a two dimensional dynamic programming method by integration of a weighting factor. To analyze the trade-off between fuel consumption and trip time a multi-objective optimization is presented.

Chapter 5 In chapter five theoretical potential gains of eco driving are discussed. The trajectory optimization problem is solved for exemplary trips for the conventional, electric and hybrid vehicle. General and real-life drive cycles are used to compute so-called eco cycles, that represent optimal vehicle operation for the corresponding mission. To verify the simulated results, the computed optimal drive cycles were experimentally tested on an engine and

chassis test bench. Important, drive train specific factors for eco driving are derived.

Chapter 6 Chapter six deals with the integration of constraints. A case study shows how traffic constraints can affect potential gains of eco driving. Traffic constraints are integrated for the case of a vehicle following situation to ensure driver safety. A second case study discusses the environmental aspects of eco driving. Ecologic advantages of eco driving are considered with the integration of emission constraints. Fuel consumption and emission measurements show the trade-off between economic and ecologic vehicle operation.

Chapter 7 An approach to integrate the developed algorithms in a driver support system for eco driving is shown in chapter seven. The direct vehicle simulation software VEHLIB was integrated on a stationary driving simulator. Using the optimization algorithms in combination with the inverse vehicle model an advanced driver support system was developed. The system was experimentally evaluated by several external subjects. Survey questions were used to investigate the driver acceptance of the system. Using simulated fuel consumption and survey results the efficiency and effectiveness of the driver support system was evaluated.

Chapter 8 In the last chapter a general conclusion of this thesis work can be found. A perspective on future work recommendations is given.

Chapter 2

Literature Review

Contents

Eco driving is a way for a driver to reduce his energy consumption immediately. With that, by applying the principles of eco driving, a driver can rapidly reduce his impact on the environment. For most people the more interesting aspect of eco driving is the cost advantage. Without extensive costs on development or production of new technologies it represents a way to rapidly reduce the operating cost of a vehicle.

The first studies on fuel reductions due to driver operation seem to be driven by this mindset. Research on effects of driver behavior on fuel consumption started in the middle of the 1970s in the US. Due to the first oil crises the oil prices in the

US increased by about 50% between 1970 and 1974. As a result the Department of Transportation published two reports in 1976 in which the effectiveness of driver aid devices to improve fuel economy are discussed [32], [33]. Further studies on the effects of driver behavior on fuel consumption were published by Evans in 1976 and 1979 [34, 35]. Evans, working for General Motors, stated that in an urban setting with traffic, on average, a 1% increase in trip time resulted in a 1.1% improvement in fuel consumption. However, Evans mentions that 'expert' drivers were able to 'skillfully' adjust their speeds, such that fuel was reduced although trip time was not increased. As a final result Evans concludes that the fuel economy meter, a gauge that indicates instantaneous miles-per-gallon values, is not accurate enough for a driver to minimize his fuel consumption.

After this period and with the second oil crisis in the 1978-1980 research continued on the subject. Several studies [36] indicate that significant savings in fuel cost are possible due to changes in driver behavior. The concept of eco driving started to become interesting for companies and transportation fleets [37]. Through continuous feedback and reinforcement of eco driving rules the fleet drivers from a major textile company were able to reduce the company's total fuel purchases and therefore reduce their expenditures.

In the last years the enforcement of the Kyoto protocol puts countries under pressure to reduce their greenhouse gas emissions. Since the transportation sector is one of the most important contributors to CO2, Methane and NOX emissions, countries are planning to achieve part of their CO2 targets by cutting emissions from vehicle transportation. While the vehicle manufacturers achieved a reduction of 13% in CO2 emissions by 2007 [38] due to the development of new technologies, several European governments are now integrating eco driving into their national reduction strategies. Countries, like The Netherlands, are developing eco driving programs to motivate people to perform eco driving strategies and educate people about eco driving [39]. Some countries integrate education on eco driving principles in the course of the drivers license tests. In general, studies show that, on average, a 10% reduction of fuel consumption is achievable due to eco driving.

Knowing the advantages of eco driving a lot of research on the subject was supported in the last years. In Europe, the European Campaign On improving DRIVing behavior, ENergy efficiency and traffic safety (ECODRIVEN) was launched in 2006. In the following years projects like the FootLITE project [40], the ECOWILL project [41], the eCoMove project [42] and the FLEAT project [43] started in

Europe. The National Highway Traffic Safety Association in the US published several reports throughout the years 2009 and 2010, in which the current eco driving assist systems are analyzed and recommendations for the development of efficient systems are given [7, 44].

Eco driving courses are offered in several countries. In general the results have been very positive and drivers have shown to be able to reduce their energy consumptions [24]. Hornungs [24] mentions in his work in 2000 that a long term reduction of fuel consumption between 10 - 15% was possible. However, in a long term study Beusen [45] followed the progress of drivers that took eco driving courses. He concludes that, while at first reducing their energy consumption, drivers fall back to their old driving habits some time after the course. In the work of Wahlberg [46] he monitors drivers that were educated in eco driving rules over 12 months and states that on average only an increase of 2% was measured over the entire period. It becomes obvious that, without constant reminder, drivers do not intuitively integrate efficient vehicle operation in their driving, even if these drivers do know how to optimize vehicle operation. Due to this, it is assumed that the potential long term savings possible with a driver assist system for eco driving cannot be achieved by a onetime eco driving course.

In Section 2.1 existing eco driving support systems will be discussed. An important part of any eco driving support system is the way the suggested 'optimal' vehicle operation is determined. A support system, which advices a driver of sub-optimal vehicle operation cannot be very effective in optimizing the vehicle operation of a driver. We therefore analyzed existing algorithms used to determine optimal vehicle operation in Section 2.2.

2.1 Eco driving support systems

With the aim to reduce energy consumption many companies are developing driver assist systems for eco driving. Some of these systems are developed by the car manufacturer themselves and directly integrated in the vehicle. This way appropriate vehicle parameters can be directly stored in the system. Other systems are developed to be implemented in various vehicle types. With the rise of the smart phone there are now eco driving applications available to be downloaded on portable devices such as a mobile phone or a laptop computer. Generally the existing support

systems can be separated into two categories: informative systems and advisory systems. In the following we will present existing systems for each of these two categories.

2.1.1 Informative systems

Informative systems transmit information about several variables of the vehicle to the driver. In contrast to advisory systems, however, no advice about optimal vehicle operation is given. Informative driver assist systems have been implemented in road vehicles for a long time. The first informative system in vehicles was the fuel gauge. An analog fuel gauge was used to show how much gasoline was left in the tank. With this the device was indicating cumulative fuel consumption. In today's vehicles a digital display often shows trip kilometers, kilometers left to drive with the remaining fuel, instantaneous fuel consumption and/or average trip fuel consumption. While most of these systems often stay unused, they can give indications on how vehicle operation influences fuel consumption. With informative systems the motivated driver has to perform trial and error experiments to identify the vehicle operation that leads to the minimum fuel consumption. While informative indicators can give a good idea of overall vehicle operation they can often lead to false assumption when looking at instantaneous fuel consumption. Instantaneous energy consumption will generally be higher in acceleration phases or on upward slopes. However, these increases do not indicate bad vehicle operation [32, 47].

Hybrid vehicles often have more advanced informative systems. Having two power sources and, with that, two energy storage devices, displaying the vehicle states becomes more complex. In hybrid vehicles the dashboard display often shows fuel consumption, battery state of charge, and the flow of energy. In Figure 2.1 the dashboard of a hybrid vehicle, the Ford Smart Gauge, can be seen. This gauge developed in 2010 can be run in two modes: The 'basic' mode just informs the driver of general vehicle parameters while the 'empower' mode is a mode where more advanced information is presented to the driver. When choosing this functionality long term fuel efficiency is shown to the driver in the form of leafs growing on the display background. With this the driver knows when his vehicle operation will result in better fuel economy

FIGURE 2.1: Ford Smart Gauge [7]

In the last years several vehicles started to have 'green' indicators like the Ford Smart Gauge. Often an 'eco' light on the dashboard informs the driver of the efficiency of his driving style. A report published by the Department of Transportation [32] in 1976 shows a comparison of driver aid devices at the time. As a response to the oil crises multiple car manufacturers presented information about instantaneous fuel consumption with help of a vacuum gauge. If the vacuum in the engine manifold dropped toward 0, which happens at wide open throttle, the system indicated increased instantaneous fuel consumption. The Chrysler Fuel Pacer is one of these driver aid systems. It can be found in some of the Chrysler/-Dodge models from 1974 to 1978. In the report the Fuel Pacer is expected to achieve a reduction of up to 23.1% in fuel consumption. The Chrysler Fuel Pacer consisted of a light that was attached on the left side of the hood. When lit up it indicated excessive fuel use. The indicator is turned on when the vacuum level in the manifold dropped below a threshold level [7]. The system was intended to help drivers reduce their fuel consumption by reducing the power they used on acceleration. Other vacuum gauges such as the Pontiac and Ford vacuum gauges are expected to achieve fuel consumption improvements between 6.9 and 24.6%

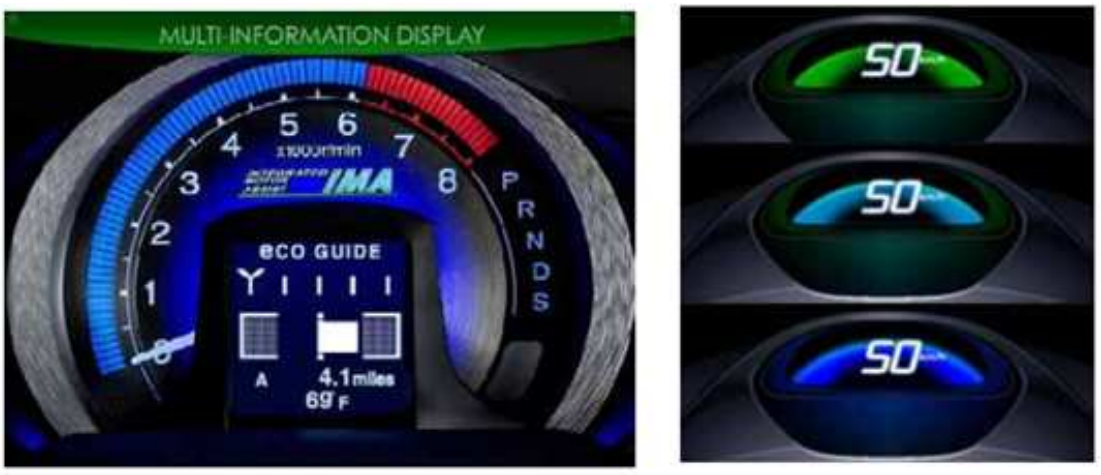

FIGURE 2.2: Honda Ecological Assist System [7]

[32]. However Hinton [32] points out in his report that the gains in fuel economy very much depend on the drivers motivation.

An 'eco' light indicator was integrated in the 2009 model of the Honda Odyssey. In this vehicle the variable cylinder management made it possible to turn off two or three of the six cylinders at low power requirements while cruising. The light indicated that cylinders were shut down and therefore fuel consumption was reduced. While trees and green leaves are very popular indicators for efficient operation [7] other vehicle manufactures indicate the efficiency level of the vehicle in color scheme on the dashboard [7]. Figure 2.2 shows one of these indicators. Here the Honda Ecological Assist System can be seen. This system can be found in the 2010 Honda Insight Hybrid. The background color of the speedometer indicates ecologic vehicle operation in green and turns blue when more fuel is consumed due to excessive acceleration and braking.

2.1.2 Advisory systems

Advisory systems are a common way to assist drivers to reduce fuel consumption. On the contrary to informative systems the advisory support systems give specific advice of how to reduce the vehicle's energy consumption. One of the most important challenges for driver assist systems today is to effectively transmit information to the driver without creating a safety risk because the driver's focus is taken off of the road.

While route indicators such as GPSs often use the auditory way to transmit information to the driver, the most popular way for driver support systems for eco driving is by visually presenting information. The most common advisory support system for eco driving integrated in vehicles today is the gear change indicator. The indicator is a simple flash that lights up on the control board to suggest an up- or down shift. With this system many vehicle manufacturers encourage the driver to operate the engine in an efficient region with the goal to keep fuel consumption low.

It is well known that operating a vehicle at constant speed is more efficient than continuously changing speeds. With this assumption we can count cruise control systems and throttle control systems into the category of eco driving support systems. Studies show small reductions in fuel consumption due to such devices, but other than general eco driving advice systems they can only be used on highways, where the vehicle is operated at constant speed. The devices usually cannot be used below speeds around 40-60km/h [47].

A vehicle's acceleration is commonly assumed to have a strong influence on fuel consumption. Many driver assist systems therefore indicate the acceleration rate and advice the driver not to exceed a certain limit. In Figure 2.2 such a system can be seen. The Honda Eco Assist system shows a horizontal bar in the middle of the display. When accelerating or braking at high rates the bar stretches to the left and right. The driver is advised not to operate the vehicle such that the bar reaches the gray shaded areas. Due to reduced acceleration and deceleration rates the overall fuel consumption is reduced.

Although most systems interface with the driver by giving visual information some driver support systems use haptic devices to generate advice by force feedback. One of the first systems mentioned in the report of the Department of Transportation was such a system. The so-called Accelerite was an acceleration pedal feedback system. When engine vacuum levels were low the pedal increased the resistance to suggest lower acceleration levels to the driver. However, the system can easily be overwritten by pushing harder on the gas pedal. Tested in several trucks the system showed an improvement in fuel economy between 3 and 17%.

Today, implementing a resistance on the acceleration pedal is still a method used when trying to reduce energy consumption. Nissan claimed in 2008 to have developed the world's first eco pedal [8]. In Figure 2.3 the operating principle of

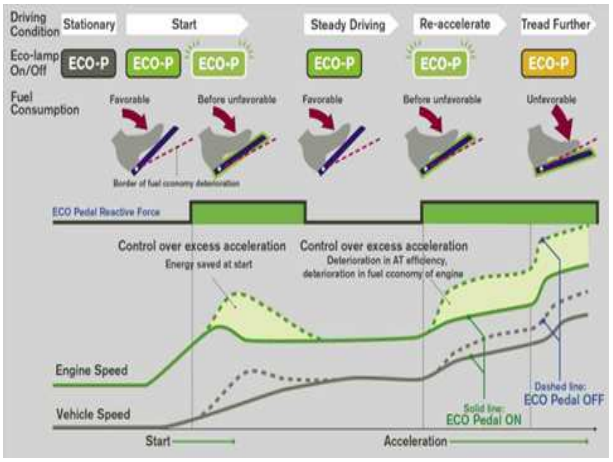

FIGURE 2.3: The Nissan Eco Pedal [8]

this system can be seen. As in the Accelerite the driver can feel a resistive force when the pedal is pressed too hard. Nissan announces that using the pedal results in 5-10% fuel reduction. The similar approach to restrict the vehicle acceleration is taken by Larson [48]. In his research the so-called Active Accelerometer Pedal (AAP) is used to increase safety by reducing acceleration rates. Larson announced that he could not find a significant reduction in fuel consumption due to the changes in acceleration. He concludes that acceleration rates are not the only important factor having an impact on fuel consumption.

There are several advanced driver assistance systems on the market today. These differ from the previously mentioned systems, in that they take into account vehicle parameters to determine the appropriate advice to the driver. In the following section a review of existing advanced driver assistance systems (ADAS) that give advice to the driver in real time while driving and systems that use recorded vehicle data to give post trip tips for improvement will be given.

2.1.2.1 Advanced Driver Assistance Systems (ADAS)

To our knowledge the first ADAS was developed in 2001 in the Netherlands. In her thesis, M. v.d. Voort describes the development of the so-called FEST (fuel efficiency support tool) [9]. In her work, v. d. Voort uses a state machine to determine the optimal vehicle operation that should be transmitted to the driver. The application uses vehicle parameters, including power characteristics of the engine, gear ratios, and a fuel consumption map of the engine. In addition, measured, real time variables, such as vehicle speed, acceleration, engine speed, clutch

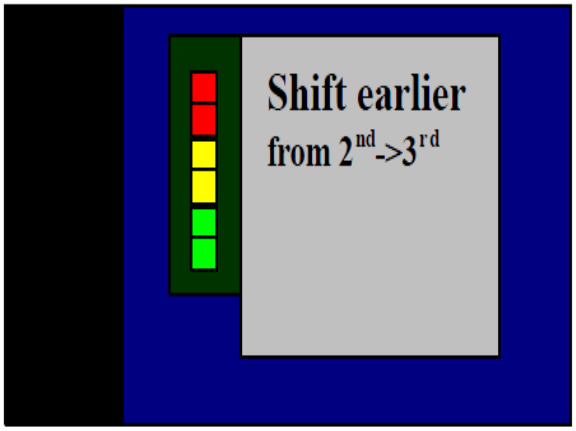

FIGURE 2.4: FEST driver assist system [9]

signal, gear, accelerator pedal position, steering angle and headway are taken into account. With the detected driver operation the vehicle is assigned to a state, for example 'deceleration phase'. Comparing optimal vehicle operation in this state to the actual, the system decides what advice to give to the driver. v. d. Voort developed a driver display that can be seen in Figure 2.4. As seen, the suggestions given to the driver are simple and very specific. In addition to written tips the driver operation is rated in a green, yellow, red color scheme.

In the context of the FootLITE project an advanced driver assistance system has been developed. The FootLITE Eco Driving Support Tool [40] consists of an LCD display which gives instantaneous feedback to the driver while on the road. The display shows route information, distance to the car in front, speed consistency and speed limits. Trying to optimize the vehicle operation for fuel consumption the system uses the eco driving rules published in the driving guide [49] by the Institute of Advanced Motorists (IAM) as a basis. Using this rule based strategy the FootLITE system is aiming to increase the efficiency of the entire vehicle network. In order to reduce the impact of vehicles on the network, alternative routes and even trip cancellations are suggested [40].

ADAS for eco driving are also being developed by companies specialized in driver support systems. Vexia[1] is a company working on navigational driver assist systems using GPS and radar. Their Econav system is an advanced system that helps drivers to reduce their fuel consumption. The system, that looks like a car's GPS (Figure 2.5), provides the driver with feedback about best speed, gear and acceleration rate for corresponding route segments. For the system to determine

[1]Vexia: Spanish brand that develops GPS navigation systems (www.vexia.co.uk/)

FIGURE 2.5: Vexia Econav system [10]

optimal operation the driver has to input his vehicle's manufacturer and the model. Unfortunately no information on the optimization process was found.

Several car manufacturers are now developing their own built-in eco driving assistance systems. These use specific drive train and engine parameters. Porsche[2] is in the process of developing their ACC InnoDrive [50]. The system, currently still in the testing phase, is using radar data, road grade and route prediction to propose a velocity profile and gear choices to the driver. While Porsche is not necessarily trying to reduce the environmental impact of their vehicles, reducing fuel consumption come as an advantage when looking at long distance racing competition. The Porsche ACC InnoDrive is supposed to reduce fuel consumption by 10% and is implemented in conventional drive trains as well as their electric and hybrid vehicle architectures.

2.1.2.2 Post-trip support systems

Giving real-time, instantaneous advice to a driver can be difficult due to missing trip information and potential safety risks. Post-trip support systems are therefore a good alternative to advice the driver about efficient driving. There are now several car manufacturers, like Fiat and Nissan, that develop and integrate vehicle specific eco driving support systems in their vehicles.

The Fiat EcoDrive is a post-trip advisory system, that can be used with the Fiat 500 and Fiat Grande Punto models [51]. The trip data is transferred by USB

[2]Porsche: German car manufacturer (http://www.porsche.com)

Port to the personal computer. Using a downloaded program the user can track his performance report and progress on mileage and emissions. Nissan introduced their program CARWINGS Eco-Drive [7] in 2007 in Japan. The program is an extension to their existing navigation program and encourages drivers to reduce their energy consumption. The Fiat EcoDrive, as well as the CARWINGS Eco-Drive includes applications where drivers can compare their fuel consumption in common city areas to that of other drivers. Calling on peoples competitive spirit the programs are trying to motivate drivers to reduce their environmental impact.

With the increasing number of smart phones there are several nomadic applications that can be downloaded to cellular phones. Two sample applications, the GreenMeter [7] and the TripAlyizer [7], are shown in Figure 2.6. The GreenMeter (on the left) was developed by Hunter Research Technology. It is an application that can be downloaded on the IPhone. The user has to enter vehicle parameters in the setup process. The device uses the IPhone's internal accelerometer together with the vehicle parameters to determine the vehicle power, engine power and fuel used. The results are shown in stacked bar graphs that indicate how much energy was used on rolling resistance, aerodynamic drag, and acceleration. With this the driver can identify how his operation can influence the energy needed.

Surich Technology's Trip Alyizer consists of an application that was developed to be used on the IPhone 3G version. It uses the 3Gs featured GPS, accelerometer and speakers. Using information on gasoline purchases the system calculates trip efficiencies by distributing scores to acceleration, idle time, speed, and time spent at the engine's 'sweet spot'. The application can be used to transmit information to the driver in an auditory way by using the cell phone's speakers.

Several other post-trip support systems to reduce energy consumption exist. For companies with vehicle fleets eco driving can be a simple way to reduce their operating cost. With this in mind eco driving support systems like the Earthrise Technologies' EcoWay [7] and the GreenRoads-Safety Center [7] were developed for fleet applications.

FIGURE 2.6: Nomadic post-trip support systems [7]

2.1.3 Conclusion

As previously presented, there are several driver support systems implemented to reduce energy consumption. In Table 2.1 a summary of the discussed representative systems can be seen. The computational effort of the systems was rated as well as their need for advanced inputs from the vehicle or GPS devices. It can be seen that, while informative systems result in small computational efforts and rarely require vehicle input, the advisory systems and in particular advanced driver assist systems require a lot of information in order to function. In addition heavy computing algorithms are commonly applied to treat the information and identify detailed driver advice. In the following we will discuss algorithms used to determine appropriate vehicle operation.

2.2 Optimal vehicle operation

There are two different ways that can be used to compute fuel reducing vehicle operation. The first method, here called Rule Based Evaluation, uses rules that can be applied depending on the state of the vehicle. This method is easily implemented in support systems or taught to drivers, but such methods are usually

system category	system	detail	computational load	vehicle input	output
informative systems					
	fuel gauge		-	-	cumulative consumption
	fuel display		-	+	instantaneous consumption
	hybrid advanced display		-	+	consumption, battery charge, energy flow
	'green' indicators	eco light, eco bar	-	-	light, leafs, color, bar
advisory systems					
	gear change indicator		-	+	up- and downshift indication
	cruise control		-	+	automatic cruise control
	acceleration limiting devices	honda bar, accelerator pedal	-	-	pedal resistance
	ADAS real time systems				
		FEST (2001)	++	++	written recommendations with color code
		FootLITE (2009)	+	++	route information, distance to car in front, speed consistency, speed limits
		Vexia Econav	?	++	best speed, gear and acceleration rate
		Porsche ACC InnoDrive (2013)	?	+++	velocity profile, gear changes
	ADAS reporting systems				
		Car manufacturers (Fiat ecoDrive, Nissan CARWINGS)	+	-	report
		nomadic devices (GreenMeter, TripAlyizer)	+	-	report
		fleet applications (Earthriese Ecoway, Greenroads)	+	-	report

TABLE 2.1: Overview of fuel efficiency support systems

sub-optimal. A second method is to develop a model of the vehicle and to apply a mathematical trajectory optimization to a specific mission. This method is not simple to be implemented in real time due to the fact that knowledge about the trip has to be provided. However, if a sufficiently accurate system model is used the result can be considered optimal. In Section 2.2.1 a literature review of rule based evaluation methods is presented. Works on trajectory optimization methods were reviewed in Section 2.2.2.

2.2.1 Rule based evaluation

Basic eco driving rules have been developed and published by several associations [52] and automobile manufacturers [53]. These generally state that, in order to drive economically, the driver should:

- Anticipate traffic flow
- Maintain a steady speed
- Shift up early
- Check tire pressure frequently
- Avoid extra weight

Mostly eco driving rules such as these are given in a very general way, such that they can be applied by any driver to any type of vehicle. Mostly such rules are developed using common sense and some knowledge about the physics in the system. Anticipating traffic flow can reduce energy wasted on accelerations, when the vehicle will need to slow down due to traffic in front. Assuming that a conventional vehicle is used, the internal combustion engine achieves its highest efficiencies at high torque, low speed operation. Higher gear engagements will therefore result in better overall system efficiency. Maintenance of a vehicle reduces energy consumption, but is also a task necessary for a responsible driver to improve safety. In addition, although it is sometimes not possible, in general it is easy for a driver to minimize the extra weight carried by his vehicle. With this the mass to be displaced is reduced and that will lead to lower energy consumption.

One way to determine appropriate rules for vehicle operation is to look at the losses and operation principle of each component in the vehicle drive train. With this

certain rules, like efficient gear shifting, can be fixed. However, using this approach, the vehicle's mission is not taken into account. A second method to determine important eco driving factors is to analyze experimental data and determine for which vehicle operation the fuel consumption was reduced.

Ericsson [54] used this approach in her work. In her study driving data from several cars circulating in a city was collected. Measuring several variables she could identify parameters such as acceleration with strong power demand, late gear shifting, time spend in a certain velocity range, time spend in some engine speed range, stops, speed oscillations and so on. She concludes her work with the specification of five most important factors for fuel consumption and emissions. Based on Ericsson's work Saint Pierre [55] used a statistical analysis to determine an eco factor using experimentally measured driving data. With this factor the efficiency of the vehicle operation can be rated.

It is assumed that, due to the lack of a priori trip information most advanced driver assist systems apply a rule based method to compute the appropriate driver advice. In her thesis, van der Voort [56], applied a rule based method in the FEST driver support system. In the FEST several vehicle states, such as 'deceleration phase' or 'cruising', are specified. The state the vehicle is currently in is determined using present information but also some history of the vehicle variables. Appropriate vehicle operations were pre-defined for each state. When the vehicle state is determined the current vehicle operation is compared to the optimal vehicle operation. With this van der Voort uses a state machine approach to apply a rule based evaluation method in real time.

While rule based methods are more simple to be implemented they can only determine sub-optimal vehicle operation. Even if the instantaneous optimal vehicle operation is determined, a globally optimal result is not achievable since the vehicle's mission is not taken into account. Implementing this method in a driver support system the maximum potential gains of eco driving cannot be reached since the advice presented to the driver is already sub-optimal.

2.2.2 Trajectory optimization

In the literature, trajectory optimization problems are very common. There are several areas of research that apply and develop mathematical methods to determine the, with respect to some objective, optimal trajectory. In robotics trajectory optimization problems are important for energy conversation and safety. Rocket scientists use trajectory optimization to determine the correct trajectory to send rockets into the orbit. In our work we will confine our review on trajectory optimization problems on the field of ground transportation. Work on road vehicle trajectory optimization will be discussed in Section 2.2.3. In addition, relevant work on railroad vehicle optimization is presented in Section 2.2.4.

2.2.3 Road vehicles

The idea to optimize the velocity profile of a road vehicle in order to save fuel was first investigated by Schwarzkopf in 1977 [11]. Schwarzkopf used a polynomial model of the vehicle to calculate fuel consumption for a given vehicle state. With this simplified cost function he used the Pontryagin's maximum principle, a method based on the calculus of variation, to minimize the fuel. Two scenarios were considered. First the energy to accelerate to a desired cruising speed was minimized. In a second problem the vehicle operation was optimized when driving over a hilly road. In Schwarzkopf's work the problem was stated with initial and final conditions in distance, velocity and time. The goal of the study was to develop and/or verify empirical driving tips given at the time. The results showed that using such an optimization algorithm, appropriate vehicle operation can be identified and theoretically fuel can be reduced. Useful tips given by the author for implementation in real life driving include:

- Reduce speed before downhill section and increase speed on downhill
- Increase speed before uphill section and reduce speed on uphill

This concept can be seen in Figure 2.7, where a vehicle is shown driving over a hill or through a valley. Most literature following Schwarzkopf refer to his publication as the first research in this area.

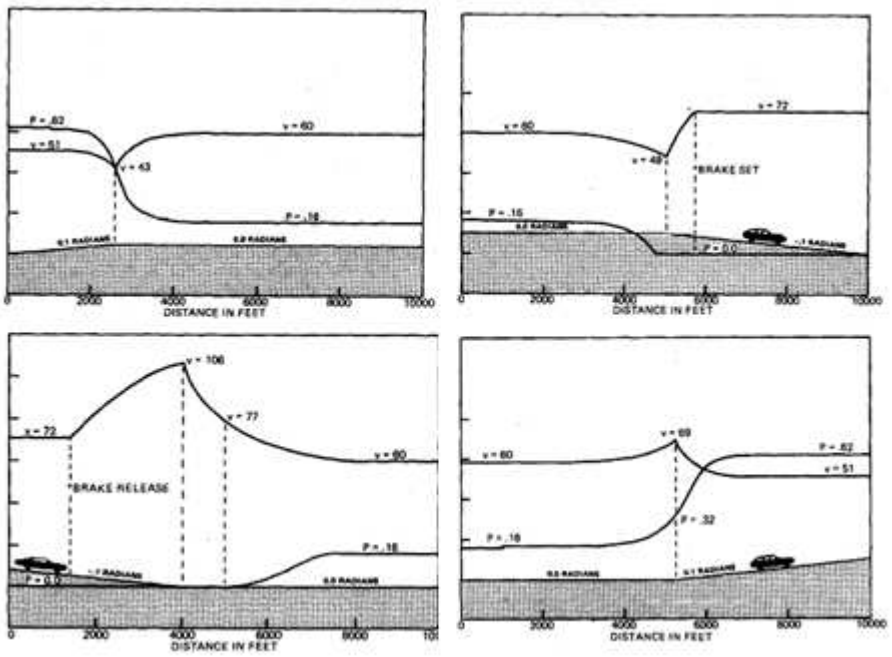

FIGURE 2.7: Driving over hills, by Schwarzkopf [11]

In the middle of the 90th century another US researcher, Hooker [12, 57], published his work on velocity profile optimization. While Schwarzkopf used a simple vehicle model, Hooker used experimental data to describe the energy consumption. From his previous experimental studies he integrated vehicle data to derive accurate fuel models dependent on the vehicle velocity and acceleration rate. In his paper [12] he considers four different optimization problems. The problem of finding the optimal cruising speed for a vehicle on a constant grade, the optimal way to accelerate a vehicle to a typical cruising speed, the optimal way to drive a block between two stop signs and the optimal way to drive over hills with a desired average speed. In his analysis Hooker uses the Dynamic Programming Algorithm to solve the optimization problems in a 3 dimensional approach, where time is placed in the x-axis and velocity and position can be chosen as states at each time step. However, linked by the vehicle's dynamic equations, time, position and velocity are not three independent variables. Hooker therefore chose the velocity of the vehicle as the state at some time and uses nearest neighbor interpolation to fix the distance to the predefined grid. In his work, Hooker found the optimal velocity profiles for 15 previously experimentally identified cars. Comparing fuel economy versus trip time he states that there is an unique optimal driving profile for time and fuel. Covering a distance in shorter time results in higher fuel economy due to high acceleration rates, while a longer travel time results in more losses due to engine idling. In comparing the vehicles he used, he found that optimal cruising speeds

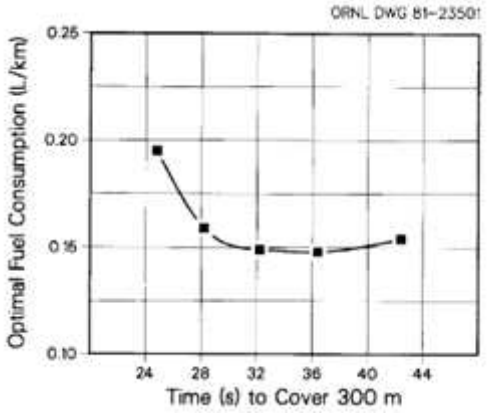

FIGURE 2.8: Fuel versus time trade off by Hooker [12]

and acceleration rates change for different vehicles. In Figure 2.8 the trade of between fuel used and trip time is shown for driving the distance of 300m between stop signs. It can be seen that the optimal trajectory for time and fuel would occur if we cover the distance in 36 seconds using .15 L/km of fuel.

Working on the same optimization problems as Hooker in 1988, Monastyrsky in 1993 [58] shows a different approach to solve the problem. He reduces the computational cost of the optimization by reducing the number of states in the dynamic programming problem. Considering the mission to drive a certain distance with fixed initial and final velocity he eliminates the time as a state. Reintroducing the time in the cost function in combination with a weighting factor achieves the desired trade-off between fuel and time. The cost function can then be written as $J = J_{fuel} + \beta T$ where T is the trip duration and β the weighting coefficient between fuel and time. However, in his publication Monastyrsky does not mention how he determines the appropriate weighting factor. In his paper Monastyrsky shows the trade off in percentage increase of fuel consumption relative to the optimum versus average speed.

Continuing the research on fuel-optimal velocity control Stoicescu published his paper in 1995 in the International Journal of Vehicle Design [59]. In his work Stoicescu states that considering the three variables time, distance and fuel, 6 optimization problems can be defined and analyzed. These are:

1. Minimize cost for fixed time T
2. Minimize cost for fixed distance
3. Minimize cost for fixed distance and time T

4. Minimize time for fixed cost
5. Maximize distance for fixed cost
6. Maximize distance for fixed cost and time T

Using a simple system model Stoicescu solves the stated problems using Pontryagin's maximum principle. Finally, he states that optimal control of a vehicle includes the following phases combined in different ways:

- deceleration without shut-off engine (zero engine power)
- emergency deceleration without shut-off engine (zero engine power)
- emergency deceleration braking
- constant velocity running
- full-throttle acceleration

Emergency deceleration phases are never utilized if the final velocity is not significantly less than the initial velocity.

All research in this field up to the year 2003 considered vehicles with internal combustion engines as power source. In 2003 a paper published by Guzzella, Sciaretta and van Balen [60] first considers the problem of finding the fuel optimal trajectory for a fuel cell powered vehicle. Applying numerical optimization methods the optimal velocity profile is found for a trip over a route with fixed average speed and for a cyclic route problem.

The dynamic programming optimization method was also applied to the fuel optimal routing problem over a complex terrain by Tsao [13]. In Tsao's work the fuel consumption is optimized in a time independent way, while considering the grade angle of a complex terrain without road system. In his paper he includes fuel levels as a constraint in his optimization. There are specified points on the grid defined to be refueling stations. The algorithm Tsao developed first evaluates if the vehicle has enough fuel on board in order to perform the fuel optimal route. If the vehicle would run out of fuel the route is recomputed with an obligatory stop at a fueling station within reach. The concept is illustrated in Figure 2.9, where

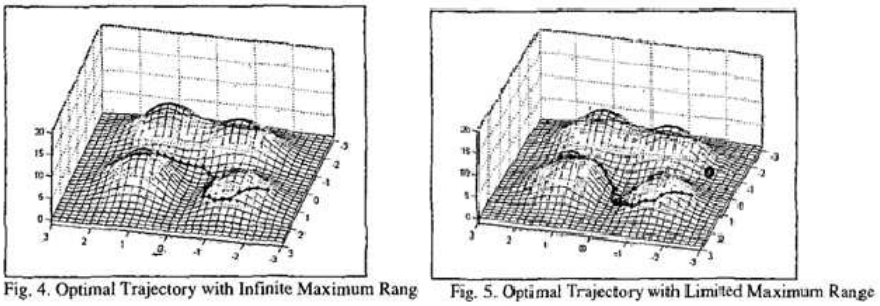

FIGURE 2.9: Complex terrain with fueling stations by Tsao [13]

the left graph shows the solution when the amount of fuel on board is not considered. The right graph presents the solution when the amount of fuel is considered and the fuel in the tank was not sufficient to perform the trip. In this solution the route is altered and the vehicle stops at a fueling station, here shown as a dot. This optimization problem can become interesting when looking at electric vehicles, where the autonomy is one of the concerns of people.

Velocity trajectory optimization was not always used to minimize fuel. In 2005 a series of three papers were published by Velenis and Tsiotras [61–63]. The work investigates velocity trajectory optimization with the goal to minimize time for a certain mission. In their research, the time a vehicle takes to drive a given route with constraints on acceleration and speed is minimized using Pontryagin's Maximum Principle. The algorithm was implemented using the receding horizon method. Test results of this strategy are shown from tests on the Silverstone F1 circuit.

In 2008 velocity profile optimization was applied to the route of a city bus. Using the predefined longitudinal profile of city buses the publication by Nouveliere [64] investigates fuel economy improvements in optimizing the velocity trajectory of a bus. Using the dynamic programming optimization approach the optimal velocity profile is found for all states in speed and distance in advance. Since a driver can not accurately follow the desired optimal velocity profile the current actual state in velocity and distance is used to update the desired optimal velocity trajectory from the precomputed result.

In the last ten years there has been a lot of research in the area of adaptive cruise control [65–68]. A cruise control in the conventional sense controls the throttle, such that the vehicle speed is constant independent of road profile. The adaptive cruise control regulates the velocity of the vehicle in a way that the

average velocity of the vehicle for a certain trip is fixed at a desired value, but the actual instantaneous velocity can vary according to the road profile with the goal that fuel economy is minimized. This strategy has been shown to have potentials in reducing fuel consumption for trucks. The problem equals the previously defined velocity trajectory optimizations in the way that it finds the velocity profile to cover a certain distance with a known grade profile keeping a desired average velocity. For implementation purposes the receding horizon method is used to simulate a final state. The optimization approaches used to solve the adaptive cruise control problem include Dynamic Programming, Pontryagin's Maximum Principle and other optimization strategies.

With the scarcity of fossil fuel hybrid vehicles have become more and more common. In 2010 Keulen published his work to show that velocity trajectory optimization can improve fuel economy of hybrid electric trucks [14, 69]. In his papers Keulen uses previous research studies to define the general shape of the optimal velocity profile. In Figure 2.10 the shape of the optimal profile used in Keulen's work can be seen. Using a predefined profile he reduces the optimization process to the search of 4 parameters, the constant velocity v_{cr}, the electric machine use during coasting P_{em}, the velocity v_d where maximum power deceleration starts and the end velocity v_e which equals the start velocity v_s of the next cyclic section. He solves the optimization using a nonlinear optimization based on Matlab's 'fmincon' command. While a lot of research has been done on energy management strategies for hybrid vehicles not many studies were published on the trajectory optimization problem for hybrid vehicles. In literature no work was found where a pure trajectory optimization problem for a manufactured hybrid vehicle is discussed. Like in Keulen's work, all studies treating hybrid vehicles approach the problem as one overall optimization where energy management is optimized together with the velocity profile. However, hybrid vehicles sold today already have a control strategy for energy management implemented. It is therefore necessary for the application in an eco driving support system to separate optimal operation of the vehicle from energy management in the drive train.

When studying trajectory optimization for road vehicles it can be helpful to investigate how trajectory optimization problems for railroad vehicles were resolved. With new drive trains, such as the hybrid and electric vehicle, the ability to recover energy will play a role in the process of finding the optimal operation. Therefore it can be interesting to look at studies treating railroad vehicles, since electric energy

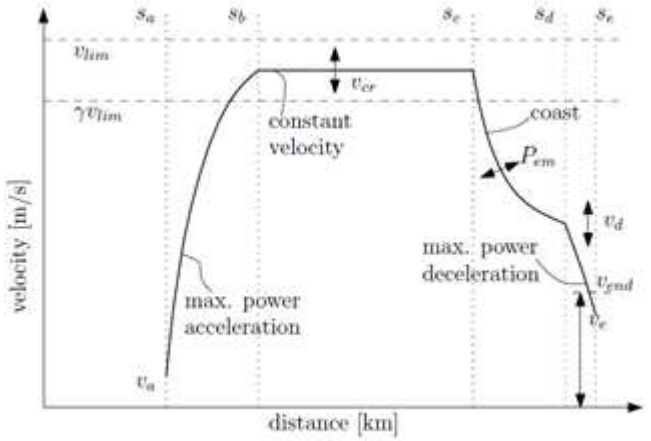

FIGURE 2.10: Predefined velocity profile by Keulen [14]

recovery has been a subject for some time in this field. With a lot of literature available on railroad vehicle optimization the following section only gives a brief overview of some interesting applications.

2.2.4 Railroad vehicles

Research on possible improvements in energy consumption for trains has started in 1968, when Ichikawa [70] published a paper in which he uses a numerical method to solve the trajectory optimization problem of a train going from one station to another in a fixed time. He does not quantize his reductions in energy consumption, but rather sees his work as a motivation for a growing research in this field that would help save a large amount of energy in transportation.

Following this publication, as desired by Ichikawa, research in train velocity profile optimization grew. Starting in the 1980s there were two main research teams starting to investigate the advantages of velocity profile optimization. Golovitcher [71], first in Russia later in the US, discusses the optimization issue in his publications between 1982 and 2003, while Howlett's group [15, 72] in Australia published on the same matter between 1980 and 2009. Both use Pontryagin's Maximum Principle to solve the problem. Golovitcher finds that optimal control has to be a combination of 5 states, namely: FB (full braking), PB (partial braking), C (coast), PP (partial power), FP (full power). Howlett [15, 72] on the other hand identifies the optimal control for a track without slope to consist of the sequence power, hold, coast, brake. Dependent on the desired final time the length of the coast phase changes. In Figure 2.11 various optimal velocity trajectories to drive

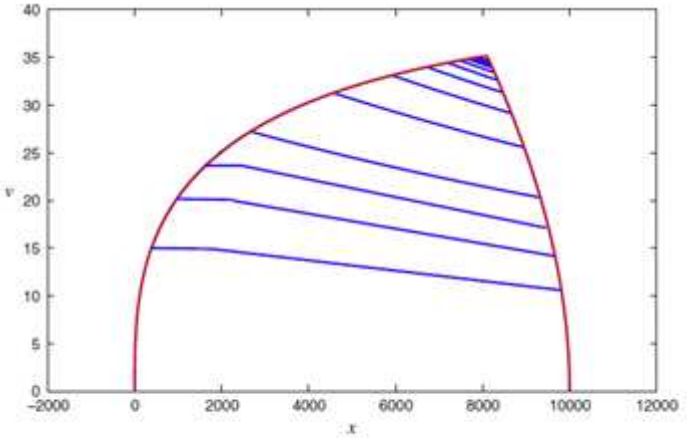

Fig. 1. The minimum time *power-brake* journey on flat track and various longer time journeys using *power-coast-brake* and *power-hold-coast-brake*.

FIGURE 2.11: Velocity Profiles for Various Time Constraints by Howlett [15]

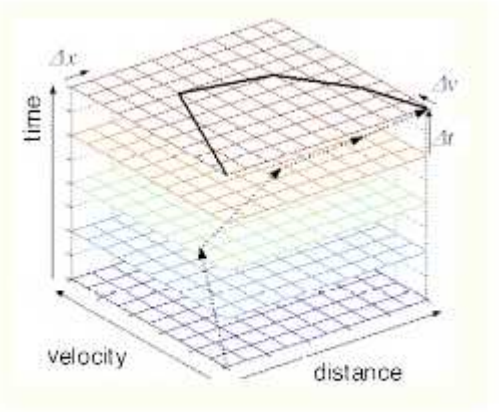

Fig. 3: Trajectory of train running profile in state space.

FIGURE 2.12: 3 dimensional Dynamic Programming by Miyatake [16]

a distance of 10000m for desired final times can be seen. In red here the velocity profile chosen if time is supposed to be minimized.

While both of their initial works were on trains without energy regeneration after 1990 their simulations included energy recuperation of the electric locomotive.

Since 2004 Miyatake [16, 73] published several papers on optimization of velocity profiles of trains. In his analysis he uses a dynamic programming approach in a three dimensional way, as seen in Figure 2.12. This gave him more freedom to introduce constraint and his work shows that several factors, e. g. the internal resistance of the capacitor, have effects on the results.

2.2.5 Conclusion

In Table 2.2 an overview of representative trajectory optimization methods applied to calculate best road and railroad vehicle operation is presented. Studying the table it becomes obvious that the Pontryagin's minimum principle and the dynamic programming optimization method are the commonly used methods to resolve these problems. It seems that there exists a relationship between model complexity and optimization method. Generally, the Pontryagin's minimum principle is applied in cases where the considered problem is rather simple. When complex, detailed models of the system are used and various constraints are to be integrated, commonly the dynamic programming method is applied. The computational cost is therefore higher, but the method allows us to easily integrate complex constraints.

2.3 Conclusion

We can conclude from this literature review that eco driving represents a good way to reduce energy consumption for the transportation sector. However, effective driver support systems are necessary to guide and remind the driver about the optimal operation of the vehicle.

It has been shown that there are several informative and advisory driver support systems that can be used to reduce energy consumption. While most systems transmit information using the visual way, there are some approaches where advice is given the auditory way or with the use of haptic devices. Advanced driver assist systems that use detailed vehicle and trip information to transmit computed best vehicle operation to the driver, have been investigated. More complex systems are able to give detailed information to the driver, but, to do so, they need to be provided with more specific information. A major difficulty with ADAS systems seems the design of an appropriate human machine interface (HMI), which is critical for the effectiveness of the system. A second important aspect of an ADAS system is the evaluation of best vehicle operation.

Generally the appropriate vehicle operation is determined in one of two ways. Most driver assist systems studied in literature used a rule based algorithm. This way best vehicle operation is determined dependent on an identified vehicle state. Rule

application	study	modeling	optimization method	optimization problem
conv. vehicle	Schwarzkopf (1977)	simple polynomial	Pontryagin's min. principle	acceleration to speed v; driving over hills
conv. vehicle	Hooker (1983)	accurate experimental date fuel(v,a)	3D dynamic programming	optimal cruising speed; acceleration to v; driving between 2 stops; driving over hills
conv. vehicle	Monastyrsky (1993)	experimental data	2D dynamic programming with weighting	as above
conv. vehicle	Stoicescu (1995)	polynomial	Pontryagin's min. principle	any combination of problem with time, distance and cost
fuel cell elec. vehicle	Guzzela (2003)	polynomial	Pontryagin's min. principle	fuel cell vehicle, cyclic trip
conv. vehicle	Tsao (2003)	simple model	dynamic programming	complex terrain with refueling
conv. vehicle	Velenis (2005)	-	semi-analytic, intuitive optimal profile	time optimal trajectory for formula 1
city bus	Nouveliere (2008)	dynamic drive train model	dynamic programming	route of bus
conv. vehicle	Hellstroem and others (2009-2010)	dynamic model, detailed model	dynamic programming, Pontryagin's min. principle, others	adaptive cruise control
hybrid vehicle	Keulen (2010)	polynomial	predefined shape of speed profile, parameter evaluation	hybrid vehicle energy management and velocity profile
railroad vehicle	Ichikawa (1968)	-	-	station to station
railroad vehicle	Golovitcher, Howlett (1980-2009)	energy consumed, no vehicle model	Pontryagin's min. principle	station to station, later with energy recovery
railroad vehicle	Miyatake (2004)	detailed model (effect of resistance of capacitors analyzed)	dynamic programming	effects of components on consumption

TABLE 2.2: Overview of trajectory optimization studies to reduce energy consumption

based algorithms can only determine sub-optimal vehicle operation since no global optimization is performed. A second way, which usually results in more accurate results, is to use a vehicle model and numerical optimization methods to determine fuel minimizing operation. In this second case the accuracy of the optimal velocity profile depends on the correspondence of the model to the actual system. In general, optimization methods applied to trajectory optimization problems are the dynamic programming method or the Pontryagin's Maximum Principle. While the dynamic programming method is usually more costly in computational effort, complex system models and constraints are easily implemented. The Pontryagin's Maximum Principle, being based on Calculus of Variation, is a fast calculation, but is not trivial to be used with complex cost functions and problems with constraints. With this approach it is often difficult to capture all loss phenomena of the system.

To complement existing studies this thesis work investigates three main areas. First, we want to determine potential gains of eco driving by identifying drive train specific optimal vehicle operation. Secondly, we will evaluate the effects of constraints on potential gains and optimal vehicle operation. Finally this work proposes a way to integrate numerical optimization algorithms in the development of an effective driver support system.

Eco driving is well known to reduce fuel consumption for conventional vehicles. While the operation of the traditional car might be somewhat intuitive for a driver, the efficient operation of new technology drive trains can be a challenge. Integrating physical vehicle models, in this work we want to develop optimization algorithms that can be applied to any vehicle drive train on the market today, no matter its complexity. With this the optimal operation can be identified in a vehicle specific way. A comparison of best vehicle operation can lead to insights about importance of modeling details. To what level is it necessary to include detailed modeling in the fuel minimization process?

To predict maximum potential of eco driving, trajectory optimization techniques will be applied, together with a detailed vehicle model, to a specified trip. With this, we will not concentrate on certain driving scenarios, such as 'driving over hills', or optimal acceleration, but rather identify the globally optimal velocity trajectory for a given trip. So called eco cycles are computed for corresponding original drive cycles. Doing so, we assume that a priori trip information, about initial and final vehicle speed and distance is given. In addition, we hypothesize that maximum speed limits on the driven roads, road grade and stops are known

in advance. In this work, trip time is considered as a given trip constraints. With this definition we can say that eco driving does not create any disadvantages for the driver. Computed potential gains are therefore solely due to changes in vehicle operation and not due to a decrease in average vehicle speed.

While most work on eco driving assumes optimal conditions this thesis shows an approach to determine more realistic vehicle operation by integration of constraints. Initially maximum potential gains are identified considering trip and road constraints, such as speed limits. This can help to identify an upper limit for possible fuel savings. However, it does not give realistic approximations of realistically reachable consumption. In this work we will evaluate the effects of traffic on potential fuel savings due to eco driving.

Another constraint that should be considered when eco driving strategies are computed are environmental constraints. While most work presents eco driving as a solution to environmental problems in the transportation sector, emission constraints were never integrated. With this thesis we aim to evaluate economic and ecologic aspects of eco driving. An approach to integrate emission constraints in eco driving optimization algorithms is proposed.

Our literature review showed that several driver support systems for eco driving exist. While the algorithms integrated in advisory systems are usually simple, we can find many works on trajectory optimization for road vehicles. In our work we want to combine the theoretical work with an implementation in a handy advanced driver assist system. With the development of a practical human machine interface we present an approach to integrate complex optimization algorithms in a driver support system.

To summarize, the original contributions of this work are:

- Potential gains of eco-driving are determined with use of physical vehicle models (conventional, electric and hybrid vehicle) at required level of detail
- Eco-driving considered without disadvantage in arrival time: Constraint of trip time is taken into account and discussed
- Potential gains of eco-driving are identified while taking into account limitations due to traffic

- Potential gains of eco-driving are identified while considering the influence of pollution emissions
- Development of a Human Machine Interface with continuous online advice and educational trip report

Chapter 3

Vehicle Modeling

Contents

With the development of powerful computers, simulations have become an important part of engineering work. Using models of complex systems, their behavior in all kinds of situations can be simulated. System simulations can never exactly predict the response of the physical system and to verify, the real systems

should always be tested. However, working with models can have many advantages. While simulation models are built faster and with less cost than most real world prototypes, the effects of component changes in complex systems is easily tested. In a system's development process a model is often used to predict its real operation. In our case, we construct a simulation model to predict consumption for specific vehicle operation. A macroscopic model to predict energy consumption is used.

In this chapter we will construct the vehicle models for the conventional, electric and hybrid vehicle drive trains. For optimization purposes an inverse modeling approach is applied. In Section 3.1 the advantages of inverse modeling versus direct modeling are discussed. The modeling of a vehicle's chassis is presented in Section 3.2. Detailed drive train models of the conventional, electric and hybrid vehicle can be found in Section 3.3-3.5. To verify simulated energy consumption values a direct modeling software VEHLIB was used. The modular software is introduced in Section 3.6.

3.1 Direct and inverse modeling

To simulate dynamic systems there are two different modeling approaches that can be applied. Using direct modeling the system is modeled with its natural input, following the energetic flow, to the output. Inverse modeling is what we call a model, where the inputs and outputs of the system are inverted. This means that we assume an output, back-calculate component operation opposed to the energy flow, to identify the required input.

Figure 3.1 shows the difference between the two modeling approaches for the specific case of a road vehicle. In the upper graph the direct modeling method can be seen. The driver specifies the inputs to the system, which are accelerator pedal, brake pedal, possibly clutch and gear, and auxiliary use. With these inputs the drive train operation can be computed, and the drive torque propelling the vehicle is determined. The output of the model is a resulting vehicle speed and acceleration.

In the inverse modeling approach a desired vehicle operation is specified as input. The chassis and drive train component operation is back calculated to identify the necessary power output from each component. In a conventional vehicle, for

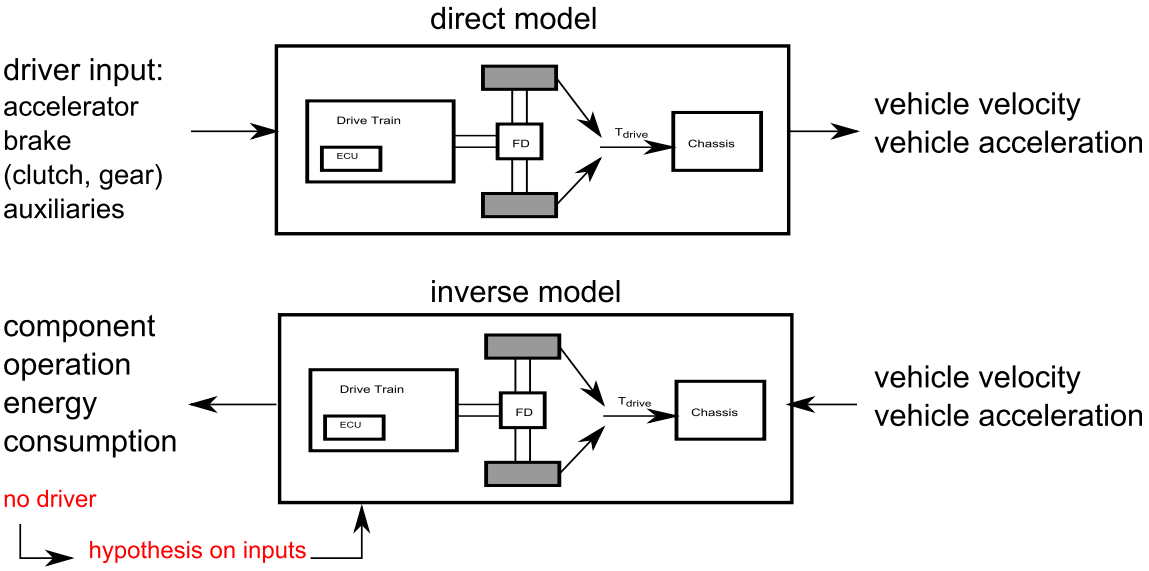

FIGURE 3.1: Direct versus inverse modeling

example, the engine operating point is computed; in an electric vehicle the electric machine operation is calculated. With this the energy consumption of the vehicle can be computed for a given vehicle operation.

An advantage of inverse modeling is to eliminate the human driver in the computation process. Component operation can be computed for an exact vehicle operation without uncertainties due to the human driver behavior (driver feedback that enables a specified profile to be tracked). However, in order to uniquely specify system operation it is often necessary to make several hypotheses on some control variables. For the conventional vehicle a driver usually specifies acceleration, friction braking, clutch and gear selection. In the process of inversion the necessary engine and brake inputs are easily identified. In our approach hypotheses were defined in order to specify clutch and gear operation. Since the goal of this study is to determine energy efficient vehicle operation, the engaged gear was specified such that fuel consumption was minimized. The clutch was assumed to be fully engaged, unless the shaft output speed dropped below idle. In this case minimum engine speed was defined to be engine idling speed, and the clutch is slipping.

The electric vehicle seems to be the simplest of the three drive train systems for inversion. Since no gear box and clutch exist in the drive train, it is unnecessary to make hypotheses. The electric motor and mechanical brake operations can be determined given the vehicle operation. In the case of the hybrid vehicle the operation of several power sources have to be computed, given vehicle operation.

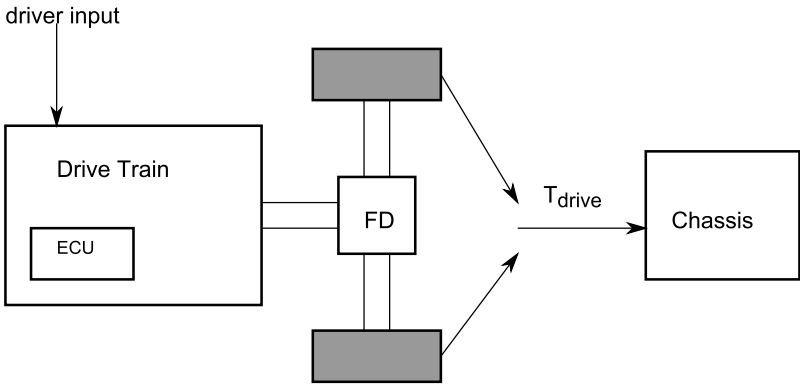

FIGURE 3.2: Vehicle modeling

Although the driver only specifies acceleration and braking the inversion process of this vehicle drive train is not trivial. The operation of the vehicle is usually determined by the electronic control unit (ECU), which uses the driver inputs as well as battery state of charge. In a model inversion we need to assume that battery state-of-charge is known downstream from the ECU at the drive train output. This is necessary to identify the correct power split and to compute the appropriate component operation. The inverted hybrid vehicle model is presented in detail in Section 3.5.

Another input that is common for all vehicle drive trains is the auxiliary power, which depends on the driver's use of vehicle accessories, such as radio, lights, and others. In our work a constant auxiliary output power was specified in the inversion process:

$$P_{aux} = 300W \tag{3.1}$$

In Figure 3.2 a generalized schematic of a vehicle's drive train can be seen. We can see that, generally, the driver input is used in the drive train to determine component operation. The drive train then transmits the drive torque to the wheels, where it is used to propel the vehicle chassis through the road contact. In the following a general model of a vehicle chassis will be constructed. The detailed, inversion based model of the drive train for each vehicle type will be discussed in Sections 3.3-3.5.

3.2 Vehicle chassis modeling

Constructing an inversion based chassis model, the goal is to determine the necessary drive train output torque T_{drive} as a function of specified vehicle speed v and acceleration a. In the following we will proceed to construct a direct chassis model which will be inverted.

3.2.1 Dynamics of chassis

The motion of the chassis is a result of the forces acting on it. In our work only longitudinal forces are considered in order to determine the vehicle's longitudinal motion. Using Newton's second law we can write

$$M_{veh_x} a_x = \sum F_x \tag{3.2}$$

$$= F_{drive} - F_{res} \tag{3.3}$$

where $M_{veh_x} \neq M_{veh}$ is a lumped parameter representing the mass that is to be accelerated, $a_x = a$ specifies the vehicle's longitudinal acceleration and F_x the sum of forces along the longitudinal axis. The drive force F_{drive}, generated by the vehicle's drive train, is used to propel the vehicle and to overcome the resistance forces F_{res}, that are generally opposing the direction of motion. In this energetic model no slipping of the wheel, on the contact patch between road and tire, is considered. With this hypothesis we can define a relationship between vehicle motion and wheel rotational speed ω_{wheel} using the tire radius R_{tire}:

$$\omega_{wheel} = \frac{v}{R_{tire}} \tag{3.4}$$

$$\dot{\omega}_{wheel} = \frac{a}{R_{tire}} \tag{3.5}$$

The inertia to be accelerated can be described by a lumped parameter, considering vehicle weight and wheel inertias:

$$J_{veh} = M_{veh} R_{tire}^2 + 2 J_{tire} \tag{3.6}$$

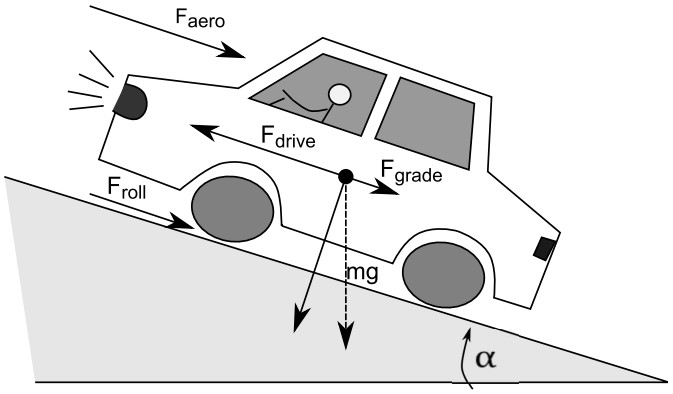

FIGURE 3.3: Resistance forces acting on chassis

With Equation 3.4-3.6 we can now rewrite Equation 3.3 by

$$J_{veh}\dot{\omega}_{wheel} = T_{drive} - F_{res}R_{tire} \tag{3.7}$$

where T_{drive} specifies the drive train output torque, which is positive in the acceleration phase and negative when braking. Inverting Equation 3.7 and assuming that there is no slipping between the tire and the road (Equation 3.4-3.5) the drive torque required for a given vehicle speed and acceleration can be determined by

$$\begin{aligned} T_{drive} &= f(v,a) && (3.8)\\ &= J_{veh}\frac{a}{R_{tire}} + F_{res}(v)R_{tire} && (3.9) \end{aligned}$$

where the resistance forces F_{res} depend on the vehicle speed and can be computed as a sum of rolling resistance, aerodynamic drag and road grade.

3.2.2 Resistance forces

In Figure 3.3 a vehicle chassis driving on a non-flat road can be seen. The schema shows the resistance forces due to rolling resistance, aerodynamic drag and road grade on the chassis.

Rolling resistance is a force that exists due to the deformation process of the tire between the vehicle and the road. Although it depends on many parameters, such as the tire pressure, tire wearing and road quality, it is generally approximated by

$$F_{roll} = C_r M_{veh} g cos(\alpha) \tag{3.10}$$

with C_r, the coefficient of rolling resistance, which is dependent on vehicle load and wheel radius. g represents the gravitational constant and M_{veh} the vehicle's mass including the chassis, drive train, engine and passengers. On a non-flat road the road grade α has to be taken into account in the computation of rolling resistance because the downward force due to gravity is not orthogonal to the road surface. The rolling resistance is independent of the vehicle operation and can therefore not be influenced by the driver throughout a trip. However, it is obvious that it changes with the vehicle's load. Reducing vehicle weight will reduce the energy needed to overcome rolling resistance. The vehicle's weight, however, influences the maximum force that can be transmitted by the wheels to the vehicle.

The aerodynamic drag is a force that manufacturers are often trying to reduce with aerodynamic vehicle designs. The aerodynamic drag is dependent on air density ρ, the vehicle's drag coefficient C_d, and the vehicle's frontal surface A. Given the vehicle speed the force can be computed by

$$F_{aero} = \frac{1}{2} \rho C_d A v^2 \tag{3.11}$$

In Figure 3.4 the power due to aerodynamic drag for various speeds can be seen for different vehicles [74]. Dependent on the vehicle's shape the drag coefficient changes. In this graph four different types of chassis are plotted for comparison. For example the aerodynamic drag coefficient of a Hummer H2 truck lies at 0.57, while a station wagon, like the Audi A5, only has a drag coefficient of 0.33. A very aerodynamic vehicle, like the Volkswagen XL1 can have an aerodynamic drag coefficient of 0.19 [75]. Changing the shape of the vehicle, automotive engineers can improve the drag coefficient and therefore reduce energy consumption of the vehicle. However, much larger savings in energy can be made by reducing the vehicle's operating speed. From Figure 3.4 it can be seen that aerodynamic drag grows quadratically with speed. Particularly at high speeds it becomes obvious that by a small reduction in vehicle velocity large amounts in energy can be saved.

When driving on hilly roads the force due to road grade has to be taken into account when modeling the vehicle chassis. When driving on a road with slope α_{road} the resistance force due to grade is calculated by

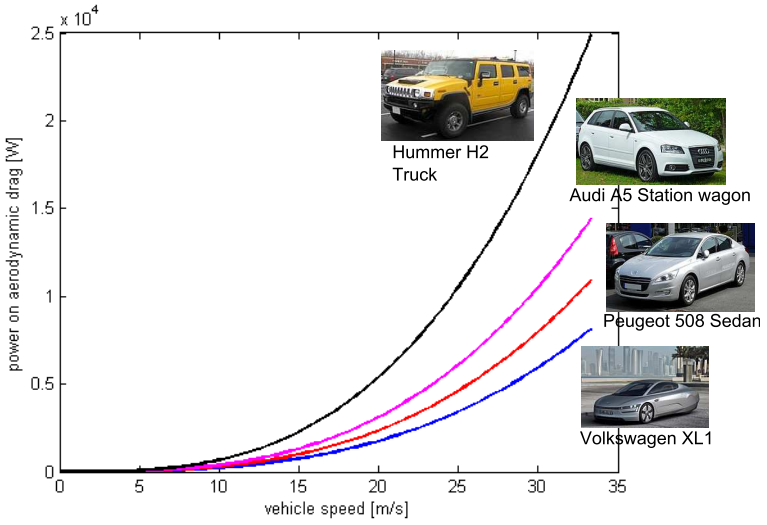

FIGURE 3.4: Aerodynamic drag for different vehicle chassis

$$F_{grade} = M_{veh} g sin(\alpha_{road}) \tag{3.12}$$

Naturally the grade resistance force acts as an accelerating force on downhill roads and slows the vehicle down on uphill sections. In order to reduce overall energy consumption for a trip it is expected that reducing vehicle speed on uphill sections and accelerating on the downhill parts and therefore converting the potential energy in kinetic energy, would be optimal.

3.3 Conventional vehicle

In this thesis gains of eco driving for passenger vehicles are discussed. A small conventional passenger vehicle was therefore chosen for modeling and testing. In Figure 3.5 the 308 vehicle model from the French manufacturer PSA Peugeot Citroen [1] can be seen. The vehicle has a weight of 1470kg. For modeling purposes the vehicle was separated in two parts: the chassis and the drive train. The chassis can be modeled as presented in Section 3.2, such that the drive train output torque is calculated as a function of vehicle speed and acceleration. In the following the inverse drive train model of the conventional vehicle is outlined.

[1] PSA Peugeot Citroen http://www.psa-peugeot-citroen.com/

FIGURE 3.5: The Peugeot 308 Vehicle

3.3.1 Drive train modeling

The drive train of the Peugeot 308 can be seen in Figure 3.6. Its major components are the wheels, a differential, the gear box, a clutch and the internal combustion engine. In this work no dynamics of the mechanical drive shaft are considered. The hypotheses made in order to uniquely define the operation of each drive train component are:

- Instantaneous gear engagement
- No losses in clutch unless shaft speed below idle
- Constant auxiliary power

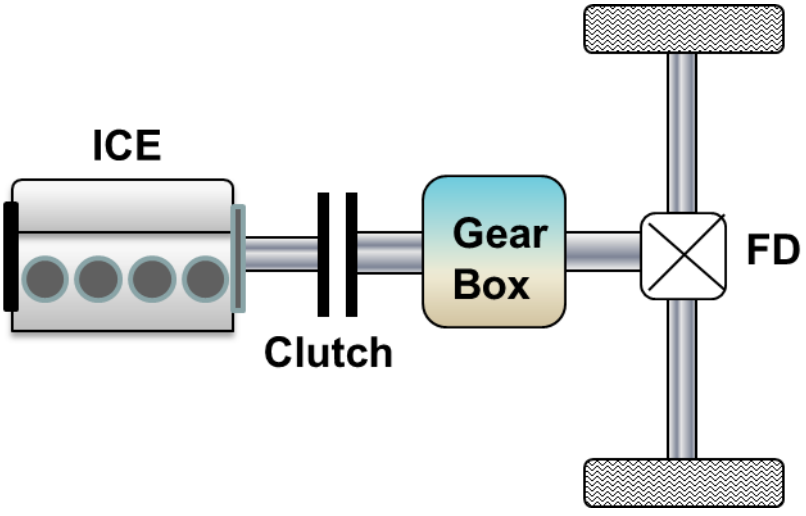

FIGURE 3.6: The Conventional Vehicle Drive Train

With these assumptions the speed of the engine output shaft ω_{eng} can be deduced from the wheel speed ω_{wheel} by

$$\omega_{eng} = max(\omega_{eng-idle}, \omega_{wheel} * R_{FD} * R_G(i_{gear})) \tag{3.13}$$

where $\omega_{eng-idle}$ specifies the engine idle speed and R_{FD} and $R_G(i_{gear})$ define the ratio of the final drive and the selected gear. Power losses exist in the clutch when the clutch plate is slipping. Simulating the efficiency of the final drive η_{FD} and the selected gear $\eta_{G(i_{gear})}$, the drive train output torque can be translated to the engine output shaft by:

$$T_{drive_{eng}} = \frac{T_{drive}}{R_{FD}\eta_{FD}^{\psi} R_G(i_{gear})\eta_G^{\psi}(i_{gear})} \tag{3.14}$$

Here η_G and η_{FD} are the efficiencies of the gear ratio R_G and final drive reduction ratio R_{FD}. The efficiency of the differential is assumed to be constant with respect to speed and torque. A unique efficiency $\eta_G(i_{gear})$ for each gear is fixed. Each gear's efficiency is assumed to stay constant for the entire range of operating speed and torque. The parameters ψ depends on the energy flow and is defined by

$$\psi = \begin{cases} 1 & \text{if } T_{drive} \text{ is positive} \\ -1 & \text{if } T_{drive} \text{ is negative} \end{cases}$$

The dynamics of the internal combustion engine can be described with

$$J_{eng}\dot{\omega}_{eng} = T_{eng} - T_{drive_{eng}} - T_{aux} \tag{3.15}$$

The load torque due to the auxiliaries is simply determined by $T_{aux} = \frac{P_{aux}}{\omega_{eng}}$. Inverting Equation 3.15 the engine torque can be computed as a function of wheel torque

$$T_{eng} = \frac{T_{drive}}{R_{FD}\eta_{FD}^{\psi} R_G(i_{gear})\eta_G^{\psi}(i_{gear})} + \frac{P_{aux}}{\omega_{eng}} + J_{eng}\dot{\omega}_{eng} \tag{3.16}$$

3.3.2 Engine modeling

The engine that was integrated in the Peugeot 308 passenger vehicle is the, by Peugeot and BMW developed, EP6 engine. It is a 1.6L gasoline engine that can provide a maximum torque of 160Nm at 4250rpm and reaches its maximum output power of 88kW at 6000rpm. The engine is modeled using an engine consumption map, which was previously identified experimentally on an engine test bench. A graph of the engine specific fuel consumption can be seen in Figure 3.7. In this graph the upper, blue line shows the maximum torque that the engine can provide for a given speed. When injection is cut and the vehicle is 'driving' the engine, the engine output torque is negative. The engine minimum torque is shown as a blue dashed line.

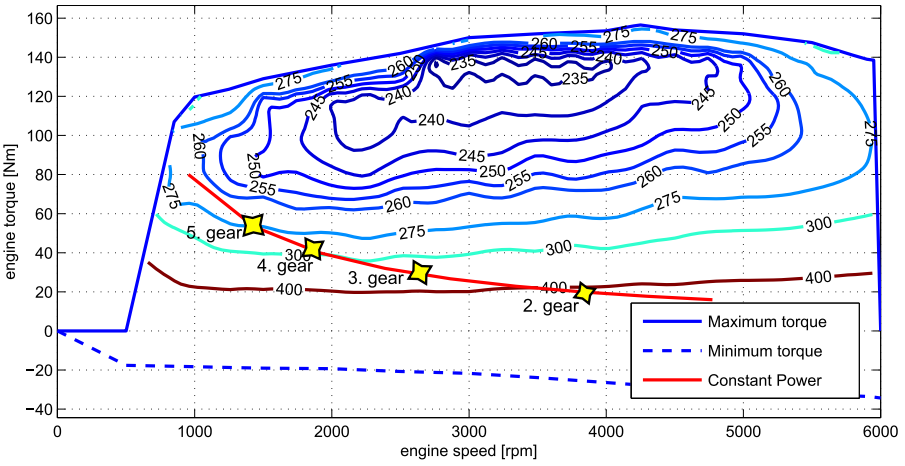

FIGURE 3.7: Engine Specific Consumption in g/kWh

In Figure 3.7 the specific consumption is shown in g/kWh. In red a constant power line is drawn for an engine output of 8kW. It can be seen that for equal power output the fuel consumption can be very different. Providing 8kW at 4000rpm the engine consumes a lot more fuel per kWh than when supplying it at 1000rpm. The engine's combustion process is most efficient at low speeds and at close to maximum torque.

In conventional vehicles the driver can influence the point of operation of the engine with the gear choice. While hybrid vehicles or continuous variable transmissions can push the engine operating point to its optimal, the manual 5-speed transmission gives only a discreet choice of engine operations. Operating a vehicle in the appropriate gear gives the driver an immediate way to reduce fuel consumption.

In Figure 3.7 the engine operating point for gear 2 to 4 were plotted for a vehicle speed of $50km/h$ and an acceleration of $0.2m/s^2$. It can be seen that if the driver chooses to operate the vehicle in 2nd gear the engine consumes around 400g of fuel per kWh. However, when a higher gear is engaged the fuel consumption of the vehicle for the same velocity and acceleration is lower. In third gear only about 350g and in 4th and 5th less than 300g per kWh is needed. To eliminate driver input for gear choice, we assume in this work that an eco driver will always want to choose the most efficient gear. After calculating the fuel consumption for all five gears the optimal gear, which means the one with minimal fuel consumption, is therefore chosen. With this the instantaneous fuel consumption of a conventional vehicle can be computed as a function of vehicle speed and acceleration by

$$\dot{m}_{fuel} = \min_{i_{gear}} \dot{m}_{fuel}(T_{eng}(i_{gear}), \omega_{eng}(i_{gear})) \tag{3.17}$$

$$= f(v, a) \tag{3.18}$$

3.4 Electric vehicle

In the last years electric vehicles have become more and more popular. There are now several car manufacturers that have electric vehicles on the market. The electric vehicle has gained in popularity due to its flexibility in energy source. While conventional vehicles commonly only use non-renewable fossil fuels the electricity used as energy source in this drive train can be generated from several different, renewable or non-renewable, sources.

The electric vehicle presented here is a test vehicle used at the IFSTTAR laboratory. The electric Mega City produced by AIXAM [2] can be seen in Figure 3.8. The vehicle is a small vehicle with a weight of 750kg. Identifying the appropriate rolling resistance coefficient and drag coefficient the vehicle's chassis can be modeled as described in Section 3.2. Given the vehicle operation in speed and acceleration the drive train torque is computed. In the following the model for the electric drive train is derived.

[2] AIXAM http://www.aixam.com/

FIGURE 3.8: The AIXAM electric vehicle

3.4.1 Drive train modeling

The drive train configuration of the AIXAM Mega City can be seen in Figure 3.9. The drive train is made up of the final drive and the electric motor/generator, which is coupled by the converter to the battery. Due to the characteristics of the electric motor, which can provide high torque at very low speeds, there is no need for a gear box. A gear box could be integrated in an electric vehicle to enable shifting the operating point of the electric motor into more efficient regions. In this work, a simple electric drive train architecture is investigated and the possibility of a gear box will not be considered in the following.

The Mega's drive train contains 12 lead acid battery packs. The battery, that has a nominal capacity of 76 Ah, weighs around 350kg. The vehicle is driven by a continuous current, separately excited, electric motor. The motor reaches its maximum output power of 14kW at 3000rpm. It can provide a maximum torque of 60Nm.

Given the vehicle's wheel speed ω_{wheel} and the drive torque at the wheels T_{drive}, the operation of the electric motor output shaft is computed by

$$\omega_{EM} = \omega_{wheel} R_{FD} \tag{3.19}$$

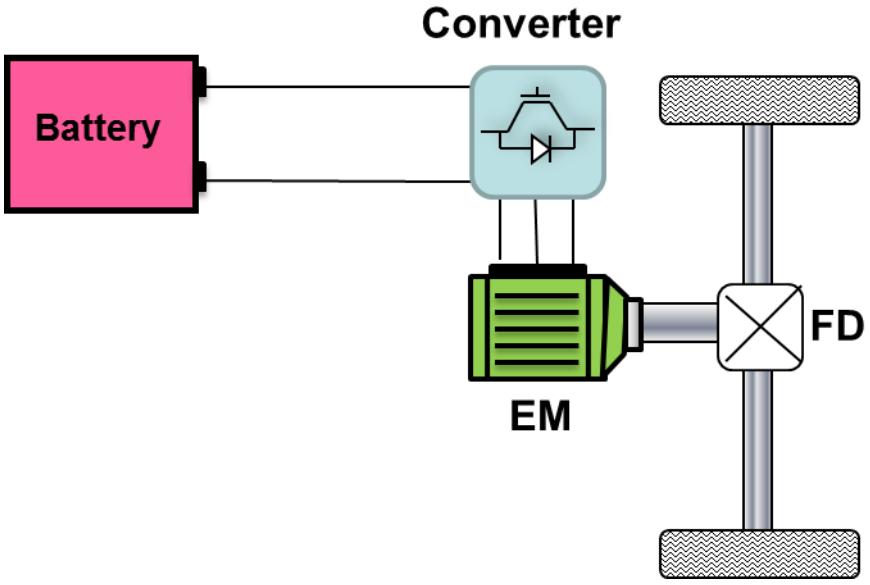

FIGURE 3.9: The Electric Vehicle Drive Train

$$T_{drive_{EM}} = \frac{T_{drive}}{R_{FD}\eta_{FD}^{\psi}} \tag{3.20}$$

where η_{FD} defines the efficiency of the differential with ratio R_{FD}. ψ is defined by

$$\psi = \begin{cases} 1 & \text{if } T_{drive} \text{ is positive} \\ -1 & \text{if } T_{drive} \text{ is negative} \end{cases}$$

The dynamics of the electric machine can be described by

$$J_{EM}\dot{\omega}_{EM} = T_{drive} - T_{drive_{EM}} \tag{3.21}$$

where J_{EM} defines the inertia of the electric motor. Without any further assumptions we can now invert the vehicle model, using Equation 3.19-3.21, to compute the torque of the electric motor as a function of drive torque necessary for a specified vehicle operation.

$$T_{EM} = \frac{T_{drive}}{R_{FD}\eta_{FD}^{\psi}} - J_{EM}\dot{\omega_{wheel}}R_{FD} \tag{3.22}$$

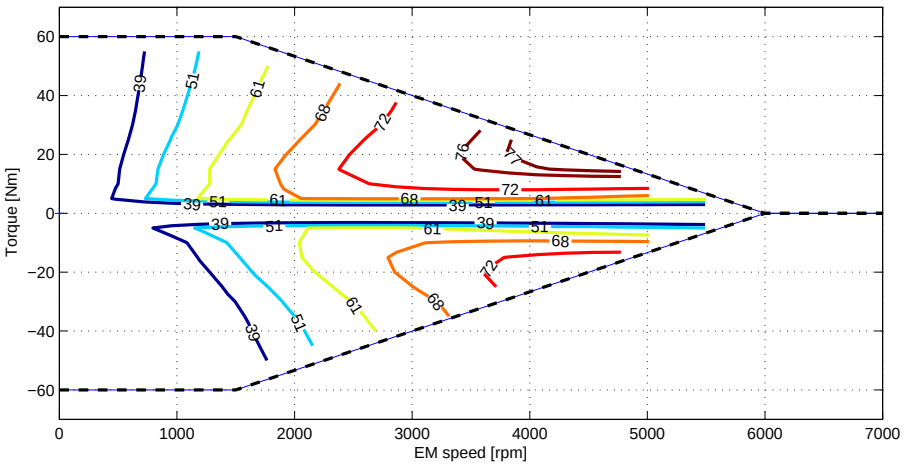

FIGURE 3.10: Efficiency map of electric motor

3.4.2 Modeling of electric components

The efficiency of the electric motor and the converter are simulated combined, with an experimentally identified loss map. The efficiency of the motor/converter unit in dependency of operating speed and torque can be seen in Figure 3.10. The upper and lower blue lines mark the maximum and minimum torque envelope. It can be seen that the functionality of this electric drive unit is very different to that of an internal combustion engine. While an engine cannot provide torque at low speed and in fact will turn off if speed drops too low below idle, the electric motor can provide its maximum torque at low speeds. In comparison, the gasoline engine, where the efficiency lies below 34%, the electric motor can reach up to almost 80%. While the thermal engine reaches high efficiencies at high torque, low speed ranges, the electric motor operation is optimized in the higher speed area.

Using a loss look-up table, the power losses of the electric motor P_{lossEM} can be computed as a function of torque and speed using interpolation methods. The driver is assumed to consume constant auxiliary power defined by P_{aux}. The demanded battery output power can now be calculated by:

$$P_{battout} = T_{EM}\omega_{EM} + P_{lossEM} + P_{aux} \tag{3.23}$$

The battery is modeled with a simple electric circuit, as presented in Figure 3.11. The battery is represented by a resistor in addition to an open circuit voltage.

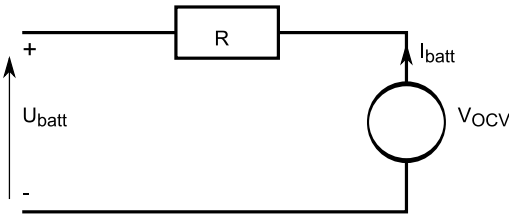

FIGURE 3.11: Simple battery circuit

The battery's resistance usually changes dependent on its operation (charging/discharging) and on the battery state-of-charge. However, while the changes in resistance due to change in SOC happen only in the low state-of-charge range, the resistance stays almost constant over 70% of the battery operating range. We therefore only consider resistance changes due to operating mode. Commonly a lower resistance is assumed for charging than for discharging.

Given the battery state-of-charge the open-circuit-voltage (V_{OCV}) and the resistance (R) can be evaluated by interpolation over battery specific data. The battery current (I_{batt}) and battery output voltage (U_{batt}) are computed using the following relationships:

$$\begin{aligned} P_{battout} &= V_{OCV} I_{batt} - I_{batt}^2 R && (3.24) \\ &= U_{batt} I_{batt} && (3.25) \end{aligned}$$

where U_{batt} is the battery output voltage and I_{batt} is the battery current. The battery power used can then be computed by

$$P_{batt} = V_{OCV} I_{batt} \tag{3.26}$$

Given the faradaic efficiency (η_{far}) and the nominal capacity of the battery C_{ah}, the instantaneous consumption of battery charge ΔSOC can be computed by

$$\Delta SOC = -\eta_{far} \frac{I_{batt}/3600\Delta t}{C_{ah}/100} \tag{3.27}$$

Given the vehicle velocity and acceleration, Equations 3.4-3.12 together with Equations 3.19-3.26 can be used to calculate the instantaneous power output from the battery for the specific electric vehicle:

$$P_{batt} = f(v, a) \tag{3.28}$$

In the electric drive train the operation of the electric motor/generator is reversible. With this the kinetic energy of the vehicle can be used to charge the battery when braking. Some electric vehicles use so-called regenerative brake pedals. In such vehicles the electric generator is used to apply a negative torque on the wheels when braking. Due to safety restrictions it is not allowed to replace the entire friction brake system with electric, regenerative braking. Therefore, using a regenerative brake pedal, implies that a control strategy is implemented to specify mechanical and electric braking. A simpler approach, where no regenerative brake pedal is used is therefore often implemented. While using the brake pedal only for mechanical friction braking, these vehicles simulate an electric 'engine braking' as in conventional vehicles. When taking the foot off of the accelerator pedal a load is simulated by applying a negative torque on the wheels through the electric generator. In the here considered electric vehicle a constant electric braking torque of 17Nm is applied when the vehicle is in coasting. With this, the vehicle has a low deceleration rate which is used to recover energy. However, once the driver steps on the brake pedal the friction brake is applied and energy is lost in heat.

The flexibility in energy source and the ability to recover kinetic energy are advantages of the electric drive trains in comparison with the conventional vehicles, where the combustion process is not reversible. However, driving an electric vehicle also comes with disadvantages. First of all, obviously energy is still necessary to operate the vehicle. And while the number of vehicles is growing and researchers are searching for alternative, renewable energy sources, the amount of energy used to drive electric vehicles should not be neglected and/or wasted. Nevertheless, the major disadvantage of the electric vehicle is its autonomy and charging time.

A simple comparison: In general a passenger vehicle has a fuel tank of abound 50L. Gasoline fuel weighs around 720g per L. A compact passenger car can usually be driven on about 6-7L/100km. With this a conventional car has a range of 700-800km per tank that initially weighs 36kg and can be refilled at any of numerous gas stations in a few minutes.

For the case of an electric vehicle recent technologies are using lithium ion batteries, which can have an energy density of up to 200Wh/kg. The Renault Zoe [3] electric vehicle is a small passenger car that has recently been released. While the vehicle's range on the standard test cycle (NEDC) is 210km, Renault announces a range of 100-150km dependent on utilization [76] for the 22kWh lithium ion battery pack. The battery, weighing around 300kg, therefore gives the driver a driving range around 5 times smaller than the gasoline vehicle for a weight 6 times the fuel tank. In addition, electric vehicles have to carry the dead weight of an empty battery since its weight is not reduced when discharged. While the range is smaller for the electric vehicle the charging can take anywhere from 1-8h for a full charge.

It can be seen that, when using electric vehicles, energy consumption can become a very important factor. It is therefore important to identify the most efficient operation of the particular vehicle. Eco driving with electric vehicles can minimize energy consumption in order to maximize the vehicle's operating range.

3.5 Hybrid Vehicle

The hybrid vehicle has become a popular solution for manufacturers to meet higher fuel consumption and emission standards. By definition, a hybrid vehicle is a vehicle that contains two or more power sources. The solutions on the market today combine the internal combustion engine with an alternative power source like a flywheel, a hydraulic accumulator, an electric battery or a fuel cell.

The flywheel stores energy in the kinetic energy of a mass spinning at high speed. This energy can be reused to boost the vehicle in the acceleration phase. This system is used in the Formula 1 to improve the vehicle performance [77]. When the alternative power is provided by a hydraulic system the energy recovered is stored in the compressed gas of an accumulator. The hydraulic hybrid solution is commonly used on heavy applications such as refuse trucks [78] or delivery vans [79] due to the high power and low energy density of the hydraulic system. However, the solution can also be implemented in passenger vehicles [80].

For passenger vehicle applications the most popular solution is the battery electric vehicle. While there are still many disadvantage due to cost, weight and power

[3] Renault Zoe Electric Vehicle http://www.renault-ze.com

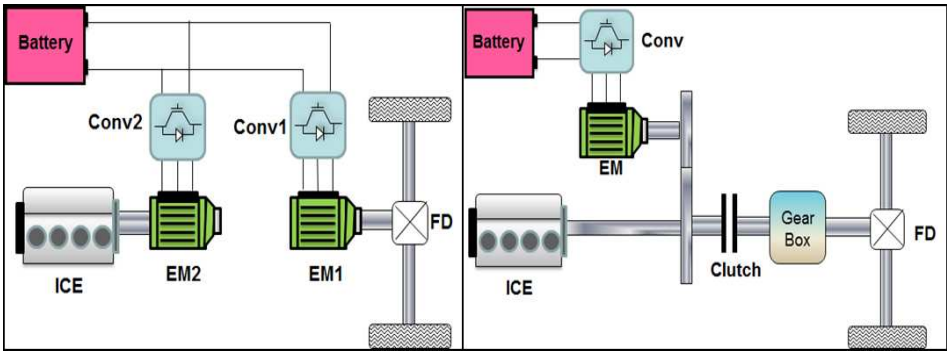

FIGURE 3.12: The hybrid drive train configurations: a) series config. b) parallel config.

output of the battery the chemical energy storage seems to be the appropriate solution for small passenger vehicles. The algorithm presented in this thesis can be applied to any hybrid vehicle system but since this work focuses on passenger vehicle applications we will only consider electric hybrid vehicles in the following.

Hybrid vehicles reduce fuel consumption due to their ability to recover kinetic energy when braking. In addition, the alternative power source can be used to move the engine operating point to a more efficient region, which therefore improves system efficiency. In a hybrid vehicle drive train, the power from the implemented sources is combined to generate the torque output at the wheel. Existing hybrid drive train configurations can be separated in three classes. In Section 3.5.1 a short review of the three hybrid architectures is presented. In this work the Toyota Prius hybrid vehicle will be used as an example of a hybrid vehicle. The construction of the drive train model is presented in Section 3.5.2.

3.5.1 Hybrid vehicle drive trains

Existing hybrid drive train vehicles are designed in parallel, series or power split configuration. In Figure 3.12 and 3.13 an electric hybrid drive train in each of the three configurations can be seen.

The first graph in Figure 3.12 shows a drive train in series configuration. In the series drive train the mechanical power from the engine is transformed to electricity by an electric generator. The electricity is then used to either charge the battery or run the electric motor that is connected to the wheels. In a series configuration there is no mechanical connection from the ICE to the wheels. All the power used to propel the vehicle is transmitted through the electric path. With this approach

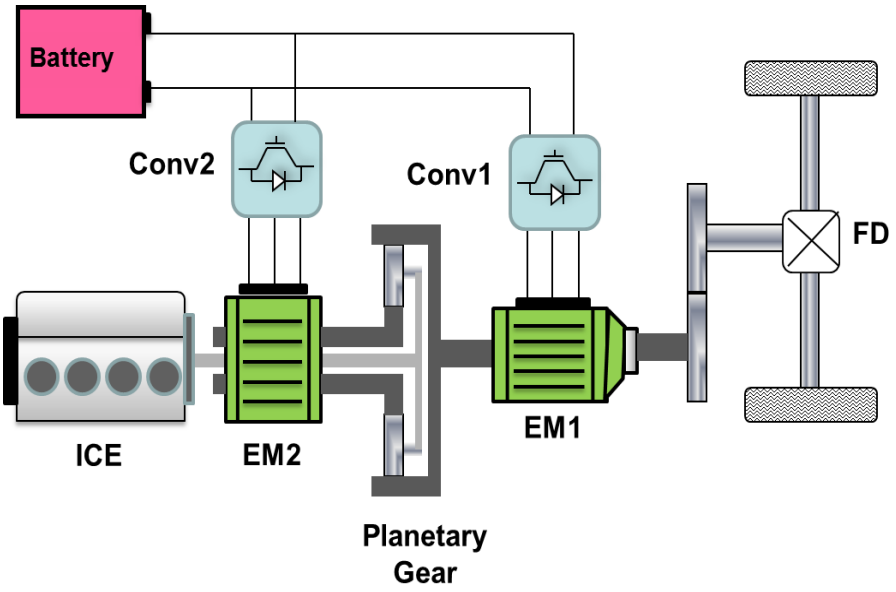

FIGURE 3.13: The Prius power split hybrid drive train

the engine operating point is entirely decoupled from the wheel operation. The ICE can therefore be run at the most optimal operating point to achieve maximum efficiency. However, in this drive train the efficiency of the electric motor/generator system is critical for overall system efficiency. In addition vehicle performance is dependent on the performance of the electric components. This often results in either a low power system or a large, heavy battery system.

In Figure 3.12 the second graph shows the hybrid drive train in parallel configuration. In a parallel hybrid configuration the engine is coupled with the mechanical shaft to the wheel. The engine can therefore transmit power directly to the wheels. An electric motor/generator is connected to the output shaft and contributes to the drive torque. With this configuration the engine operating point is not entirely decoupled from the wheels. With the electric machine the engine can only be assisted in torque, while the speed stays proportional to the wheel speed. All power is transmitted through the mechanical shaft, which has a very high efficiency.

The third hybrid configuration, seen in Figure 3.13, is the power-split configuration. This configuration, often also referred to as parallel-series drive train, combines the advantages of the parallel and series configuration. In the power-split drive train the engine operating point can be controlled to its optimal. But, if needed, all power can be transmitted from the engine to the wheels through the very efficient mechanical shaft. However, with the advantages of this drive train comes a system that is very complex and hard to control. For power-split

FIGURE 3.14: Toyota Prius

hybrid vehicles the control strategy is a critical factor that is important to achieve optimal system efficiency.

The Toyota Prius was one of the first hybrid vehicles on the market and still is one of the most common hybrid passenger vehicles on the road today. With its complex power-split drive train it will therefore be used in this work as representative hybrid passenger vehicle. In the following the drive train model will be presented and the control strategy, implemented by Toyota, is simulated.

3.5.2 Toyota Prius hybrid vehicle

The Toyota Prius II Hybrid Vehicle can be seen in Figure 3.14. The vehicle is a compact passenger car with a mass of 1360kg, which includes the battery and all other drive train components. As mentioned above, the vehicle is configured as a power-split hybrid drive train. A detailed schematic of the drive train components can be found in Figure 3.13.

The vehicle is driven by a 1.5L gasoline engine which operates on a high expansion ratio cycle [81] and therefore achieves efficiency values higher than a similar conventional gasoline engine. The power provided by the IC engine is split by the planetary gear set into electrical and mechanical path. The electric generator (EM2) is connected to the sun gear, while the electric motor (EM1) is turning with the output shaft, which is connected to the ring gear. Both machines are permanent magnet synchronous AC motors. The electric machines are connected by an inverter to the NiMh battery pack. The battery consists of 28, each 7.2V battery cells connected in series. The resulting battery pack has a nominal voltage of 201.6V and a nominal energy rating of 1.3kWh. The inverter contains a boost

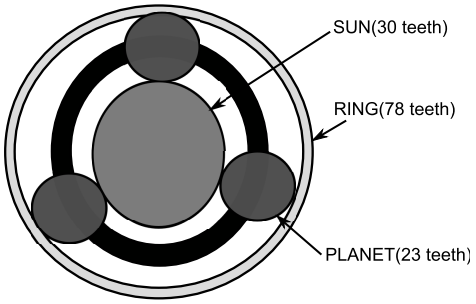

FIGURE 3.15: Planetary Gear Set

converter in order to increase the battery voltage if needed. The losses in the converter are neglected in this model.

The vehicle chassis can be modeled similar to the conventional and electric vehicle chassis, using Equations 3.4-3.12 with experimentally identified aerodynamic drag and rolling resistance coefficients. As with the conventional and electric drive train, it is assumed that the efficiency η_{FD} of the final drive reduction R_{FD} is constant with respect to torque and speed. The electric motor/generator (EM1) is connected to the output shaft and is therefore always turning with a speed proportional to the wheel speed. Given the wheel speed and torque the speed and torque of the ring side of the planetary gear can be computed by

$$\omega_{ring} = \omega_{EM1} = \omega_{wheel} R_{FD} \tag{3.29}$$

$$T_{ring} = \frac{T_{drive} - T_{brakemech}}{R_{FD} \eta_{FD}^{\psi}} - T_{EM1} \tag{3.30}$$

Here, $T_{brakemech}$ represents the mechanical brake torque, which is only non-zero if the minimum negative torque of the two electric motor/generators is exceeded.

In this power split drive train the power from the engine is split by a planetary gear set to the electric generator or the wheel output. A schematic of this gear can be seen in Figure 3.15. The planetary gear set has three inputs: the ring, sun and carrier/planet. In this work the gear set is modeled in a static way. With this assumption the geometry of the planetary gear results in two degrees of freedom in speed, but only one degree of freedom in torque. Hence, if one of the input torques is fixed the remaining two can be calculated. The speed and torque relationship of the planetary gear set can be described by:

$$\omega_{sun} = R_g \omega_{ring} + (1 - R_g)\omega_{planet} \tag{3.31}$$

$$T_{sun} = -\frac{1}{1 - R_g} T_{planet} = \frac{1}{R_g} T_{ring} \tag{3.32}$$

where R_g is the ratio parameter, which is calculated by $R_g = -\frac{T_R}{T_S}$ with $T_R = 78$, the number of teeth on the ring gear and $T_S = 30$, the number of teeth on the sun gear. Implemented in the Prius vehicle, the sun gear is connected to the electric generator, the planet part is run by the engine and the ring gear is connected to the electric motor and the output shaft.

Given the engine speed (ω_{eng}) and torque (T_{eng}) the fuel consumption is calculated using a look-up table, that has been identified in experiments on an engine test bench. The electric motor and generator with their respective inverters are modeled using look-up tables to determine the power losses as a function of motor speed ($\omega_{EM1,EM2}$) and motor torque ($T_{EM1,EM2}$). Given the motor/generator operation and the auxiliary power (P_{aux}) the battery operation is derived by:

$$P_{battout} = T_{EM1}\omega_{EM1} + PlossEM1 + T_{EM2}\omega_{EM2} + P_{lossEM2} + P_{aux} \tag{3.33}$$

The battery is modeled with a simple electric circuit, including voltage source and a resistance, similar to the electric vehicle. The resistance changes with the state-of-charge of the battery. Figure 3.16 shows the resistance for the Prius NiMH batteries in charge and discharge mode. Using experimental data the open-circuit-voltage (V_{OCV}) and battery resistance (R) are evaluated using interpolation methods. The battery current (I_{batt}) and battery output voltage (U_{batt}) can be calculated with the following relationships:

$$P_{battout} = V_{OCV} I_{batt} - I_{batt}^2 R \tag{3.34}$$

$$P_{battout} = U_{batt} I_{batt} \tag{3.35}$$

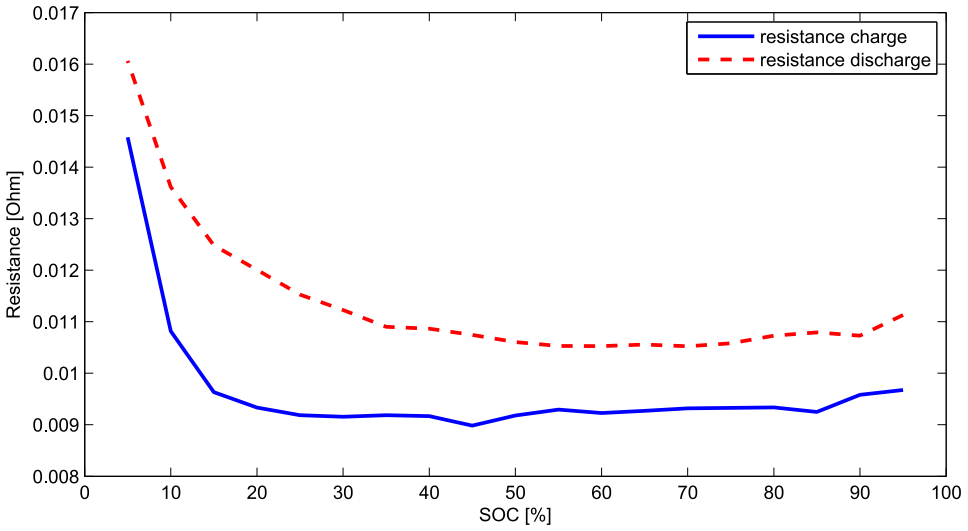

FIGURE 3.16: Battery resistance in charge and discharge mode

Due to the drive train complexity we can not determine the operation of each vehicle component given the drive train output ω_{wheel} and T_{drive}. Combining multiple power sources in the vehicle architecture there are multiple ways to achieve a specified vehicle operation. This is why an energy management strategy is needed. The control strategy is usually drive train specific and has a strong influence on fuel consumption. In our work we assume that the control strategy of the vehicle is known. It can therefore be simulated but not altered.

3.5.2.1 Prius control strategy

The control strategy implemented in the Prius II has been experimentally identified [82] and will be integrated in the vehicle model. At this point it should be noted that this work does not optimize the energy management of the hybrid vehicle, but rather identifies optimal utilization, given vehicle architecture and control strategy.

The Prius II is operated in two modes: the hybrid mode, where the engine provides power to the battery and/or the wheel, and the electric mode, where the engine is turned off and the electric motor satisfies the entire driver demand. The mode is chosen dependent on vehicle operation, battery state-of-charge and battery management system (BMS). In the following the two modes are discussed in more detail.

Hybrid mode

The vehicle is operated in hybrid mode given that either the state-of-charge is lower than SOC_{minhyb} or the vehicle speed exceeds maximum electric speed ($v_{vehmaxelec}$). When the vehicle is operated in hybrid mode the engine is turned on and provides the needed power to charge the battery and to propel the vehicle.

The BMS computes the demanded power ($P_{dembatt}$) of the battery as a function of battery state-of-charge. The power losses (P_{loss}) in the system are estimated. The total power required from the engine is determined by:

$$P_{reqeng} = P_{out} + P_{loss} - P_{dembatt} \tag{3.36}$$

The engine speed and torque are chosen, such that the efficiency of the engine is maximized along the constant power curve to provide P_{reqeng}. With this the operation of all drive train components can be calculated given the vehicle operation.

Electric mode

In electric mode the engine is turned off and EM1 provides the output power. The operation of the drive train can be calculated using Equations (3.29)-(3.33) and

$$\omega_{eng} = T_{eng} = T_{EG} = 0 \tag{3.37}$$

The vehicle is operated in electric mode if the battery state-of-charge is greater than the minimum state-of-charge boundary value ($SOC_{minelec}$ (Note: $SOC_{minhyb} \neq SOC_{minelec}$, hysteresis)) and the vehicle speed does not exceed $v_{vehmaxelec}$.

With this simulated control strategy the vehicle operation can uniquely be identified for any vehicle velocity and acceleration. With a complex drive train, like the power-split hybrid vehicle, it is hard to predict fuel optimal operation. Most efficient component operation for electric machines, battery and ICE is easily identified, however optimizing overall system efficiency is very difficult. Due to this numerical optimization methods will be used to compute optimal drive train operation and to identify important factors for eco driving for hybrid vehicles.

3.6 Dynamic vehicle simulation with Vehlib

In our approach inversion based modeling is used in the optimization process to identify a vehicle's optimal velocity trajectory without taking into account driver specific inputs. In the inversion process some dynamic phenomenons, such as dynamic gear changes, clutch engagements and the resulting torque interrupts, were omitted to simplify the simulation. In order to verify that the optimization results are realistically implementable a direct vehicle simulation software is used.

The Vehlib simulation software is a tool that was developed by the IFSTTAR laboratory for energetic simulation of drive trains. The software uses the Matlab simulink interface. With Vehlib component operation as well as energy consumption is computed for given drive cycles, which are specified in speed as a function of time. The direct vehicle simulation takes the speed profile as an input and uses a virtual driver to operate the vehicle in a realistic way. In order to follow the desired speed profile we represent the driver by a PID controller.

Due to its modularity the Vehlib library can easily be used to construct any kind of drive train. In Figure 3.17 the model for the conventional P308 vehicle can be seen. Separating each drive train component comes with the advantage that any other conventional vehicle can easily be simulated simply by replacing the appropriate engine or gear box components. Similarly the electric and hybrid vehicles were simulated using modules of the appropriate electric machines and batteries. Most component models were identified using experimental data, which results in a very realistic loss approximation of the system.

The Vehlib simulation, while primarily used to verify energy consumption for computed velocity profiles, was also used in the implementation process of this thesis work. Using the modularity of the software it can easily be adapted to a hardware-in-the-loop setting. The vehicle drive train simulation was used when verifying the vehicle performance on the engine test bench. A more detailed description of this setup will be discussed in Section 5.1.2.

In the scope of this work the Vehlib simulation software was adapted to be used in a driving simulator environment. This enabled us to experimentally test the developed advanced driver assist system for eco driving on the driving simulator. Changes to the vehicle model and experimental results of these studies can be found in Chapter 7.

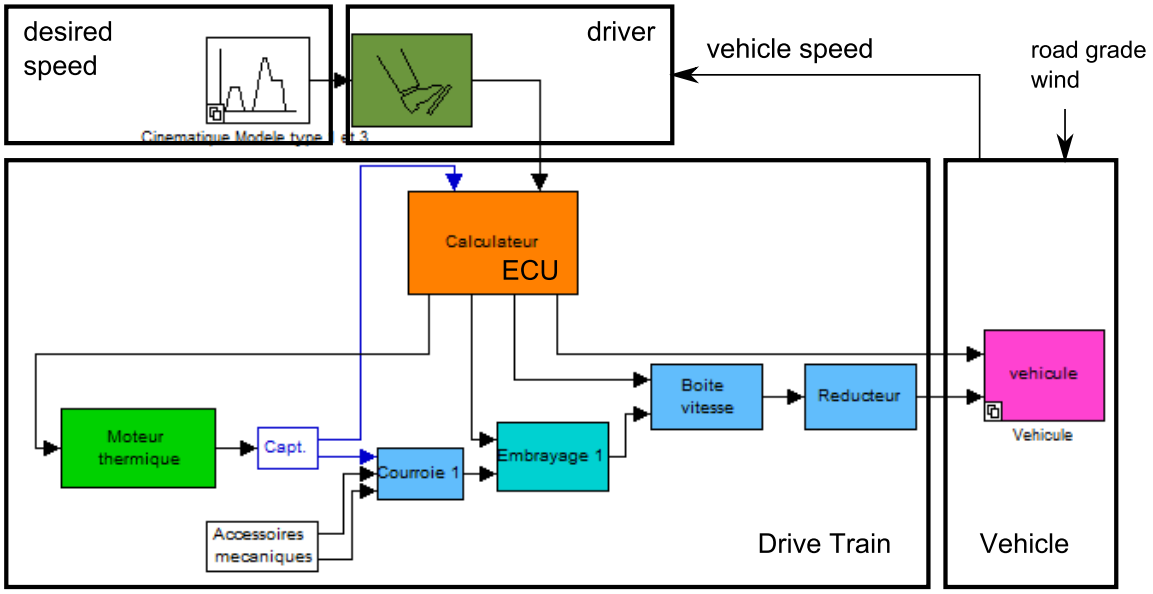

FIGURE 3.17: The VEHLIB vehicle simulation software

3.7 Conclusion

The content of this chapter dealt with the modeling of the three main drive trains considered for optimization in this thesis work. The differences and importance of inverse and direct model approaches were outlined. The modeling of the vehicle chassis was described. Using an inversion based model approach three different drive trains were modeled: the conventional, electric and power-split hybrid vehicle. The constructed models can be used to compute vehicle specific energy consumption for a given vehicle speed and acceleration. The direct Vehlib simulation software was introduced and will serve as a tool to verify and experimentally implement the resulting velocity profiles.

Analyzing the physical models of the different vehicle drive trains the dependency of system efficiency was discussed. It was found that the energy necessary due to the resistance forces acting on the vehicle chassis can be reduced with a smarter choice of vehicle velocity. This is a drive train independent factor that can reduce energy consumption. To identify most efficient system operation the losses in all components have to be taken into account. Inefficient components, such as the internal combustion engine, have to be considered. For the hybrid vehicle the control strategy, which varies with battery state-of-charge, has a very strong influence

on overall system efficiency. Manufacturers need to make sure that appropriate control strategies are applied for predicted system operation.

Chapter 4

Optimization

Contents

In Chapter 2 it was shown that a variety of methods can be used to compute energy reducing vehicle operation. While some works use a rule based strategy to optimize the velocity trajectory of vehicles, others apply numerical optimization techniques. To achieve good results and accurately define the best vehicle operation, we applied a mathematical optimization to the problem.

From the literature review in Chapter 2 it can be seen that several previous studies applied optimization methods to solve a trajectory optimization problem.

While most studies were searching for the energetically best velocity trajectory [11, 57, 64], others computed the time optimal speed profile [61–63]. As shown by Stoicescu [59], using the decision variables time, distance and energy, there are several different optimization problems that can be defined. The objective of our work is to identify potential gains of eco driving for passenger vehicles. The objective to be considered is therefore limited to the vehicle's energy consumption for a trip.

In this chapter the optimization methods applied to solve the trajectory optimization problem will be outlined. The problem is defined mathematically in Section 4.1, where the cost function and optimization constraints are specified. To guaranty driver acceptability of an eco driving system we keep trip time constant between general driving habits and the energetically optimal velocity trajectory. Initially, we therefore consider a fixed time problem. In Section 4.2 a solution to the single-objective constraint problem is presented applying the dynamic programming method.

Some eco drivers might, however, accept increases in trip time with the goal to further reduce energy consumption. In Section 4.3 a multi-objective optimization problem is studied, where time and energy consumption is considered as cost. An optimization approach is shown, where the dynamic programming method is used to solve the multi-objective optimization problem without integrating a weighting factor. The constructed algorithm was also used to discuss the sensitivity of the optimal speed profile.

4.1 Problem definition

A road vehicle's longitudinal motion can be described using two state variables: the distance d that the vehicle has traveled, and the vehicle's velocity v.

$$X = \begin{bmatrix} x_1 \\ x_2 \end{bmatrix} = \begin{bmatrix} x \\ v \end{bmatrix} \tag{4.1}$$

The motion of the vehicle system is described by the following set of state space equations:

$$\begin{bmatrix} \dot{d} \\ v \end{bmatrix} = \begin{bmatrix} 0 & 1 \\ 0 & 0 \end{bmatrix} \begin{bmatrix} d \\ v \end{bmatrix} + \begin{bmatrix} 0 \\ 1 \end{bmatrix} u \tag{4.2}$$

where the input u is given by the acceleration a, which is a result of some power demanded by the driver. For optimization purposes it is often required to represent the system in discrete time form. Using the two states, distance d and velocity v, and the input variable, acceleration a, the vehicle's motion can be described in discrete time form by:

$$d_{i+1} = d_i + v_i \Delta t + \frac{1}{2} a_i \Delta t^2 \tag{4.3}$$

$$v_{i+1} = v_i + a_i \Delta t \tag{4.4}$$

where Δt represents the time step of the discretization.

4.1.1 Optimization objective

An eco driving driving style is generally assumed to be environmentally friendly. However, usually the objective is to reduce energy consumption. Conveniently, for conventional vehicles reducing fuel consumption also reduces CO2 emissions. Still, we cannot assume that reducing energy consumption is equivalent to reducing our environmental impact. Since the economic advantage of eco driving is a strong motivator for people to apply it, we will start by defining our objective to be the energy consumption of the vehicle. The objective function is therefore specified by:

$$\Gamma_1 = \int_t \gamma_{veh}(t) dt \approx \sum_{i=1}^{n} \gamma_{veh_i}(t_i -> t_{i+1}) \tag{4.5}$$

where the value of γ_{veh} depends on the vehicle's acceleration and speed. The continuous cost function is approximated as a discrete sum. In such an approximation the grid choice can be critical to achieve good results. The appropriate grid choice for this application is discussed in Section 4.2.2.

The measure of γ_{veh} changes with the drive train configuration. The objective function represents fuel consumption for the conventional, but represents electric energy for the electric vehicle.

$$\gamma_{veh}^{conv}(t) = \dot{m}_{fuel_i}(t_i -> t_{i+1})\Delta t_i \tag{4.6}$$

$$\gamma_{veh}^{elec}(t) = P_{batt_i}(t_i -> t_{i+1})\Delta t_i \tag{4.7}$$

For the hybrid case the objective takes into account a combination of fuel consumption and battery use. This will be discussed in more detail in Section 5.3.3.

$$\gamma_{veh}^{hyb}(t) = \dot{m}_{fuel_i}(t_i -> t_{i+1})\Delta t_i - \alpha\Delta SOC(\Delta t_i) \tag{4.8}$$

4.1.2 Optimization constraints

For real time applications of eco driving in a driver assist system, the optimization constraints have to be identified with the help of positioning systems, navigational systems and/or mapping services. With today's technologies, the driver's position and his route can be defined in advance using a destination input from the user. With this, many constraints such as distance, speed limits and arrival times can be predefined.

In this study the first step is to identify potential maximum gains of eco driving. In order to discuss the gains of eco driving a baseline, to compare optimal operation to, has to be specified. Here, standard and real-life, experimental, drive cycles were used to represent ordinary driving. In Figure 4.1 a recorded velocity profile from a driver in an urban setting can be seen. In the following this velocity profile is used to define the optimization constraints.

Trip constraints Initially, the driver's mission has to be defined. Using drive cycle data, as seen in Figure 4.1, the trip constraints can be specified. In this graph the first plot shows the driver's velocity as a function of time, whereas the second plot shows the vehicle speed as a function of distance. There are three variables that describe the driver's mission: distance, time and velocity. The trip constraints are defined by setting boundary values for each of these:

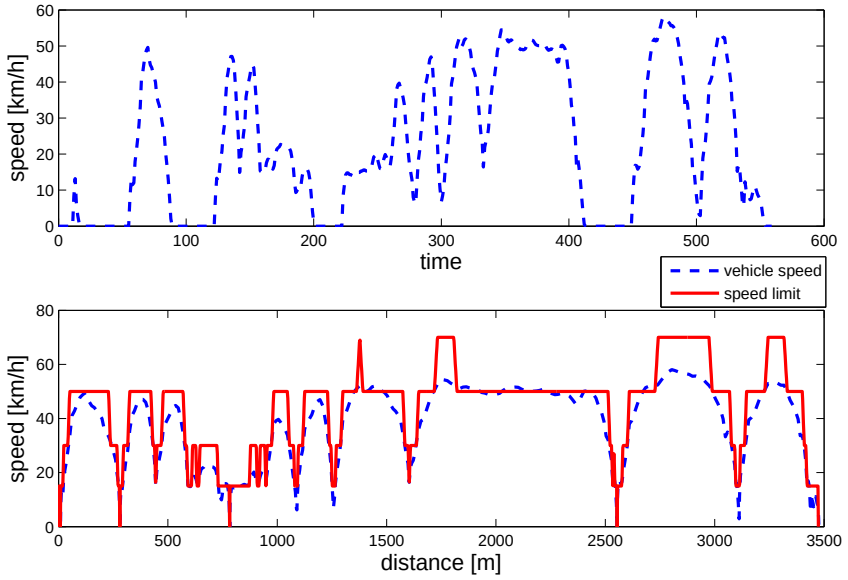

FIGURE 4.1: Urban real life drive cycle

$$d(0) = d_0 \qquad d(t_f) = d_f \tag{4.9}$$

$$v(0) = v_0 \qquad v(t_f) = v_f \tag{4.10}$$

$$t_f = T \tag{4.11}$$

It is assumed that the time is always initialized to zero. Defining these constraints we assume that the driver starts at some distance at a fixed initial speed and arrives at the final distance with a predefined final speed within some specified trip time. Many eco drivers might be willing to take into account time delays with the goal to reduce the energy consumption. Initially, it is here assumed that time is a fixed trip constraint. With this, the driver does not have any disadvantages due to eco driving and gains in fuel consumption, that are solely due to eco driving, can be identified. To discuss the trade-off between fuel and time a multi-objective optimization is considered in Section 4.3.

Road constraints In order to make a fair comparison between the driver's real-life vehicle operation and the optimal velocity trajectory, road constraints that

limit the driver's choices, need to be respected. There are multiple possible road constraints. It is here assumed that all limiting constraints on speed, as for example speed constraints due to road curvature, are included in official speed limitations. Due to the fact that speed limit data was not available for the considered drive cycle the limitations were approximated using the driver's velocity profile.

To specify the maximum allowable speeds, the legal speed limits in France were applied. While the lowest legal speed limitation is at $30km/h$ we used an additional, low speed, speed limit at $15km/h$ to simulate very slow driving in pedestrian zones or roundabouts. The resulting speed limiting vector can be written as $v_{lim} = [15, 30, 50, 70, 90, 110, 130]$ km/h. Since most drivers generally tend to exceed legal speed limits once in a while, it was assumed that a vehicle operation that exceeded a speed limit up to $3km/h$ was supposed to be within the lower boundary. The process of identifying the appropriate speed limit for some distance d_i can be described in two steps:

- find index j for which $v_{lim}(j-1) + 3 < v(d_i)$ and $v_{lim}(j) + 3 >= v(d_i)$
- $v_{max}(d_i) = v_{lim}(j)$

Establishing these rules the maximum velocity was computed as a function of distance. In Figure 4.1 the second plot (dashed blue line) shows the car's velocity as a function of distance. The imposed maximum speed limits can be seen in red (solid line). It is shown that, in addition to maximum speed limitations, the maximum speed limit enforces required stopping distances. If the real life driver had to stop the vehicle due to a stop sign or a red light, the optimal eco driving velocity profile will result in a stop at the same distance. In this study, no stop light timings were taken into account. It was assumed that the eco driver will have to stop at the same distances as the original driver. The computed optimal eco driving profile has to satisfy the following road constraint:

$$v(d_i) < v_{max}(d_i) \tag{4.12}$$

Another road specific parameter that is taken into account in this study is road grade. Due to changes in road grade the demand on the vehicle drive train changes for the same vehicle velocity and acceleration. Road grade therefore might have an effect on optimal vehicle operation. In our work road grade is integrated as an

optimization input, rather than a constraint. The grade resistance force (Equation 3.12) acting on the chassis is determined as a function of road grade, which is a distance dependent variable.

$$F_{grade} = M_{veh} g sin(\alpha_{road}(d_i)) \tag{4.13}$$

Other constraints In addition to trip and road constraints, traffic constraints represent an important factor for eco driving. Especially in an urban setting the traffic has a strong influence on the driver's vehicle operation. While traffic is an unpredictable variable, it is important to consider it when talking about realistic gains due to eco driving. In Chapter 6 traffic constraints will be introduced and the effect of traffic constraints on potential eco driving gains will be discussed.

Eco driving is often considered environmentally friendly. However, in the majority of studies only energy consumption is minimized. Pollutant emissions are a second important factor. The impact of eco driving on emissions will be evaluated in Chapter 6. An approach to integrate environmental constraints will be proposed.

4.2 Single-objective optimization

In a first analysis, we consider the single-objective optimization problem to minimize energy consumption. A variety of optimization methods are available to solve this problem. Heuristic methods as well as deterministic methods can be applied. With heuristic methods, such as for example the genetic algorithm [83], the difficulty consists in defining an appropriate evolutionary criterion. Heuristic methods might not determine the global minimum and dependent on the initialization parameters, the result can be a local minimum.

The trajectory optimization problem can be solved using deterministic methods like the Pontryagin's minimum principle [84] or the dynamic programming method [57, 58]. From the literature review in Chapter 2 it can be seen that these two methods are most commonly chosen to solve trajectory optimization problems for ground transportation. The Pontryagin's minimum principle is based on the concept of Calculus of Variation. This approach has the advantage that the problem can commonly be reduced to an algebraic equation that can be solved in very

little time. With this method constraints are not easily integrated. For complex problems it often becomes difficult to determine initial conditions that lead to an optimal solution, which satisfies all optimization constraints. The method is sometimes used in combination with evolutionary algorithms [85] to determine appropriate initial conditions before solving the problem analytically.

The dynamic programming method is based on Bellman's Principle of Optimality [86]. With this method non-linearities and optimization constraints are easily integrated in the optimization process. In general, the method breaks down a complex problem into smaller, simpler sub-problems, which can be solved recursively. The method leads to a functional equation that can easily be solved with the digital computer. If appropriate discretization is applied, dynamic programming generally identifies the globally optimal solution. However, the disadvantage of the dynamic programming method is its 'curse of dimensions'. The time of computation grows exponentially with the problem's dimensions. With this, it often takes a lot longer to solve than when applying the Pontryagin's Minimum Principle.

In this work the dynamic programming optimization method was chosen due to the complex cost function of the system and the set of constraints. Using this method enabled us to implement similar optimization procedures for all vehicle types: the conventional, electric and hybrid vehicle. Due to the flexibility of the method it was simple to integrate trip, road and any additional constraints that were studied.

In Figure 4.2 a general overview of the treated optimization problems can be seen. Initially a three dimensional dynamic programming method [25] was applied, in order to accommodate all constraints in time, distance and speed. With the goal to reduce computational time the optimization was later reduced to two dimensions by integration of a weighting factor. A nested approach, where the two dimensional dynamic programming method is integrated in combination with a root finding method, was applied to fix all constraints in time, distance and speed. Finally, we will introduce a dynamic programming based method to solve the multi-objective problem without weighting factor. With this algorithm, computing the Pareto optimal front, the tradeoff between energy consumption and trip time is discussed. In addition, the method can be used to analyze the sensitivity of fuel consumption to changes in the optimal velocity trajectory.

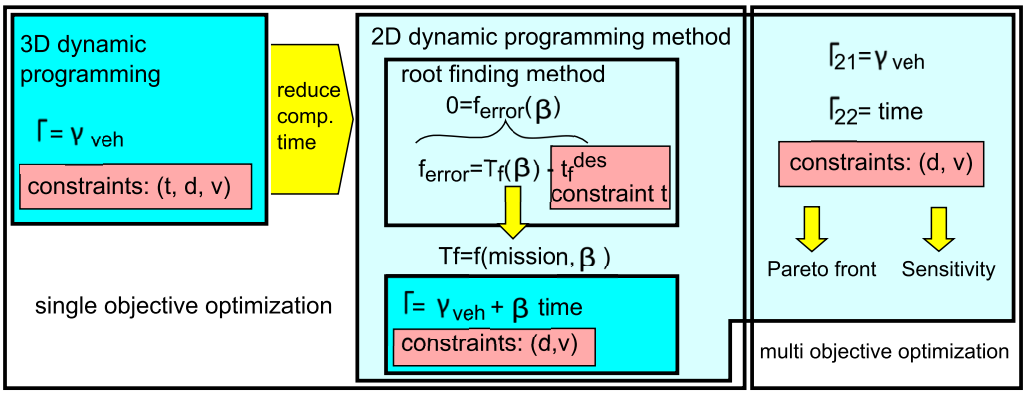

FIGURE 4.2: Overview of optimization problems

4.2.1 Three dimensional dynamic programming

In the dynamic programming optimization the search for the optimal trajectory is simplified using the Bellman principle while searching from the final state backward in time. The Bellman principle states the following [86]: 'An optimal policy has the property that whatever the initial state and initial decision are, the remaining decisions must constitute an optimal policy with regard to the state resulting from the first decision.'

The dynamic programming method generally consists of two parts. In the first part possible states are searched backwards in time for the optimum while storing the indices. In a second part the optimal path is found by retracing the stored indices from the initial state to the final.

The problem defined in Section 4.1 is solved while satisfying constraints in three dimensions. Although the system's motion can be described using two states, the three dimensional dynamic programming method was therefore used with the states distance d, velocity v and time t:

$$X = \begin{bmatrix} x_1 \\ x_2 \\ x_3 \end{bmatrix} = \begin{bmatrix} t \\ d \\ v \end{bmatrix} \tag{4.14}$$

Applying the optimization method the first step is to discretize the state vectors over the desired range. In the following the notation $X_{k,i,j}$ refers to the state $\begin{bmatrix} t(k) & d(i) & v(j) \end{bmatrix}^T$. The initial and final distances (d_o, d_f) and speeds (v_o, v_f) at t_o and t_f are fixed and denoted

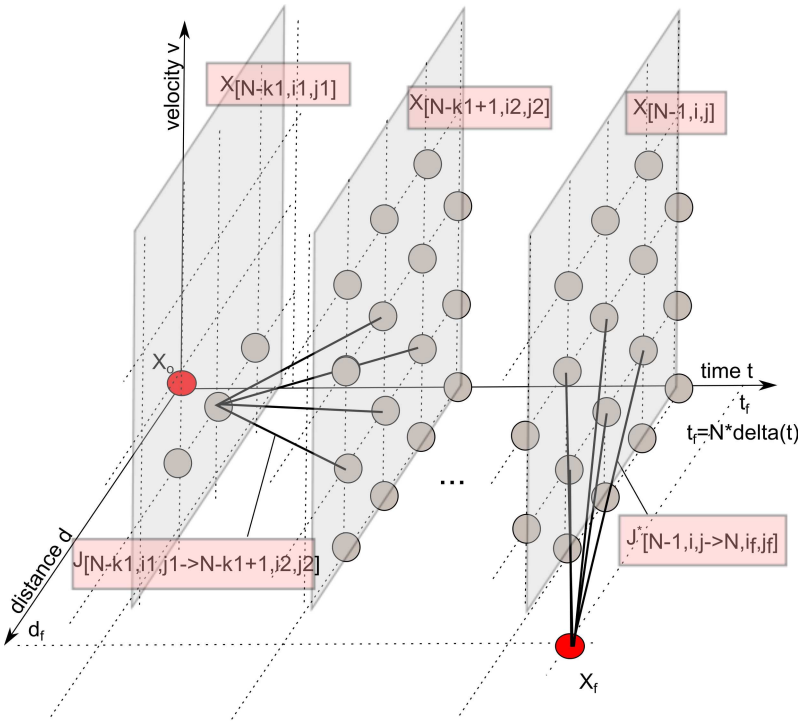

FIGURE 4.3: 3D Dynamic programming optimization method

$$X_o = \begin{bmatrix} t_o \\ d_o \\ v_o \end{bmatrix} \qquad X_f = \begin{bmatrix} t_f \\ d_f \\ v_f \end{bmatrix} \tag{4.15}$$

Beginning the search for the optimal trajectory from the final state the optimal costs $J^*_{[N-1,i,j]} = J_{[N-1,i,j->N,i_f,j_f]}$ and indices $I_{[N-1,i,j]}$ of the respective trajectories are stored for all possible states at the last time step $N-1$. The state transition diagram to visualize the process can be seen in Figure 4.3.

If we can define the cost of $J_{[N-1,i,j]}$, we can assume that the optimal trajectories for all possible values of i_2 and j_2 at some point in time $N-k_1+1$ are known and their costs to reach the desired final state are given by $J^*_{[N-k_1+1,i_2,j_2]}$. The optimal trajectory from some state $X_{[N-k_1,i_1,j_1]}$ to the final state can then be found by comparing the sum of costs of the state transitions between $X_{[N-k_1,i_1,j_1]}$ to $X_{[N-k_1+1,i_2,j_2]}$ and the optimal cost from $X_{[N-k_1+1,i_2,j_2]}$ to X_f for all possible $[i_2, j_2]$. The cost of the optimal trajectory at $N-k_1$ is given by:

$$J^*_{[N-k_1,i_1,j_1]} = \min_{i_2,j_2}(J_{[N-k_1,i_1,j_1->N-k_1+1,i_2,j_2]} + J^*_{[N-k_1+1,i_2,j_2]}) \tag{4.16}$$

Storing the costs $J^*_{[N-k1,i,j]}$ and indices $I_{[N-k1,i,j]}$ for all k_1, i, and j the optimal cost from X_o to X_f is found after N iterative steps. In order to find the sequence of states used to result in the minimum cost the indices are used to retrace the trajectory.

Hooker [57] first proposed in 1988 to apply a three dimensional dynamic programming method to optimize vehicle operation for several predefined scenarios. Our approach is based on his work, and as he did, we here used the three dimensions time, distance and speed. Due to the dependencies of these three dimensions a free choice of distance and velocity at each time step is not possible. Choosing the desired vehicle velocity Hooker used interpolation to fix the resulting distance, d_i, for a given time, t_i, and speed, v_i, to the grid. In our studies it was found that the dependency of the three dimensions allows us to make an intelligent choice of grid size that makes interpolation unnecessary. The step size of each dimension is determined by the following procedure:

Initially v_i is assumed to be 0. Equations (4.3) and (4.4) can then be reduced to

$$\Delta d = \frac{1}{2} a_i \Delta t^2 \tag{4.17}$$

$$\Delta v = a_i \Delta t \tag{4.18}$$

When we solve equation 4.18 for a_i we can replace a_i in equation 4.17. Choosing Δd and Δt the grid size for Δv is then found by

$$\Delta v = \frac{2\Delta d}{\Delta t^2} \Delta t \tag{4.19}$$

With this definition all resulting distances, d_i, for a chosen speed, v_i, at time t_i fall on the defined grid. This holds true for any other chosen initial value of v_i. However, when in our work initial and final conditions in velocity were often specified to zero. So this seemed to be the most appropriate choice.

Due to the fact that the three dimensions (d, v, t) in the dynamic programming computation are dependent, the initial state might not be reachable by all paths within one final step in the backward calculation process. This becomes obvious looking at the last step where d_i, v_i, d_{i+1}, v_{i+1}, and Δt are fixed by the computed

optimal paths up to the $(i+1)$th step and the initial conditions (at time i). Given these values the resulting system of equations consists of two equations with only one unknown, which is not solvable. Hookers publication [57] does not mention any adaptation of his calculation to this fact. In our calculation it was found that leaving the second to last iterative step (at $t = 1$) free, and independent of the grid, can ensure that all possible, computed trajectories can reach the initial state.

This process is demonstrated in the following. Expanding Equations (4.3) and (4.4) for two time steps results in the following four equations:

$$d_{i+1} = d_i + v_i \Delta t + \frac{1}{2} a_i \Delta t^2 \tag{4.20}$$

$$v_{i+1} = v_i + a_i \Delta t \tag{4.21}$$

$$d_{i+2} = d_{i+1} + v_{i+1} \Delta t + \frac{1}{2} a_{i+1} \Delta t^2 \tag{4.22}$$

$$v_{i+2} = v_{i+1} + a_{i+1} \Delta t \tag{4.23}$$

Replacing d_{i+1} and v_{i+1} in Equations (4.22) and (4.23) with Equations (4.20) and (4.21) results in

$$d_{i+2} = (d_i + v_i \Delta t + \frac{1}{2} a_i \Delta t^2) + (v_i + a_i \Delta t)\Delta t + \frac{1}{2} a_{i+1} \Delta t^2 \tag{4.24}$$

$$v_{i+2} = (v_i + a_i \Delta t) + a_{i+1} \Delta t \tag{4.25}$$

With these two equations, which represent the second to last and last time step in the dynamic programming process, the two unknowns a_i and a_{i+1} can be computed with the fixed variables d_i, v_i, d_{i+2}, v_{i+2}, and Δt. Using this concept all possible trajectories can be explored for optimality.

4.2.2 Two dimensional dynamic programming

When implementing the dynamic programming method to solve an optimization problem the solution is found by strategically searching all possible solutions. The method looks at all possible state values at each step on the time-axis. This is why the computational cost of a three dimensional approach is much higher than that of a two dimensional method. To illustrate this 'curse of dimensions' we will look at an example.

We consider a problem defined in two dimensions, where the time-axis is discretized into N steps and at each step we have to choose from N state values. The dynamic programming method then searches N possible states at each of the N time steps. The computational cost to find the solution can be described by $N*NC = N^2*C$, where C is the computational cost to calculate one edge. However, assuming the problem consists of three dimensions, then at each time step N there are N^*N possible states to be investigated. The resulting computational cost becomes $N * N^2C = N^3 * C$. The problem is solved in exponential time. The computation takes $C * N^x$ time, where x is the number of dimensions. Dynamic programming is therefore known as a weak NP (nondeterministic polynomial) complex problem.

In order to reduce computational time the two dimensional dynamic programming method [26] was therefore applied. In this approach the same strategy is implemented simplifying the search for the optimal solution by use of the Bellman principle. However, the search space is reduced to only two variables. Using the two state variables that describe the vehicle's motion, the distance d and velocity v define the decision space. In Figure 4.4 the problem setup is illustrated.

$$X = \begin{bmatrix} x_1 \\ x_2 \end{bmatrix} = \begin{bmatrix} d \\ v \end{bmatrix} \tag{4.26}$$

A state can be described by $X_{j,i}$ and initial and final constraints are defined in distance and velocity.

$$X_0 = \begin{bmatrix} d_0 \\ v_0 \end{bmatrix} \qquad X_f = \begin{bmatrix} d_f \\ v_f \end{bmatrix} \tag{4.27}$$

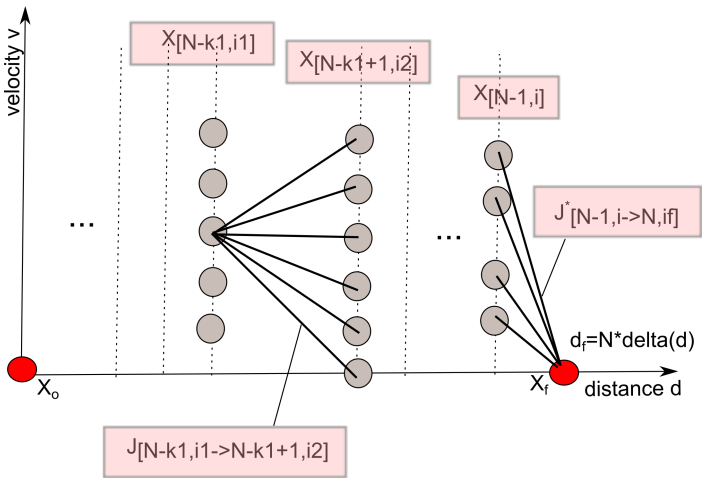

FIGURE 4.4: Dynamic programming optimization method

As for the three dimensional case, once the optimal costs $J^*_{[N-1,i]} = J_{[N-1,i->N,i_f]}$ for the second to last state are fixed the problem can be solved recursively, while incrementing k_1, by comparing the optimal costs of the possible choices at each step on the x-axis.

$$J^*_{[N-k_1,i_1]} = \min_{i_2}(J_{[N-k_1,i_1->N-k_1+1,i_2]} + J^*_{[N-k_1+1,i_2]}) \tag{4.28}$$

Storing the costs $J^*_{[N-k,i]}$ and indexes $I_{[N-k,i]}$ for all k, and i's the optimal cost from X_0 to X_f is found after N iterative steps and the optimal path can be retraced.

With this approach the computational cost is significantly reduced in comparison to the three dimensional method. But, as seen in the graph, the initial and final conditions are only set in distance and speed, not in time. To implement a fixed final time a second term was introduced in the cost function of the optimization. Adding the trip time with a weighting factor β in the objective function, the arrival time of the resulting optimal velocity trajectory can be controlled. The new objective function is specified by:

$$\Gamma_2 = \int_d \gamma_{veh}(d)dt + \beta\Delta t(d) \approx \sum_{i=1}^{n} \gamma_{veh_i}(t_i - > t_{i+1})\Delta t_i + \beta\Delta t_i \tag{4.29}$$

To compare the results between the three and the two dimensional method a simple trip was optimized for a conventional vehicle. Starting from rest a distance of 300m was covered to arrive at a full stop. For the three dimensional approach

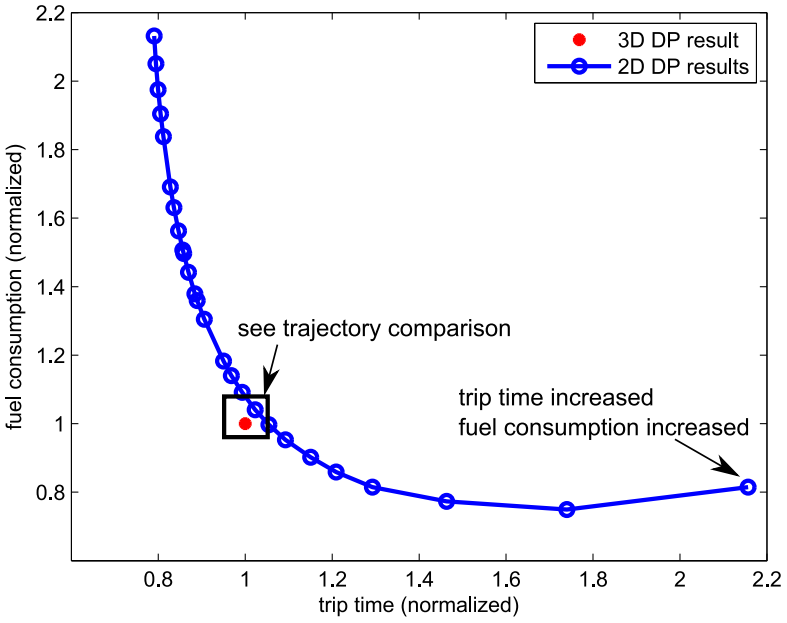

FIGURE 4.5: 3D DP solution versus 2D DP solution

the arrival time was fixed to 30s. The maximum speed limit was relaxed and set very high, such that it did not interfere with the result. The problem was solved for several different β values using the two dimensional method. In Figure 4.5 a comparison of the minimum fuel consumption computed with the two methods can be observed. The figure shows a normalized graph, the red point visualizing the result from the 3 dimensional method and the blue line representing the cost of the optimized trajectories computed with the 2 dimensional dynamic programming method.

From Figure 4.5 it can be seen that, applying the two dimensional dynamic programming method using various β values, we can analyze the tradeoff between energy consumption and trip time. Optimal velocity profiles with various final times can be computed by changing the weighting factor β. To increase the arrival time to very large values a negative weighting factor has to be chosen. Such a case is pointed out in Figure 4.5 on the lower right. While this point is not optimal in time neither in fuel it has to be considered when forcing the arrival time to a desired value. The tradeoff between energy consumption and trip time will be discussed in more detail in Section 4.3. To ensure that only optimal points are computed a multi-objective optimization method that does not require a weighting factor is applied.

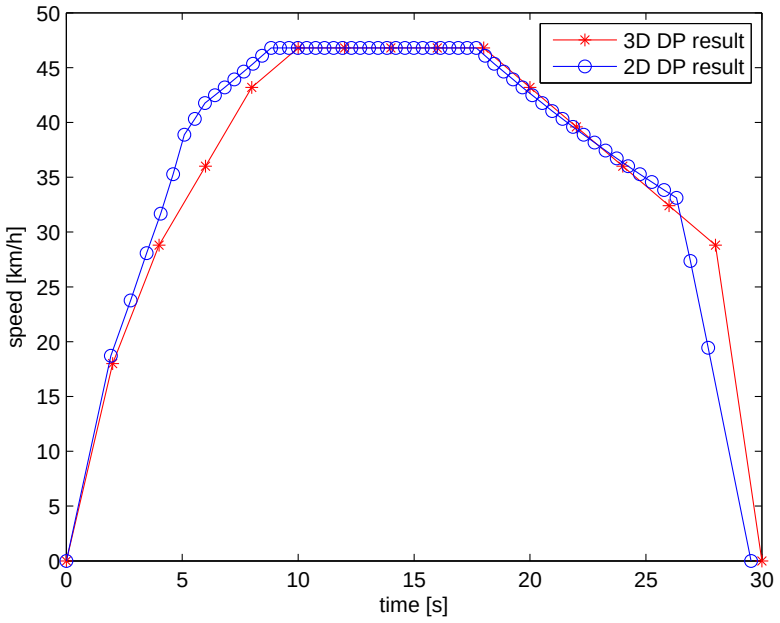

FIGURE 4.6: Velocity profile of similar points of 3D solution and 2D solution

For a β value of 0.9 the solution of the two dimensional dynamic programming method gave results very close to the three dimensional solution. We therefore compare the respective speed trajectories to analyze the differences. Figure 4.6 shows the solution using the three dimensional algorithm in red. The vehicle arrives at the destination at exactly 30sec, as specified by the time constraint. The blue speed profile shows the solution using the two dimensional method with a weighting factor of $\beta = 0.9$. It can be seen that without time constraint integration, the vehicle reaches the destination in a shorter time and consumes slightly more fuel. From the graph it can be seen that the three and weighted, two dimensional solutions are very similar.

Figures 4.5 and 4.6 showed that the two methods give very similar results with respect to energy consumption and velocity trajectory. The variations are assumed to be due to the difference in grid choice between the three and two dimensional method. The same grid choice is impossible for the two methods due to the fact that, in the three dimensional method the time step is set, however in the two dimensional method it is the distance step that is fixed. For the two dimensional method it is necessary to specify the distance step sufficiently large, with respect to possible velocity changes, to enable the vehicle to accelerate and reach high velocities. The choice of distance and velocity are therefore not independent.

Δ d	Δ v	fuel consumption [g]	computation time [sec]
10	1	17.11	.9
5	0.5	16.2	1
5	0.2	15.24	1.75
2	0.5	15.45	88
2	0.3	15.15	617

TABLE 4.1: Analysis of grid choice for two dimensional dynamic programming method

While the increment in distance is chosen rather large the grid size of the velocity vector is kept small.

To identify the appropriate grid choice, different step sizes and their effect on fuel consumption and computational time were analyzed. The 300m problem was used with a weighting factor β of 0.9. In Table 4.1 the resulting fuel consumption values for different grid size combinations can be seen. Fuel consumption values seem to stabilize just above 15g of fuel for this trip. It can be seen that, once grid size becomes too small, the computational cost increases significantly. For further computations we therefore specified the grid size to $\Delta\, d = 5m$ and $\Delta\, v = 0.2m/s$.

A reduction from three to two dimensional dynamic programming using a weighting factor was first proposed by Monastyrsky [58]. However, in his work, Monastyrsky never mentioned how to specify an accurate weighting factor β to achieve a desired final time. To solve the single-objective time constraint problem the weighting factor β has to be identified such that an optimization with cost function Γ_2 results in an optimal velocity profile that satisfies the time constraint (Equation 4.11).

In a real-time application the factor β could be directly defined by the driver. With this parameter the significance of time versus energy consumption for each individual driver can be described. However, to compare trips and compute gains due to eco driving it is important to respect the initial and final conditions of the mission.

When a β is fixed the optimization problem can be solved using the two dimensional dynamic programming method. As a result a velocity profile, which is optimal for some final time T_f, is computed. For a specified vehicle's mission the final time can then be defined as a function of the weighting factor β:

$$T_f = f(mission, \beta) \tag{4.30}$$

In our work, several methods to identify an appropriate weighting factor for a specified time constraint were considered. Initially a mapping technique was used. This approach is presented in Section 4.2.2.1. As a second solution we propose in Section 4.2.2.2 to implement a nested technique, using the dynamic programming method in combination with root finding methods. Several root finding methods were discussed for their efficiency when applied to the considered problem.

4.2.2.1 Mapping of weighting factor

Considering a problem where constraints are only defined on the initial and final state, the weighting factor β can be computed using a pre-calculated mapping function. Assuming that the vehicle starts from rest and stops at the destination, the trip time of the resulting optimal velocity trajectory only depends on the traveled distance, $d_{trav} = d_f - d_0$, and β. Equation 4.30 can be replaced by

$$T_f = f(d_{trav}, \beta) \tag{4.31}$$

Applying a sufficiently small grid size the expected range of distance and β values is discretized. An optimal velocity profile is calculated for all combinations of possible travel distances and β values using the presented two dimensional dynamic programming method. Storing the final time values for each distance and β combination, T_f can be expressed as a function of distance and β by the use of a look-up table. The shape of T_f is presented as a contour in Figure 4.7 a). The relationship between the weighting factor and arrival time is clearly visible: decreasing β values result in increased trip time, and also lower energy consumption. For longer missions similar β values result in longer trip times than for shorter missions.

The function shown in Figure 4.7 a) can be inverted to compute β values as a function of desired trip time and travel distance. Figure 4.7 b) shows β in dependency of final time and distance. The left boundary of the contour shows the minimum possible time for a given distance. This line depends on the performance of the vehicle. On the other side the slowest trip time for optimal fuel consumption

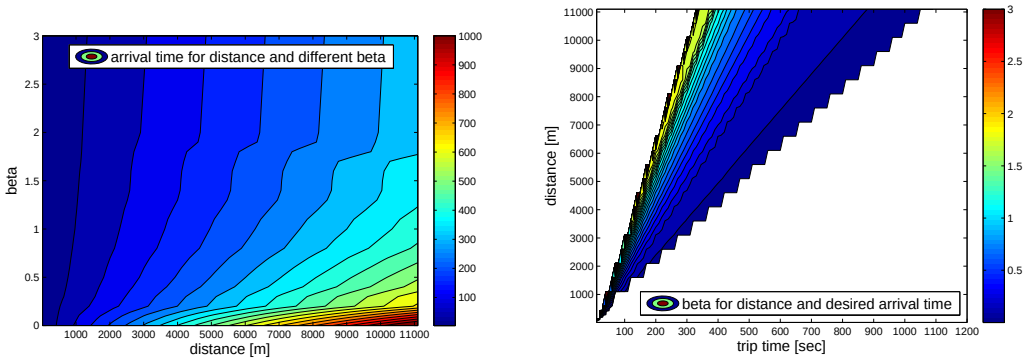

FIGURE 4.7: a) T_{res} as function of d_f and β, b) β as function of d_f and desired T_{res}

is shown. Here, only positive β values were used. It can be seen that a finite optimal arrival time to minimize fuel consumption exists. When β is set to zero only energy consumption is considered in the optimization process. In this case the driver accepts any time delay necessary to reduce the trip's energy consumption. Today it is often assumed that reducing average speed will always reduce energy consumption. With this graph it can be seen that this is not the case. Optimal final time to minimize fuel consumption will be discussed in more detail in Chapter 5. The steps seen on the contour boundaries are due to the discretization step, which can be further reduced.

The mapping method is a very simple approach to pre-calculate the defined range of distances and arrival times. However, when applied to more realistic problems, where maximum speed limits and/or road grade have to be considered, this approach only gives approximations and no exact solutions. For a theoretical comparison of eco driving potentials this method is not sufficient. In Section 4.2.2.2 we will therefore develop a more accurate solution to solve the time constraint single objective optimization problem.

4.2.2.2 Nested evaluation of weighting factor

Due to the drawbacks of the mapping method a second approach to identify the appropriate weighting factor for a fixed time constraint was proposed using a nested evaluation. As previously stated, the arrival time of the optimized velocity profile can be defined as a function of the vehicle's mission, where all trip, road and other constraints have to be satisfied, and the weighting factor β. Given the desired arrival time t_f^{des} for the mission, an error function is defined:

$$f_{error} = T_f - t_f^{des} \tag{4.32}$$

If, for some given β, the computed optimal velocity profile does not satisfy the predefined fixed time constraint, the function f_{error} will not be zero. In the proposed nested solution this error function is used to choose a new β. Using the shape of the error function the new weighting factor, when used in the optimization process, should return a velocity profile with a final time closer to the desired arrival time than the previous evaluation.

Using this method two minimization processes are performed. The first is using the dynamic programming optimization method to compute the optimal velocity profile given some pre-defined weighting factor. The output of this first method is a velocity profile with an arrival time that is most likely not equal to the desired final time. The second process consists of a β-update, where the knowledge of the original beta value and the error between the desired and the resulting trip time are used to generate a new beta value. This identification process of the weighting factor can be defined as a root-finding problem.

Initially a trial and error method was used to identify the desired range of β values. Several drive cycles were used to compute the error f_{error} between arrival time of optimized velocity profile for a variety of β values. The values were computed for the New European Drive Cycle (NEDC), which is a standard drive cycle used in Europe to test fuel economy values. In addition three drive cycles were used to simulate urban (HYZURB), highway (HYZROUT) and freeway (HYZAUTO) driving. The shape of the error function can be seen in Figure 4.8. The red line in the graph shows the x-intercept. Each function has a root where it crosses this level. When the root of the mission specific error function is found the single-objective fixed time optimization can be solved.

The simplest method to determine a function's root is the bisection method. However, this method is generally considered not very intelligent and slow. We therefore investigated five different root finding methods: the Bisection Method, the Secant Method, the False-Position Method, Ridder's Method and Brent's Method. In the following we will briefly discuss the advantage and disadvantage of each one. A detailed description of each method can be found in the Appendix.

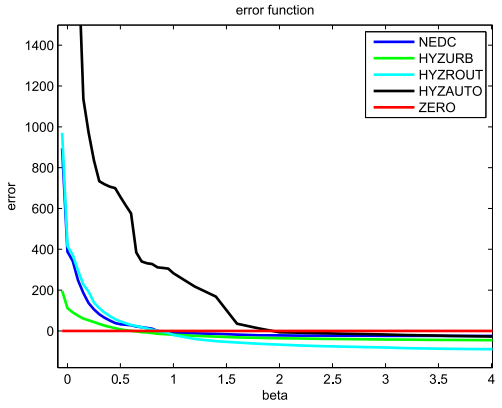

FIGURE 4.8: Shape of error function for different missions

The bisection method is a method applied to find the root of a continuous function. Assuming that there exists at least one zero in an interval the root is found by iteratively bisecting the interval. With this method the length of the interval is reduced by one half at each step. Its convergence time is linear and therefore considered slow (depending on the shape of the function f). Other methods have therefore been developed with the intention of reducing the number of iteration, and therefore computational time.

The Newton Method is a root-finding method commonly used to reduce the number of iterations. With this method the x-intercept is approximated using the slope at a search point. However, when the function's derivative cannot be defined analytically the method cannot be used. The False Position Method and Secant Method are algorithms derived from the Newton Method, and applicable in this case. The approach used is to approximate the slope of the function linearly with two points. A negative aspect of these methods is that they assume the function is approximately linear in the region of interest. The two methods differ only in their choice of which point the new value will replace. The Secant method, while often the faster method, is not guaranteed to converge. A schematic of the Bisection, False Position and Secant Method can be seen in Figure 4.9.

The application of these Newton based methods is usually faster than using the Bisection Method because the search can converge faster than in linear time. However it depends strongly on the shape of the function f and even linear convergence rates are not guaranteed.

In 1979 Ridder [87] developed a method that resolves the issues encountered with the Secant and False Position Method. In his approach, Ridder takes the bent out

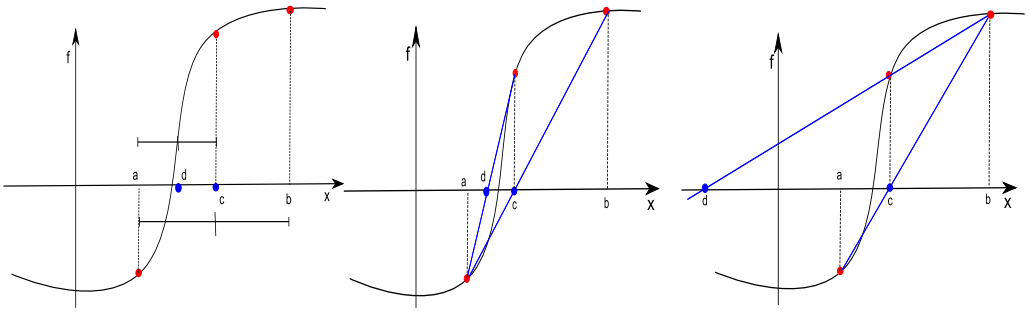

FIGURE 4.9: a) Bisection Method, b) False Position Method, c) Secant Method

# of iterations	Bisection	Secant	False-Position	Ridder's	Brent's
NEDC	11	101	150	9	15
HYZURB	13	22	37	13	12
HYZROUT	11	35	81	13	10
HYZAUTO	12	61	150	13	15

TABLE 4.2: Computational Cost of Root-finding Methods

of the function by using an exponential. The algorithms convergence is supposed to be super linear and robust [87].

To combine fast convergence with the guaranty of at least linear convergence Brent developed an algorithm in 1970 on the basis of an approach previously taken by Dekker [88, 89]. With his method, Brent ensures that the search converges in at least linear rate but often much faster. To achieve this the method uses a combination of Bisection Method, Secant Method and Inverse Quadratic Interpolation.

Analysis of Computational Cost An analysis of the computational cost of the discussed algorithms is shown to identify the most suitable method for our application. Since the cost function of the vehicle depends strongly on the drive train model, we will here represent the cost in numbers of iterations. It was defined that a maximum error in final time of 0.5s was acceptable. This seemed sufficient since the analyzed drive cycles have final times between 800 and 2000s.

In Table 4.2 the resulting number of iterations can be seen for four different drive cycles: the NEDC standard drive cycle, an urban cycle called HYZURB, a highway cycle called HYZROUT and a cycle that represents freeway driving, named HYZAUTO. The results were computed with the use of the Peugeot 308 vehicle model, and applying the 2 dimensional dynamic programming method with a grid size of 5m for distance and 0.2m/s for velocity.

It can be seen that, due to the shape of the error function, which is not approximately linear, the Secant and False-Position Methods do not perform very well. The maximum number of iterations was set to 150 in this study and it was found that the False-Position Method did not converge within this range for two of the drive cycles. It can be seen that the Bisection Method is a good choice for the here studied shape of error function. In comparison to the Secant and False-Position Method more advanced root-finding methods, like Ridder's or Brent's Method, perform much better. In general, Ridder's and Brent's methods performed about as good as the Bisection method for the considered error function. The advantage of these methods is that they are applicable to any function and (in most cases) converge faster than the Bisection Method.

In comparison with the three dimensional dynamic programming, a reduction to a two dimensional approach leads to a very large gain in computational time. For a 300m mission, driven in 30s, the three dimensional method needed around 250s to solve the problem. The two dimensional approach, where the cost arrays are calculated in the first iteration, solved the problem in 1.9s CPU time[1].

4.2.3 Conclusion

In Section 4.2 a solution to the single-objective time constraint trajectory optimization problem was presented. Applying the dynamic programming optimization method a three dimensional approach was used initially. Using a weighting factor a faster, two dimensional solution to the problem is proposed.

For a specified weighting factor the problem can be solved using the two dimensional dynamic programming method. It was shown that for simple problems a mapping method is appropriate to identify the correct weighting factor. If more complex constraints have to be satisfied a nested method can be used combining the 2 dimensional dynamic programming method with advanced root finding methods. In this study several different advanced root finding methods were considered and it was found that the bisection, Ridder's and Brent's method are good choices for the considered error function. All further computations will be using the two dimensional dynamic programming method in combination with Brent's root finding method.

[1]The computations were done with a laptop computer with a i5 Intel Core Processor M520 running at 2.40GHz using 8GB random access memory

4.3 Multi-objective optimization

The single-objective optimization problem considered in Section 4.2 uses time as a trip constraint that defines a driver's mission. However, many drivers, and in particularly eco drivers, might be flexible in their arrival time. Some might consider taking into account some time delays, in order to achieve reductions in their energy consumption. Therefore the trade-off between trip time and energy consumption for a given mission has to be discussed.

The simplest method to resolve a multi-objective control problem is to construct one single cost function using weighting factors to combine the different objectives. However, as shown in [90], depending on the shape of the cost function, this approach may not be able to compute all optimal solutions. In this work, the multi-objective optimization problem is solved without the use of weighting factors.

First, we will introduce the multi-objective trajectory optimization problem. Removing Equation 4.11 from the constraints, only trip constraints on initial and final distance and velocity are specified. No time constraint is fixed. Instead two objective functions were defined: the energy consumption, as seen in Equation 4.33, and the arrival time of the optimal velocity profile, as described in Equation 4.34. Together with the equations of motion of the system (Equation 4.3 and4.4) and the trip and road constraints specified in Section 4.1.2 the multi-objective problem is defined.

$$\gamma_{21} = \sum_{i=d_0}^{d_f} \gamma_{veh_i}(d_i) \tag{4.33}$$

$$\Gamma_{22} = \sum_{i=d_0}^{d_f} \Delta t_i(d_i) \tag{4.34}$$

The result of a multi-objective optimization problem is often presented in the form of a Pareto front. A Pareto front is a graph that shows the trade-off between several objectives. The Pareto front is usually a x-dimensional hyperface where x is the number of objectives defined in the optimization problem. For our problem, where two objective functions are specified, the Pareto front can be represented by a curve, hence with two dimensions. A Pareto front is computed by calculating points on this curve, so called Pareto optimal points. The Pareto optimality is

originally a concept used in economics. A point is Pareto optimal if it is impossible to improve on one of the considered objectives without making another worse.

This means that if a point p lies on the Pareto optimal front it satisfies

$$J_n(p) < J_n(i) \tag{4.35}$$

for all point i and for at least one objective n. Given a set of points we can compute the Pareto optimal front looking at all possible solutions and then identifying the points that are not Pareto optimal and deleting them. A point q is not Pareto optimal if there exists a point p such that

$$J_n(p) < J_n(q) \tag{4.36}$$

for all cost functions n. With this strategy all points that are not Pareto optimal can be identified and the resuming points create a Pareto optimal front.

There are several methods used to find the Pareto optimal front given multiple cost functions. A very common one is the genetic algorithm, where evolution rules are defined and used to create generations. After several generations the algorithm is supposed to converge to the optimal solution [91]. Since this algorithm is often not very intuitive and might not converge, we will here use the dynamic programming algorithm [27] to find the Pareto optimal points [90]. In the following the multi-objective dynamic programming optimization is described in more detail.

4.3.1 Multiobjective dynamic programming

In our problem setup each Pareto optimal point corresponds to a velocity profile from some speed v_{i_1} at distance d_{k_1} to some speed v_{i_2} at d_{k_2}. Each trajectory is associated with some cost one (Γ_{21}), here the energy consumed, and some cost two (Γ_{22}), the time of the trip. Similarly to Section 4.2.2, the problem, with constraints in initial and final distance and velocity, is defined as a two dimensional dynamic programming problem, plotting the distance on the x-axis and the speed on the vertical axis. The geometric setup can be seen in Figure 4.10. In the search for the optimal solution a Pareto optimal set is stored at each state. This means that at each state (each possible velocity $v(i)$ at some distance $d(k)$) not only one

optimal trajectory is stored but rather a set of optimal trajectories that make up the Pareto optimal front.

The optimization process follows the same steps as described in Section 4.2.2. Initially, the possible ranges in both states are discretized and the notation $X_{k,i}$ will refer to the state $\begin{bmatrix} d(k) & v(i) \end{bmatrix}^T$. The initial and final states are fixed by

$$X_o = \begin{bmatrix} d_o \\ v_o \end{bmatrix} \qquad X_f = \begin{bmatrix} d_f \\ v_f \end{bmatrix} \tag{4.37}$$

Beginning the search for the optimal trajectory from the final state the cost array is initialized at $N-1$ with $J^1_{[N-1,j]} = J^1_{[N-1,j->N,if]}$ and $J^2_{[N-1,i]} = J^2_{[N-1,i->N,i_f]}$. In the next step the trajectories at $d(N-2)$ from v_{i_1} to v_{i_2} for all i_2's are computed with $J^1_{[N-2,i_1->N-1,i_2]}$ and $J^2_{[N-2,i_1->N-1,i_2]}$. Once these costs have been calculated the Pareto optimal front of trajectories from $[d(N-2) \quad v_{i_1}]^T$ to $[d(N) \quad v_{i_f}]^T$ can be established. All trajectories that are not Pareto optimal are not stored.

Assuming that a Pareto optimal front of points j is stored at some state $X_{[N-k_1+1,i_2]}$ we can iteratively compute the Pareto optimal front of $X_{[N-k_1,i_1]}$ by calculating

$$J^1_{[N-k_1,i_1]} = (J^1_{[N-k_1,i_1->N-k_1+1,i_2]} + J^{1,j}_{[N-k_1+1,i_2]}) \tag{4.38}$$

and

$$J^2_{[N-k_1,i_1]} = (J^2_{[N-k_1,i_1->N-k_1+1,i_2]} + J^{2,j}_{[N-k_1+1,i_2]}) \tag{4.39}$$

at each i_1 for all i_2 and for all j's in the Pareto front at $v(i_2)$. Comparing the costs, non-optimal points are deleted and the new front at $X_{[N-k_1,i_1]}$ is constructed. The optimization terminates when the Pareto optimal front of $X_{[1,i_0]}$ is found.

Moving backwards in time on the x-axis the sets of Pareto optimal trajectories will get larger and an increasing number of Pareto optimal points appear at each step. This results in an increase in calculations per step and therefore in computation time, since more trajectories are searched at each distance. However, in order to find the Pareto front only a certain amount of points are needed. Therefore a truncation method, presented in 4.3.1.1, was used to reduce the number of points in the Pareto front in order to reduce the computational load of the optimization.

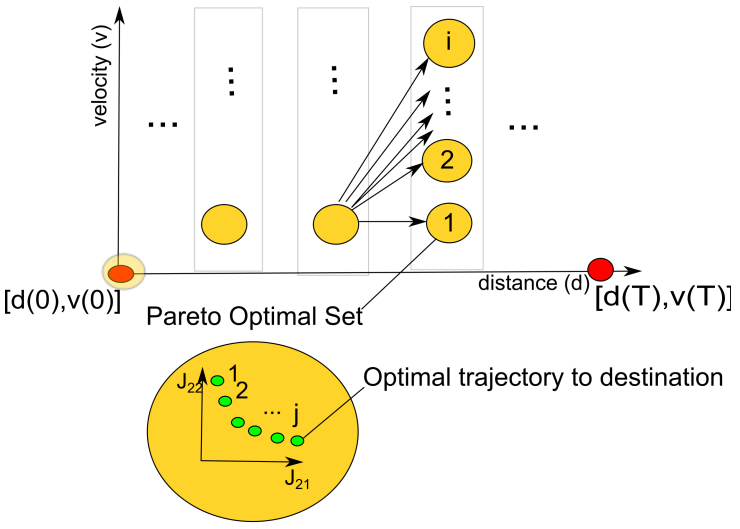

FIGURE 4.10: Pareto Front with Dynamic Programming

4.3.1.1 Truncation method

Storing an entire set of optimal points at every state, it becomes impossible to only store the indices of the optimal path and retracing the velocity profile later. In order to be able to construct all optimal trajectories in the Pareto optimal front it is necessary to store the optimal speed profile for each trajectory while calculating them. This implies storing multiple velocity trajectories at each state. The algorithm is therefore not only costly in computational time but also requires a large amount of memory. Due to this fact it is important to use truncation methods with an appropriate maximum number of trajectories that should be maintained throughout the calculation process. The proposed truncation method [92] deletes points from a curve while maintaining the shape of the curve visible. In order to achieve this, points in high density areas are erased.

In this method the distances to the first, second and third closest points are calculated for each point in the set. The points are then sorted in order of increasing distance to other points. When two points have the same distance to the first closest point, the distance to the second closest point is taken into consideration. After deleting the first in order, the process is repeated, distances are re-calculated and the points are sorted.

This process can be explained with the help of Figure 4.11. Here, in a first iteration, point one is erased because it has the closest first and second point, then point two is deleted and finally, in a third iteration, point three as well. With this method

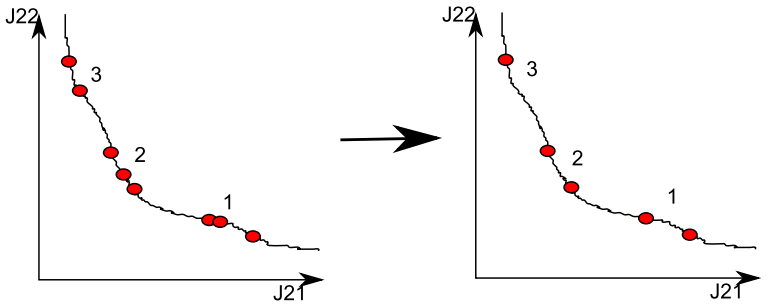

FIGURE 4.11: Truncation Method for Pareto Optimal Front

the number of points in a set can be reduced to a desired amount while the Pareto optimal front stays visible.

This multi-objective optimization was found suitable for off-line optimization. The approach can be used to identify the relationship between several objectives. However the computation process is costly in calculation time and memory. In the following the algorithms is demonstrated on a simple example.

4.3.2 A simple example

To illustrate the described multi-objective trajectory optimization method a simple mission was chosen. The vehicle operation of a conventional vehicle is optimized for a 300m road section between stop signs. With this mission the constraints on initial and final states can be fixed by

$$X_o = \begin{bmatrix} d_o \\ v_o \end{bmatrix} = \begin{bmatrix} 0 \\ 0 \end{bmatrix} \qquad X_f = \begin{bmatrix} d_f \\ v_f \end{bmatrix} = \begin{bmatrix} 300 \\ 0 \end{bmatrix} \tag{4.40}$$

No maximum speed constraints are defined for now, only the limitations on acceleration due to the mechanical constraints of the vehicle are taken into account.

The example problem is solved using the fixed time dynamic programming optimization method and the multi-objective optimization method. In the following the results and computational time of the two methods are compared. We will briefly discuss the trade of between trip time and energy consumption.

4.3.2.1 Comparison of the two optimization methods

To discuss and compare the two methods of computation, the optimal solution to the mission was computed using the fixed time method for several final time constraints. Considering the flexible time problem, the Pareto optimal front was calculated for two different values of truncations. A truncation value of j implies that j points (here j velocity trajectories) were saved at each state. Therefore, not only j trajectories in the final Pareto optimal set are considered, but rather the amount of points in the front at each state within X_f and X_o is truncated. With this, we expect that the calculation with higher truncation values will give better results.

With the results in fuel consumption, trip time and computation time the advantages and disadvantages of the two methods can be compared. In Figure 4.12 the results of this study are shown. The plot shows the calculated Pareto optimal front for a truncation number of 10 as green stars. The Pareto front with a truncation value of 30 is represented by blue circles. We can see that the results of the two options fall onto about the same curve. However, the solution with higher truncation value shows a much smoother result.

In addition, plotted as red crosses in Figure 4.12, the solution to the fixed time constraint method is presented. It can be seen that the differences of the two methods are not very significant. With both methods we can evaluate the optimal velocity trajectory of a given vehicle, for a specified mission. Using the fixed time method the trade-off between fuel and time does only become apparent when calculating multiple points. Here, we can see four solutions to the fixed time problem with desired final time $T_f = [25, 30, 35, 40]$s. The advantage of the multi-objective optimization approach is that it provides several solutions with different final times with only one calculation.

Dynamic programming is an optimization method for which the computational effort grows exponentially with the number of dimensions. In the computation of the Pareto optimal front the three dimensional dynamic programming problem is reduced to two dimensions. However, because it is a multi-objective optimization and, at each state, we search all possible trajectories in the Pareto optimal front, the problem has to evaluate the cost function more than K^2-times. By using the method of truncation described above the computation time can be reduced to

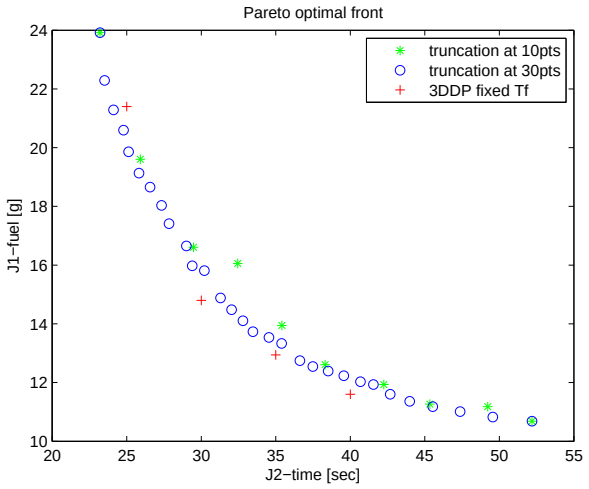

FIGURE 4.12: Pareto optimal front

Optimization method	Δ t	Δ d	Δ v	trunc pts	computation time [sec]	trajectories calculated
3D Fixed time method	2	1	1	-	240-280	1
2D Flexible time method	-	5	.2	10	155	10
2D Flexible time method	-	5	.2	30	241	30

TABLE 4.3: Grid sizes and computation time for fixed and flexible time problem

some maximum at each iteration. If no truncation is used the number of function evaluations grows with each iterative step.

In the following, computational times of the fixed time problem, solved using the three dimensional dynamic programming method, are compared to those of the multi-objective method. At this point we have to note that the computation time strongly depends on the grid choice. Larger steps in the grid obviously result in less function evaluations and therefore lower computation time. This is true for both methods. However with large steps in grid optimality cannot be guaranteed. A well balanced solution has to be found. In Table 4.3 the meshes used to compute the presented results can be seen. As mentioned in Section 4.2.2 it was found that the grid specification for the 3-dimensional dynamic programming method has to be very different from that of a 2-dimensional method.

In Table 4.3 the resulting computational times for each method can be seen. For each calculation of the fixed time problem a calculation time between 240 and 280s was needed. The difference in computation time results from the difference in the final time constraint. A longer trip time results in a longer evaluation process. Further, it can be seen that the flexible time solution, where the entire Pareto

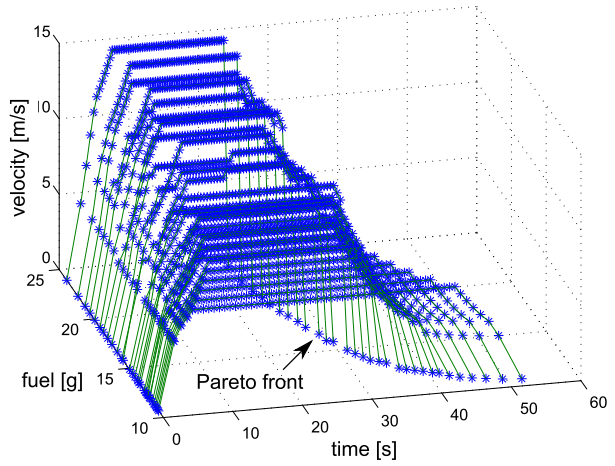

FIGURE 4.13: Velocity trajectories of Pareto optimal front

optimal front of velocity trajectories is computed, was computed in less or equal time as the fixed time problem. The entire Pareto optimal front consisting of 30 optimal trajectories was calculated in about the same time as a single solution to the fixed time problem. With these results it seems that for an analysis of eco driving gains the flexible time method is a better choice.

4.3.2.2 Trade-off between energy consumption and trip time

Using a truncation value of $j = 30$ the multi-objective dynamic programming method was used to compute 30 Pareto optimal velocity trajectories. The resulting Pareto optimal front can be found in Figure 4.12 in blue. It can be seen that due to the shape of the Pareto front a small compromise in trip time can result in large reductions in fuel consumption. This is especially true in the area where the trip time is short, here between 25s and 35s. A driver flexible in his arrival time can significantly reduce energy consumption in comparison to a driver with fixed arrival time.

In Figure 4.13 the velocity trajectories, corresponding to the 30 points in the Pareto front, are plotted in three dimensions with time on the x-axis, fuel on the y-axis and velocity on the z-axis. The drivers consuming more fuel (higher on the y-axis) are driving at higher vehicle speeds, and arrive therefore in less time. The Pareto optimal front is still slightly visible on the right in this graph.

In the following, four of the 30 trajectories were used to analyze the gains. In Figure 4.14 the four selected trajectories can be seen. In this graph the differences

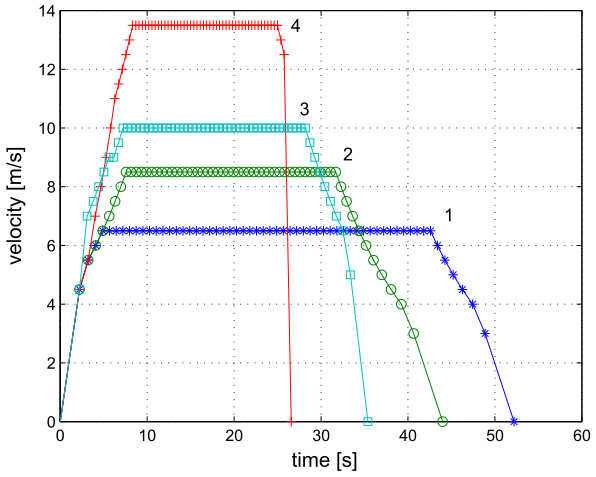

FIGURE 4.14: 4 Pareto optimal velocity trajectories

trajectory	arrival time [sec]	fuel consumed [g]
1	52	10.68
2	44	11.36
3	36	13.33
4	28	18.66

TABLE 4.4: Arrival time and fuel consumption of Pareto optimal trajectories

in vehicle speed are visible. The respective arrival times and fuel consumption of the four trajectories are presented in Table 4.4.

It can be seen that, a driver operating his vehicle at up to 14m/s will arrive within 28s, but consume 28.6% more fuel than the driver that arrives only 8s after him, driving at a maximum speed of 10m/s. However, it can also be observed from Table 4.4 that, the driver with a trip time of 44s, consuming 11.36g, can only reduce his consumption by about 6% when driving at a slower speed to arrive 8s later. Again, we can see the potential gains for very fast drivers to reduce their energy consumption.

4.4 Sensitivity analysis

In this Section we briefly want to discuss the sensitivity of the computed optimal velocity profile. The effect of minimal diverges from the optimal speed profile on energy consumption is investigated. To do so, we will use the two dimensional optimization method with a predefined weighting factor β. However, similar to the

multi-objective approach, we will store multiple velocity trajectories at each computational step. With this, not only the optimal velocity trajectory is determined but several, close to optimal, suboptimal velocity profiles.

The optimization algorithm works in the following way. Like for the multi-objective optimization, a set of multiple velocity trajectories is stored at each state. A percentage value p_{subopt} is specified to define the maximum level of sub optimality taken into account. At each step we will then not eliminate all sub-optimal trajectories, but all profiles that result in a cost higher than the cost of the most efficient trajectory plus p_{subopt} percent. This implies that, if the optimal fuel consumption at a state is given by x then the worst velocity trajectory in the stored set consumes $x + p_{subopt}$ of fuel.

The optimization approach is visualized in Figure 4.15. Similarly to the multi-objective optimization, we store multiple trajectories with costs between the optimal fuel consumption and optimal plus $p_{suboptimal}$ percent. This implies that, at each search, several trajectories have to be evaluated for each possible state. A trajectory is only eliminated from the stored set if its cost is more than p_{subopt} percent more than the optimal. With this, many trajectories have to be stored and considered at each calculation step. The truncation method, presented in Section 4.3.1.1, is therefore used to reduce the density of possible solutions.

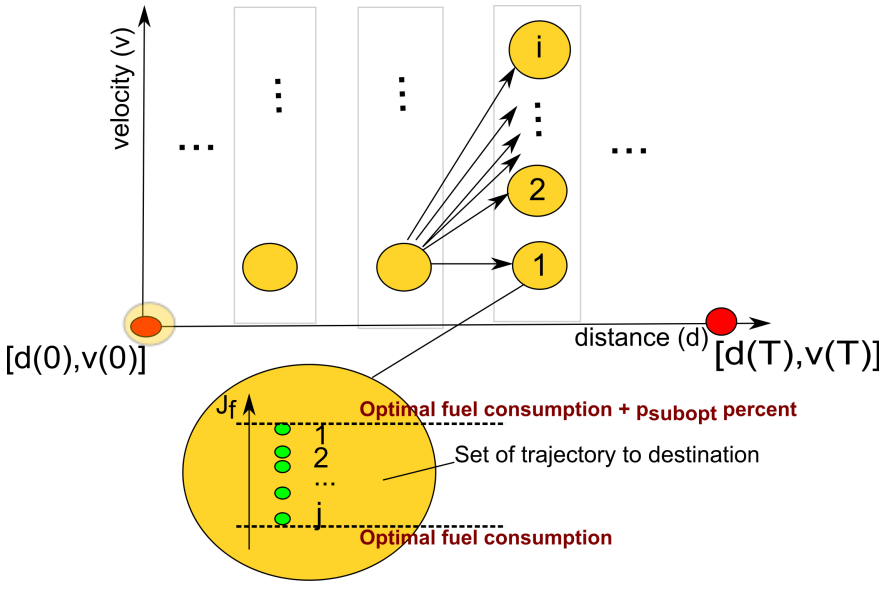

FIGURE 4.15: Sensitivity analysis with Dynamic Programming

Using this approach we were able to analyze the sensitivity of energy consumption to trajectory changes for a 300m trip. The calculation was done fixing the weighting factor β to 1 and using a truncation number of 50. Specifying $p_{subopt} = 5$, 50 suboptimal trajectories with cost up to 5% higher than the optimal trajectory were computed. The trajectories are plotted in Figure 4.16. We compare the set of suboptimal trajectories, in blue, to the optimal velocity trajectory, which can be seen in red.

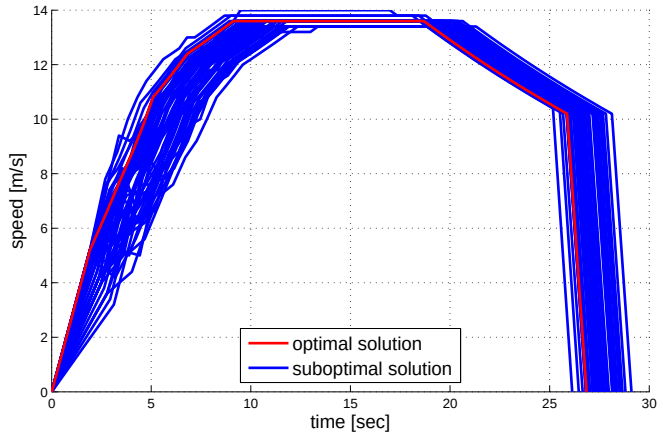

FIGURE 4.16: Optimal velocity trajectory versus suboptimal solutions

It was found that, while the acceleration phase changes drastically, we do not see much change in the stabilized cruising speed. Generally, the cruising speed is kept rather low and constant. None of the suboptimal trajectories show small accelerations or decelerations in the cruising phase. In the acceleration phase however, a variety of different rates are used to reach the stabilized speed. The deceleration phase for the different trajectories generally uses similar slopes for all the calculated suboptimal trajectories. The envelop surrounding the trajectories is much larger for acceleration and deceleration phase, while at stabilized speeds only a limited choice of velocity is given. It seems that changes to the optimal speed profile in the acceleration phase only have a limited effect on fuel consumption, here up to 5% increase. Stabilized speeds, however, seem to be very important to keep fuel consumption close to optimal.

With this analysis we can conclude that the energy consumption is very sensitive to changes in the stabilized speed phase. However, variations in the acceleration phase seem to have only little impact on fuel consumption. These findings will later be taken into account in the design of a driver assist system.

4.5 Conclusion

In this chapter the constrained trajectory optimization problem, used to identify optimal vehicle operation, was defined. The equations of motion of the dynamic vehicle system were specified in discrete time form. Using specific drive cycles and real life driving data the driver's mission can be defined. The mission parameters were used to identify trip constraints that were imposed on the initial and final states. In addition road constraints, such as distance dependent maximum speed limits were fixed.

A fixed-time single objective problem was considered at first. Due to the complexity of the cost function and to simplify constraint integration the dynamic programming method was applied. Initially, a three dimensional dynamic programming method was used to solve the problem. To reduce computational time the problem setup was reduced to two dimensions by integrating a weighting factor in the cost function. To solve the fixed time problem the two dimensional dynamic programming method was used in a nested process, in combination with root finding methods. Several root finding methods were investigated and it was found that the bisection, Ridder's and Brent's method were appropriate choices to be applied to this problem. The single objective fixed-time problem will be used in the following to compute potential gains of eco driving, while satisfying the desired trip time. For further computations the two dimensional dynamic programming method is used in combination with the Brent's root finding method.

To discuss the trade-off between trip time and energy consumption a multi-objective problem, where time is considered as a second cost, is presented. A multi-objective dynamic programming method, that can be used to solve the problem without cost function weighting, is applied to find the Pareto optimal front that presents the solution to the problem. It was found that the method has a high computational cost due to the computation of several velocity trajectories at each state. In addition a large amount of memory is necessary due to the fact that the entire velocity trajectories are stored throughout the calculation. To solve these issues a truncation method, that allowed us to reduce the number of calculated optimal velocity profiles to a desired maximum amount, was used. With this the shape of the Pareto optimal front remains visible while the computation time is reduced. Comparing the multi-objective approach to the three dimensional fixed time solution, it was found that the multi-objective dynamic programming method

represents an efficient algorithm when analyzing multiple optimal trajectories and the trade-off between trip time and energy consumption.

Finally, the developed optimization algorithms were used to identify the effects on fuel consumption when diverging from the optimal velocity profile. A sensitivity analysis showed that, while the acceleration phase is less important for optimality, the appropriate stabilized cruising speed seems very important to keep energy consumption low.

Chapter 5

Potential Gains of Eco Driving

Contents

One objective of this thesis work is to identify the potential gains of eco driving for different drive train technologies. It is well known that certain vehicle operations reduce energy consumption. However, to justify further research efforts on the

concept of eco driving it is important to investigate how high these reductions could be. To compute the upper limit, the maximum theoretical potential gains of eco driving need to be determined. This implies that no unpredictable constraints, such as traffic, are considered. In addition the driver is assumed to be perfect, which means that the velocity profile is driven as computed, without delays or other human errors.

In Chapter 3 a simulation model of three different vehicle drive trains, the conventional, electric and hybrid vehicle, were constructed. With the optimization method presented in Chapter 4 these models can be used to compute vehicle specific optimal velocity trajectories for given missions. Comparing the optimal velocity profile to the original mission, represented by a standard drive cycle or real-life driving data, the theoretical gains in energy consumption can be evaluated. Applying an optimization algorithm with a physical vehicle model, the optimal, mission dependent, vehicle operation is calculated. With this, vehicle specific, energy efficient operation can be identified. An analysis of the resulting vehicle operation can provide insights on important factors for eco driving.

In this chapter the potential gains of eco driving and drive train specific optimal vehicle operation are discussed. The optimal velocity profiles are calculated by use of the two dimensional dynamic programming trajectory optimization method. Three types of drive trains are considered: the conventional, the electric and the hybrid vehicle. In Table 5.1 an overview of the studied problems is given.

Section 5.1 deals with the optimal vehicle operation of the conventional vehicle. First we evaluate the ideal velocity trajectory for four vehicle missions (Section 5.1.1). The simulated vehicle operation is then verified in a hardware-in-the-loop setting on an engine test bench. Experimental results and fuel consumption measurements can be found in Section 5.1.2. Potential gains of eco driving for different missions are computed. In Section 5.1.3 the optimal vehicle operation is analyzed and important factors for eco driving are discussed in Section 5.1.4.

Energetically optimal operation of a vehicle with electric drive train is presented in Section 5.2. With the help of real-life driving data, the most efficient operation of a small electric vehicle was computed (Section 5.2.1). A chassis test bench is used to verify the theoretical results and measure the energy consumption for the ideal eco cycles (Section 5.2.2). With the analysis of optimal operation of the electric drive train vehicle, in Section 5.2.3, important factor for eco driving with electric

drive train	problems studied	method of verification
conventional	• NEDC standard cycle • urban driving • extra-urban driving • freeway driving • road grade integration	engine test bench
electric	• ECE-15 standard cycle • urban driving • adapted extra-urban driving	chassis dynamometer
power split hybrid	• extra-urban driving	-

TABLE 5.1: Overview of studied problems

vehicles can be deduced. Recommendations on most efficient driving for electric vehicles are found in Section 5.2.4.

In Section 5.3 the hybrid vehicle is studied. As a representative example, the velocity trajectory of the Toyota Prius, power-split hybrid vehicle was optimized. For the hybrid vehicle, being a more complex case, the optimization algorithm had to be adapted (Section 5.3.1). Due to their two power sources, hybrid vehicles are known to achieve lower fuel economy values than conventional vehicles. However, in order to reduce energy consumption, the consumption in both power sources needs to be considered. Appropriate methods to evaluate the energy consumption of the Prius hybrid vehicle for a trip are discussed in Section 5.3.2. The vehicle operation was optimized for a representative real-life driving cycle. The vehicle specific, ideal velocity trajectory is analyzed in Section 5.3.3.

5.1 Conventional vehicle

The Peugeot 308 vehicle was presented as an example of a conventional vehicle in Section 3.3. Modeling the drive train components and the vehicle chassis, it has been shown that the operating efficiency strongly depends on vehicle velocity and acceleration. In the drive train it is important to make the best choice of gear in order to move the engine operating point to a desired region and therefore increase its combustion efficiency or decrease pollutant emissions. In addition, it was found that the energy needed to propel the vehicle is related to the driven velocity by the resistance forces. With several parameters to be taken into account it is difficult to select the appropriate vehicle operation for a mission applying simple rules.

In this section a numerical optimization method is applied to compute the energetically best velocity profile for the conventional vehicle for a desired mission. The ideal velocity profile is calculated for four different drive cycles that represent urban, highway and freeway driving. Section 5.1.1 presents a comparison between original driving mission and computed eco driving cycle. In Section 5.1.2 an engine test bench is used to verify the results in an experimental hardware-in-the-loop setting. Finally, an analysis of most efficient vehicle operation is shown in Section 5.1.3 and most important factors for eco driving will be highlighted (Section 5.1.4).

5.1.1 The ideal velocity trajectory

For the case of the conventional vehicle four different drive cycles were used for comparison of optimal and general vehicle operation. We expect that gains due to eco driving depend on the situation the vehicle is in. For example, for freeway driving the vehicle operation is usually rather constant and engine efficiency is generally high, we therefore expect smaller gains due to eco driving behavior than in an urban setting where a lot of acceleration and deceleration phases are necessary due to frequent stops. We therefore consider drive cycles representing various real life situations.

In Figure 5.1 the original velocity trajectory of the four examined drive cycles can be seen. In this graph the velocity profile as a function of time are represented in the first plot and the vehicle speed as a function of distance is shown in the second plot. The data is used to identify trip and road constraints for the optimization

drive cycle	maximum speed [km/h]	number of stops	distance [m]	time [s]
NEDC	120	12	11010	887
HYZURB	58	4	3475	560
HYZROUT	103	5	11220	754
HYZAUTO	138	3	46200	1741

TABLE 5.2: Drive cycle specification

setup. From the first plot the initial and final velocity can be determined, as well as the intermediary stops and stop duration. The second plot shows initial and final distance. Shown in red on the second plot is the road constraint. The maximum speed limitation is defined as a function of distance. Table 5.2 shows a summary of drive cycle parameters, such as distance, time, maximum speed and number of stops.

The first graph in Figure 5.1 shows the New European Drive Cycle (NEDC). This is a standard drive cycle used in Europe to compute fuel economy and emission values for conventional vehicles. With its squared shape we suspect that it does not give a good representation of actual driving behavior. Therefore, to simulate general driving behavior three drive cycles were used, which represent real-life driving [93]. The HYZURB cycle, shown on the top right in Figure 5.1 presents an urban drive cycle, where the vehicle speed rarely goes above 50km/h. We can see that many short acceleration and deceleration phases are present in this cycle. A third cycle, called HYZROUT, stands for extra-urban driving. The cycle is shown in the second graph on the left. Here, vehicle speed reaches a maximum of around 100km/h. There are still many acceleration and deceleration phases present, but not as frequent as in the urban setting. The last cycle, HYZAUTO, models freeway driving. In this case the profile has an initial acceleration phase and a final deceleration phase. Throughout the trip only one stop is shown and the average vehicle speed is rather high.

The described cycles were used to specify trip and road constraints. The nested two dimensional dynamic programming optimization method with a discretization step of $\Delta d = 5$ and $\Delta v = .2$ was then applied to derive the corresponding eco cycles, that resulted in the same driving mission but minimized the vehicle's fuel consumption. The inverse vehicle model constructed in Section 3.3 was used to ensure optimal, fuel efficient gear choices. Figure 5.2 presents the computed optimal vehicle operation for the four different cycles. For each cycle the original velocity profile (blue) is plotted in comparison with the eco drive cycle (red,

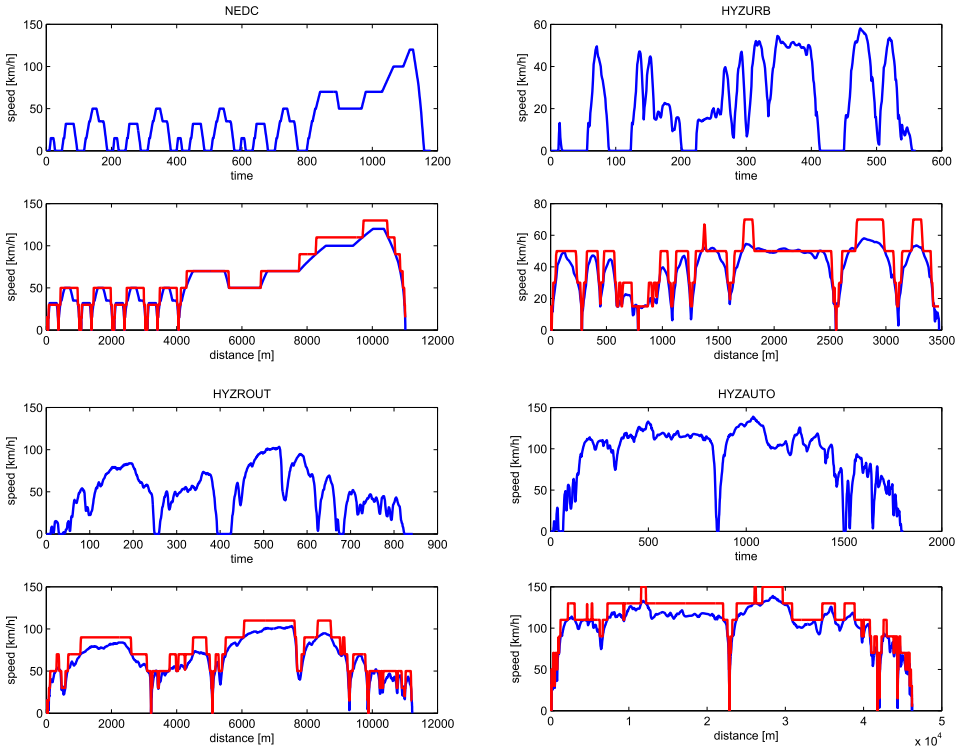

FIGURE 5.1: Maximum speed constraints for various drive cycles

cycle	gain in fuel consumption due to eco driving
NEDC	17.9%
HYZURB	27.2%
HYZROUT	25.1%
HYZAUTO	7.9%

TABLE 5.3: Gains in fuel consumption

dashed) in the first plot. The gear selection for the two cycles is shown in a second plot, where the original driver's gear selection is shown in blue and the optimal gear selection for the eco cycle is drawn in red. A summary of the gains in fuel consumption between the original cycle and corresponding eco cycle can be seen in Table 5.3. It can be seen that potential gains in fuel consumption lie between 8 and 27%.

From the results in Figure 5.2 we can observe that the optimal velocity trajectory uses rather high acceleration rates, increasing the vehicle speed rapidly, to reach a lower cruising speed than used in the original drive cycle. Since the problem was solved as a fixed time problem the average velocity of the two cycles stays the same. It can be seen that the vehicle stops are sometimes shifted in time. This is due to the fact that a constraint for a stop was defined in distance. This means

the vehicle has to stop at a certain distance, but independent of its arrival time at that distance. The idling time is added post-optimization at each stop. This way to integrate the constraint is useful for stop signs. However, for stop light timing this approach might not be the best. In this work we did not include the timing of stops, in future work if the time of stop light phases is known, this could be integrated in the optimization.

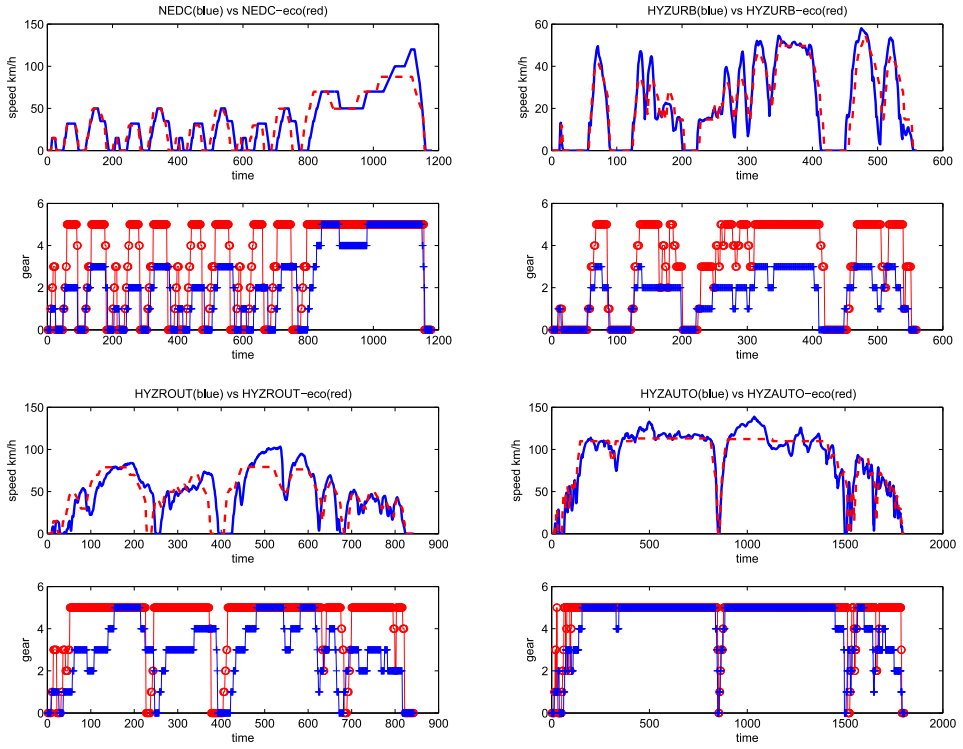

FIGURE 5.2: Standard drive cycle vs computed eco-driving profile

From the second plots it can be seen that the optimal gear selection is very different from the choice taken by the original driver. In general the gears are chosen higher in the eco cycle. It is assumed that this is to improve the engine efficiency. An in depth analysis of the vehicle operation is presented in Section 5.1.3, where engine and drive train efficiencies will be discussed. To identify the potential gains of eco driving the calculated optimal velocity profiles were tested in an experimental setup.

5.1.2 Verification on engine test bench

Hardware-in-the-loop experiments are often used to verify simulated concepts. With this approach a certain part of the hardware is running in real time, while

the rest is simulated on a computer. With this setup algorithms can be tested in a controlled experimental setting. In our case, the calculated drive cycles were tested on an engine test bench, where the engine is running in real time while the rest of the vehicle is simulated.

Figure 5.3 shows the experimental setup of the engine test bench. Here, the vehicle chassis, drive-shaft and clutch are simulated using the VEHIL software [94]. The Peugeot 308's EP6 internal combustion engine, being the hardware component in the loop, is running in real time. The DSpace MicroAutoBox Controller is used to run the vehicle simulation and command the EP6 engine in real time. The input to the vehicle model is the driver's demand for acceleration or deceleration which is directly translated into throttle and break command. In the VEHIL software the driver is modeled by a simple PID controller, which ensures that the desired drive cycle is followed as good as possible.

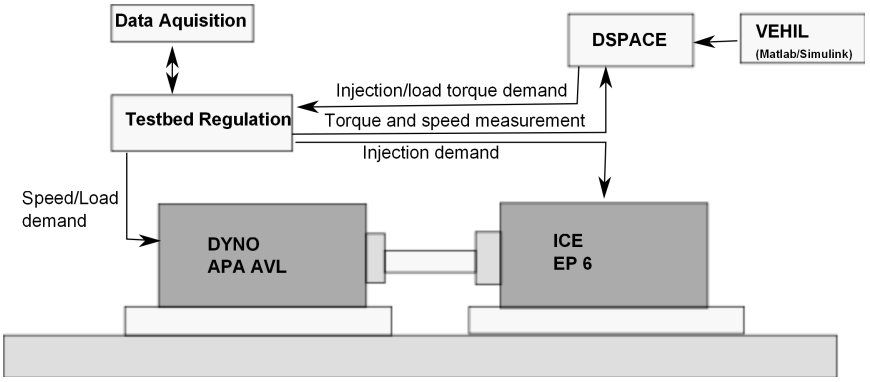

FIGURE 5.3: Engine test bench set-up

The AVL[1] engine test bench consists of an electric machine, that is connected to the engine output shaft, and a controller that regulates the shaft speed. The AVL electric machine simulates the vehicle load on the engine shaft by regulating the shaft to the speed calculated by the vehicle simulation. The fuel is measured by the AVL fuel balance that allows us to measure fuel dynamically throughout the experiment. In Table 5.4 details of the test bench components can be found. The described hardware-in-the-loop setup allowed us to measure the engine's actual fuel consumption and therefore compute the fuel economy of the vehicle for a given cycle.

In a real life implementation of eco driving strategies the driver will never be able to exactly follow the calculated optimal velocity profile. In this experimental

[1] AVL is a company for the development of power train systems, https://www.avl.com/

Electric machine	AVL APA 102/E
EM maximum torque	255Nm
EM speed range	0-10000rpm
EM force sensor	Z6FC3, 200kg
EM speed sensor	ROD 426 001B-01024
Speed sensor on engine shaft	AVL 364C/364X Angle Encoder
Fuel measurement	AVL Fuel Balance 730

TABLE 5.4: Parameters of Engine Test Bench Equipment

setup the driver is represented by a PID controller, simulating an automated, ideal, driver. Still, the desired drive cycle will not be followed exactly. This is also due to the fact that it was calculated using an inverse vehicle model where gear changes happen instantaneously. In Figure 5.4 the desired drive cycle input can be seen together with the actual velocity trajectory driven by the virtual vehicle. It can be seen that the used PID controller results in satisfactory tracking of the desired velocity profile. Due to this difference and non simulated dynamic phenomena there was a slight difference in fuel consumption between the simulated inverse model and the measured consumption in the dynamic hardware-in-the-loop setting. For the NEDC cycle, seen in Figure 5.4 the simulated fuel consumption was found to be 6.6L/100km. With the measurements we calculated 6.7L/100km. The difference seemed to be acceptable for the 11.8km cycle.

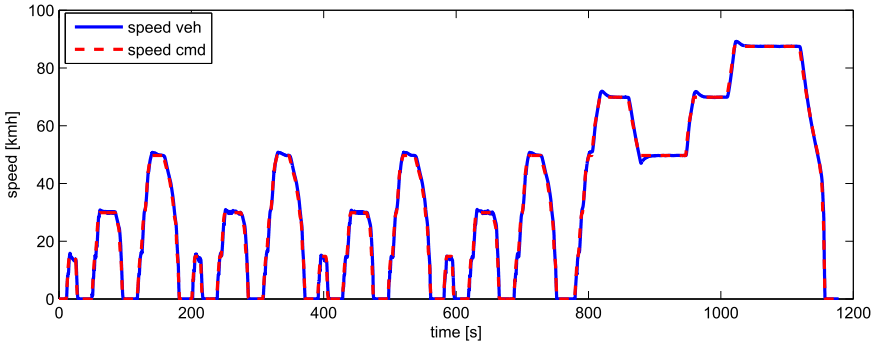

FIGURE 5.4: Velocity trajectory simulated and followed in experiment

Each drive cycle was experimentally tested three times to eliminate measurement errors. In Table 5.5 the average fuel economy values can be seen for the four tested cycles. When comparing the original drive cycle to the computed optimal eco drive cycle we found that between 8 and 27 % less fuel was used for the eco cycle. As expected higher gains due to eco driving were detected in urban settings than when driving on the highway. For the highway cycle eco driving showed a potential reduction in fuel consumption of 8%, while the consumption of the real

drive cycle	original [L/100km]	eco [L/100km]	reduction [%]
NEDC	6.7	5.5	17.9
HYZURB	9.76	7.11	27.2
HYZROUT	7.22	5.41	25.1
HYZAUTO	6.92	6.37	7.9

TABLE 5.5: Fuel Consumption [L/100km] Original Drive Cycle vs Eco-Drive Cycle

life urban cycle could be reduced by 27%. Although the standard NEDC cycle already shows very squared use a reduction of up to 17.9% is possible for this cycle when applying optimal vehicle operation.

We should remind the reader at this point that the eco driver performs the same mission and therefore covers the same distance in the same time. Changes in energy consumption are solely due to the choice of gear and the selected rates of velocity and acceleration. In Section 5.1.3 the optimal vehicle operation is discussed in detail to investigate the origin of the savings in fuel consumption

5.1.3 Analysis

In order to understand the reasons for the reductions in energy consumption the vehicle operation needs to be analyzed. This will help us gain an understanding of most efficient vehicle operation. Identifying most important factors for eco driving can be helpful to encourage drivers to apply eco driving strategies. Further the knowledge can be applied in the development of driver support systems for eco driving.

For comparison of optimal vehicle operation and original drive cycle the NEDC cycle will be investigated in more detail. Table 5.5 tells us that the fuel consumption was reduced by almost 18% between the baseline and eco cycle. The optimal velocity trajectory of this cycle together with the original cycle are presented in Figure 5.2 on the top left. As previously mentioned the gear was chosen for the eco driving cycle such that the engine operation results in the most efficient combustion process. We can therefore see that the gear choice between the original cycle and the eco cycle are very different. Generally, the engaged gear is much higher for the eco cycle. In Figure 5.5 the resulting engine operation for the two tested cycles can be observed.

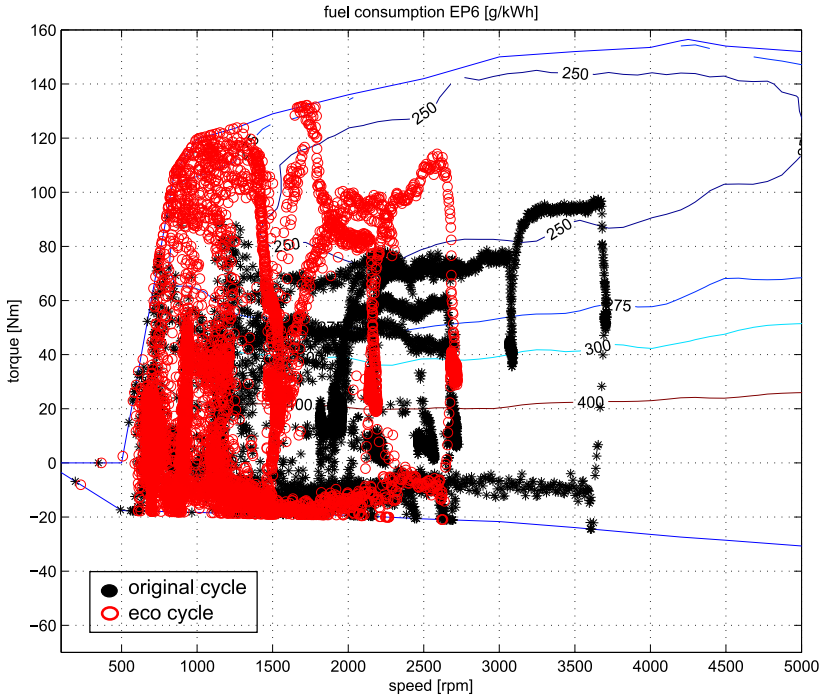

FIGURE 5.5: Engine operation of NEDC standard cycle and eco-cycle

In black (stars) the engine operation of the original NEDC cycle can be seen. For this cycle the engine is used up to a speed of over 3500rpm and the torque of the engine output is mostly lower than half of the maximum available engine torque. For the eco cycle, plotted as red circles, it is shown that due to the gear selection the engine is running at low speed, up to just over 2500rpm, and high torque. The engine's maximum torque output is used especially at low engine speeds. In addition when looking at the negative torque range it becomes obvious that the deceleration rates used in the eco cycle are chosen such that engine braking can be used at its maximum. The operating points mostly lie close to the minimum torque line. At this point injection is cut and no fuel is needed to keep the engine running.

With the operation, seen in Figure 5.5 ,the engine efficiency was improved from 19% for the original cycle to 24% for the eco drive cycle. When computing efficiency values for other major components in the drive train, such as clutch, gear box, and final drive, it was found that variations in efficiency were minimal. However, a 5% increase in engine efficiency can hardly be responsible for an 18% reduction in fuel consumption over the drive cycle. Computing the mechanical energy needed to perform the drive cycle, it was found that, while the standard

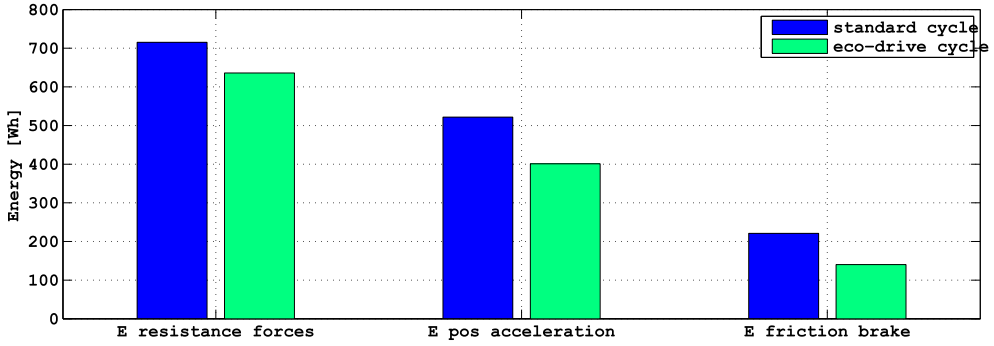

FIGURE 5.6: Energy saved on resistance forces, acceleration and braking

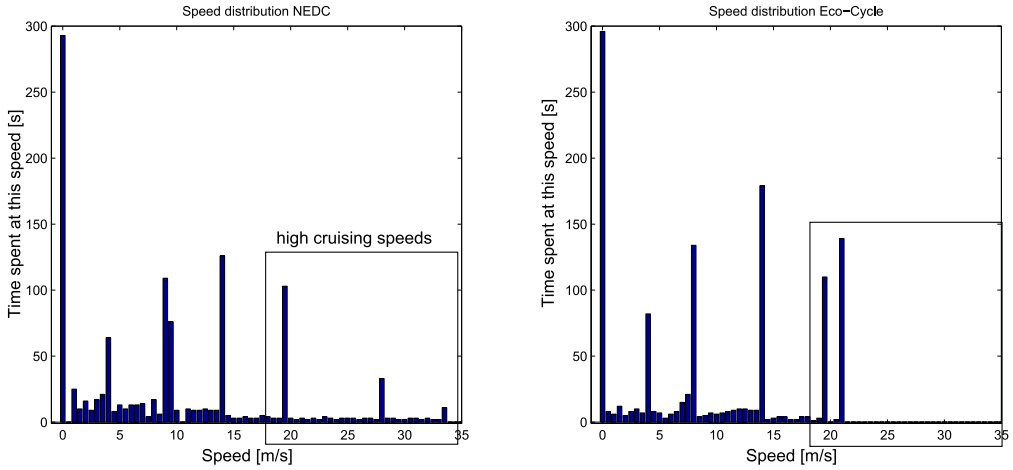

FIGURE 5.7: Velocity distribution of standard cycle (left) and eco-cycle (right)

cycle uses 1237Wh, the eco-drive cycle only consumed 1036Wh. This reduction in energy is due to the choice of velocity and acceleration rates.

In Figure 5.6 three bar graphs can be seen. The figure is used to compare energy consumed for the original and the eco cycle. The energy used to overcome the resistance forces, the aerodynamic drag and the rolling resistance, is represented by the first bars, on the left. The force needed to overcome the aerodynamic drag grows quadratically with the vehicle speed. The constant speeds, where acceleration rates are zero, chosen for the two cycles can be observed in Figure 5.7. It can be observed that the standard cycle uses much higher cruising speeds than the eco cycle. Therefore, the energy needed to overcome the aerodynamic drag, which grows quadratically with speed, is much higher. This results in 11% more energy that the vehicle needs to provide, to overcome the resistance forces.

The bars in the middle of Figure 5.6 show energy used on positive acceleration. It

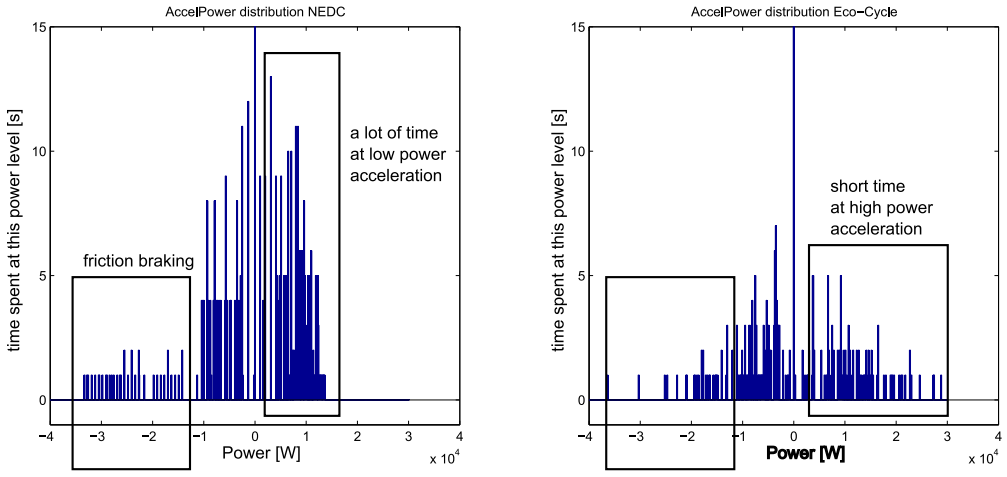

FIGURE 5.8: Acceleration power distribution of standard cycle (left) and eco-cycle (right)

was found that the energy on acceleration needed for the eco drive cycle is much lower than for the original cycle. Figure 5.8 shows the distribution of acceleration power, which is calculated as a product of mass, acceleration and velocity. ‘

$$\dot{E}_{posaccel} = \frac{d}{dt}(\frac{1}{2}mv^2) = Mv\dot{v} = Ma^{+}v \tag{5.1}$$

We can observe that the eco cycle uses higher acceleration power rates. However, it was found that the cumulative power used for acceleration was less for the eco cycle than for the standard cycle. Due to the choice of higher but short acceleration phases at rather low speeds the energy is lower than that for the standard cycle. Over the entire cycle the optimized velocity trajectory uses 23.2% less energy on positive acceleration.

The third group of bars in Figure 5.6 shows energy lost in friction braking. Using deceleration rates that allow for engine braking results in lower fuel economy. This is because the kinetic energy is then used to run the engine while, when braking with the mechanical friction brake, the energy is lost in heat. In the standard drive cycle the energy lost on friction braking is 36% higher than that of the eco-cycle. In Figure 5.8 this can be seen in the range of negative acceleration power. The original drive cycle uses much higher power rates for vehicle deceleration. Such high negative rates of output power can only be provided by the friction brake in a conventional vehicle.

5.1.4 Important factors for conventional vehicle eco driving

From the analysis of the optimal vehicle operation we can conclude that there are several factors that are important to reduce energy consumption for the conventional vehicle. It should be noted that these factors are derived for a desired mission with constraints in distance, velocity and time.

The gear selection in the conventional vehicle is important to improve the combustion efficiency in the engine. It was shown that an engine operation at low speed but high torque is best for the examined vehicle drive train. To push the engine operating point into the high torque, low speed region usually the highest possible gears are engaged.

It was shown that, in order to reduce fuel consumption the cruising speed of the vehicle has to be selected as low as possible. With this the energy necessary to overcome the aerodynamic drag is reduced. This seems to be a very important parameters. In order to reduce the cruising speed, rather high acceleration rates are used to acceleration the vehicle rapidly to the desired speed. Loosing time in the acceleration phase would result in higher cruising speeds in order to reach the target within the fixed trip time.

The deceleration phase usually consists of a coasting phase, where engine braking is used at its best. This phase uses rather low deceleration rates. However, the second part of the deceleration phase uses hard friction braking to come to a full stop. Here, engine braking is not used to fully decelerate the vehicle because this would result in a long deceleration phase and, in order to respect the average trip velocity, the maximum vehicle speed would have to be selected higher. With the aim to reduce the time used on acceleration and deceleration, rather high rates are used. This then allows us to use lower maximum vehicle speeds while still satisfying the time constraint.

From these results it could be expected that reducing the vehicle speed will always result in lower fuel consumption. With this assumption, simple rules for eco driving could be stated. However, it is not as simple as that. With the vehicle velocity the energy needed to overcome the aerodynamic drag is reduced. The aerodynamic drag force, as stated in Section 3.2, grows quadratically with the vehicle speed. This implies that, reducing the vehicle's velocity at high speeds, a significant reduction in energy consumption due to aerodynamic drag can be achieved. For

small vehicle velocities this reduction is rather small for the same changes in vehicle speed. Increasing the trip time, the vehicle velocity and acceleration rates are reduced. This results in lower efficiencies of the drive train components. Engine efficiency is reduced and the clutch is slipping. When average vehicle speed drops below a certain value, we found this to be around 25km/h, the decreasing efficiency outweighs the gains in energy due to reductions of aerodynamic drag. Similarly to the studies of Hooker [12] we found that an optimal trip time exists at which fuel consumption is reduced to its minimum. Further increasing the travel time results in losses in the drive train that cannot be compensated for by reductions in resistance forces.

5.1.5 Effect of road grade

In order to identify overall optimal vehicle operation the road profile needs to be taken into account. In our work road grade is directly integrated in the vehicle model, simulating the grade resistance force on the chassis. While we will not investigate the effects of road grade in detail, a simple example will here be used to show that grade is an important factor that cannot be neglected.

As an example a real life driving profile was used. The drive cycle together with the road profile is presented in Figure 5.9. The profile represents a driver that leaves the city of Grenoble at the bottom of the mountain, drives up to the skiing region Chamrousse, and finishes back down in the valley at Grenoble. The road grade of the trip reaches a maximum of 12%. The trip is almost a hundred kilometers long and takes 6929s, which converts to almost 2 hours. The imposed maximum speed constraint derived from the driver's velocity profile can be seen in red in Figure 5.9.

The cycle was used to derive trip and road constraints. The two dimensional dynamic programming method was then applied to identify the optimal speed profile. Two different cases were considered for comparison. First, the velocity profile was computed not taking into account road grade. We here assumed the mission was taking place on a flat road. In a second calculation the road grade was included in the optimization process. The resulting velocity profiles can be seen in Figure 5.10. While it is generally assumed that an increase in vehicle speed in downhill sections leads to more fuel efficient operation we could here not confirm these assumptions.

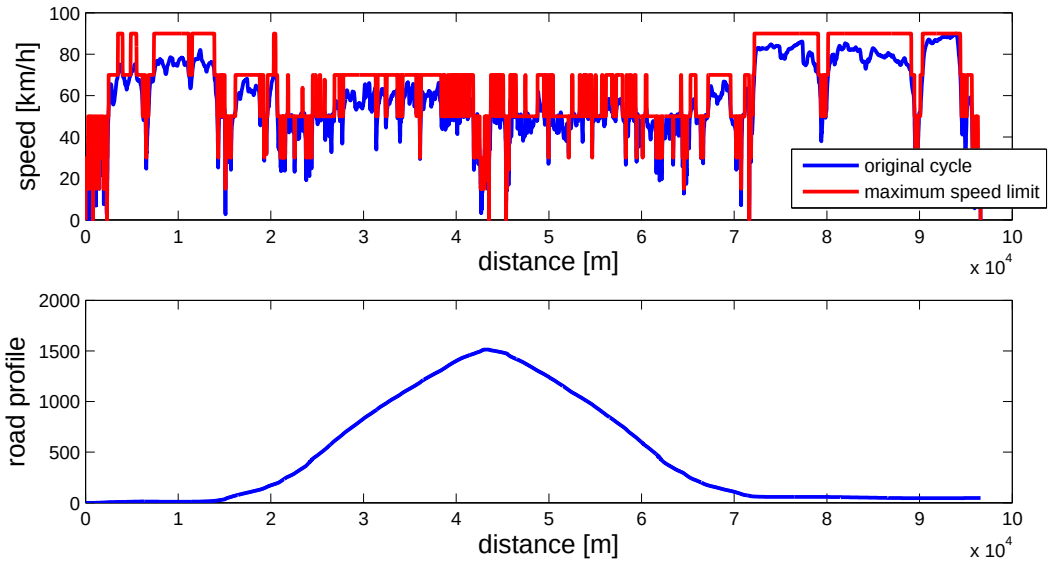

FIGURE 5.9: Drive cycle with grade

Investigating Figure 5.10 it was found that the velocity profile determined with grade used lower speeds prior and after the hill. The zones where the velocity of the cycle calculated with grade exceeds the cycle computed without grade are here highlighted in pink. The green zones mark the parts where the grade optimal speed is inferior. Throughout driving on hills the vehicle speed for the grade optimization trajectory was sometimes higher. However, this occurred on uphill as well as on downhill driving. Using the direct VEHLIB simulation the fuel consumption for both velocity profiles over the hilly road was simulated. For the velocity trajectory that was optimized without taking into account road grade, the vehicle consumed 5.06L/100km. Using the grade information as an input a fuel consumption of 4.96L/100km could be achieved. Integrating the road grade in the optimization process the globally optimal velocity profile can be calculated which results in 5% less fuel consumption for the trip.

With this study we can see that road grade is an important criterion to be taken into account when identifying the optimal velocity trajectory for a trip. However, it seems that optimal vehicle operation when driving over hills is not easily identified. To further analyze the problem different up- and downhill situations need to be investigated in future work.

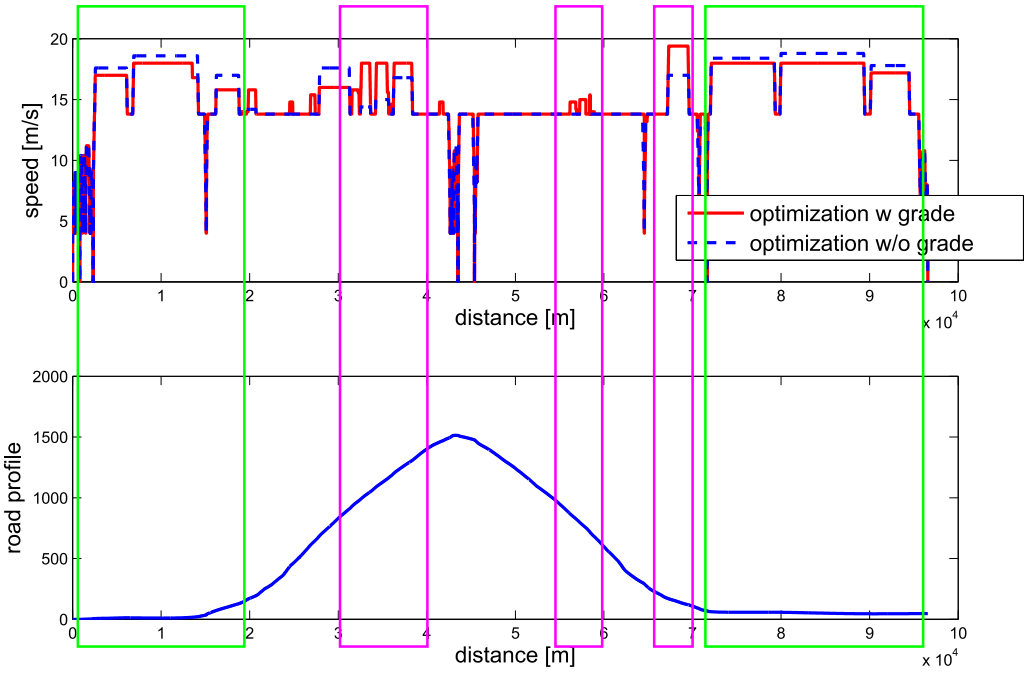

FIGURE 5.10: Optimal speed profile with and without road grade integration

5.2 Electric vehicle

With today's environmental problems the electric vehicle is becoming more and more popular. Due to the differences in drive train, optimal vehicle operation will not necessarily be the same as for the conventional vehicle. In this section the optimal vehicle operation of a small electric test vehicle, the AIXAM Mega City, is investigated. The goal is to minimize battery power used (P_{batt}) for an entire trip. The vehicle model described in Section 3.4 is used in combination with the two dimensional dynamic programming method (Section 4.2.2) to compute the eco cycle for a given driving mission.

In Section 5.2.1 the considered drive cycles are presented and corresponding optimal, eco drive cycles are calculated. To verify the simulated potential gains of eco driving, the drive cycles are tested on a chassis test bench (5.2.2). Section 5.2.3 shows an analysis of the identified optimal vehicle operation, comparing general driving to eco driving. A summary of important factors for eco driving for electric drive train vehicles can be found in Section 5.2.4.

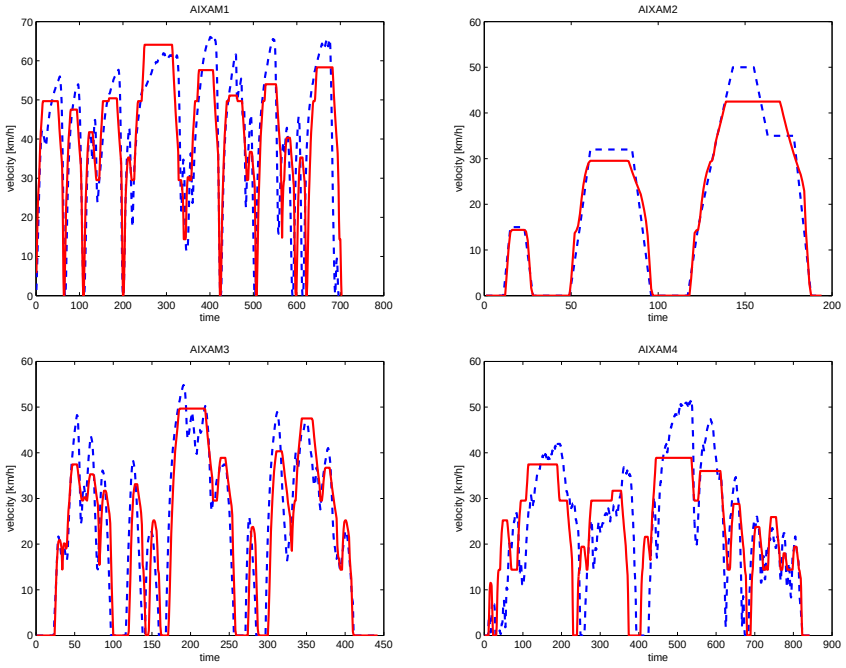

FIGURE 5.11: Standard drive cycle vs computed eco-driving profile electric vehicle

5.2.1 The ideal velocity trajectory

The AIXAM Mega City electric vehicle can reach a maximum speed of about 65km/h. Due to this constraint it was not possible to test standard cycles, like the NEDC, where the vehicle speed reaches up to 120km/h. Therefore, specific cycles for the electric vehicle were constructed. The baseline cycles can be seen in Figure 5.11 in blue (dashed line). Four cycles were considered. The cycle on the top left (AIXAM1) and bottom left (AIXAM3) represent real life drive cycles. Here, stored velocity profiles of a driver, that used the AIXAM Mega City vehicle in an actual trip was used. The plot seen on the top right (AIXAM2) shows the first part of the standard NEDC cycle, often referred to as ECE-15. This is a very short cycle, where the vehicle runs for less than 200s. The fourth cycle, here named AIXAM4, is a scaled cycle. The cycle is usually used to represent extra-urban driving. Here, the velocity was divided by two such that the electric vehicle's maximum speed was not exceeded.

Figure 5.11 shows the computed optimal velocity profiles in red. Due to the fixed time constraint in the optimization the eco cycles arrive at the destination at the same time as the baseline drive cycles. The vehicle has therefore covered the same distance in the same time. As previously seen for the conventional vehicle, the

maximum speeds of the eco cycles are lower than those of the original cycles. It is expected that this is due to the energy that can be saved when reducing the aerodynamic drag forces.

From Table 5.6 we can see that potential gains between 5 - 19% can be achieved due to eco driving. In the following, the simulated, theoretically optimal velocity profiles are tested in an experimental setup on a chassis test stand. With this the actual energy consumption can be measured for the original and for the computed eco drive cycles.

5.2.2 Verification on chassis test bench

On a chassis dynamometer the vehicle is running in real-time while the driver follows a desired velocity profile. A schematic of the CLEMESSY[2] chassis test bench is presented in Figure 5.12. The tested electric vehicle has a front-wheel-drive drive train configuration. The vehicle is therefore placed with the front wheels on the test bench rollers. The two test bench rollers are connected to an electric machine to simulate the resistance and inertial forces of the vehicle. The electric machine has the ability to output a maximum torque of 3000Nm and can provide up to 132kW. For safety an emergency brake is attached to the dynamometer shaft on the right to bring the rollers to a stop when needed. The test bench can simulate vehicle speeds up to 200km/h. A ventilation system is used to simulate air motion proportional to vehicle speed. This is necessary such that the cooling mechanisms controlling the temperature of drive train components can work properly.

A picture of the experimental setup can be seen in Figures 5.13. The small electric vehicle is attached such that it stays stationary. The vehicle's front tires are turned on the rolling dynamometer, while the rear wheels are at rest. The drive cycle is presented to the driver in the form of a vertical line that is displayed on a computer screen in front of the vehicle. Each one of the cycles was driven three times, in order to get sufficient data to support conclusions. To eliminate effects of varying battery losses due to different battery charge, the cycles were alternated, testing always pairs of original and eco cycle with similar battery charge. The battery was never depleted lower than 50% of charge. An on-board storage device was used to

[2]CLEMESSY: French company that works on design and integration in the fields of electrical engineering, process automation and mechanized systems; http://en.clemessy.com/

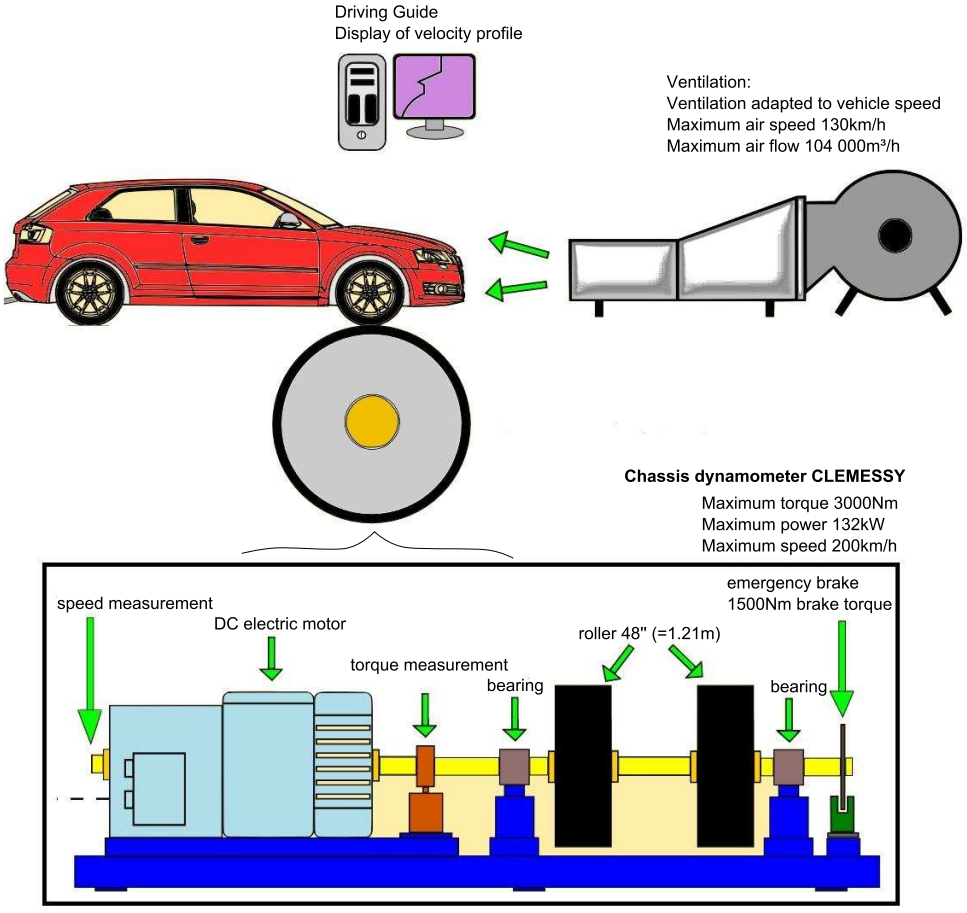

FIGURE 5.12: Chassis dynamometer schematic

cycle	original cycle	eco cycle	gain
AIXAM1	872.2	705.56	19.3%
AIXAM2	89.4	85.56	4.5%
AIXAM3	283.3	248.89	12.1%
AIXAM4	427.78	386.11	9.4%

TABLE 5.6: Energy Consumption in Wh

store the battery operation throughout each experiment. The energy consumption for the four original and eco drive cycles computed in Wh can be seen in Table 5.6.

The results show that for the four tested cycles a reduction in energy consumption between 5 and 19% was possible. The AIXAM2 cycle shows the smallest gain due to eco driving. This was to be expected, since the cycle represents the rather squared standard cycle and represents a very small driving period. The two real-life driving cycles AIXAM1 and AIXAM3 show the highest potential gains. The

FIGURE 5.13: Chassis test bench

reason for this could be that electric vehicles are still new to drivers, and are not used as intuitively as conventional vehicles. The scaled extra-urban cycle showed a 9.4% improvement in energy consumption between the original and the eco cycle.

In the following the drive cycles will be analyzed in more detail. In Section 5.2.3 the operation of each component in the drive train is investigated in order to gain insights on most important parameters for eco driving of electric vehicles.

5.2.3 Analysis

The AIXAM1 cycle was chosen for comparison between most efficient vehicle operation and original cycle. Since the electric vehicle considered does not contain a gear box the gain of 19.3% in energy consumption has to be uniquely due to vehicle operation. First, the changes in efficiencies of drive train components were investigated. It was expected that the optimal vehicle operation results in a more efficient electric motor/generator operation. However, it was found that this was not the case.

In Table 5.7 the efficiencies of major drive train components can be observed. For the electric components the motoring and generating phases are listed separately. We found that the electric machine's efficiency values improved slightly for the generating phase, but decreased a little for the motoring phase. Similarly the efficiency of the battery was not found to change significantly. It can therefore be

assumed that the changes in energy consumption over the drive cycles are not due to increases in component efficiency.

components	original cycle (motor/generator phase)	eco cycle (motor/generator phase)
Final Drive [%]	94	94
Electric Motor [%]	70.82/57.14	69.4/59.5
Battery [%]	92.8/99.31	92.87/99.29

TABLE 5.7: Component efficiency

Looking at the energy output at the wheels it was found that, similarly to the case of the conventional vehicle, due to the correct choices of vehicle velocity and acceleration the eco cycle simply requires less energy. Due to lower choices of vehicle speed the resistance forces where reduced. Energy necessary to accelerate the vehicle's inertia was reduced by applying appropriate acceleration rates at low vehicle speeds. In Figure 5.14 a comparison of the energy necessary to overcome the resistance forces and to accelerate the vehicle's inertia for the two cycles is shown on the left. The stacked bar graph on the left shows the original cycle, while the right bar represents the eco cycle. It can be seen that, while a small amount is saved due to a reduction in resistance forces, namely the aerodynamic drag and the rolling resistance, a larger amount of energy is saved due to the energy necessary to accelerate the vehicle's mass. It was found that for optimal vehicle operation rather short, high acceleration rates should be used at low speeds, to rapidly reach the lowest possible constant speed necessary to reach the destination in a desired time.

Figure 5.14 displays the energy distribution for the deceleration phase on the right. The sections of the stacked bar graphs represent the energy lost on mechanical friction braking, the energy lost on losses in the drive train components while regenerating energy, and energy that is regenerated and used to charge the electric battery. As mentioned in Section 3.4.1, the electric vehicle considered in this study does not utilize a regenerative brake pedal. Only deceleration rates up to a fixed torque can be used to recover electric energy. Deceleration rates exceeding this limit are realized by the use of the mechanical friction brake. For the original drive cycle, using higher deceleration rates, more energy is lost in heat due to friction braking than with the optimal velocity trajectory. Even when the regenerative braking capability is used the component operation results in losses. A certain amount of recovered energy is therefore lost on the way and never reaches the

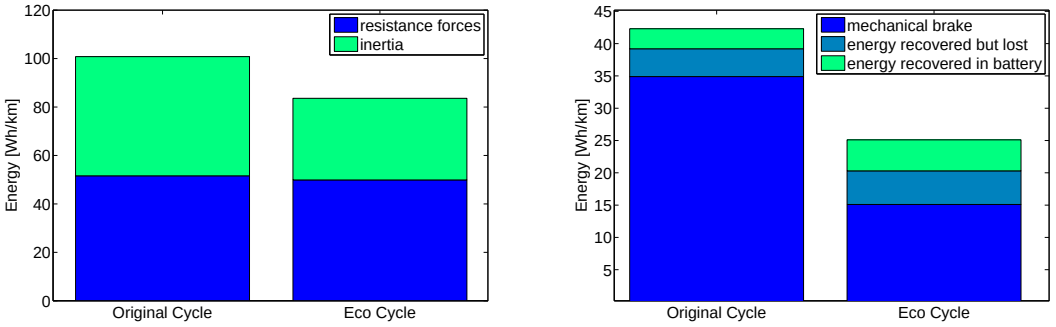

FIGURE 5.14: Energy Consumption in Motoring and Deceleration Phase of AIXAM1

battery. Due to inappropriate deceleration rates these losses are high in the case of the original drive cycle. For these reasons the original drive cycle cannot regenerate more energy than the eco drive cycle, although a lot more energy is available for recovery (Figure 5.14).

5.2.4 Important factors for electric vehicle eco driving

From the analysis it was found that for urban and extra-urban missions the efficiency of drive train components has little influence on the energy consumption of an electric vehicle. The choice of acceleration rates, operating speeds and deceleration rates are most important for eco driving.

Similarly to the conventional vehicle, the losses due to aerodynamic drag grow with increasing vehicle speed. To reduce the energy needed to overcome aerodynamic forces, vehicle speeds have to be kept as low as possible. High acceleration rates are therefore used to accelerate the vehicle in a short time to the desired cruising speed. In the braking phase, vehicle specific deceleration rates should be used. Drive train specific deceleration rates can ensure that the maximum possible amount of energy is regenerated using the reversible electric components.

As for the conventional vehicle, driving an electric vehicle an energetically optimal arrival time exists. The efficiency of the electric motor, presented in Section 3.4.1, decreases with its operating speed. Running the motor at speeds close to zero results in very low efficiencies. Using the electric machine in generator mode at low speed we sometimes even draw current from the battery, although the drive train should be operated in charging mode. This is due to very high losses in this mode of operation. Running the vehicle at low speeds it was found that losses,

such as the ones in the electric motor/generator, outbalanced the improvements in energy consumption due to reductions in aerodynamic forces. In comparison to the conventional drive train discussed previously, however, this speed was found to be below 20km/h for the simulated electric drive train.

5.3 Hybrid vehicle

The third type of vehicle treated in this work is the hybrid drive train vehicle. Containing two or more power sources, this vehicle architecture presents a more complex case than the conventional and electric vehicle. Since vehicle functionality of the hybrid vehicle is not at all intuitive it is important to use numerical optimization methods to identify the optimal vehicle operation. With this we hope to be able to specify eco driving factors for hybrid vehicles.

As a representative hybrid vehicle the well-known Toyota Prius power split hybrid vehicle was used. The vehicle model was constructed in Section 3.5 together with a simulation of the control strategy integrated to manage the vehicle's power split. Due to the complexity of the hybrid vehicle the dynamic programming optimization method cannot be used in its classic way. In the hybrid drive train the power split control strategy uses the battery state-of-charge to determine the vehicle's operation. A computation of the eco cycle in reverse time is therefore not possible. Small changes are needed to adapt the optimization algorithm to the particular case of the hybrid vehicle. These are presented in Section 5.3.1.

For a driver of a hybrid vehicle the energy consumption is represented by the fuel used. However, to analyze the energy consumption over a trip the initial and final battery charge of the vehicle have to be taken into account. In Section 5.3.2 several different approaches to compare energy consumption of hybrid vehicles are discussed. Section 5.3.3 shows the results of an optimization of the Prius over an extra-urban drive cycle and the analysis of the ideal velocity profile for hybrid vehicles.

5.3.1 Hybrid vehicle optimization

The applied dynamic programming optimization method, used in the standard way, computes the optimal solution by searching from the final state backwards

on the time-axis to the initial state. However, this implies that the cost of some edge on the graph only depends on its initial and final state. For the conventional vehicle drive train this is true. The operating cost of the vehicle only depends on the initial and final distance and speed at each step. For the electric vehicle a simplified model was constructed, such that the energy consumption of the vehicle does not depend on the battery state-of-charge. This is a justified simplification since the losses in the battery only vary minimally with changes in SOC.

However, for the case of the hybrid vehicle, the vehicle operation strongly depends on the battery state (3.5). Dependent on the battery SOC the engine can be turned off, or used to propel the vehicle. This means that the cost of vehicle operation will vary significantly with the battery state-of-charge. Therefore the cost of vehicle operation depends not only on initial and final states, but also on the previous vehicle operation, which is used to compute the current SOC. Starting the optimization process from the final state in distance the SOC of the vehicle is not known. However the SOC is known at the initial distance at initial time.

To adapt the optimization method to the vehicle model, we therefore used the dynamic programming approach while computing the optimal trajectory from the initial state, keeping track of the current battery state, to the final state. This variation of the method was tested on the conventional and electric drive train vehicles. The results of the forward and backward dynamic programming method are identical. For the optimization of the Prius vehicle this method can be used to optimize the drive train operation taking into account battery SOC variations.

The two dimensional optimization process can be described by the following steps:

- Initialize optimal costs at $k_1 = 2$: $J^*_{[2,i]} = J_{[1,i_0->2,i]}$
- Increment k_1 and find the optimal cost at each state by comparing $J^*_{[k_1,i_2]} = \min_{i_1}(J_{[k_1-1,i_1->k_1,i_2]} + J^*_{[k_1-1,i_1]})$ while storing the optimal indices
- Compute the optimal trajectory by retracing the stored indices

The control strategy applied to a hybrid drive train represents a key aspect of the vehicle, which has a strong influence on the vehicle's fuel economy. In addition, the energy management strategy in hybrid vehicles makes sure that battery charge never exceeds a certain upper limit or drops below a specified lower boundary. With this in mind, we initially assumed that the battery charge level is

controlled by Toyota's energy management strategy. However, first optimization results showed that only considering fuel consumption when optimizing the vehicle's operation over a drive cycle is not sufficient. The optimization algorithm seems to make the best instantaneous choice of vehicle operation, however, without taking into account the effect this operation has on future computational steps. As an example, if the vehicle is at a low battery level the vehicle's velocity is decreased to avoid turning on the internal combustion engine. At this point deceleration might not be optimal, but since all-electric mode is considered of no cost at this point the lower vehicle speed is chosen. This, instantaneous optimal operation, leads to a high battery depletion and later, possibly inefficient charging.

It was concluded that, although the control strategy balances the battery charge, to optimize the vehicle trajectory we still need to consider the total instantaneous energy consumption in the objective function. A weighted cost function that combines fuel consumption and battery use, is therefore proposed:

$$\gamma_{veh}^{hyb}(t) = \dot{m}_{fuel_i}(t_i -> t_{i+1})\Delta t - \alpha \Delta SOC(\Delta t_i) \tag{5.2}$$

With this cost function the changes in energy in the battery are taken into account as well as fuel consumption. Charging the battery will result in a positive change in SOC. An increased charge in the battery can later be used to propel the vehicle. It should therefore have a positive effect on the cost. A discharge will show in a negative change in SOC. A discharged battery needs to be re-charged later, and more fuel will therefore be used later. This operation needs to be weighted negatively. With this analysis we chose to subtract the cost of battery use from the cost due to fuel consumption. The required weighting factor α will therefore take on a positive value. However, an exact value for α is not easily specified.

In Section 5.3.3 the appropriate value for α will be investigated for a specific driving mission. Before comparing the optimization results for different velocity trajectories the 'consumption' of a hybrid vehicle needs to be defined. Section 5.3.2 shows commonly used fuel consumption definitions that can be used for comparison of drive train efficiency or to test the effectiveness of implemented energy management strategies.

5.3.2 The consumption of a hybrid vehicle

It is difficult to compare fuel consumption for hybrid vehicles and draw conclusions about fuel economy. For a specified cycle the final fuel consumption can be very different, dependent on initial state-of-charge in the battery. Also, due to the logic in the control strategy the fuel consumption does not only depend on distance driven. Dependent on the level of power demand the battery might be more or less discharged. Comparing the energy consumption of a cycle to another one result, might show low fuel consumption but a significant discharge in the battery, while another velocity profile resulted in higher fuel consumption and a high final SOC in the battery. Only using fuel consumption values to determine the trip efficiency might lead to false conclusions.

There are several approaches to solve this problem. A rating procedure of fuel economy was first published in 1999 by the Society of Automotive Engineers (SAE). Their standard SAE J 1711 presents a 'recommended practice for measuring the exhaust emissions and fuel economy of hybrid-electric vehicles' [95]. For an overall use of electric energy smaller than 1% of the energy consumed in fuel, the SAE guidelines claim that the energy consumption of the battery is negligible. This implies that only fuel consumption has to be considered if the following equation holds:

$$\frac{|electric \quad energy|}{energy \quad in \quad fuel} <= 1\% \tag{5.3}$$

If the difference between consumed electric energy and fuel consumption is to large one way to reduce this difference is to test the vehicle over a longer distance. Due to the control strategy, implemented to keep battery charge around a target value, the battery charge should stay balanced over very long trips. Running a drive cycle multiple times should therefore lead to a continuous increase in fuel consumption, but not in the change of final battery charge. For this procedure it is necessary to start the test at some battery charge within the limitation boundaries of the control strategy. A disadvantage of this procedure is the (experimental or computational) cost.

In 2002 an additional SAE guideline was released [96]. It presents a method that is applicable if the change in battery charge is less than 5% of the fuel consumption. The approach uses linear interpolation to approximate the fuel economy of a hybrid

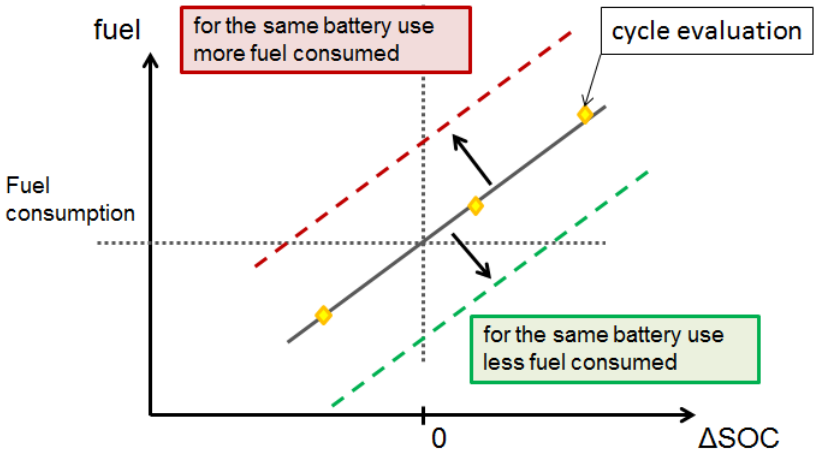

FIGURE 5.15: Definition of Fuel Consumption for Hybrid Vehicle

vehicle for charge sustaining battery use. This process can be explained with the help of Figure 5.15. In this figure the consumption of the hybrid vehicle over a cycle is plotted in a graph with the axis of fuel consumption and ΔSOC. ΔSOC stands for the electric energy consumption and represents the difference in battery state-of-charge between the beginning and the end of a trip.

Using the method proposed in the 2002 SAE guidelines the vehicle is tested over a cycle at least two times. For the two tests, two different initial battery charge levels are used. If the target battery charge value of the control strategy is known, these two initial SOC values can be chosen intelligently. A first test should use an initial battery charge below the target value, but within the boundary values of the energy management, such that the battery is being recharged throughout the cycle. This would lead to a high fuel consumption and positive ΔSOC. An initial SOC value higher than the target value should be used for the second test. With this the control strategy will operate in charge depleting mode and fuel consumption will be low. The ΔSOC will be small or negative for the cycle. In Figure 5.15 the computed cycles are shown as yellow diamonds. In our example a third point was computed for verification.

Given the two points a linear interpolation can be used to compute fuel consumption for a change in battery charge level. To compare fuel consumption, we usually search for the actual fuel used by the vehicle, when operated in charge sustaining mode, meaning that the change in battery state-of-charge over the cycle is small or equal to zero. From Figure 5.15 the charge sustaining fuel consumption can be approximated by evaluating the fuel consumption value, where the line intersects the displayed zero ΔSOC line.

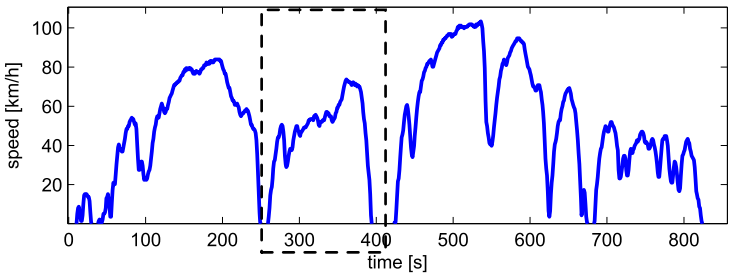

FIGURE 5.16: Real-life drive cycle for Prius

The slope of the line in Figure 5.15 is usually drive train and control strategy dependent. However, for different drive cycles, such as urban or highway cycles, the efficiency of the vehicle operation changes. This can be observed in a shift of the line. A cycle represented by a parallel line shifted to the upper left represents a velocity profile that has worse fuel economy. In this case the vehicle used more fuel for similar battery discharges. A shift to the bottom right corresponds to less fuel consumption. Here, less fuel was used for the same battery discharge. This method will be used in the following to evaluate the optimized velocity profiles.

5.3.3 The ideal velocity trajectory

To investigate potential gains of eco driving for hybrid vehicle we optimized the operation of the Prius hybrid vehicle for a mission that represents real-life, extra-urban driving. The tested drive cycle is presented in Figure 5.16, where vehicle velocity is plotted as a function of time. With their ability to regenerate energy, hybrid vehicles usually have an advantage in urban settings, where the vehicle has to perform a lot of stops. This cycle was chosen for testing because, although vehicle speeds go up to almost 100km/h, there are several acceleration and deceleration phases where the use of the alternative power source will be useful. Using the cycle data, optimization constraints in distance, velocity and time were defined. To solve the fixed time constraint optimization the nested optimization method, combining two dimensional dynamic programming with root finding methods, was applied.

In order to solve the optimization problem the weighting factor α in Equation 5.2 needs to be specified. α represents the trade-off between the electric energy, used from the battery, and the gasoline fuel consumption. To choose an appropriate weighting factor, we need to understand the effect different α values have on the

optimization result. Initial wide range calculations showed that an appropriate value for α needs to be selected at around 3. An array of different α values was defined, with a fine grid around the value 3.

$$\alpha = [0, 2, 3, 3.25, 3.5, 3.75, 4, 5, 6] \tag{5.4}$$

With the vehicle model constructed in Section 3.5 and the optimization approach described in Section 5.3.1 it is now possible to compute the optimal velocity profile for the specified extra-urban trip. To compare the optimization results using the linear interpolation method, presented in Section 5.3.2, vehicle operation needs to be evaluated for at least two different initial battery charge levels. The trajectory optimization method was therefore solved for each α_i for three different initial battery charge levels: $SOC_{ini} = [40, 50, 60]\%$.

The results are presented in Figure 5.17 and 5.18. The graphs show the changes in battery charge over the cycle on the x-axis and the fuel consumed on the y-axis. Figure 5.17 illustrates the effect of the weighting factor α on the optimization result. Each plotted curve in this graph represents an initial battery charge level. The points on the curve represent an optimized solution for one of the α factors. To reduce the complexity of the graph the corresponding α values were only labeled for one of the three curves. It can be seen that choosing different weights on the electric energy results in very different consumption and battery charge levels over the cycle. A high α value, corresponding to the right most solution points on the curve, will lead to a high positive ΔSOC. In this case the battery is charging most of the time, since charging has a reducing effect on the cost. Reducing the weighting factor α the battery charge level at the end of the cycle is lower and fuel consumption is reduced. Less fuel was transformed into electric energy. However, for an α value of zero the ΔSOC value is further reduced, but fuel consumption is increased. In this case, less energy is recovered in the battery while more fuel was consumed. This leads to the conclusion that overall more energy must have been consumed.

In Figure 5.18 the same solution points were plotted. However, while Figure 5.17 showed the dependency on initial SOC value, we can here see the solution points plotted dependent on the weighting factor α. This graph can be used to compare the energy efficiency of the optimization results using the method proposed by SAE. For each α value the optimal velocity trajectory was computed

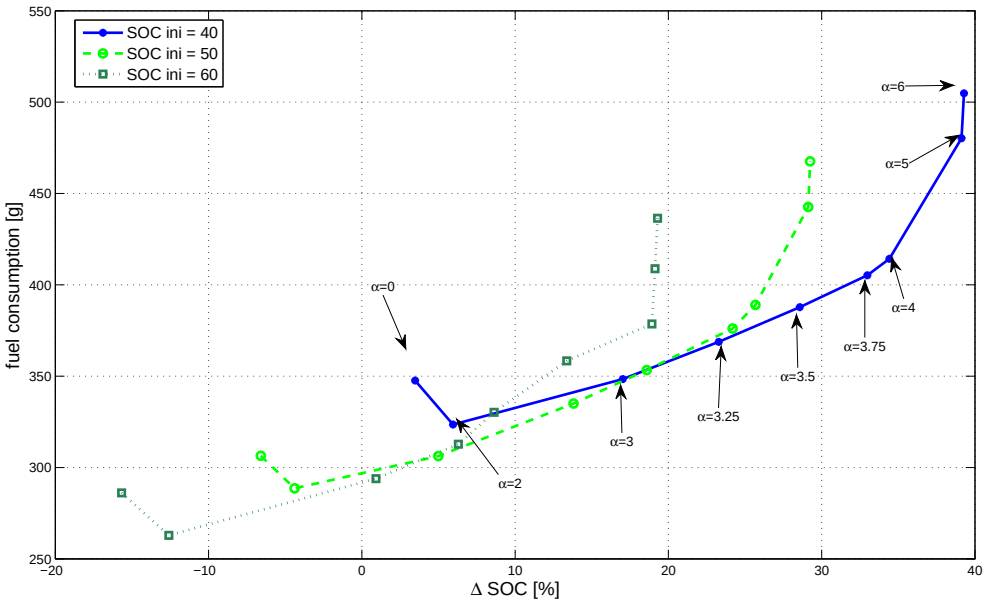

FIGURE 5.17: Fuel consumption versus ΔSOC dependent on initial SOC

for three different initial battery charge values. Each line in this graph represents the solutions to an optimization with a specified α value. In addition, the vehicle consumption was simulated for the original cycle and added to the graph for comparison. The linear interpolation line of the original drive cycle is represented by the magenta line (non-dashed). For all α values it can be seen that using a lower initial battery charge results in battery charging vehicle operation and high initial battery charges lead to battery depleting vehicle operation.

Figure 5.18 shows that the consumption of the original cycle is much higher than that of some of the optimization results. Using an α factor of 3 or 3.25 the vehicle's fuel consumption can theoretically drop more than 20% for similar final levels of battery charge. Nevertheless, it can be seen that the α value has to be specified in an appropriate range in order to achieve global energetically optimal vehicle operation. A lower α value, close to zero, results in less battery charging but still increases the overall energy consumption for the trip. A very high choice of the weighting factor can result in unnecessary battery charging and therefore wasted energy in transformation losses.

To analyze most efficient hybrid vehicle operation in detail a section of the previously studied drive cycle was chosen. The selection in Figure 5.16 shows a 150s segment between two stops. As previously, the optimal velocity trajectory was

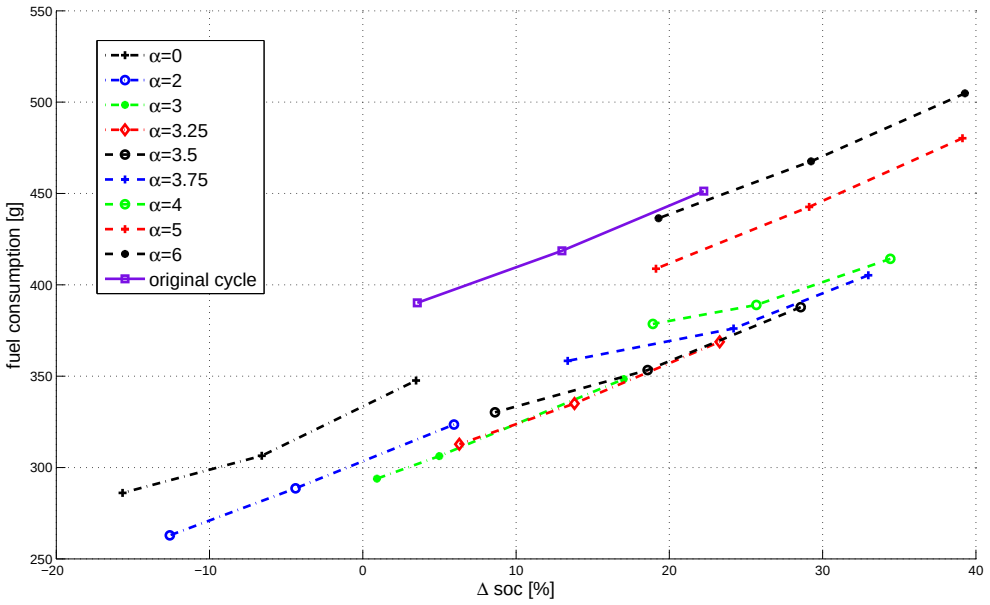

FIGURE 5.18: Fuel consumption versus ΔSOC dependent on α

computed for different α values. For an initial battery charge of 50% the resulting velocity profiles are plotted for $\alpha = [0, 3, 6]$ in Figure 5.19. The original velocity profile for this segment is shown in red. The black (dotted) line represent the optimal velocity trajectory when specifying an α value of 6 in the optimization process. The energetically best velocity profile computed with a weighting factor of 3 can be seen in green. If electric battery use is not taken into account, and α is set to zero, the optimization resulted in the blue velocity profile.

The three velocity trajectories show clearly the effect of a non-appropriate weighting factor in the cost function. When battery use was weighted to high, here seen as the black velocity trajectory, the optimal velocity trajectory shows oscillations. The vehicle is never operated at constant speed. It is either accelerated, with high power demand, or regenerative braking is used. To operate the vehicle in charging mode at all times the vehicle speed is used to force the control strategy to demand battery charging. The energy management in the Prius hybrid vehicle is constructed such that, when high power demands occur, the engine is turned on. The engine output is used to satisfy the wheel demand and/or charge the battery. At high acceleration rates the battery is therefore rarely discharged. When the vehicle is decelerated the electric system is always in regenerative mode and the kinetic energy is used to increase battery charge levels. The velocity trajectory results in high fuel uses, but also in a high final battery charge. However, due to

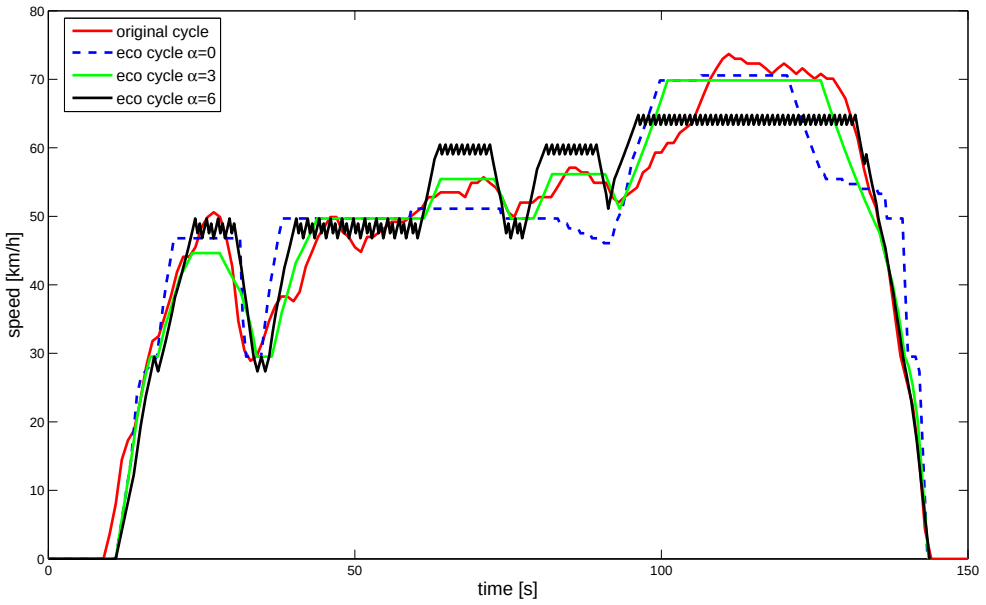

FIGURE 5.19: Eco drive cycles for different alpha values

the transformation losses this operation cannot be globally optimal. In addition, following the specified velocity profile would result in very fast mode switching, which was not penalized in the inverse vehicle model.

When battery operation is not taken into account, it seems that electric energy is freely used at inappropriate times and the internal combustion engine is only turned on when necessary. With this the battery is used in depleting mode. Nevertheless, the engine has to be used at some point, when sufficient electric energy is not available. In Figure 5.19 the blue profile represents the solution to the optimization where α was set to zero. The engine is mostly turned off. When the battery's discharge reaches levels close to the control boundaries the vehicle's speed is reduced such that the engine does not have to be started. This operation can be seen at $t = 85 - 100s$ and at $t = 130s$ in Figure 5.19. With this, the vehicle can stay in electric mode, which results in zero cost. This vehicle use does not result in globally optimal operation. While final fuel levels are rather low, the battery is discharged and will eventually have to be recharged. Low α values might be applicable to the case of a plug-in hybrid vehicle, where battery charge depletion is normal at the end of a trip.

The energetically optimal velocity trajectory can be computed with a weighting factor of around three. The green velocity profile in Figure 5.19 shows globally

efficient vehicle use in comparison to the originally driven segment.

The entire extra-urban drive cycle and its corresponding optimal eco cycle were tested using the dynamic VEHLIB vehicle simulation. Considering the correct balance of electric and fossil fuel energy the vehicle consumed 4.02 L/100km to perform the trip, while the original drive cycle used 4.83 L/100km. The battery, having an initial SOC value of 50% for both profiles, was charged to 64.1% while the original profile resulted in a final battery charge of 60.3%. With this the overall energy consumption was reduced. To understand most efficient vehicle functionality the operation of each major drive train component was analyzed. In Table 5.8 the average efficiency of each component in motoring and regenerative phase can be observed.

components	original cycle (motor/generator phase)	eco cycle (motor/generator phase)
Final Drive [%]	97	97
EM1 [%]	86.2/87.2	87.2/89.4
EM2 [%]	88.1/88.2	90.8/90.7
Engine [%]	35.1	35.0
Battery [%]	96.3/91.4	96.7/94.7

TABLE 5.8: Component efficiency

We found that, while the efficiencies of the electric components increased slightly for the eco cycle, the engine efficiency was reduced by a small amount. Nonetheless, we can assume that a major reduction in energy consumption is not due to small increases in component efficiencies in the drive train. The chassis operation was therefore investigated. Similarly to the electric and conventional vehicle, it was established that, as a result of intelligent choice of acceleration and velocity rates, the energy necessary to overcome resistance forces and to accelerate the vehicle's inertia was reduced. Likewise, it seems that the rate of deceleration is critical in order to regenerate a maximum amount of energy. In Figure 5.20 bar graphs are used to illustrate the energy consumption of the Prius over the original and the optimal drive cycle in motoring and in deceleration phase.

In the first graph the energy needed to overcome resistance forces, which includes rolling resistance and aerodynamic drag, can be seen in blue. The energy used to accelerate the vehicle's mass is shown in the stacked graph in green. It was found that the sum of energy is a lot higher for the original cycle than for the eco cycle. This leads to higher overall energy consumption of the original cycle. Investigating

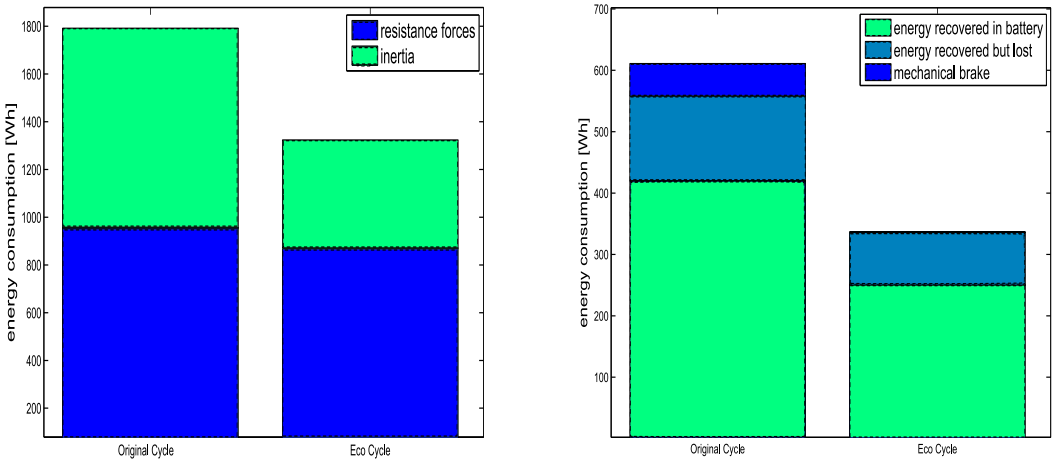

FIGURE 5.20: Energy Consumption in Motoring and Deceleration Phase of Prius

the deceleration phase, it was found that, with the applied deceleration rates, less energy was available for recovery for the eco drive cycle. However, from the second graph in Figure 5.20 it can be seen that for the original cycle the deceleration phase was not adapted to the vehicle architecture. Hence, the percentage of kinetic energy regenerated and actually used to charge the battery is lower. In the original drive cycle a small percentage of energy is lost in friction braking, while the eco cycle uses almost never the mechanical brake. The eco cycle recovered 74.3% of the energy available for regeneration, while the original cycle was able to regenerate only 68.7%.

With this analysis it was concluded that, for the hybrid vehicle discussed, the losses in the drive train due to varying efficiencies are not as important for eco driving as the losses due to increasing resistance forces and acceleration power. In order to reduce energy consumption the vehicle speed should be kept as low as possible to reduce energy spent on resistance forces, and particularly to overcome the aerodynamic drag forces. High acceleration rates were used over short times in order to reduce the energy needed to accelerate the vehicle's mass. Although hybrid vehicles have the ability to regenerate kinetic energy, frequent acceleration and decelerations result in an increase of energy consumption. To use appropriate deceleration rates the vehicle configuration and control strategies should be considered to allow for maximum energy recovery.

drive train	cycle	gain in energy consumption
conventional	NEDC	17.9%
	HYZURB	27.2%
	HYZROUT	25.1%
	HYZAUTO	7.9%
electric	AIXAM1	19.3%
	AIXAM2	4.5%
	AIXAM2	12.1%
	AIXAM3	9.4%
hybrid	HYZROUT	17%

TABLE 5.9: Overview of potential gains due to eco driving

5.4 Conclusion

Potential gains of eco driving were discussed for three representative vehicle architectures: the conventional, the electric and a power-split hybrid vehicle drive train. Optimizing drive cycles that simulated different vehicle missions, the optimal, vehicle specific, velocity profile was identified taking into account speed limits, stops, time constraints and road grade. Comparing the resulting vehicle operation with general driving, important factors for eco driving were discussed for each drive train type. An overview of potential gains identified for different vehicle architectures can be seen in Table 5.9.

The conventional vehicle operation was optimized for four drive cycles, representing a standard cycle, urban, extra-urban and freeway driving. For verification the resulting optimal velocity profiles were tested in a hardware-in-the-loop setting on an engine test bench. The measurements showed that applying ideal vehicle operation can reduce fuel consumption up to 27 % for an urban setting. Analyzing the velocity profile we established that, while component efficiency has increased only slightly, the energy needed to drive the eco cycle was much lower than that used for the original missions. It was found that low stabilized vehicle speeds, and rather short, but high acceleration rates lead to decreases in energy consumption due to reductions in resistance forces and inertial acceleration forces. In the deceleration phase engine braking can result in better fuel economy because fuel consumption on engine idling is reduced.

Operation of the electric AIXAM Mega City vehicle was optimized for four adapted

drive cycles. With these, real-life and standard drive cycles were simulated, without exceeding the vehicle's maximum speed of 65km/h. The energy consumption of the vehicle over the specified original and eco cycles was measured in an experimental setup. Testing the vehicle on a chassis test bench a real-life driver was used to follow the drive cycles. It was found that for electric vehicle's eco driving presents an important potential to reduce energy consumption. Especially for real-life drive cycles gains in consumption of up to 19% were identified. The simulation results show that drive train component efficiency is generally not a critical factor for globally ideal vehicle operation. Appropriate choices of vehicle velocity and acceleration resulted in decreases of the overall energy consumption. This is due to the reduction in resistance forces and energy spend on acceleration and deceleration phases. The use of accurate deceleration rates is important in order to maximize energy regeneration. Hence, vehicle specific modeling is necessary.

To optimize the more complex, hybrid vehicle operation the dynamic programming method was applied in a non-classic way. Using a forward facing optimization allowed us to take into account battery state dependent drive train functionalities. A new objective function was defined such that fuel consumption and battery use were considered in the optimization process. The factor α was introduced to construct a weighted cost function. To compare the energy consumption of different trips, when final battery SOC is not identical to the initial, a linear interpolation method was applied as suggested by SAE. We computed optimal vehicle operation for an extra-urban, real-life, drive cycle. The mission was optimized, considering various α-weighting factors, for three different initial battery charge levels. From the results it can be seen that eco driving has high potentials even for fuel efficient hybrid vehicles. However, the appropriate weight between fuel consumption and battery use is critical for good results. For the simulated real-life drive cycle a reduction in energy consumption of about 17% was calculated. While the optimal velocity profile showed slight increases in efficiency of the electric drive train components, it seems that a major reduction in energy consumption is achived due to the choice of velocity and acceleration rates. Low, stabilized velocities are ideally used in combination with short high acceleration rates. In the deceleration phase the regenerative capacity of the vehicle drive train has to be taken into account to optimize kinetic energy recovery.

An overview of optimal vehicle operation for the studied vehicle drive trains can be seen in Table 5.10. In general it can be concluded that, above a certain minimum

drive train	acceleration	stabilized speed	deceleration	gear shift
conventional	high	low, constant	engine braking, hard mechanical braking	highest possible gear
electric	high	low, constant	electric brake, hard mechanical braking	-
hybrid	high	low, constant	regenerative braking, rarely friction braking	-

TABLE 5.10: Overview of optimal vehicle operation

speed, increases in drive train component efficiencies have negligible effects on overall energy consumption. Using short, high acceleration rates to reach rather low, constant operating speeds seems to result in minimum energy consumption due to reductions in resistance force and inertial acceleration forces. We can therefore define eco driving factors for acceleration rates and stabilized speed phases drive train independent. In the deceleration phase it is very important to consider drive train specific models in order to maximize energy recovery.

Chapter 6

Constraint integration: Traffic and Emissions

Contents

Up to this point ideal velocity trajectories were discussed. The trajectory optimization problem solved in Chapter 5 considered only drive train specific limitations and trip or road dependent constraints. This chapter deals with the integration of more complex constraints. We will here study the influence of traffic limitations and emission constraints on potential gains of eco driving.

Traffic is an unpredictable variable when optimizing vehicle operation for a desired trip. However, in the development of driver assist systems it is also one of the most important parameters that have to be taken into account. Neglecting a vehicle's traffic environment could result in advice that leads to safety risks for the driver. While energy consumption is the objective to be optimized, we do not want to trade-off driver safety in order to reduce consumption. In Section 6.1 the effect of traffic on fuel consumption gains in an urban setting is analyzed. Since secondary vehicle behavior is hard to predict, experimental data was used to compute fuel optimal and safe vehicle operation for a conventional test vehicle.

Eco driving strategies are often applied due to their economic advantages. For eco driving to also show ecologic advantages the emissions of the energetically optimal velocity profiles have to be investigated. Section 6.2 presents an approach to integrate environmental constraints in the trajectory optimization process. Using hardware-in-the-loop experimentations on an engine test bench the pollutant gas emissions were measured for the fuel optimal drive cycles. From initial experimental results optimization constraints for emissions were derived. Economically and ecologically optimal vehicle operation is discussed in Section 6.2.4.2.

6.1 Eco driving with traffic constraints

Driver safety should be the most important criterion in the development of a driver assist system. Advice given by a support system should never have a negative effect on the driver's safety. When computing potential energetic gains of eco driving, we therefore need to take into account traffic constraints. Yet, to our knowledge, there is no work in literature that treats the dependency of eco driving strategies on traffic constraints. In the context of this thesis work studies investigated potential gains due to eco driving in an urban setting where traffic influences the vehicle operation [30]. A vehicle following situation is considered.

Experimental data was used to specify the vehicle's mission. Section 6.1.1 lays out the format of experimental data. Vehicle and trip parameters are specified. The optimization constraints are defined in Section 6.1.2. Various vehicle following criteria, like the total-time-to-collision (TTC), the time-inter-vehicular (TIV) and the safe distance to brake, are discussed. A brief description of the adapted optimization process is given in Section 6.1.3. For comparison the optimal velocity

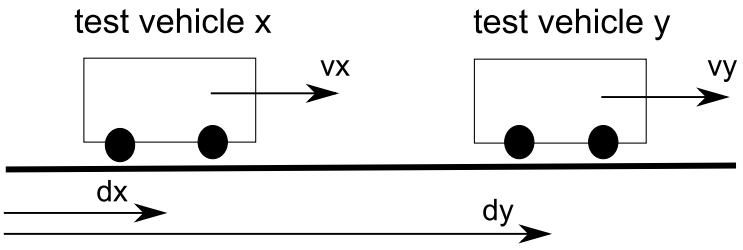

FIGURE 6.1: Vehicle Following Situation

profile is computed for the case of no traffic influences. Considering the vehicle following situation the trajectory optimization problem is solved for a low risk driver and a high risk driver. The optimization results is found in Section 6.2.4.2. The unconstrained velocity profile can be compared to a velocity trajectory that is adapted to the traffic surrounding the vehicle.

6.1.1 Trip specification

A vehicle following situation is illustrated in Figure 6.1. The schematic shows a vehicle x which is following vehicle y. Vehicle y is often referred to as 'preceding vehicle' or 'vehicle in front'. In our case the goal is to optimize the vehicle operation of vehicle x without safety risks due to the presence of vehicle y.

To define baseline energy consumption a real-life drive cycle was used. A Renault Clio test vehicle equipped with speed sensors, radar and camera was used to record a real-life drive cycle with a corresponding traffic situation. With this setup the vehicle speed (v_x) of the test vehicle as well as relative speed (Δv_{xy}) and acceleration (a_y) of the preceding vehicle were stored.

Integrating the vehicle speed (v_x) the distance of the test vehicle (d_x) can be found as a function of time.

$$d_x = \sum^{t} v_x(t)\Delta t \tag{6.1}$$

When given the relative speed of the preceding vehicle (Δv_{xy}) the distance (d_y) and the velocity (v_y) can be calculated as a function of time:

$$v_y = v_x + \Delta v_{xy} \tag{6.2}$$

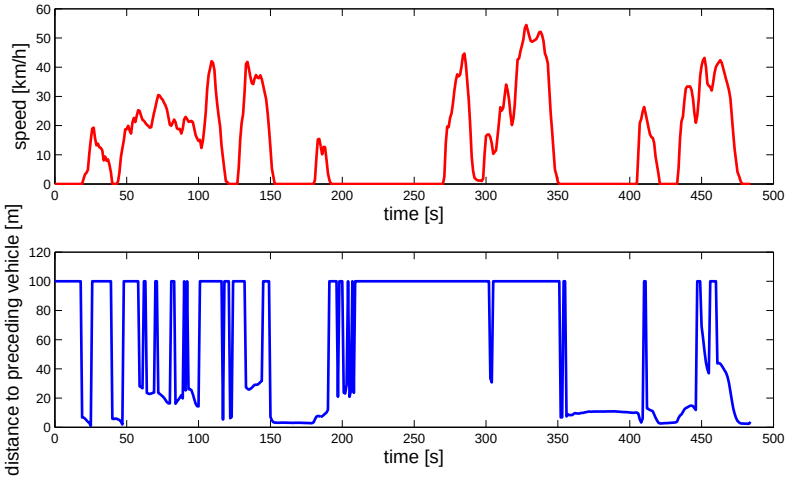

FIGURE 6.2: Real-life drive cycle with car following

$$d_y = \sum^{t} v_y(t)\Delta t \tag{6.3}$$

With these computations we can assume that the distance, velocity and acceleration of vehicle x, the test vehicle, and vehicle y, the preceding vehicle, are known. Figure 6.2 shows a sample cycle. The plotted drive cycle represents urban driving. The first plot shows the recorded vehicle speed as a function of time. In the second plot the distance between the test vehicle and the preceding vehicle can be observed. Inconsistencies in traffic result in periods where no vehicle is being followed. At other times, often at stop lights where the vehicle is at rest or at low speeds, the distance between the vehicle x and y is very small. At periods where no preceding vehicle was identified by the sensors the distance to the vehicle in front was fixed to a very large value (here 100m), such that this cannot have an influence on optimal vehicle operation. It can be seen in Figure 6.2 that at certain times the vehicle following distance for the used real-life driver was very small. It was found, that in an urban setting sufficient safety distances are often not respected, especially in acceleration and deceleration phases.

The drive train of the Renault Clio can be modeled similarly to the Peugeot 308 conventional drive train presented in Section 3.3. The vehicle is a small passenger vehicle with a mass of 1020kg. The power is transmitted through the mechanical shaft and a 5-speed manual transmission to the engine. The vehicle is propelled by a 1.5L diesel engine that can achieve a maximum combustion efficiency of 40%.

Using the vehicle model of a conventional drive train the fuel consumption can be computed instantaneously as a function of vehicle speed and acceleration.

In the following the experimentally recorded vehicle data is used to identify potential gains due to eco driving while satisfying established safety criteria.

6.1.2 Optimization constraints

Previously only trip and road constraints were considered in the trajectory optimization. To derive trip and road constraints the experimental data, shown in Figure 6.2, can be used, applying the procedure described in Section 4.1.2. Constraints are specified on the initial and final states. In addition we defined maximum speed limits as a function of distance. Further, we will here integrate traffic constraints considering a vehicle following situation. It is assumed that the vehicle in front cannot be passed, and the vehicle speed therefore has to be adapted. Hence, constraints on vehicle velocity and distance have to be specified to ensure safe vehicle following. Three factors for safe vehicle following are investigated: the safe braking distance, the time-inter-vehicular (TIV) and the time-to-collision (TTC).

Although it is not often used in rules for safe vehicle following, the safe braking distance seems a rather intuitive way to specify a good following distance. To compute the safe braking distance the maximum deceleration rates of vehicles x and y are estimated by $a_{minx} = a_{miny} = -g = -9.81 m/s^2$, which was identified as an appropriate value for the maximum braking capacity of passenger vehicles [97]. If, for some reason, vehicle y brakes at its maximum deceleration rate the safe distance is defined by the distance that is needed for vehicle x to come to a full stop without colliding with vehicle y. This distance includes the driver's reaction time. A realistic reaction time, T_{react}, for a driver can be specified by 1s. The time to decelerate vehicle x and y from the current speed to a full stop is then defined by

$$\Delta t_y = \frac{-v_y}{a_{miny}} \tag{6.4}$$

$$\Delta t_x = \frac{-v_x}{a_{minx}} \tag{6.5}$$

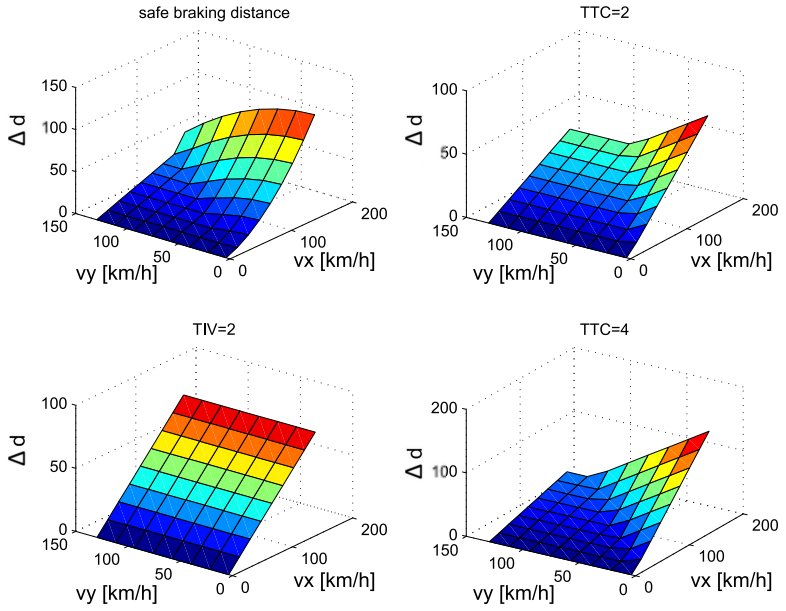

FIGURE 6.3: Safe Following Distance Criterion

With this the distance needed to slow down can be calculated with

$$d_y = v_y \Delta t_y + 0.5\, a_{miny}\, \Delta t_y^2 \tag{6.6}$$

$$d_x = v_x T_{react} + v_x \Delta t_x + 0.5\, a_{minx}\, \Delta t_x^2 \tag{6.7}$$

The safe distance (d_{safebr}) to avoid collision when braking is then given by the difference of the two distances. Theoretically the safe distance can be zero or negative when vehicle y is faster than vehicle x. In real life the minimum distance between two vehicles necessary for safe vehicle following is always the distance the vehicle covers in the reaction time. The minimum is therefore set to the distance driven during reaction time.

$$d_{safebr} = max(v_x T_{react}, d_x - d_y) \tag{6.8}$$

To illustrate the shape of this distance, it has been plotted for different vehicle speeds v_x and v_y in a 3D graph. The surface is shown on the top left in Figure 6.3.

A measure often used by drivers in real-life driving on highways is the time-inter-vehicular (TIV). The French highway code [98] specifies the minimum allowable TIV to be 2s. Instantaneously, this measure does only take into account the own vehicle speed and neglects the speed of the vehicle in front. The minimum safe distance (d_{TIV}) between two vehicles using the TIV is calculated by:

$$d_{TIV} = v_x TIV \tag{6.9}$$

A TIV of 2s is often recommended. This time window takes into account the drivers reaction time of about 1s, which then leaves him 1s to slow down his vehicle. The shape of the distance computed using a TIV of 2s can be seen in Figure 6.3 in the bottom left graph. It can be seen that the shape is independent of the v_y speed.

A third criterion, often used for implementation in collision warning devices, is the time-to-collision (TTC) [99]. Assuming that the vehicle speeds stay unchanged this parameter specifies the time it will take until the two vehicles collide. The TTC is calculated using the following equation:

$$TTC = \frac{(d_y - d_x)}{(v_x - v_y)} \tag{6.10}$$

If a desired TTC is specified, the minimum allowable distance can be derived. Figure 6.3 shows minimum, safe following distances for a TTC of 2s in the top right graph and for a TTC of 4s in the bottom right graph. When v_y is greater than v_x the equation does not hold. Theoretically the distance is zero, since no collision will occur if the vehicle in front is driving faster than the vehicle following. Nonetheless, for safe vehicle following, the lower boundary for the minimum allowable distance was chosen to be the distance driven during the time of reaction $d_{react} = v_x T_{react}$. It can be seen that doubling the TTC from 2s to 4s results in much larger allowable minimum distances between the two vehicles.

From Figure 6.3 it can be seen that the shape of the minimum allowable following distance for the considered criteria is very different. The TIV criterion is independent of the speed of the preceding vehicle. However, for the safe braking distance and the TTC factors the safe following distance is increasing when the speed of vehicle x is much larger than that of vehicle y. To compare the characteristics

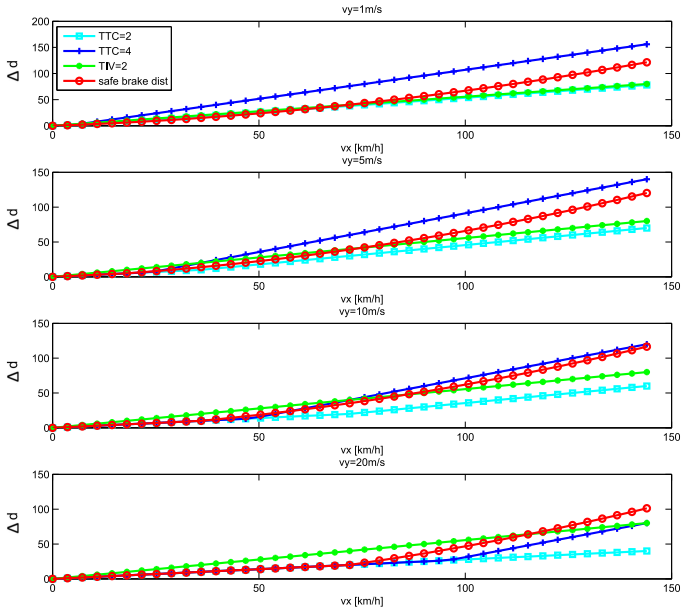

FIGURE 6.4: Safe Following Distance Criterion in Comparison

of the three parameters the minimum allowable distances are illustrated in a 2D graph for 4 different values of v_y. The four plots in Figure 6.4 show the computed minimum allowable, safe following distance as a function of vehicle speed. The preceding vehicle speed is assumed to be very slow in the first graph, it is set to 1m/s. The lower three graphs show the change in allowable following distance if the velocity of the preceding vehicle is increased to 5m/s, 10m/s and 20m/s.

As previously noted the TIV parameter, here represented by the green line (points), is a v_y independent function and therefore does not change shape throughout the four graphs. For low preceding vehicle speed it seems that this parameters can be categorized as a high risk vehicle following criterion since it specifies the lowest minimum following distance. The graph shows clearly the difference between a TTC of 2s, plotted in light blue (squares), and a TTC of 4s, drawn in dark blue (crosses). While the higher TTC represents very safe driving, a TTC of 2s represents the most risky vehicle following distance for the four computed preceding vehicle speeds. The safe braking distance seems to represent a medium risk vehicle following criterion. However for high v_y the safe-braking-distance parameter recommends very high distances between the two vehicles.

Any of the three criteria can be integrated in the proposed algorithm. For urban driving we want to discuss a low and a high risk vehicle following case. It seems

that for vehicle speeds in the urban range this can be done using a TTC of 2s for a risky driver and a TTC of 4s for a cautious driver. From experimental data the distance of the preceding vehicle, d_y, is given. Fixing the TTC value, the minimum allowable distance between the two vehicles, d_{TTC}, can be computed using the two vehicle speeds, v_x and v_y. Therefore, we define the optimization constraint on the distance d_x:

$$d_y(t) - d_x(t) > d_{TTC} \tag{6.11}$$

6.1.3 Optimization Method

The trajectory optimization problem can be defined as presented in Section 4.1. For optimization purposes the motion of the system is specified in discrete form. The objective of the optimization is to minimize fuel consumption of the tested conventional vehicle for a given mission, while trip, road and traffic constraints are respected. The optimal velocity profile is identified using a nested optimization algorithm, where a two dimensional dynamic programming method is used in combination with advanced root finding methods. The trajectory optimization was presented in detail in Section 4.2.2.

There are two ways to integrate the considered traffic constraints: as a constraint on time or as a constraint on distance. The two dimensional method chosen for optimization uses the axis distance and velocity. In this work we therefore integrate the traffic constraint as a limitation on the distance of the vehicle. However, time still plays an important role, since the distance of the preceding vehicle is defined as a function of time. It is therefore necessary to keep track of the time at which the test vehicle passes a certain distance. Computing the optimal velocity trajectory backward on the x-axis, it is not possible to specify the time the vehicle passes at a certain distance. Similarly to the optimization strategy applied to the hybrid vehicle (Section 5.3.1) we therefore applied the dynamic programming algorithm in a non-standard way, computing the optimal trajectory in a forward facing way. With this method the optimal trajectory is identified starting from the initial distance, calculating forward in distance, and therefore time.

Searching for the best solution from the initial to the final state, we can keep track of the time at which the vehicle passes a certain distance. Given the experimental

data, distance and velocity of the preceding vehicle are known as functions of time. Given the operating time of the optimal velocity trajectory at some distance the possible choices of vehicle speeds can be constraint. With this, at time t, for some distance d certain choices of velocity are not allowed in order to satisfy the traffic constraint.

6.1.4 Results

The urban real-life drive cycle, seen in Figure 6.2, was used to define a driver's mission and the surrounding traffic constraints. Applying the optimization algorithm the ideal velocity profile was computed with and without traffic constraints. For comparison a high risk driver scenario (TTC=2s) was imagined as well as a cautious driver (TTC=4s).

Figure 6.5 shows the resulting vehicle operation. The first graph shows the original drive cycle in red and the unconstrained optimal velocity profile in green (dashed). In the second graph the traffic constrained solutions can be seen together with the original drive cycle. A high risk driver, respecting a TTC constraint of 2s, is represented by the dark blue (dashed) curve. The light blue (dashed) line shows the ideal vehicle operation for a cautious driver.

The resulting velocity trajectories show that ideal, unconstrained vehicle operation uses short, hard acceleration phases and low constant speeds. Variations in vehicle speeds are rare because any acceleration and deceleration phase results in a waste of energy. The constrained velocity trajectories show more variations in vehicle velocity. When a preceding vehicle is present the recommended ideal vehicle speed is reduced to ensure safe operation. In Figure 6.5 an example of such a situation is given at $t = 60s$. The unconstrained optimization solution shows constant vehicle speed while the traffic constrained velocity profile reduces the operating speed, similarly to the original driver, to avoid a collision. However, reducing the vehicle speed results in a lower average trip velocity. To compensate for sections, where lower vehicle speed is recommended due to traffic, the constrained ideal velocity profile uses higher maximum speeds to satisfy the fixed time constraint. In the second plot of Figure 6.5 it can be seen that these phenomenons are stronger when low risk driving is considered. More frequent variations and higher maximum speeds are present in the velocity profile computed with a TTC of 4s than for the one calculated with a TTC of 2s.

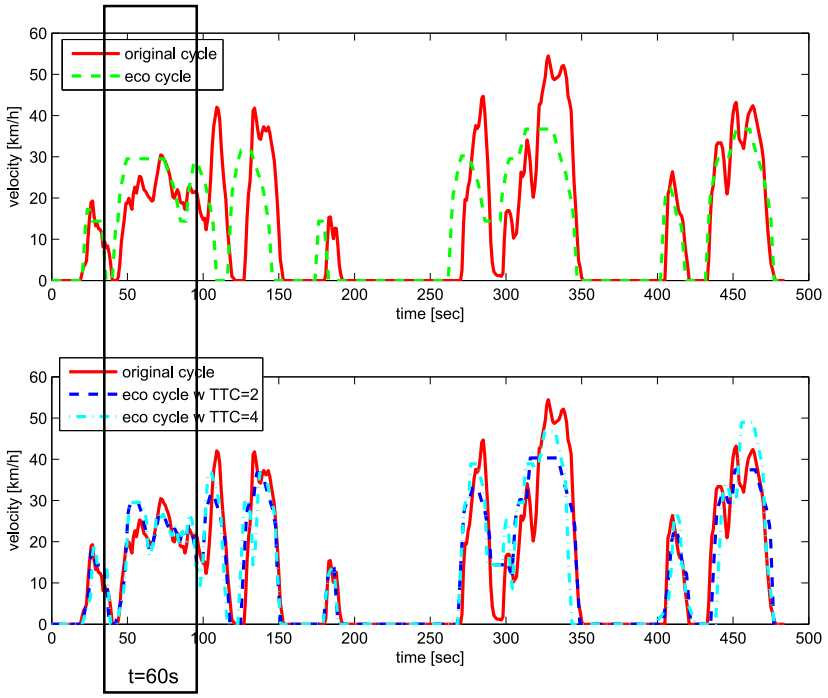

FIGURE 6.5: Optimal Velocity Trajectory

All computed ideal velocity profiles result in the same mission. From Figure 6.5 it can be seen that trip constraints in initial, final state and arrival time were satisfied. Before comparing energy consumption for the identified drive cycles the road and traffic constraints need to be verified. The left graph in Figure 6.6 shows the optimal velocity trajectories as a function of distance. The distance dependent maximum speed limit can be seen in red. The calculated ideal velocity profiles never exceed the maximum velocity limitations and road constraints are therefore respected.

To verify the traffic constraint integration the TTC-values throughout the cycles were computed. For comparison Figure 6.6 shows the resulting TTC values in the right graph. To evaluate the effect of the constraint, the TTC values are plotted for the traffic constraints eco cycles as well as the unconstrained ideal velocity profile. The purple and red lines show the TTC limitations of 2s and 4s. In green the TTC operating points of the optimal eco-cycle without traffic constraints can be seen. It is shown that the cycle does not respect any safety constraint and the TTC values drop well below the boundary lines. Multiple negative TTC values can be observed for this cycle. From Equation 6.10 it can be concluded that in this case either the distance of vehicle x is greater than that of vehicle y, or the velocity of vehicle x is smaller than the velocity of vehicle y. The points, where vehicle x

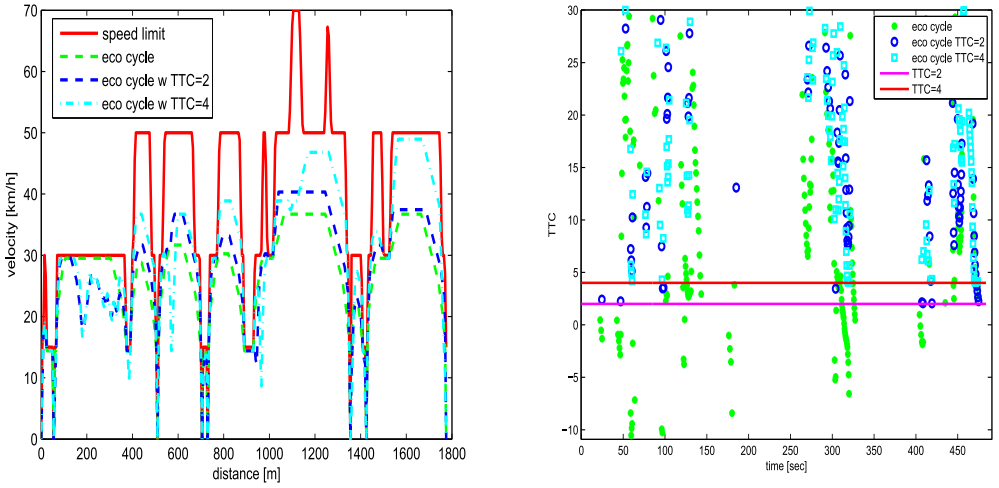

FIGURE 6.6: Road and traffic constraints of ideal velocity trajectories

is following vehicle y but the speed of vehicle x is smaller than that of vehicle y, are not plotted in this graph. The points were deleted because they do not show any importance in TTC, since no collision is possible in this case. Therefore, since the remaining points correspond to the first case, we can conclude that with the choice of this velocity trajectory a collision would already have happened.

In dark blue the TTC values of the optimal vehicle operation with TTC=2s is plotted. We see that the TTC values never drop below the 2s boundary. The light blue TTC values, which represent the optimal operation with TTC=4s, never show a TTC lower than 4s. Due to the restriction of traffic the optimization of the trajectories for these two cases is limited. Vehicle speeds were adapted to those of the preceding vehicle. Due to the forced change of the velocity profile an increase in fuel consumption is expected.

To compare the gains of eco-driving with and without traffic constraints, the fuel consumption was calculated for the computed cycles. In Table 6.1 the fuel used for each of the cycles can be seen. The fuel consumption was computed applying an optimal gear for the eco cycles as for the original cycle. To drive the originally specified drive cycle the vehicle consumed 97.36g of fuel. Without traffic constraints this number can be improved to 64.10g for the same mission. Not considering the preceding vehicles the driver can theoretically arrive at his destination in the same time while consuming 34% less fuel. Applying safety distances to integrate traffic constraints the optimal fuel consumption has increased to 69.62g for a TTC of 2s and to 82.3g for a TTC of 4s. In total, an optimal velocity trajectory resulted in a

cycle	constraint	fuel consumption [g]	gain [%]
original cycle	driver	97.36	-
eco-drive cycle	-	64.10	34
eco-drive cycle	TTC=2sec	69.62	28
eco-drive cycle	TTC=4sec	82.30	15

TABLE 6.1: Fuel Consumption of Optimal Velocity Trajectories

gain of only 15% when traffic constraints were integrated with a TTC of 4s. The decreases in optimal fuel consumption are due to increased velocity fluctuations and higher vehicle velocities.

Note: When we computed TTC-values for the original cycle, as performed by the driver, it was found that the real-life TTC-values fluctuate a lot. Some very small TTC-values, close to zero, were found. The driver's natural vehicle operation resulted in situation close to collisions. It is assumed that these were times when the driver was overtaking the preceding vehicle.

6.1.5 Conclusion

Considering a vehicle following situation, the effects of traffic on potential fuel consumption gains of eco driving were discussed. Experimental data from a radar equipped vehicle was used to specify a real-life vehicle mission and its surrounding traffic situation. Several safe vehicle following criteria were discussed and compared in their minimum allowed inter vehicular distance. It was found that dependent on test vehicle speed and velocity of preceding vehicle the criteria can result in very different constraints. For the presented studies the time-to-collision factor was implemented. It can be used to represent a high risk and a low risk driver.

Using the adapted, non-classical dynamic programming optimization method the ideal velocity trajectory was identified for an urban trip. The best velocity profile was computed with and without traffic constraints. For the constrained optimization it was found that the resulting ideal velocity profile had frequent acceleration and deceleration phases due to the fact that vehicle speed had to be adapted to the traffic. The optimal velocity fluctuated more, and due to time constraints higher maximum cruising speeds had to be used in order to achieve the same resulting average speeds for the trip.

Due to speed fluctuations and increases in maximum velocities the optimal fuel consumption increased when traffic is taken into account. For the urban scenario considered an unconstrained optimal driver was able to reduce fuel consumption by 34%. The potential gains due to eco driving were reduced when considering a risky driver by 16.6%. If a cautious driver is simulated, the gains due to eco driving decrease by more than half. However, optimizing the vehicle mission with known traffic parameters a gain due to eco driving of 15% can still be achieved, even if safety precautions are taken.

We can conclude that it is important to consider traffic constraints in the investigation of maximum potential gains of eco driving. Due to the constrained vehicle velocity the gains of eco driving are reduced. However, an important fact that we need to point out is that safe eco driving did not result in increasing fuel consumption. In order to gain more knowledge about effects of eco drivers in traffic situations more studies are necessary on various traffic situations. We can conclude that it is important to take into account traffic constraints in the development of driver assist systems in order to ensure driver safety. An approach to do so will be presented in Chapter 7.

6.2 Eco driving with environmental constraints

Eco driving is generally considered to be environmentally friendly due to the reduction in fuel consumption and therefore CO2 emission. With the rising fuel prices the interest in eco driving lies for most drivers in the cost reduction. In literature a lot of work on energy and fuel efficient eco-driving can be found, but only one study was found where emission values are considered when discussing eco driving. Johansson [100] measured fuel consumption and emission values for 16 test drivers that were educated on eco-driving. In his study Johansson found that due to more time spent in high throttle engine operation some emission values increased.

In this work the trade-off between fuel consumption and pollutant emission is discussed. Economic, fuel optimal, and ecologic, fuel and emission reducing, vehicle operations are compared. Using hardware-in-the-loop testing the fuel and emission values of the computed, optimal drive cycles were measured. A simple method is proposed to integrate fuel and emission optimal gear operation in a dynamic

setting. It will be shown that eco driving can be applied in a way such that it represents economic and ecologic advantages.

In the following the optimization problem, integrating environmental constraints, is discussed. Section 6.2.2 gives a detailed description of the experimental setup. We will first investigate economic, and therefore cost and fuel reducing, vehicle operation in Section 6.2.3. Using the experimental results, an approach to integrate environmental constraints is presented in Section 6.2.4. Ecologic vehicle operation is analyzed and the trade-off between fuel consumption and environmental constraints is elaborated.

6.2.1 Optimization

The operation of a conventional vehicle is to be optimized for economic and ecologic operation. As representative compact passenger vehicle the Peugeot 308 vehicle will be used to demonstrate the algorithm. A detailed drive train model of the conventional vehicle, including engine parameters, can be found in Section 3.3. The vehicle is simulated using an inverse model, such that fuel consumption can be computed as a function of instantaneous vehicle speed and acceleration.

Emissions are a very important factor to be reduced for environmental reasons. In addition, exhaust emissions should be decreased in an urban setting in order to improve air quality and therefore our health. We will thus analyze a drive cycle that represents real-life urban driving behavior. The original velocity profile together with the driver's gear selection can be seen in Figure 6.7 in blue. The shown mission was used to deduce trip and road constraints, which were to be respected by the optimized velocity trajectory.

In the setup of the optimization problem we can now define two objective functions. A first cost function is used when economic vehicle operation is computed. In this case overall fuel consumption is minimized. The cost function can be computed as a sum of instantaneous fuel rates, derived using the presented non-linear vehicle model (Equation 3.18):

$$\Gamma_{veh_1} = \int \gamma_{fuel}(t)dt \tag{6.12}$$

or in discrete time

$$\Gamma_{veh_1} = \sum_{i=1}^{n} \dot{m}_{fuel_i}(t_i -> t_{i+1})\Delta t_i \tag{6.13}$$

When ecologic vehicle operation is to be calculated, fuel consumption as well as emission values have to be taken into account. The cost function can then be expressed as a weighted function with the two objectives: Pollutant emission and fuel.

$$\Gamma_{veh_2} = \int (\gamma_{fuel}(t) + \lambda\gamma_{emission})dt \tag{6.14}$$

which corresponds to

$$\Gamma_{veh_2} = \sum_{i=1}^{n} \dot{m_{fuel}}(t_i -> t_{i+1})\Delta t_i + \lambda_i Emissions_i \Delta t_i \tag{6.15}$$

in discrete time form.

Solving the optimization problem for objective functions Γ_{veh_1} and Γ_{veh_2} would be a simple way to identify the economically and ecologically optimal vehicle operation. However, in order to implement cost function Γ_{veh_2} in an optimization process the variable λ which describes the weighting between fuel and emission values has to be known. Target emission values could be specified for a cycle using the governmentally fixed norm or the initial cycle values. It seems that such parameters should be cycle dependent and it was found that fixing a cycle's emission target is not obvious. Second, in order to compute Γ_{veh_2}, emission values have to be available as a function of engine operation. Such values were not available at the time of this study and the experimental identification of such a mapping was not possible due to difficulties with the regulation of the test bench. Moreover, transient effects may lead to a very complex mapping of the emissions with respect to vehicle operation. The pollutant reduction systems integrated in vehicles today commonly have their own control strategy and dynamics.

Due to these reasons the optimization problem was solved initially considering Equation (6.13) as unique objective. Using the experimental results of this optimization we will later come back to define the emission values in the objective function in Section 6.2.4.

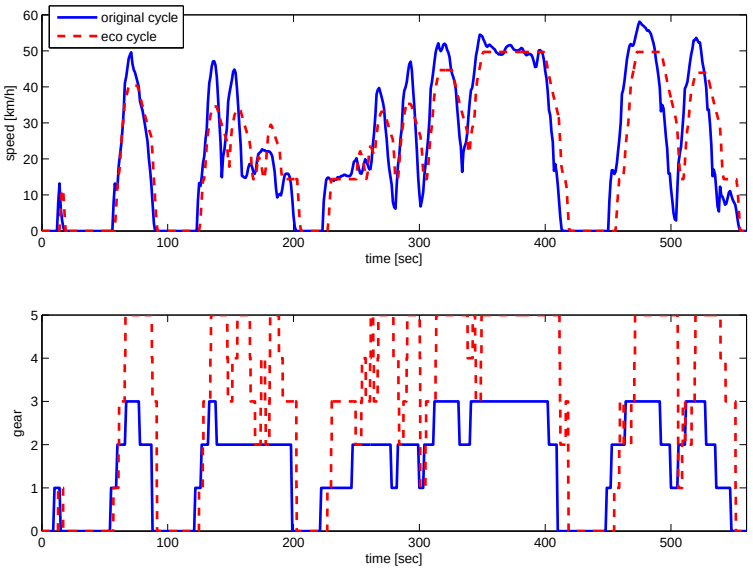

FIGURE 6.7: Original and fuel optimal drive cycle

Applying the two dimensional dynamic programming method in a nested approach, as described in Section 4.2.2, the most efficient speed profile for a considered mission can be identified. We solved the optimization problem, minimizing objective function Γ_{veh_1}, for the presented urban, real-life drive cycle. Trip constraints in distance, velocity and time were taken into account. In addition, the resulting velocity trajectory does not exceed the defined maximum speed limitations. The identified, fuel optimal, eco cycle can be seen in Figure 6.7 in red (dashed).

To measure fuel consumption and emission values for the drive cycles, the velocity profiles were tested in an experimental setup on an engine test bench.

6.2.2 Experimental Setup

A hardware-in-the-loop setup was used to test the conventional vehicle for the described drive cycles. In this approach the EP6 gasoline engine is running in real time, while the rest of the vehicle is simulated using the Vehlib software (Section 3.6). The load on the engine shaft is simulated by an electric machine. With this setup the fuel and emission values of the engine can be measured without the inconvenience of testing an entire vehicle on the road.

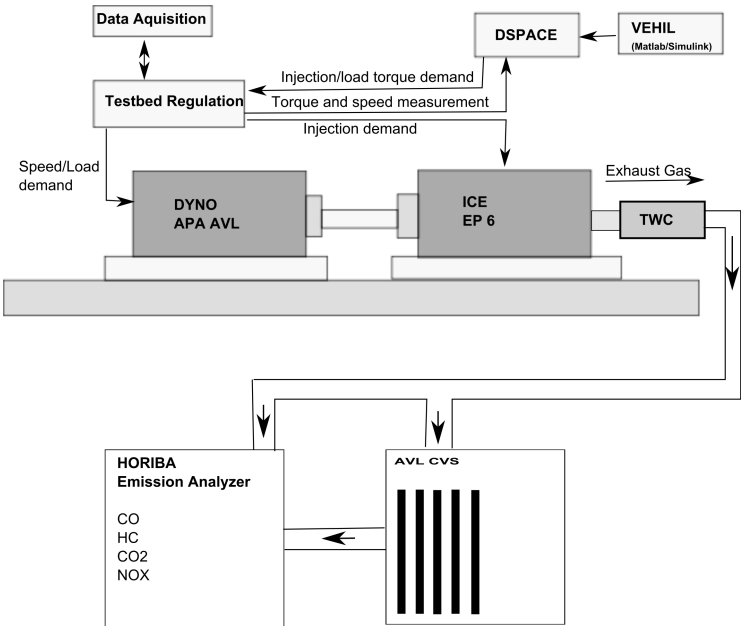

FIGURE 6.8: Engine Test Bench Schematic

A schematic of the engine test bench can be seen in Figure 6.8. The Peugeot 308 passenger vehicle drive train is simulated using the VEHIL vehicle simulation software [94]. A PID controller is used to simulate a driver that forces the vehicle to track the specified drive cycle. The DSpace MicroAutoBox Controller runs the vehicle simulation and commands the EP6 engine in real time. The AVL[1] engine test bench consists of an electric machine, that is connected to the engine output shaft, and a controller that regulates the shaft speed. Test bench specific parameters can be found in Table 6.2.

The exhaust gas of the engine is passed through the vehicle's three way catalytic converter (TWC) to reduce the emission of pollutants. To measure the vehicle's exhaust gas emissions the AVL CVS (constant volume sampler) system was used as well as the HORIBA[2] emission analyzer. Throughout the drive cycle the diluted gases are stored in the bags of the CVS system and later passed by the HORIBA emission measurement to evaluate emissions over a drive cycle. All measurements were recorded at a frequency of 10Hz.

With the described experimental setup the emission of the gases carbon dioxide (CO2), carbon monoxide (CO), Nitrogen Oxide (NOx) and Hydro Carbons (HC)

[1]AVL is a company for the development of power train systems, https://www.avl.com/

[2]HORIBA is a supplier in the fields of engine test systems, drive line test systems, brake test systems, wind tunnel balances and emissions test systems, http://www.horiba.com/

Electric machine	AVL APA 102/E
EM maximum torque	255Nm
EM speed range	0-10000rpm
EM force sensor	Z6FC3, 200kg
EM speed sensor	ROD 426 001B-01024
Speed sensor on engine shaft	AVL 364C/364X Angle Encoder
Fuel measurement	AVL Fuel Balance 730
Continuous emission measurement	HORIBA OBS 2000 PEMS (1Hz)
Average emission measurement	AVL CVS i60 Exhaust gas dilution system

TABLE 6.2: Parameters of Engine Test Bench Equipment

can be measured. Because CO2 is a naturally occurring compound and a product of perfect combustion it has not been considered as a pollutant in the past. However, the EPA (U.S. Environmental Protection Agency) has started to view CO2 as an environmental concern because it is a greenhouse gas and therefore contributes to global warming [101]. Together with water vapor, CO2 is a product of perfect combustion. In the non-perfect case the amount of CO2 emitted while driving stays approximately proportional to fuel consumption.

CO is produced when incomplete combustion occurs. The carbon in the fuel is only partially oxidized when the engine is running under rich conditions (air/fuel ratio less than 14.7). At this operation, rather than fully oxidizing the carbon to CO2, the gas CO is emitted. CO is a pollutant and reduces the flow of oxygen in the bloodstream. It therefore reduces reaction times, causes dizziness and can be dangerous to people with heart disease.

In high pressure and high temperature conditions in the engine nitrogen and oxygen atoms can react to form various nitrogen oxides. When emitted to the environment and exposed to sunlight the nitrogen oxides can form ozone.

HC, which includes methane (CH4) and non-methane hydro carbons (NMHC), can be a product of the combustion process in the engine if fuel molecules are not burned or only partially burned. In sunlight HC can react with nitrogen oxides to create ozone. HC is also considered a potential cause of cancer. As CO, hydrocarbons can be produced under rich conditions due to the lack of oxygen. In addition, HC emissions are increased in lean conditions due to engine misfires [102]. All of the four gases are currently considered pollutants and should be reduced in environmentally friendly driving.

In our setup the pollution values from the engine are measured downstream from the three way catalytic converter. With this approach the pollutants emitted to the environment are measured. Each test was repeated three times to compensate for emission measurement errors.

6.2.3 Economic vehicle operation

The economically optimal vehicle operation is presented together with the original, real-life, urban drive cycle in Figure 6.7. The first plot shows the velocity profile and in the second plot the gear selection for the two cycles can be seen. While the driver used rather low gear choices the eco cycle minimized fuel consumption with higher gear engagements. This has an immediate impact on engine operation and therefore fuel consumption and pollutant emissions.

It was found that for fuel efficient vehicle operation it is best to use hard, short acceleration phases to attain the lowest, with the time constraint possible, cruising speed. This leads to low acceleration power and short acceleration time. Reducing the aerodynamic drag loss due to the reductions in average vehicle velocity reduces the overall energy consumption. To satisfy the time constraint each segment ends with a short, rather hard deceleration phase.

Testing the two cycles on the engine test bench the fuel consumption was measured. It was found that fuel consumption was reduced by 27.8% from 9.0 l/100km for the original cycle to 6.5 l/100km for the eco cycle. The AVL emission measurement system was used to evaluate the gas emission values over the two test cycles. In Table 6.3 the measured values can be observed. Similarly to fuel consumption, the optimal cycle was able to reduce CO2 emissions. However, while fuel consumption and CO2 emissions decreased, the measurements show that emission values of CO and HC increased significantly.

The tested EP6 gasoline engine is certified for the emission norm Euro IV. This implies that for the standard test cycles the engine emits less than 1g/km of CO, less than 0.08g/km NOx and less than 0.1g/km of HC. To analyze the measured emission values these values can be used as a reference. The average NOx values seen in Table 6.3 show that the NOx emissions stayed well below the norm for both drive cycles. After several measurements no trend was identified for the two

Emission in g/km	CO2	CO	NOx	HC	fuel consumption [l/100km]
Original Cycle	207.0	2.06	0.0055	0.068	9.0
Eco Cycle	141.0	5.78	0.0046	0.12	6.5
Euro IV norm (NEDC)	-	1	0.08	0.1	

TABLE 6.3: Emission Measurement Original Cycle versus Eco Cycle

drive cycles and we therefore concluded that the measured NOx values were too small to show any significance.

In comparison with the Euro IV norm the measured CO emission values were very high. Since engine norms are certified over specified drive cycles it is possible that these limitations are exceeded by non-standard cycles, as here with the urban cycle. While the original, real-life cycle results in two times the legal emission the identified economically optimal cycle produces almost six times as much CO emissions as specified by the European norm. For the HC, the original cycle was able to stay within the limitations of the norm, while the fuel efficient eco cycle exceeds the European limitations for HC emissions.

To identify the source of such high CO and HC emissions the engine operation was compared for the two cycles. In Figure 6.9 the operating points of the engine on the test bench can be seen for the original cycle on the left and the optimized vehicle operation on the right. Due to the high acceleration rates and high gear choices of the eco cycle the engine is operated mostly in very high torque and low speed regions (Figure 6.9 b) while the original cycle uses the low torque and high speed region (Figure 6.9 a). In order to run the engine near maximum torque more fuel has to be injected. The air/fuel ratio is therefore reduced. At this point the engine is operated at rich conditions.

With this analysis it is assumed that the increases in CO and HC emissions come as a direct result of high torque engine operation. To support this assumption the measured continuous emission values were associated to the instantaneous engine operation. In Figure 6.10 a contour plot of the CO and HC emission values for the eco cycle engine operation can be seen. In the left plot the CO emission for used engine operating points is plotted in parts per million (ppm[3]) in ambient air. In the right graph, HC is plotted as a function of engine operation in ppmC (parts per million carbon). The black line shows the maximum engine output torque for

[3]ppm, parts per million: notation often used for very small quantities, denotes one part per 1,000,000 parts(or 1% = 10,000 ppm)

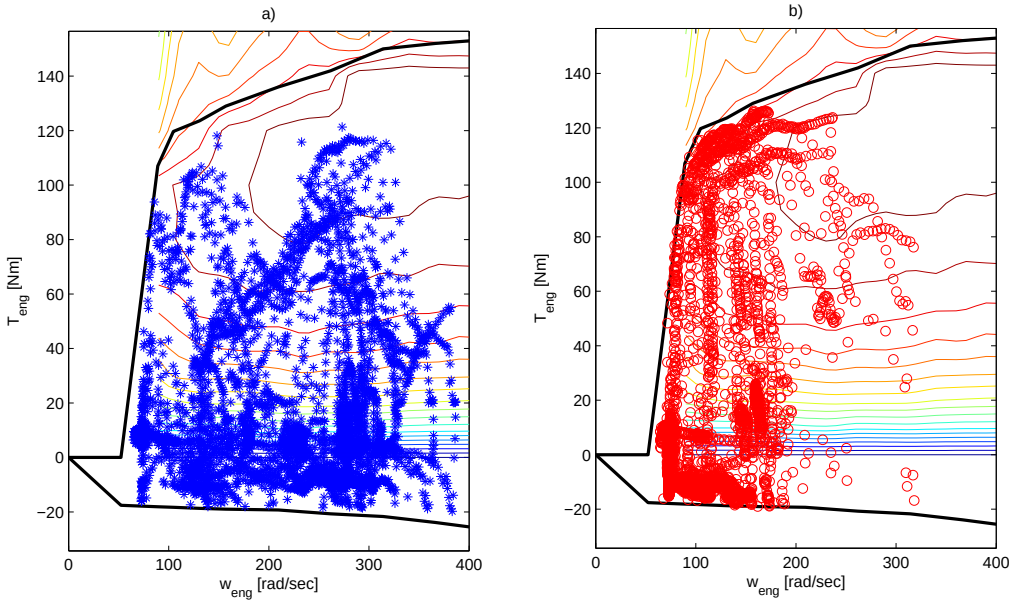

FIGURE 6.9: Engine Operation of Original Cycle (a) and Eco Cycle (b)

a specific speed. The black dashed line represents 85% of maximum torque. From this figure we can deduce that high density regions, where a lot of CO and HC were emitted, are found in the high torque range. It is therefore concluded that the elevated emission values are due to rich, high torque engine operations.

While low speed, high torque operation results usually in more fuel efficient operation, it also increases pollutant emissions. We can see that there exists a trade-off between fuel efficiency, and therefore economic vehicle operation, and emission reducing, ecologic, vehicle operation.

6.2.4 Ecologic vehicle operation

In this section we propose an approach to integrate pollutant limiting constraints in the optimization process to ensure environmentally friendly eco driving. Due to its economic and ecologic advantages the resulting velocity profile will be called eco^2 cycle.

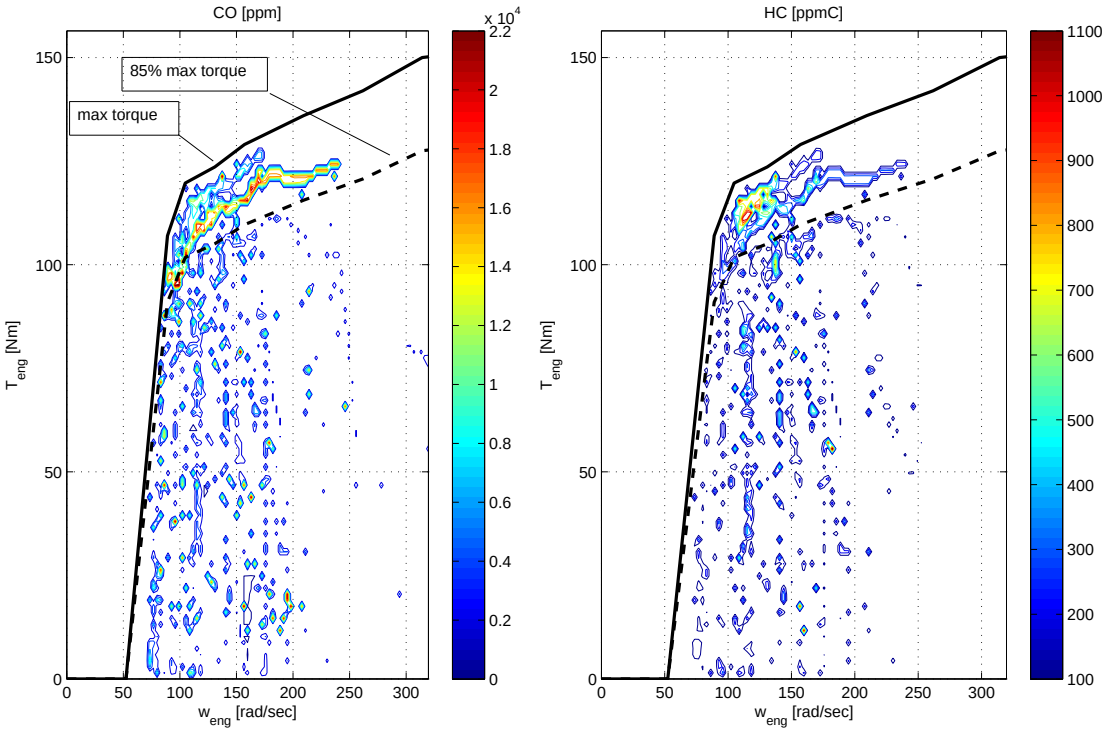

FIGURE 6.10: Identification of High Emission Zones

6.2.4.1 Emission integration

With the analysis in Section 6.2.3 it was shown that exhaust emission is strongly dependent on engine torque. Investigating the economically optimal vehicle operation we can assume that high emission engine operation occurs in the 85% to 100% torque range. We can now define an objective function Γ_{veh_2} to optimize the vehicle's trajectory for ecologic operation. To reduce the time the engine is operated in the high torque region the weighting factor λ (Equation 6.15) is used as a constraining parameter. Using the experimental results from Section 6.2.3 to fix the values of λ the objective function Γ_{veh_2} is defined as [4]:

$$\Gamma_{veh_2} = \sum_i (\gamma_{fuel}(t_i) + \lambda_i) \tag{6.16}$$

with

$$\lambda_i = \begin{cases} \lambda_0 & if\ T_{eng} > \chi T_{engmax}(\omega_{eng}) \\ 0 & if\ T_{eng} <= \chi T_{engmax}(\omega_{eng}) \end{cases} \tag{6.17}$$

In our case χ was fixed to 0.85. The objective on emissions is hereby integrated as a soft constraint. When lower torque solutions can be used to satisfy all other hard constraints the high torque engine operation is never chosen. However, if, due to fixed time constraints, high torque vehicle operation is necessary the engine can be operated in the high emission zone.

Considering cost function Γ_{veh_2} the environmentally optimal velocity trajectory was computed for the treated urban mission. The velocity profile, resulting in emission optimal vehicle operation, can be seen in Figure 6.13. In this graph the original cycle is plotted in blue, while the economic, fuel optimal profile can be seen in red. The ecological, emission optimal velocity trajectory can be seen in green. Computing the emission optimal vehicle operation we found that the differences between the eco cycle and the eco^2 driving profiles were minimal. However, the derived emission optimal gear choices had drastically changed from the economic operation. This is due to the fact that most engine operating points had to be moved from the high torque, low speed region to a lower torque, higher speed operation.

In the optimization process an inverse modeling approach was used, where gear changes are assumed to occur instantaneously. However, to simulate a cycle's consumption and to measure fuel economy experimentally on the test bench, a direct vehicle model is used, where gear changes take a certain amount of time and torque interrupts exist. Testing the computed ecologically optimal vehicle operation it was found that gear changes are demanded too frequently. The vehicle simulation was not able to follow the specified velocity profile due to frequent up- and down shifts in the gear box. We therefore propose a method to select the ecologically optimal gears automatically in a dynamic setting.

Automatic optimal gear selection In simulations of automatic gear boxes the gear changes are often triggered dependent on engine demand (throttle or torque demand) and engine rotational speed (ω_{eng}). Commonly engine minimum speed as a function of engine demand ($\omega_{gearmin}(T_{eng})$) and engine maximum speed as a function of engine demand ($\omega_{gearmax}(T_{eng})$) are defined. With this, when engine

[4] $\lambda_0 = 10000$; A number was chosen that, in comparison with the cost of allowable operating points, is infinitely big. However, we cannot set the cost at these points to infinity since the operation has to be possible if necessary due to a hard time constraint

speed drops below engine minimum speed, a down shift is induced. Similarly, if engine speed passes above the engine maximum speed a higher gear is engaged. The functions $\omega_{gearmin}$ and $\omega_{gearmax}$ can be chosen gear independent or may vary for different gears. Dynamic models usually consider the time it takes to disengage and engage a gear. Throughout the gear change a torque interrupt occurs. The time of a gear change was fixed in our simulation to 1s.

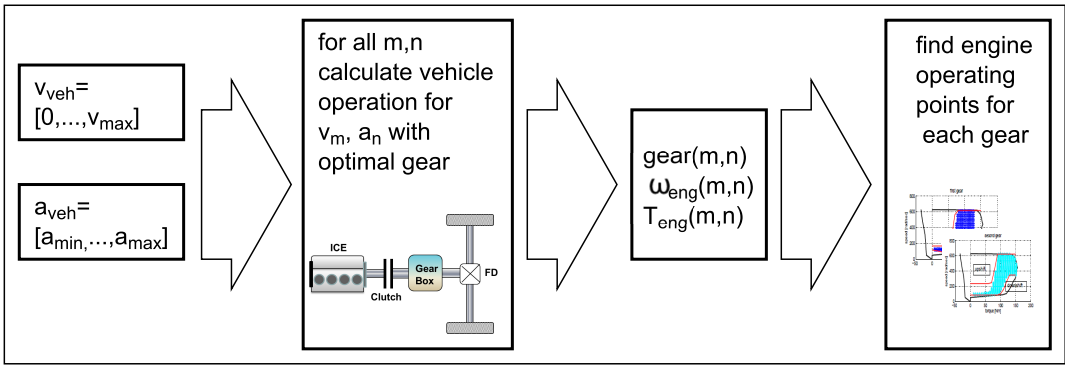

FIGURE 6.11: Calculation of optimal gear for Engine Operation

In our approach the model of the conventional vehicle, derived in Section 3.3, was utilized. The schematic in Figure 6.11 illustrates the process that was implemented. First the range of vehicle velocity (v_{max}) and vehicle acceleration (a_{min}, a_{max}) needs to be specified. The vectors v_{veh} with length m and a_{veh} with length n can be defined using some reasonable step size. With the constructed vehicle simulation the optimal gear choice, and therefore the emission optimal vehicle operation, can be computed using the cost function defined in Equation 6.16. Consequently, matrices of size (m, n) of gear choice, engine speed (ω_{eng}) and engine torque (T_{eng}) are computed for all possible vehicle operations (v_m, a_n). With this the engine operating points for optimal gear selections for gears 1 through 5 can be identified.

In Figure 6.12 the engine operation in speed and torque are plotted for gears 1 through 4. Since maximum and minimum allowable speeds are derived as functions of torque the figure shows the engine operation with torque on the x-axis and rotational speed on the y-axis. The region of operating points can be used to define minimum and maximum allowable engine speeds for each gear. Figure 6.12 illustrates the minimum allowable engine speed, $\omega_{gearmin}$, and maximum allowable engine speed, $\omega_{gearmax}$, as a red line surrounding the operating area. When engine operation crosses the lower red line a down shift occurs. When engine speed increases, to move above the upper red line, an up shift follows. To leave some

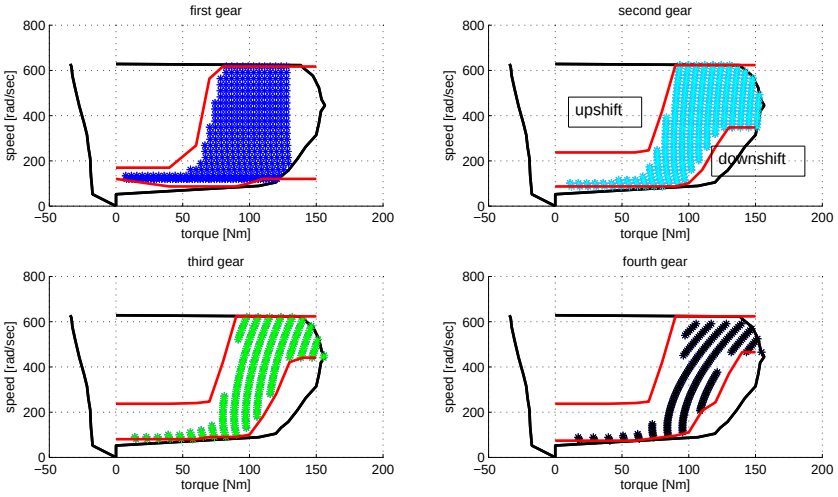

FIGURE 6.12: Optimal Ecologic Gear Shift

time between gear shifts in the acceleration and deceleration phases the minimum distance between $\omega_{gearmin}$ and $\omega_{gearmax}$ was fixed to 50rad/s for the first gear and 150rad/s for gears 2 through 5.

The proposed method allows us to select emission optimal gears when testing the cycles with the direct, dynamic vehicle simulation. Implementing this method, we were able to test the computed ecologically optimal drive cycle on the engine test bench to verify fuel consumption and emission values.

6.2.4.2 Results and comparison

The eco^2 drive cycle derived for the considered urban mission is presented in Figure 6.13. The first plot shows the velocity profile of the original, eco and eco^2 cycle, while the second graph shows the tested gear selection for the three cycles. As previously stated, we can observe that the velocity profile of the ecologic vehicle operation is approximately equal to that of the fuel optimal operation. However, as seen in the second plot, gear selections are very different. While the economically optimal operation engages very high gears to increase engine efficiency to its maximum, an ecologic driver would rather choose an intermediate gear. The higher speed and lower torque engine operation should lead to lower pollutant emission values over the cycle. It needs to be pointed out that, optimizing drive train operation for emissions still results in higher gear choices than the original baseline driver had selected.

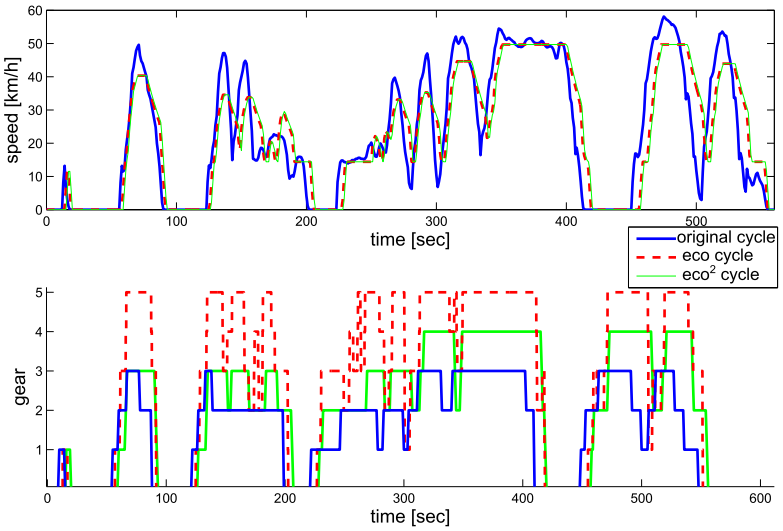

FIGURE 6.13: Original, Economic and Ecologic Drive Cycle

Emission in g/km	CO2	CO	NOx	HC	fuel consumption [l/100km]
Original Cycle	206.96	2.06	0.0055	0.068	9.0
Eco Cycle	140.96	5.78	0.0046	0.12	6.5
Eco^2 Cycle	151.51	2.18	0.0025	0.063	6.7

TABLE 6.4: Emission Measurement Final Results

Testing the eco^2 drive cycle on the engine test bench the fuel and emission values were measured (Table 6.4). The measured NOx values were considered too small to draw any conclusion. Any changes in this range could be a result of measurement errors. As expected, we can see that CO2 emissions are approximately proportional to the measured fuel consumption.

To visualize the data the results were plotted in a bar graph, presented in Figure 6.14. The figure shows fuel consumption and CO and HC emission values for the three tested drive cycles in a normalized graph. In comparison to the original drive cycle, fuel consumption was reduced with both, the eco and the eco^2 cycle. However, the economic cycle led to a drastic increase in CO and HC emissions, whereas emissions could be reduced to the baseline for the emission optimal vehicle operation.

Fuel optimal vehicle operation achieved a fuel consumption of 6.5L/100km for the considered urban mission. With environmentally friendly eco driving, fuel consumption was still reduced by 26% to 6.7L/100km in comparison with the original cycle (9.0L/100km). The compromise in energy consumption seems to be small

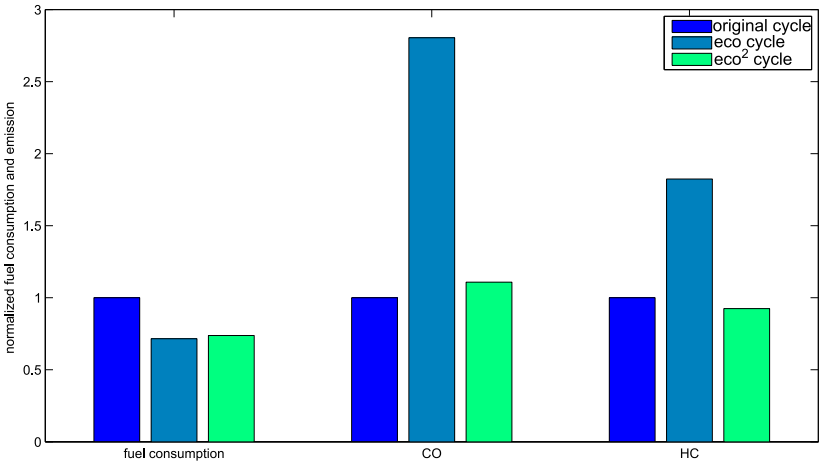

FIGURE 6.14: Fuel Consumption and Emission Results

with respect to the reductions in pollutant emissions. Considering ecologically optimal vehicle operation, eco driving can be performed without emitting any additional pollutants.

From these results it can be assumed that fuel optimal vehicle operation is achieved due to the selected velocity profile. With good choices of velocity and acceleration rates the energy necessary for the trip is reduced. In order to reduce emissions the drive train operation has to be considered. Using the gear box, engine operation can be adjusted such that fewer pollutants are emitted.

6.2.5 Conclusion

Eco driving is a driver behavior that is commonly considered environmentally friendly, while often implemented due to its economic advantages. The presented study shows a comparison of economic, fuel optimal, vehicle operation and eco-logic, emission optimal, vehicle operation.

A trajectory optimization problem was presented where an urban real-life drive cycle was optimized for eco driving. Considering two different objective functions, the fuel optimal vehicle operation was compared to environmentally friendly driving. A nested approach, combining the dynamic programming method with advanced root finding methods, was used to solve the constrained trajectory optimization problem using an inverse vehicle model. To avoid rapid gear switching a simple method to dynamically integrate the optimal gear selection was proposed

for experimental testing. Testing the original, economically optimal and ecologically optimal cycles the fuel consumption and pollutant emissions were measured. Advanced emission measurement systems were used to evaluate each cycle's CO2, CO, NOx and HC emission values.

The results show that eco driving can not always be considered environmentally friendly. Initial tests showed that fuel optimal vehicle operation resulted in increased emissions of CO and HC, while significantly reducing fuel consumption and CO2. It can be concluded that it is important to consider emission constraints in the trajectory optimization process. Taking into account a small trade-off in fuel consumption, pollutant emission values can be reduced such that the original baseline values for CO and HC are not exceeded. The ecological drive cycle still achieved a 26% reduction in fuel consumption with respect to the original driver.

Comparing economic and ecologic vehicle operation it was observed that the optimal velocity profile of the two cycles is very similar. Yet, the gear selection is very different between fuel optimal and emission optimal vehicle operation. We therefore conclude that energy consumption is reduced by the appropriate choice of velocity and acceleration rates, while the pollutants emitted depend on the drive train operation.

6.3 Conclusion

This chapter dealt with constraint integration to evaluate advantages of eco driving in more realistic situations. While previous studies only considered trip and route constraints, we here showed an approach to integrate traffic and environmental constraints in the energetic optimization process. With this, potential gains of eco driving can be approximated more realistically.

Considering a vehicle following situation influences of traffic constraints on maximum theoretical gains of eco driving were discussed. It was found that, while potential gains decreased due to traffic constraints, eco driving still represents a way to reduce fuel consumption and most importantly does not result in disadvantages for the driver. To get a better idea of advantages and disadvantages of eco driving in high density traffic situations further studies of different traffic scenarios are necessary.

Measuring emissions of computed fuel optimal velocity trajectories, it was found that eco driving cannot always be considered environmentally friendly. We therefore proposed a simple method to integrate emission constraints in the optimization process. It was shown that, taking into account a minimal trade-off in fuel consumption, the pollutant emission values can be reduced. Considering emission constraints it was shown that eco driving can represent economic and ecologic advantages.

Chapter 7

A Driver Assist System for Eco Driving

Contents

In the previous chapters the theoretical, maximum potential gains of eco driving were investigating. An ideal case was assumed, where the vehicle was simulated, however a driver model was not considered. It was assumed that the vehicle operator followed exactly the optimal velocity trajectory. Taking the driver out of the loop is a good way to evaluate potential energy savings and optimal vehicle operation. However, for real life implementations of eco driving strategy the information has to be transmitted to the driver.

Previous studies have shown that educational courses of eco driving show improvements in consumption only for a short time period. In long-term studies it has been found that drivers fall back to their original behavior [45]. It is therefore necessary to design a driver assist system to educate and remind the driver of optimal vehicle use. In contrast to off-line studies, when developing a driver support system, several driver related factors need to be taken into account. First, driver safety cannot be neglected. In addition, ergonomic aspects need to be considered in the development of a human-machine-interface (HMI). Driver acceptance and understanding is necessary to achieve good results.

In this chapter we propose an approach to integrate the developed trajectory optimization algorithms in an advanced driver assist system (ADAS). With this, we want to not only evaluate theoretical gains of eco driving, but identify realistic advantages in real-life situations. To demonstrate the effectiveness of the ADAS system it was tested in a controlled environment on a driving simulator.

An internal project at the institute IFSTTAR, called VERONESE, units several researchers from different laboratory groups for the work to increase energy efficiency in the transportation sector. Within the scope of this project the LTE (Laboratoire de Transport et Environment), LESCOT (Laboratoire Ergonomie et Sciences Cognitives pour les Transports) and LEPSiS (Laboratoire Exploitation, Perception, Simulateurs et Simulations) laboratories collaborated to develop, integrate and test the here designed ADAS system. The driving simulator, maintained by the LEPSiS laboratory, allowed us to test the support system in a controlled setting. While the simulator environment does not exactly represent real-life driving, it allows us to test a driver's behavior on similar scenarios.

To realize this project the workload was balanced between the laboratories in the collaboration. How this thesis work integrates in the overall project can be seen in Table 7.1. While the simulator was maintained by the LEPSiS laboratory, specific changes had to be made to test the developed ADAS system. In the development of the HMI of the ADAS, previous studies at LESCOT on a simple rule-based assist system were used as a basis. A survey was conducted on each subject to evaluate driver acceptance and understanding.

In Figure 7.1 the setup used to experimentally test the developed support system can be seen. The simulator hardware, which will be explained in more detail in Section 7.1, consists of the vehicle and the virtual environment. Inputs from

task	LEPSiS	LESCOT	thesis work (LTE)
simulator	+++		++
ADAS HMI		++	++
ADAS algorithm			+++
ADAS integration	+	++	++
experimentation		+	+++
user survey		++	+

TABLE 7.1: Contribution of each laboratory

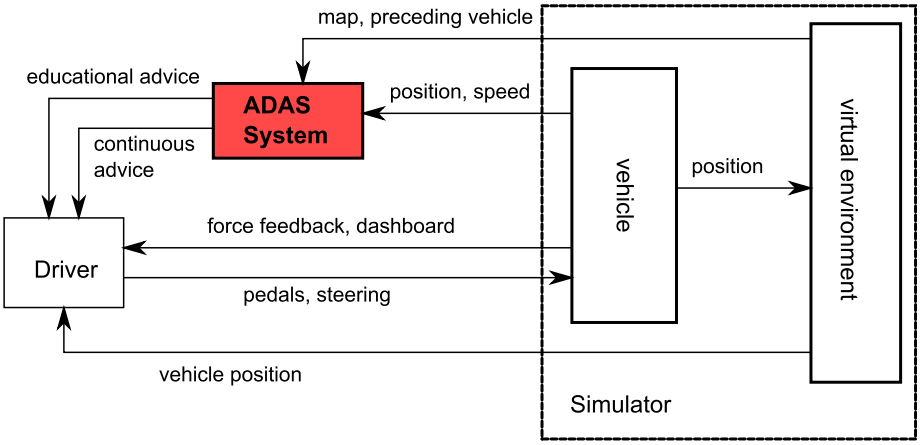

FIGURE 7.1: Schema of experimental setup

both, the vehicle and the environment will be used in the ADAS algorithm to compute information for the driver. The advice provided by the designed system consists of an educational advice and a continuous advice. The ADAS system will be described in more detail in Section 7.2. The physical driver uses the inputs from the environment, the vehicle and the ADAS system to decide on his vehicle operation, which is transmitted through the pedals and steering wheel.

In Section 7.1 the driving simulator at the IFSTTAR laboratory is presented. A brief outline of the dynamic vehicle simulation, installed on the simulator is given. The simulator environment is introduced and the setup of the communication network is specified. In Section 7.2 the driver support system is discussed. The implemented algorithm is outlined and the interface, which is used to transmit information to the driver, is presented. Section 7.3 describes the experimental evaluation of the developed ADAS system. First, the experimental setup and the testing routine applied to validate the ADAS's performance is outlined. To conclude this chapter, the results are evaluated with respect to fuel consumption and driver acceptance.

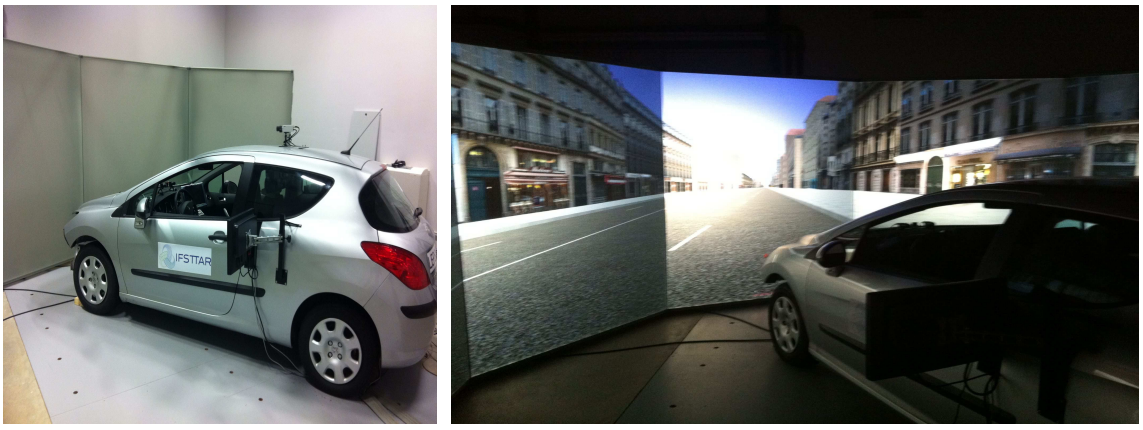

FIGURE 7.2: Driving Simulator

7.1 Driving simulator

The setup of the driving simulator at the IFSTTAR laboratory is shown in Figure 7.2. The simulator consists of a stationary Peugeot 308 vehicle that is placed in front of five projector screens. The screens are each 220cm high and 165cm long, which results in a horizontal forward view of 180° and a vertical view of 47°. When driving, the video projectors display the environment on the screens. The rear view is simulated by three monitor screens (48x56cm), that are attached in the rear of the vehicle interior and on each side of the vehicle. This way, when the driver looks in the rear view mirror a realistic image of the environment behind the vehicle can be seen.

The driver operates the vehicle in the same way a conventional vehicle is driven on the road. The accelerator, brake and clutch pedals are equipped with sensors to send a displacement signal to the control computer. There is no force feedback implemented on the pedals, only pedal position is taken into account. An electric motor is installed in the steering wheel to simulate tire force feedback to the driver. This makes driving in the simulator, where no real tire forces are acting on the wheels, more realistic to the operator. The angular position of the steering wheel is recorded to compute the trajectory of the vehicle and calculate its position in the environment. Gear selection and auxiliary use are additional input signals specified by the driver and recorded by the control computer.

Testing driver operations and reactions on a driving simulator has the advantage that the test can be run in a controlled environment. In addition safety risks are no concern, since the vehicle is not actually moving. However, it is difficult to achieve

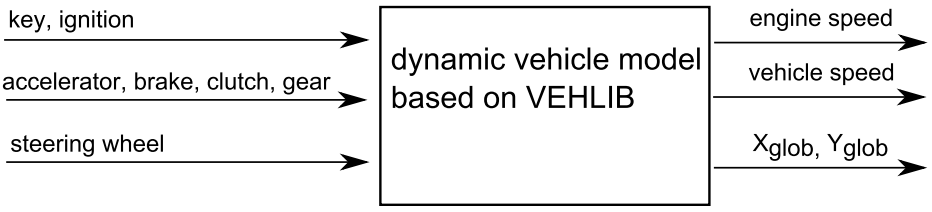

FIGURE 7.3: Inputs and outputs direct vehicle model

the same drive feelings in a driving simulator as in real life driving. Driving a stationary simulator vehicle, the human eye detects motion, but the person itself is not actually moving. This can provoke sickness and nausea. In a simulator environment, drivers often have difficulties estimating distances. Operations such as hard turns, strong acceleration and deceleration should be avoided.

The initial vehicle simulation implemented on the driving simulator was a ready to use software package that left no visibility of actual component parameters and operation. We therefore integrated the VEHLIB dynamic vehicle simulation of the Peugeot 308 vehicle on the simulator. Doing so we can be sure that the vehicle driven on the simulator and the one optimized in the driver assist system are the same. The VEHLIB vehicle simulation was initially designed for energetic vehicle simulation over a drive cycle. In the following section changes to the vehicle simulation to adapt it to the simulator environment are briefly outlined.

7.1.1 Vehicle simulation

Initially the VEHLIB software used a velocity profile as input to compute the energy consumption of the vehicle. A driver was implemented with a PID controller. In a driving simulator the real-life driver inputs define the inputs. The inputs and required outputs to the dynamic vehicle simulation are shown in Figure 7.3. Key and ignition inputs are used to identify the state the vehicle is in. The key signal specifies that the vehicle is in the 'ON' state. The ignition signal is used to turn over the engine to start it at the beginning of a trip or when it has been stalled due to inappropriate clutch use.

Once the engine is running, acceleration, brake and clutch pedals are used together with the gear selection to drive the vehicle. All pedal inputs are detected on a range from 0 to 1, where 0 defines no pedal displacement and 1 full pedal displacement. The input of the acceleration pedal can be translated directly to

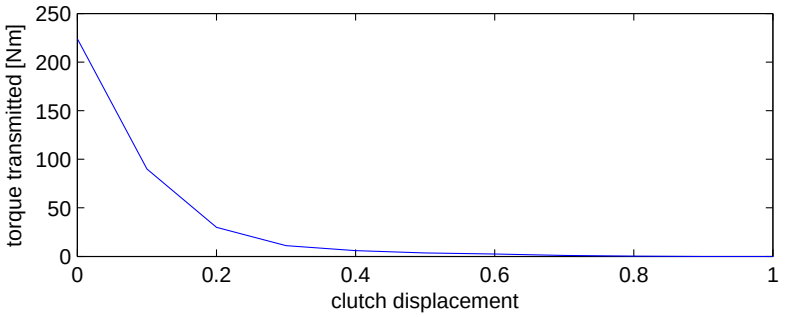

FIGURE 7.4: Clutch torque transmitted

throttle command. An accelerator pedal displacement therefore corresponds to a power demand of the engine. Similarly, we define the clutch signal to correspond to some clutch displacement. Zero displacement of the clutch pedal specifies an engaged clutch state. The clutch is disengaged when the pedal is fully displaced. The engine torque transmitted by the clutch can be defined as a function of clutch displacement, as seen in Figure 7.4. No torque can be transmitted when the clutch is disengaged. According to the real system, when the clutch is fully engaged a maximum torque of 225Nm can be transmitted. The engine maximum output torque in this drive train is 156Nm. The clutch therefore never slips when it is fully engaged.

In a detailed model the brake pedal command should be used as an input to the brake system. The pedal command is transformed in a torque applied to the wheels through the hydraulic brake system. To keep the vehicle model simple and focus on major drive train components, the brake force was here specified by multiplying the brake command by a realistic gain. To identify the appropriate gain we assumed that full brake pedal displacement corresponds to maximum possible brake force, which results in maximum deceleration without locking the wheels. The maximum brake force transmitted depends on the friction between the tires and the road and can be computed by

$$F_{decelmax} = M_{veh} g \mu \tag{7.1}$$

where M_{veh} is the vehicle mass and g is the gravitational acceleration. The tire road friction is specified by the adherence coefficient μ, which depends on road surface and condition. In our study, the value of μ was fixed to 0.6, which corresponds to an asphalt road surface in dry conditions. The brake torque corresponding to

some brake pedal displacement can be identified by interpolating between zero and maximum brake force. The wheel slipping factor is here neglected, the tire to road contact is always perfect.

In order to place the vehicle in the simulated environment the longitudinal and the lateral motion need to be computed by the vehicle model. The VEHLIB software, initially developed to compute energy consumption of drive cycles, only simulates longitudinal vehicle motion. Here, a simple lateral vehicle model is constructed using a bicycle representation of the vehicle, where the two front wheels and the two rear wheels are respectively represented by one central wheel. The so-called 'kinematic model' [103] is based only on geometric relationships and therefore does not consider the forces that affect the motion. A detailed outline of the model construction can be found in the appendix.

With this the vehicle longitudinal and lateral speed is defined as a function of vehicle speed and wheel angle. Given the steering wheel position the angle of the wheels can be computed with a steering ratio [104]. Measurements have shown that the ratio can be specified to a value around 16 for passenger vehicles. In our work the steering ratio is specified as a parameter that is fixed to 16 for very small speeds, but grows proportionally with the vehicle speed. Due to increasing slip angles the vehicle usually turns less with increased speeds. Since the implemented lateral model does not consider tire slip angles, using a changing steering ratio can lead to more realistic vehicle operation.

The dynamic vehicle model is constructed using the Matlab Simulink software. A Dspace Microautobox is used to run the simulation in real time. Communication between the vehicle model and the control computer of the simulator is ensured using the CAN protocol. In the following the simulator environment and communication is discussed in more detailed.

7.1.2 Simulator environment and communication

The driving simulator system is made up of several different components that are all controlled from a central computer unit. In Figure 7.5 the simulator environment is visualized. A control computer is used to manage the communication

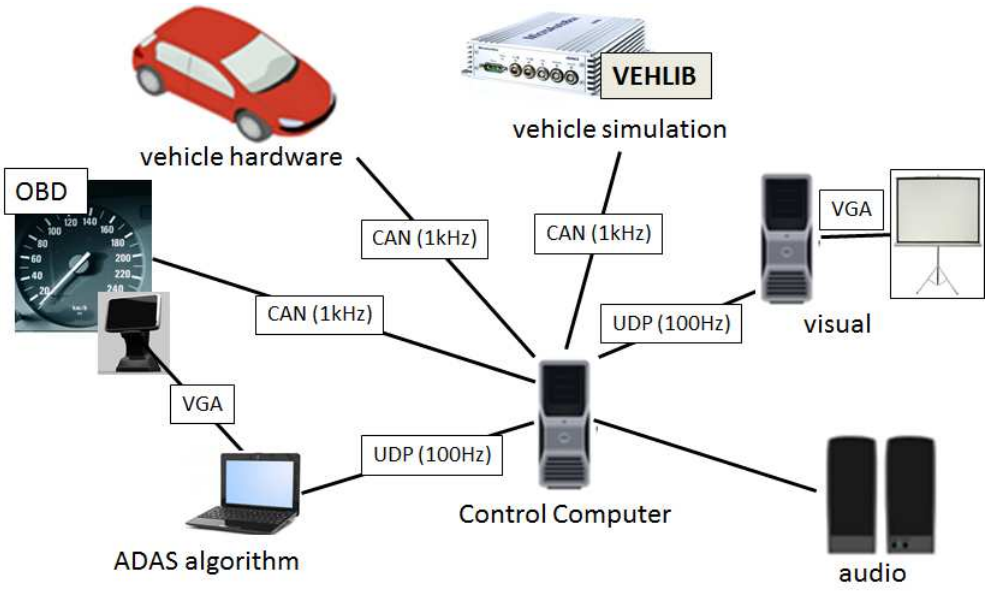

FIGURE 7.5: Simulator communication

and command the simulator components such as the auditory components, the visual control computer, the vehicle simulation, the vehicle hardware, the dashboard devices, and the advanced driver assist system.

Speakers are installed in the vehicle in order to simulate driving sounds. Appropriate driving sounds are calculated by the control computer as a function of vehicle speed, engine speed and traffic. Playing operation sounds to the driver can make driving on a simulator more realistic. Vehicle sounds such as the engine rotation can help the driver to operate the clutch and to select the appropriate gear. In order to display the appropriate environment on the visual screens the control computer transmits the vehicle position and heading to the visual machines. With these inputs the appropriate image can be computed and projected on the screens.

The driver input on the vehicle hardware is communicated from the vehicle hardware via CAN network to the control computer, which then transmits it to the dynamic vehicle simulation (Section 7.1.1). Inputs, such as accelerator, brake and clutch pedal, gear choice and steering wheel displacement, are used in the vehicle simulation to determine the vehicle states. Engine speed, vehicle speed and position in the global X-Y-plane are calculated. This information is sent back to the control computer, which processes them to indicate the appropriate signals on the vehicle dashboard. Here, the vehicle's odometers are used to present vehicle speed and engine rpm to the driver.

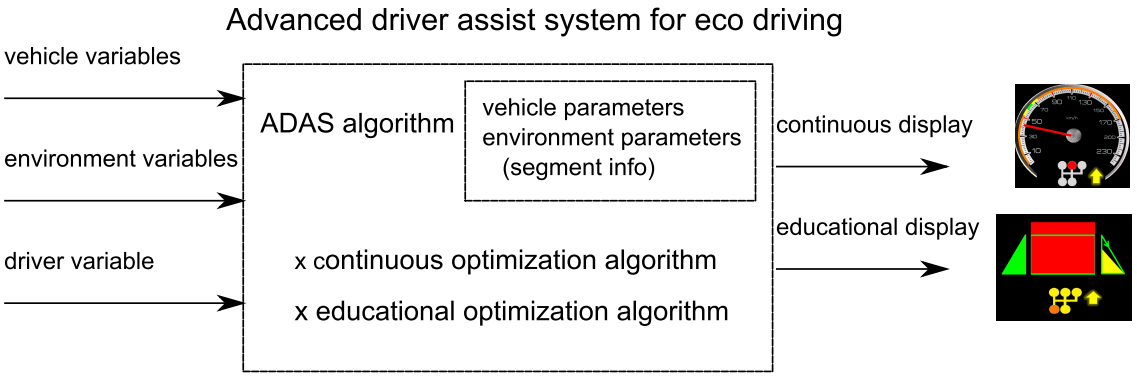

FIGURE 7.6: Inputs and outputs of ADAS

To integrate the ADAS system in the simulator network an Ethernet connection was used to communicate information from the control unit to the ADAS algorithm. Using this connection environment and vehicle data can be used to calculate optimal vehicle operation. A VGA cable is used to display the eco driving advice to the driver. In the following the functionality, algorithm and human-machine-interface of the designed advanced driver assist system is presented in more detail.

7.2 Advanced Driver Assist System (ADAS)

The here presented ADAS design is based on the optimization algorithms constructed and the knowledge acquired throughout this thesis work (Chapter 3 -6). Figure 7.6 shows a global overview of the driver assist system. The ADAS system input variables include vehicle information, road environment information and driver input. The setup used in this work assumes that access to real time vehicle variables, such as vehicle speed (v_{veh}), distance driven (d_{veh}), gear selection ($gear$), engine speed (ω_{eng}) and engine torque output (T_{eng}), is given. In addition we assume that the vehicle is equipped with radar and can therefore provide information about possibly existing preceding vehicles. If a vehicle is being followed, it is assumed that relative distance and speed of the preceding vehicle is known. We can therefore calculate preceding vehicle speed (v_y) and preceding vehicle distance (d_y).

In real life, environmental variables can be provided by GPS systems or other road mapping techniques. In our case the simulator central computer transmits the necessary road data to the driver support system. To identify the vehicle placement in the simulator environment the control computer associates each road

with a number (road number). Defining the start and end of a road the vehicle position can be defined by the road number and the position on this road (d_{road}). Communicating the road number and current road distance , d_{road}, to the support system enables the device to fix the vehicle's position in the road environment and, more importantly, on a road segment.

An operator input to the support system is used to classify the driver type. With this input the willingness of the driver to reduce fuel consumption with a trade-off in trip time is specified. This factor directly translates to the weighting factor implemented in the two dimensional dynamic programming optimization. Specifying a driver specific weighting factor between energy consumption and trip time leads to a simplification of the optimization algorithm and therefore computation time. In our experiment a constant weighting factor was implemented, which enables us to make a comparison of the results. A trade-off value of $\beta = 0.5$ was chosen, which represents an average driver type (see Figure 4.8).

Using predefined vehicle parameters and environment parameters together with the system inputs the ADAS algorithm generates advice for the driver. Figure 7.6 shows that the support system combines two different functionalities. Two optimization algorithms are applied to generate continuous advice and educational advice to support the driver. This system design uses two in-vehicle displays as human-machine-interface to transmit advice to the driver. The physical system can be seen in Figure 7.7. The interface will be discussed in detail in Section 7.2.2.

FIGURE 7.7: Installation of HMI

The construction of the ADAS algorithm implemented in the support system is described in detail in Section 7.2.1. We will outline the utilized logic and state the optimization algorithms used to evaluate driver advice. Section 7.2.2 deals with

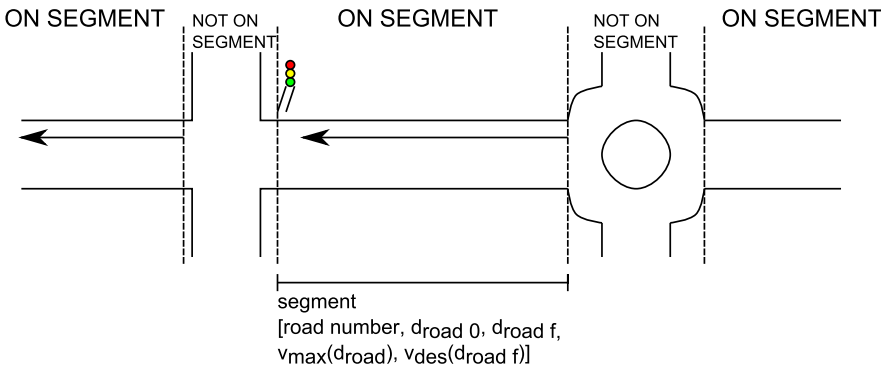

FIGURE 7.8: Definition of segment

the design of the human-machine-interface. The continuous and the education display is introduced to the reader.

7.2.1 ADAS algorithm

To understand the logic of the ADAS system, we first need to define a road segment. Figure 7.8 shows a typical road segment. A road segment starts at the point where the vehicle leaves an intersection and ends at the next intersection. In this work a road segment is defined by a segment of the road that lies between two 'intersections', where an 'intersection' can be a stop sign, a stop light, a crossing or a roundabout. Figure 7.8 shows a road segment between an urban intersection and a roundabout. In the initialization process the ADAS system loads a map of all road segments of the planned trip into memory. With this, given the road number and road distance of the vehicle it can easily detect on which segment and at which distance on the segment the vehicle is operated. In this algorithm the parts of a road that lie in between segments, such as intersections or roundabouts, are not considered for optimization. This is due to the fact that driver safety always has to be considered more important than potential fuel savings. In an intersection a driver needs to concentrate on its surroundings and the vehicle maneuvering rather than thinking of fuel efficiency. In addition, we believe that fuel consumption gains due to improvements on these parts of a trip are minimal.

With this method we can define for a vehicle to be on a segment or not on a segment. The driver assist system detects when the vehicle enters a (known) segment. The goal of the system is to compute the best vehicle operation for the current segment and guide the driver throughout the segment. This is what we call continuous advice. When the driver arrives at the end of a segment the optimal

velocity trajectory corresponding to his speed profile is computed and compared to his driving. With this information the driver can be educated on positive and negative aspects of his recent driving style. To manage the continuous and educational advice taking into account safety aspects a control logic was defined.

7.2.1.1 Control logic

The logic of the ADAS algorithm is presented in Figure 7.9. The graph shows algorithm components that contribute to the continuous advice evaluation in dark blue, while sections that are used to compute the educational advice are displayed in green. In the control logic the two states, 'on segment' and 'not on segment', are clearly visible.

In contrast to the educational display, that presents advisory information at the end of a sequential line, the continuous display is supplying information to the driver at all times. However, while the continuous display is always 'on', it does not always provide advice on optimal vehicle operation. General information, such as current vehicle speed and gear choice, is presented to the driver at all times. Optimal vehicle speed, on the other hand, is not necessarily shown. The continuous advice display design is discussed in more detail in Section 7.2.2.1.

When the vehicle enters a segment the optimal vehicle operation v_{opt} is computed for the detected segment, taking into account the vehicle's initial state. Most efficient vehicle operation is presented to the driver if the proposed optimal vehicle speed does not interfere with driver safety due to a preceding vehicle. In the case that a vehicle in front is detected and the optimal advice would result in safety risks the information is not shown. A so-called vehicle following state is specified, in which the control logic blocks critical driver advice. No information is presented to the driver until the preceding vehicle leaves, that is the vehicle has turned or accelerated to leave a safe following distance. In this case the optimal velocity trajectory is re-calculated for the segment, taking into account the current initial state. If no further safety risks are detected advice on most efficient vehicle speed can now be presented to the driver.

Continuous driver advice not only concentrates on optimal vehicle speed but also on appropriate gear choice. As we see from Figure 7.9, information on best gear selection is not segment dependent. The most efficient gear choice is continuously

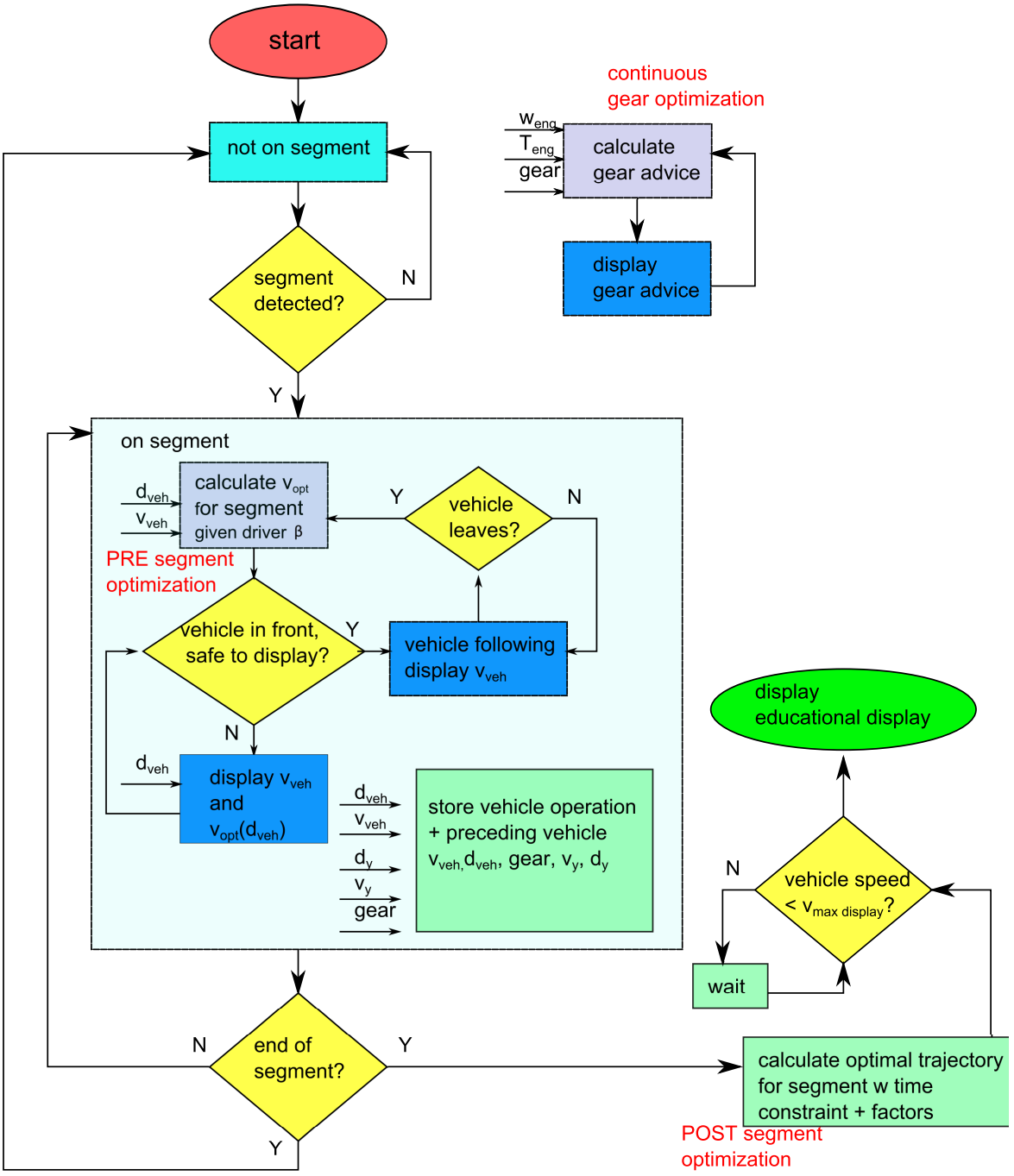

FIGURE 7.9: Logic of ADAS algorithm

calculated using the engine speed and torque. Detailed information about the advice given to the driver can be found in Section 7.2.2.1.

In order to give educational advice after a driven segment the vehicle operation is stored throughout a road segment. In Figure 7.9 the algorithms concerning the educational advice are shown in the bottom right in green. While the vehicle is covering a detected segment, vehicle distance (d_{veh}), vehicle speed (v_{veh}), gear selection, and preceding vehicle information is recorded. When the end of a road segment is detected this information is used to compute the optimal velocity trajectory for the driven segment, taking into account traffic. Comparing the best vehicle operation to the actual driving profile, four factors are evaluated to educate the driver on positive and negative aspects of his recent driving style. The display of this advice is discussed in more detail in Section 7.2.2.2. Due to safety risks educational advice is only presented to the driver if vehicle speed is lower than some threshold velocity ($v_{maxdisplay}$). In our case educational advice was given at vehicle speeds lower than 5km/h. With this choice educational advice was shown for scenarios such as stop light situations, priority situations in an intersection. No advice is presented at right turns on green or roundabouts.

In the ADAS algorithm the constructed trajectory optimization techniques developed in this thesis work are applied. In the logic flow, in Figure 7.9, the optimization components are pointed out in red. The pre-segment, continuous gear and post-segment optimization algorithms and resulting driver advice generation will be described in the following section

7.2.1.2 Optimization and Advice Evaluation

Three optimization algorithms are used to determine best vehicle operation for a specified scenario:

- Pre-segment optimization: approximates best vehicle operation for the segment to be driven
- Continuous gear optimization
- Post-segment optimization: evaluates the driver's recent vehicle operation

Of these algorithms, the first two are applied throughout vehicle use and generate advice for the continuous in-vehicle display (Figure 7.7). The post-segment optimization provides advice to the driver on an educational display (Figure 7.7).

Pre-segment optimization The pre-segment optimization algorithm, visualized in Figure 7.10, is applied in two cases. When the vehicle is detected to enter a new segment, or if the vehicle was considered in the 'vehicle following' state and the preceding vehicle had left. The trajectory optimization algorithm is then used to identify the optimal velocity trajectory of the vehicle for the segment to be driven. The two dimensional dynamic programming method is applied to solve the problem. The weighting factor β is defined prior to the trip by the driver. Utilizing the developed trajectory optimization algorithms together with the conventional vehicle model the trip and road constraints need to be defined. Trip constraints are fixed specifying initial and final vehicle states in distance and velocity. Initial conditions are easily defined by the current vehicle distance (d_{veh}) and speed (v_{veh}). In order to define constraints on the final state, we assume, similarly to the Audi Travolution Project [22], that stop light position and phase at vehicle arrival is known. Associating the end of the segment with a desired final speed ($v_{des}(d_{roadf})$) the final vehicle state can easily be specified by d_{roadf} and $v_{des}(d_{roadf})$ (Table 7.2).

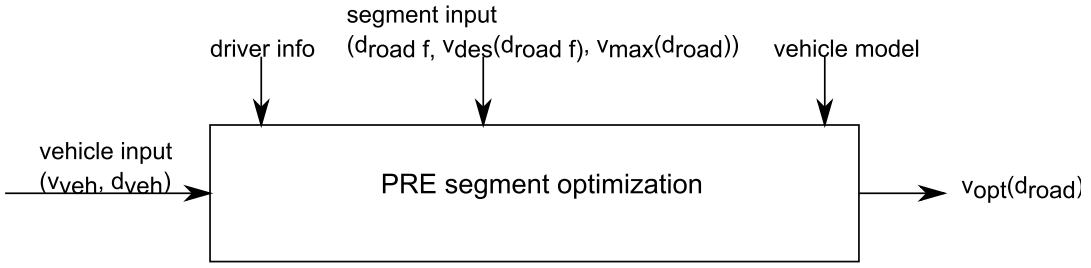

FIGURE 7.10: PRE segment optimization

situation at end of segment	$v_{des}(d_{roadf}$
red stop light, left turn on green, stop sign	0
roundabout, right turn on green	10km/h
going straight through green light	legal speed limit

TABLE 7.2: Segment final speed association

In our case a desired arrival speed was defined for any situation where the vehicle will need to come close to a stop. A corresponding situation could be a stop light that is red, a left turn on green or a stop sign. For arrival scenarios where the

vehicle does not have to come to a full stop, such as a roundabout or a right turn on green, a small vehicle speed, around 10km/h, was defined as desired arrival speed. When the segment ends with a vehicle going straight through a green light the desired arrival speed was set to the legal speed limit. Within a realistic range it was found that the accurateness of a desired arrival speed was not very important. This is due to the fact that the system's advisory function was turned off at some safety distance from the intersection ending a segment.

To specify road constraints it was assumed that the legal speed limitations are known for each segment. Appropriate maximum speed limits can easily be defined with the placement information of speed limit signs. A variable $v_{max}(d_{road})$ defines the maximum speed constraints as a function of road distance. With these hypotheses trip and road constraints can be fixed. Using the driver input to define his individual weighting of fuel consumption and trip time the vehicle specific optimal velocity trajectory is identified as a function of distance ($v_{opt}(d_{road})$).

Continuous gear optimization A second optimization that contributes to the functionalities of the continuous driver display is the continuous gear optimization. Gear advice can be given to the driver at any time, and does not depend on the vehicle position on or off a road segment. The computed gear advice is independent of optimal speed advice. This means that it only depends on the driver's vehicle operation, but is not influenced by other information presented on the display. As seen in Figure 7.11, the algorithm uses the engine operating point to determine if a gear change is appropriate. The method to identify gear changes has previously been presented in Section 6.2.4.1. Using the vehicle model gear dependent minimum and maximum allowable engine speeds for a requested torque are defined. With this, when the engine speed moves above the gear specific maximum engine speed an up-shift is recommended. Similarly, if the engine speed drops below the lower engine speed limit, the advice indicates a downshift.

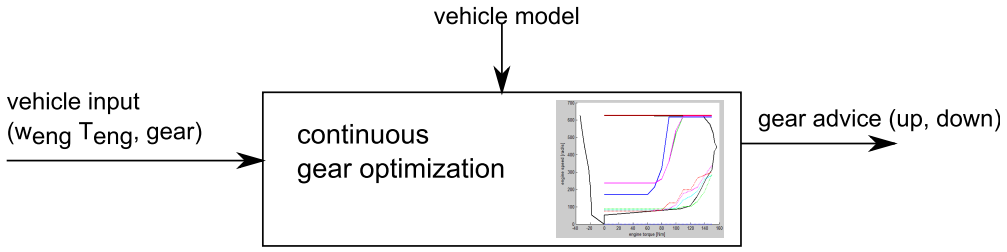

FIGURE 7.11: Continuous gear optimization

Post-segment optimization A driver's vehicle operation is evaluated once a segment is driven. To do so, the vehicle operation ($v_{veh}(t)$, $dveh(t)$) as well as information about preceding vehicles ($v_y(t)$,$d_y(t)$) is recorded throughout a segment. A general overview of the post-segment optimization algorithm can be seen in Figure 7.12. The recorded vehicle and traffic information, together with driver, segment and vehicle inputs, is used to identify the best speed profile for the last road segment. With the stored data the final time constraint can be fixed. The optimal trajectory can therefore be computed with the β specified by the driver, or as a fixed time problem identifying an appropriate beta for a given final time. In our experiments a simple β look-up method, as presented in Section 4.2.2.1, was applied to keep computational time low. In addition, the vehicle model is used to evaluate the best gear selection for the driver's vehicle operation. Using the computed optimal vehicle operation and comparing it to the driver's vehicle operation positive and negative aspects of the driving style are evaluated. Four factors, corresponding to acceleration phase, constant speed phase, deceleration phase and gear selection, are determined to educate the driver about ways to improve his driving and minimize fuel consumption.

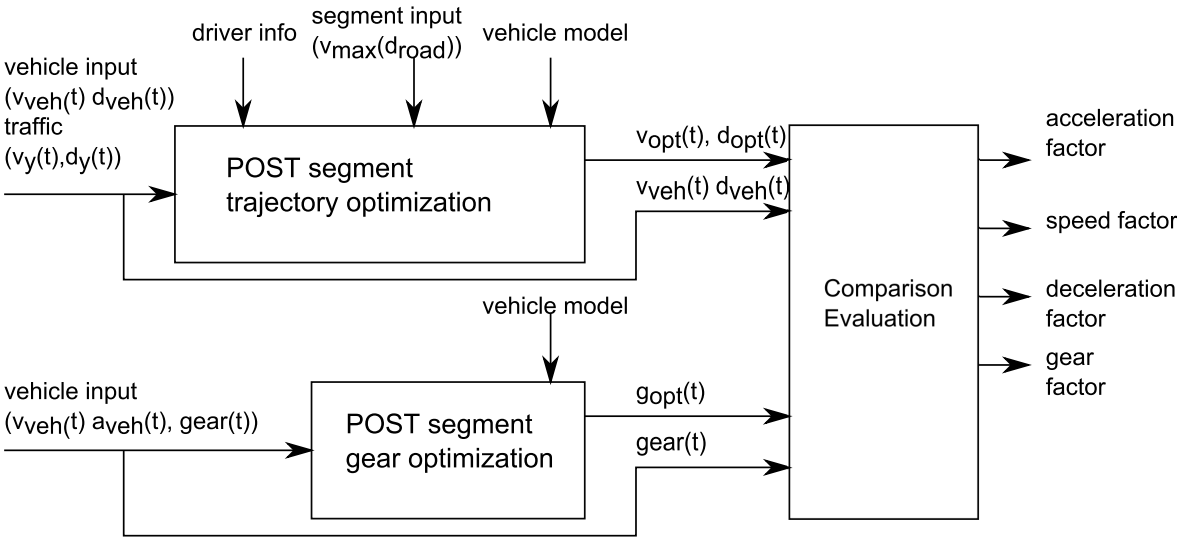

FIGURE 7.12: POST segment optimization

To transmit the computed information to the driver an efficient, easy-to-use human-machine-interface was designed.

7.2.2 Human Machine Interface (HMI)

The Human Machine Interface (HMI) used here, is based on a simple rule based approach taken in a study at LESCOT. In previous studies only a single display was used, on which an engine rotational speed was recommended. In our work the interface between the algorithm and the driver consist of two in-vehicle displays. In Figure 7.7 the installation of the driver assist system in the vehicle is shown. The continuous display is fixed within the driver's vision on the dashboard. Since the display shows a vehicle speed odometer it can replace the vehicle's odometer reading or could be integrated directly in the vehicle's own odometer display. The second, educational display is attached, similarly to navigational devices, in the front between the driver and passenger seat. In this position it is not in the vision of the driver and cannot distract the driver's general vehicle operation. In the following the design of the two interfaces is described.

7.2.2.1 Continuous display

The continuous display is used to assist a driver in minimizing his energy consumption throughout a trip. The display continuously shows information unless it considers the advice to interfere with driver safety. An image of the continuous display without advice is presented in Figure 7.13. A simple vehicle speed odometer is used as a basis of the system. Similarly to general dashboard devices we use a gauge to indicate current vehicle speed to the driver. In addition, the display includes an indication of current gear selection. The symbol of a manual gear box is shown in the bottom of the display. Within this symbol the engaged gear is indicated by a green point. The continuous display is shown like this if the vehicle cannot be placed on a segment, or a vehicle following situation is detected.

When advice about best vehicle speed is presented to the driver the display is shown as seen in Figure 7.14. On the outside of the vehicle speed odometer circle a zone indicates optimal velocity. This zone starts indication at the current vehicle speed and moves up, presenting optimal acceleration, to stabilize at an appropriate constant speed for the segment. When approaching the end of a segment advice on the best deceleration rate is given while the zone moves to lower vehicle speeds. In order to minimize his energy consumption a driver is advised to keep vehicle speed in the middle of the indicated zone.

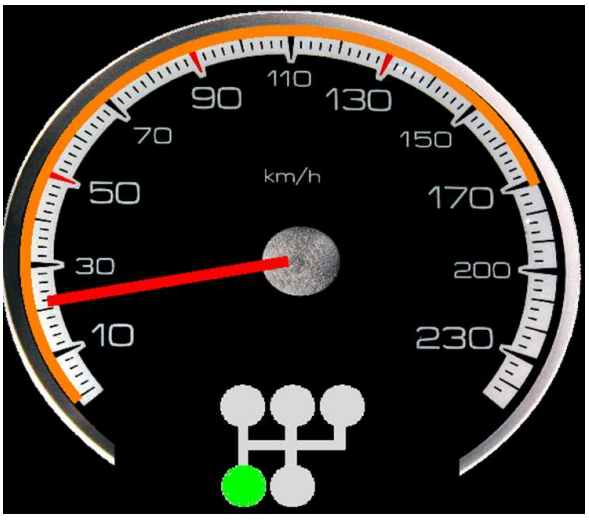

FIGURE 7.13: Continuous display without advice

In Section 4.4 the sensitivity of the identified optimal velocity trajectory was discussed. It was found that diverges from optimal solution in the acceleration and deceleration phase result in minor disadvantages in fuel consumption. In comparison, keeping the vehicle speed at the defined stabilized speed seems very important. This knowledge was implemented here. As seen from Figure 7.14, the optimal speed zone was indicate much larger in an acceleration or deceleration phase (left figure) than for the stabilized speed phase (right figure). This also had practical advantages since it is much harder to follow the indicated target speed when it is moving than when it is stationary.

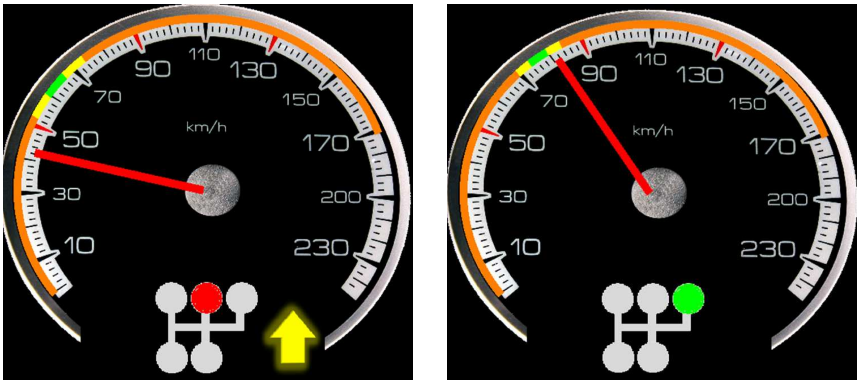

FIGURE 7.14: Continuous display with advice

In addition to optimal vehicle speed the continuous display also recommends gear changes to the driver to operate the internal combustion engine in a more efficient region. When an appropriate gear is selected the engaged gear is indicated in green in the gear box image. When the gear should be changed the gear indication changes to red and a flash indicates the direction of the recommended gear change.

An upward change is advised by a yellow upward arrow on the right of the gear box, as seen in Figure 7.14 on the left. A downward flash on the left of the gearbox indicates that a downshift is recommended.

7.2.2.2 Educational display

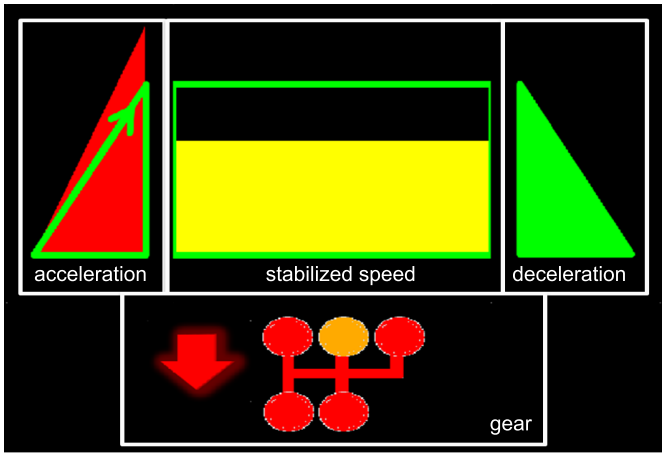

FIGURE 7.15: Educational display organization

An educational display is used to present an evaluation of the driver's recent driving style. To do so, four factors are indicated to the driver. In Figure 7.15 the screen organization and symbol placement for the different factors can be seen. The display shows the acceleration factor, stabilized speed factor and deceleration factor on the top. The symbols are organized such that we can image a velocity trajectory. The factor evaluating gear operation is placed at the bottom of the screen. In Figure 7.15 an example of an educational display is presented. We will now brake down the display to discuss the symbols of each factor and their meanings.

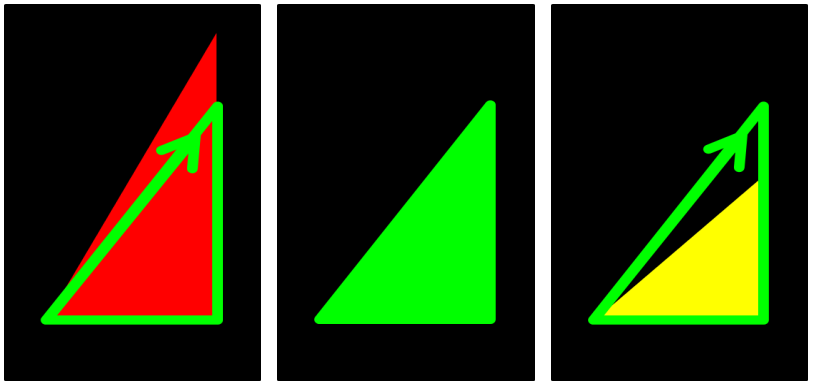

FIGURE 7.16: Acceleration factor symbols

Figure 7.16 presents the symbols designed to advice the driver of his performance in the acceleration phase. A driver might have accelerated to hard, applied correct acceleration rates or used acceleration rates below the optimal. The respective symbols indicated on the educational display advice lower acceleration, good acceleration and harder acceleration.

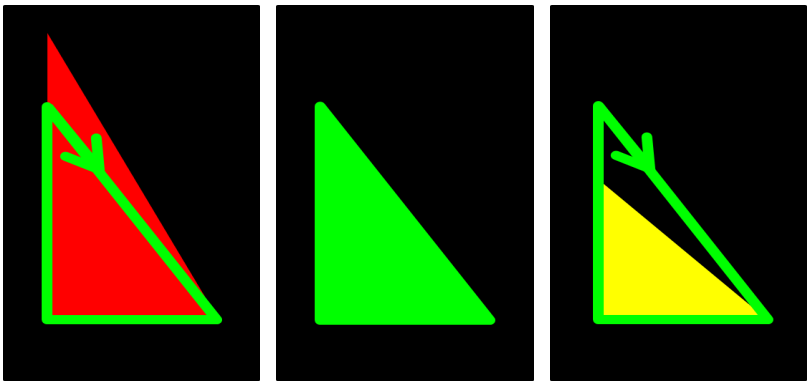

FIGURE 7.17: Deceleration factor symbols

Similarly to the acceleration phase, triangular symbols were used to indicate too hard deceleration, correct deceleration and deceleration rates below optimal. The respective symbols can be observed in Figure 7.17. In order to facilitate the use of the display a color code was implemented as well as representative symbols. A green triangular shape was used to represent fuel efficient vehicle operation. When driver operation exceeded the reference a red symbol was displayed, where the triangular area exceeded the best vehicle operation. When a driver operation was identified inferior to the reference a yellow symbol indicated a triangular area that did not entirely fill the green triangle. With this design we aim to reduce processing time for the operator to understand the indicated information.

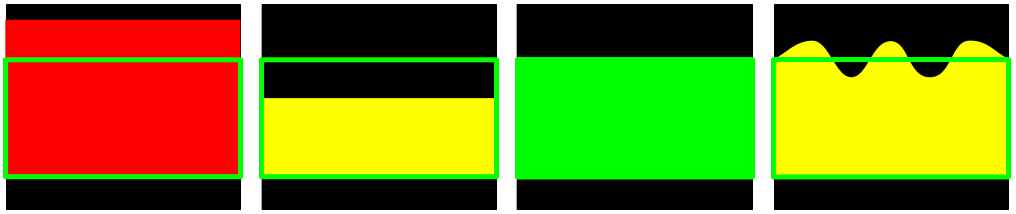

FIGURE 7.18: Speed factor symbols

The stabilized speed zone was evaluated with the help of four factors. The symbols presented in Figure 7.18 represent too high, too low, correct and unstable vehicle speeds. In addition to velocity profile evaluation the driver's gear selection is compared to most efficient gear operation for the respective vehicle velocity and acceleration. Using the red-green-yellow color code in combination with indicating

arrows, advice on gear choices is presented. The three symbols displaying gear recommendations to the driver can be observed in Figure 7.19. While the red gear box with a downward flash indicates a generally to high gear selection, the yellow gear box with an upward flash recommends, on average, higher gear engagements. To point out the gear that was used least efficient an orange circle is displayed. With this the driver can focus on improvements that result in the maximum gains in energy consumption.

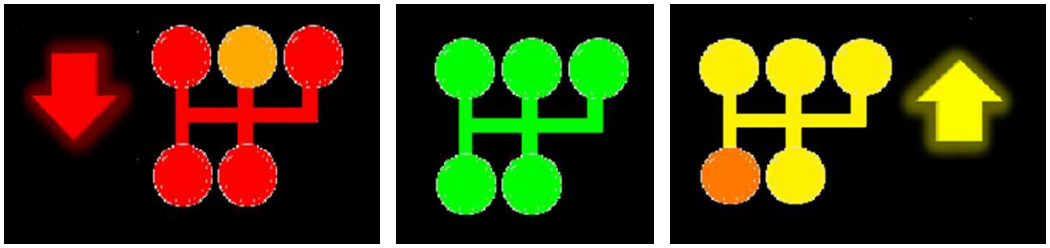

FIGURE 7.19: Gear factor symbols

The developed ADAS system was tested for gains in fuel consumption and driver acceptance in an experimental setup on a group of external human subjects using the driving simulator.

7.3 Experimentation

In this section the experimentation of the ADAS system is described, discussing experimental setup and testing routine. The results will be analyzed in Section 7.3.2.

7.3.1 Experimental setup

To experimentally test the developed driver support system three trips were designed in the simulator environment. A first trip, P0, represents a journey that takes about 7min and is mainly in an urban environment. P0 is used to train the test person on the simulator and therefore integrates multiple turns, and roundabouts. The trips PI an PII are designed to be similar, but to use different road segments. Both journeys take about 20min and consist of a first extra-urban part, where speed limitations go up to 90km/h, and a second urban part. PI and PII were used to run the baseline test, where fuel consumption without driver assist

system is measured, and test with support system. Prior to the test the subject is not informed of the course. Deviation signs at each intersection indicate the direction to be taken. To eliminate the effect of the mission on the fuel reduction the two missions were counterbalanced. This means that half of the subjects were tested for a baseline on PI, while identifying the fuel consumption with the driver assist system on PII. The second group started the test with PII and was using the support system on PI.

Prior to the experimental test two surveys were designed to gather information about the test person and their thoughts on the ADAS system. A first survey was used to identify personal parameters, such as gender, age, technical and environmental background. In addition the frequency of a person's vehicle use was identified. A second survey was used after the ADAS system was tested to evaluate the driver's acceptance and the understanding of the advice given. In addition, questions on driving effort were asked to identify disturbances due to the system. The exact questions asked can be found in the appendix.

The system was tested on a group of subjects that was recruited externally of the laboratory. 15 subjects took part on the experimentation. However, due to the difficulties of driving on a simulator 3 could not finish the tests and felt sick. Of the 12 remaining subjects 7 were female and 5 male. Within a realistic range the age of the driver was of no importance since the developed system should be usable for any driver. The oldest person to take part in the experimentation was 57 and the youngest 26 years old. A requirement was that the subject has had the driving license for at least two years.

The testing routine usually took between 1h30 and 2h and went by the following agenda:

- After welcoming the test driver a vision test was taken
- To familiarize with the simulator a training course (P0) was driven
- Baseline test of the driver's vehicle operation on course PI (or PII)
- Survey (QI)
- An introduction to eco driving and the advanced driver assist system is given
- A second training course (P0) is driven to familiarize the driver with the system

- The system is tested on course PII (or PI)
- Survey (QII)

7.3.2 Results

In the following we will analyze the gains in fuel consumption of the 12 tested subjects. The effects of subject specific parameters, like age, gender, environmental concerns and technical understanding, on gains in fuel consumption will be discussed.

7.3.2.1 Gains in fuel consumption

Overall, the results of the tested driver assist system were very satisfying. On average the 12 subjects were able to reduce their fuel consumption by 11%. A slight difference in general fuel consumption was detected between PI and PII. The baseline consumption values of PII were on average 10% lower than the consumption of PI. Counterbalancing was used to detect the effect of mission specific fuel consumption changes. Group A of 6 subjects performed the baseline on PI while the assisted driving was measured on PII. Group B of 6 subjects used PII to evaluate baseline driving and PI for the test with ADAS system. Due to the difference in mission the gains measured with the driver assist systems of group A were much higher than those measured for group B. Although differences between the two driving missions existed, in no test case did we measure increases in fuel consumption between the baseline driving and assisted driving. We can therefore be sure that the designed ADAS system has a positive effect on energy consumption.

In Figure 7.20 the gains in fuel consumption are shown per group. We can see that, while group A was able to achieve very high reductions in fuel consumption, group B showed rather small, although not insignificant, improvement in energy consumption. In order to eliminate this effect average fuel consumption of each mission was compared when driven with and without the support system. The bar graph in Figure 7.21 shows that a driver can safe on average 15% due to the ADAS system for mission PI and 5% for mission PII.

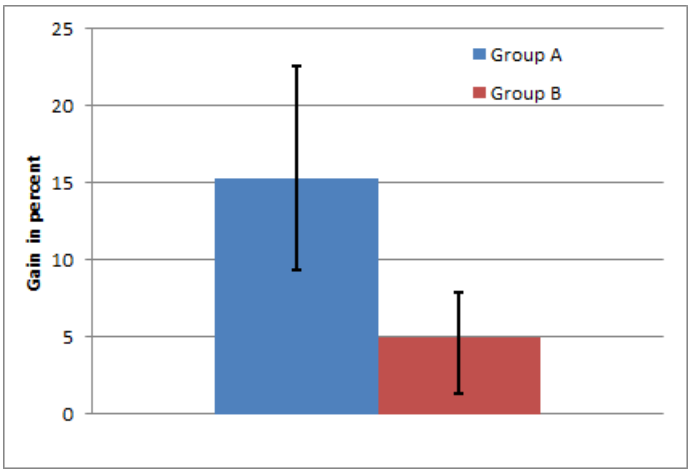

FIGURE 7.20: Gains in fuel consumption per group

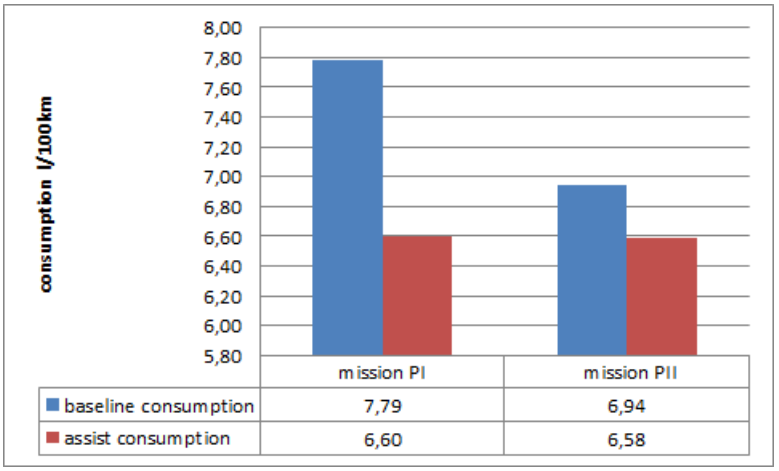

FIGURE 7.21: Fuel consumption per mission with and without ADAS

The mission profiles tested consisted of an extra-urban part, where driving on the countryside is simulated, and an urban part, where traffic and stop lights have a strong influence on the driving style. As expected it was found that, with less distractions in the extra-urban driving part, it was possible for drivers to focus more on the ADAS system. Much higher reductions in fuel consumption in extra-urban driving were identified than when using the eco driving support system in an urban environment. In Table 7.3 the measured consumption values can be found. While the ADAS system resulted in a reduction in fuel consumption of 15.25% in an extra-urban environment, the gains due to the system were only 8.74% in city driving.

setting	baseline [L/100km]	assisted [L/100km]	gain [%]
urban	8.31	7.58	8.74
extra-urban	7.00	5.90	15.25

TABLE 7.3: Fuel consumption gains in urban and extra-urban settings

7.3.2.2 Driver influence on eco driving gain

Due to the limited number of tested subjects we need to be cautious about drawing conclusions with respect to personal parameter data. Nonetheless, we want to analyze the influence of personal parameters on possible gains in fuel consumption due to an advisory system. Of the subjects tested every single one seemed to be more or less concerned with environmental problems of our planet. All of the subjects indicated that they contribute their part to reduce their environmental impact by using recycling techniques, using public transportation, biking or other environmentally friendly behavior. Some subjects stated that, in their daily vehicle use, they applied economic driving techniques. However, in the evaluation of the test results it was found that the baseline fuel consumption of these subjects was equal (for extra-urban driving) or higher (for urban driving) than those who did not indicate such behavior. It seems that insufficient knowledge of people limits their desired minimized fuel consumption without the help of an advisory system.

In the survey the drivers were asked to list several eco driving rules in order of importance. With a choice of 'vehicle speed', 'vehicle acceleration', 'anticipation', 'braking', and 'engine speed', most subjects listed 'anticipation' and 'acceleration' as the most important parameters to reduce energy consumption. In this these it has become clear that due to the aerodynamic drag vehicle speed is the most important parameter to be considered for eco driving when vehicle speeds are above 30km/h. We conclude that people generally need to be informed in more detail about vehicle specific eco driving rules.

The survey results indicated that subjects that possess basic mechanical knowledge achieved lower fuel consumption on the baseline testing. In addition, subjects with frequent vehicle use, here defined by more than 10 000km driven per year and everyday use, seemed to have lower basic fuel consumption. In Table 7.4 the baseline consumption and gains in fuel consumption for urban and extra-urban driving are listed for different categories. It can be seen that people with mechanic knowledge and frequent vehicle users had lower baseline energy consumption in an

parameter	baseline urban [L/100km]	gain urban [%]	baseline extra-urban [L/100km]	gain extra-urban [%]
w mechanical knowledge	8.10	7.30	6.90	15.86
wo mechanical knowledge	8.60	10.76	7.13	14.39
frequent vehicle use	8.00	6.84	6.77	15.35
infrequent vehicle use	8.93	12.53	7.46	15.03

TABLE 7.4: Baseline fuel consumption versus mechanical knowledge and vehicle use

urban and extra-urban environment. With respect to this reference, however, the gain in fuel consumption with the ADAS system was lower than for the subjects without mechanical knowledge and infrequent vehicle use.

In Figure 7.22 the consumption gains for different aged subjects can be seen. Although the small number of subjects is not sufficient to draw any conclusions we want to point out that the youngest subjects, with age lower than 30, showed the largest gains due to the use of the eco driving assist system. In the bar graph consumption gains for the entire driving mission can be seen, as well as separated gains for urban and extra-urban driving. In all three categories the youngest subjects seemed most capable to improve their driving behavior with the help of the system. Analyzing the survey responses it was also found that this group was the one that indicated to understand the system the most, showed the lowest effort due to its use with high acceptability. However, this group specified to have no mechanical experience. It seems that a motivated, young user can easily use the system without any mechanical background knowledge.

7.3.2.3 Driver acceptance and design

Overall it seems that the interface was easily understood. Drivers generally felt that the system's indications were justified and reasonable. From the measured fuel consumption values it seems that driver acceptance is an important factor to ensure the effectiveness of the system. In Table 7.5 the fuel consumption gains for urban and extra-urban driving are shown for drivers that tend to believe in the advantages of the ADAS system. In comparison we can see the gains of people less convinced of the system. The trust in the system seems to be an important requirement for the system to reach its maximum potential.

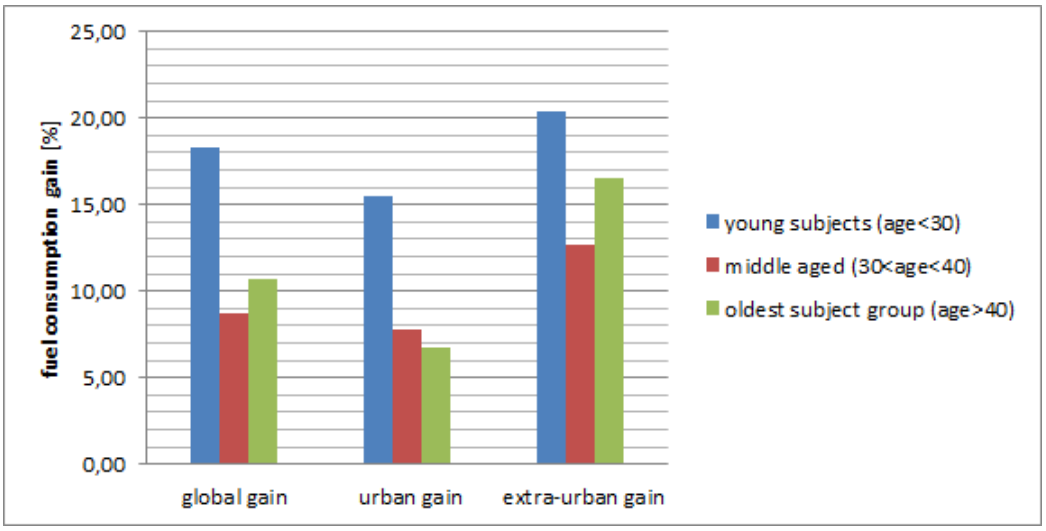

FIGURE 7.22: Consumption gains for different age groups

subject group	gain in urban driving [%]	gain in extra-urban driving [%]
ADAS accepted	9.37	16.78
ADAS less accepter	8.29	14.15

TABLE 7.5: Gains in fuel consumption dependent on system acceptance

The design of the interface was generally perceived as appropriate. However, several drivers commented on the visibility of the continuous display. While the display was attached to the dashboard it seems that drivers would prefer the system to be directly in the field of vision, similarly to displays integrated in the vehicle's front screen. Most people indicated that a driver assist system, as the one tested, could be useful. Many subjects would appreciate an ADAS system for eco driving integrated in a purchased vehicle. However, in order to separately buy a driver support system, they would have to be convinced about the advantages it represents for them.

7.4 Conclusion

This chapter dealt with the validation of the thesis work. The developed vehicle models and optimization algorithms were used to design an advanced driver assist system for eco driving. The collaboration with the LEPSiS and LESCOT laboratories allowed us to test the developed ADAS system experimentally. To evaluate the system's effectiveness, it was tested on a driving simulator on external subjects.

The simulator environment was introduced. To test the vehicle specific optimization algorithms on the driving simulator the VEHLIB direct vehicle simulation was integrated in the simulator environment. The software was adapted to the simulator with the development of a simple braking model. In addition a simplified model of the steering and lateral vehicle motion was implemented. A communication network between vehicle simulation, driving simulator environment and driver assist system was set up.

The ADAS system, that integrates the developed trajectory optimization algorithms in an operating logic that ensures minimum intervention in unsafe driving conditions, was introduced. To advice the driver of fuel optimal vehicle operation the tested ADAS system presents information to the driver on two in-vehicle displays. With this approach the human-machine-interface communicates continuous advice while driving and educational advice when the vehicle is at rest.

Testing the ADAS system in an experimental setup on the driving simulator 12 external subject were used to measure the gains in fuel consumption. On average the ADAS system was able to help the driver to reduce fuel consumption by 11%. It was found that higher gains in fuel consumption were achieved in an extra-urban environment than in city driving. In general it seems that personal parameters, such as mechanical knowledge, vehicle use frequency, age and system acceptance, have a strong impact on possible gains in fuel consumption. In addition, it was found that education on fuel minimizing vehicle operation needs to be improved. Overall we conclude that the designed ADAS system was effective and easily usable.

Chapter 8

Conclusions

Contents

To conclude this thesis we will summarize the work and its contributions. A perspective on potential future studies in this area is given.

8.1 Conclusion

A literature review has shown that several driver support systems exist to assist the driver to reduce his energy consumption. To identify most efficient vehicle operation several studies on velocity trajectory optimization exist. To complement existing work this thesis identifies drive train specific optimal vehicle operation and effects of constraints on potential gains due to eco driving. In addition an approach to integrate numerical optimization algorithm in combination with detailed physical vehicle models in the development of an effective driver assist system.

Three representative vehicle types were used to demonstrate the algorithms developed in this thesis: a conventional passenger vehicle, a small electric vehicle and the Toyota Prius hybrid power split vehicle. In Chapter 3 the advantages and disadvantages of inverse and direct modeling were discussed. A detailed physical model of each drive train has been shown. For optimization purposes the inverse modeling approach was applied. A direct vehicle modeling software VEHLIB was

used to verify the vehicle operation and consumption for the computed velocity profiles.

For modeling purposes the vehicle chassis and drive train can be separated. While the three considered vehicle's chassis can be modeled in a similar way, their drive train configuration changes. Factors influencing vehicle operating efficiency were discussed. Chassis dependent, and therefore drive train independent, losses include aerodynamic drag and rolling resistance, which depend on vehicle speed. Drive train specific factors include component operating efficiencies and the hybrid vehicle's control strategy. To identify the best vehicle operation the use of numerical optimization methods was proposed.

To identify potential gains of eco driving standard and real world cycles were used to define a vehicle's mission. Respecting the specified trip and road constraints the aim was to compute corresponding eco cycle for some baseline mission. The trajectory optimization problem is specified in Chapter 4. The continuous optimization problem was approximated with a discrete trajectory optimization. Initially the three dimensional dynamic programming method was applied due to its advantage in constraint integration. To reduce computational time the problem was reduced to a two dimensional setup by integration of the time constraint in a weighted objective function. A nested approach, where two dimensional dynamic programming was combined with advanced root finding methods was shown to given good results in an acceptable time.

A multi-objective optimization method on the basis of dynamic programming was presented to evaluate the trade-off between trip time and fuel consumption. It was found that drivers with critical trip times are able to achieve significant gains in fuel consumption for small increases in trip time. The multi-objective optimization method was used to analyze the sensitivity of the fuel consumption to divergences from the optimal velocity profile. It was found that a low constant cruising speed is important to keep fuel consumption low. Small changes in the acceleration and deceleration phase result in limited increases in fuel consumption.

Using the developed optimization algorithms potential gains of eco driving in ideal conditions were computed for the three representative vehicle types in Chapter 5. With this we were able to define an upper limit for potential gains in energy consumption. The computed eco cycles were used to compare baseline and energy efficient vehicle operation. Important factors for eco driving were determined. Fuel

minimizing vehicle operation of the conventional vehicle was computed for different drive cycles, representing urban, extra-urban and freeway driving. The resulting velocity profiles were tested in an experimental hardware-in-the-loop setting to measure fuel consumption. Various low speed cycles were used to evaluate energy efficient operation of the small electric vehicle. To verify and measure the energy consumption the cycles were tested on a chassis test bench. Optimizing hybrid vehicle operation it was found that it is important to take into account battery use although the vehicle's control strategy manages the battery level of charge. It was found that choosing an appropriate weighting of battery use and fuel consumption was critical to identify energy efficient vehicle operation.

In general, it was shown that eco driving strategies have high potentials to reduce fuel consumption for the conventional, electric and hybrid vehicle. Higher energetic gains are possible in an urban and extra-urban environment than for freeway driving. Comparing the results we determined that, while component efficiency was only showed limited increases, the energy consumption was overall reduced due to more appropriate choices of vehicle velocity and acceleration. At average trip speeds higher than 30km/h it was found that the losses due to aerodynamic drag, which increase rapidly with the vehicle speed, were a dominating factor in the optimization. Vehicle cruising speeds were chosen as low as possible to reduce losses due to aerodynamic drag.

Overall it was found that the acceleration and deceleration phase were chosen drive train dependent, while the stabilized vehicle speed was most dependent on the vehicle's chassis. The efficiencies of the drive train components usually resulted in maximum acceleration. This phase is therefore dependent on drive train performance. A lowest possible constant speed was applied in the cruising phase to respect the trip's time constraint. A drive train specific deceleration rate was chosen to maximize energy recovery. However, short deceleration phases were realized with the use of hard braking in the second phase of deceleration. With this deceleration time was minimized and lower cruising speeds could be chosen to result in the required average trip velocity.

In Chapter 6 the integration of additional constraint is presented. To identify realistic gains in fuel consumption in an urban setting the constraints due to traffic were considered. Imitating a vehicle following situation necessary safety constraints and their effect on eco driving strategies are discussed. It was shown that with reduced flexibility of vehicle operation due to traffic the gains achievable

with eco driving are limited. However, we found that while it is important to take into account traffic to ensure driver safety, eco driving still represents significant advantages in energy consumption.

In a second case study emission constraint were discussed. Eco driving is generally considered to be environmentally friendly. This study analyzed the economic and ecologic advantages of eco driving. Using hardware-in-the-loop testing the fuel consumption and pollutant emissions were measured on an engine test bench for an urban drive cycle. It was found that CO and HC emissions increased for the computed fuel efficient eco cycle. Eco driving does therefore not necessarily have to be considered ecological. In our work an approach to integrate emissions in the optimization process was proposed. A method to dynamically select emission optimal gears was presented. The measured results show that, with a small trade-off in fuel consumption, the CO and HC emissions can be reduced. It was concluded that eco driving can represent economic and ecologic advantages. However, it is important to consider emission constraints.

An approach to integrate the developed optimization algorithms in a driver assist system was shown in Chapter 7. The design of the advanced driver assist system was presented. A driving simulator was used to test the support system on external subjects. On average the ADAS system was able to help the drivers to reduce fuel consumption by 11%. It was found that higher gains in fuel consumption were achieved in an extra-urban environment than in city driving. With a survey given to the subjects it was evaluated that personal parameters, such as mechanical knowledge, vehicle use frequency, age and system acceptance, have a strong impact on possible gains in fuel consumption. In general it was found that the designed ADAS system was effective and easily usable.

This work shows that, among several other solutions, it is necessary to consider energetic optimization and its application to eco driving in order to help resolve problems in the transportation sector.

8.2 Perspectives

Future work on this subject could be envisioned in three areas: First, we envision a simplification of the optimization process. Secondly the algorithm could be generalized by applying it to other vehicle architectures. Finally we see future

work in the further development of the ADAS system and its integration in a real life scenario.

The optimization algorithms work on the basis of detailed physical models and are therefore complex and rather time consuming. In the further progress of this work the detailed optimization results could be used to identify important and unimportant aspects of detailed modeling. Developing simplified optimization without the loss of results can be helpful in the integration process.

In this work three main vehicle architectures were discussed: the conventional, the electric and a representative hybrid vehicle. In order to further analyze vehicle specific operation the algorithm can be applied to other driver trains on the road today or in the near future. The optimal operation of a fuel cell or hydraulic hybrid vehicle could potentially lead to changes in the eco driving velocity profile.

Since the aspect of the ADAS system was only briefly aborted in this thesis there remains much work to optimize the system for everyday use. It was found that driver acceptance has a strong influence on system effectiveness. Ergonomic studies are therefore necessary to evaluate the most appropriate design of the human machine interface. The system should then be tested in real life. Particularly in-vehicle tests in a Prius hybrid vehicle can be interesting to validate the gains in energy consumption.

Appendix A

Root finding methods

A.1 Bisection-Search

The bisection method is a method to find the roots of a continuous function. Given a function f the method is used to approximate the scalar value of x that satisfies the equation $f(x) = 0$. Assuming that there exists at least one zero in the interval $[a, b]$ the value of x is found by iteratively bisecting the interval. The process is illustrated in Figure 4.9 a).

Given the interval $[a, b]$ the iterative process is started by identifying the midpoint c between a and b. The values $f(a)$, $f(b)$ and $f(c)$ of the function at a, b and c are computed. Depending on the sign of $f(c)$ c is assigned to be the new lower or upper boundary value. For example, as here, if $sign(f(c)) = sign(f(a))$ then $a = c$ else $b = c$. We can now be sure that the zero lies in the new interval $[a, b]$. Repeating the same process the point d would be found next and assigned to be the new upper boundary. With this strategy the zero is approached. Defining a tolerance value ε the iterative process is continued until a value x is found for which $f(x) < \varepsilon$. In our problem the function f is represented by the final time error function and the found root x is the desired β-value to be used for the fixed time constraint optimization.

With this method the length of the interval is reduced by one half at each step, its convergence time is linear and therefore considered slow (depending on the shape of the function f). Other methods have therefore been developed with the intention of reducing the iteration number, and therefore computational time.

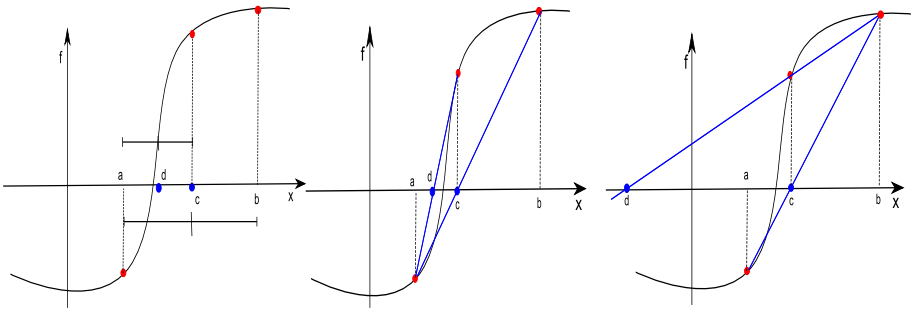

FIGURE A.1: a) Bisection Method, b) False Position Method, c) Secant Method

A.2 Newton Method

The Newton Method is a root-finding method commonly used to reduce the number of iterations. With this method the search for a zero is started with a point a and its function value $f(a)$. Using the slope of the function at point a, $f'(a)$, the next point b is fixed at the x-intercept of the line with slope $f'(a)$ through a. In our application the function $f(\beta)$ is in fact the error to the chosen final time t_f. Therefore we can not compute $f'(\beta)$.

There exist two method to solve this problem, which are derived from the Newton Method and can be applied for the case that the function's derivative can not be defined analytically. These are the False Position Method and the Secant Method. With these methods two points are chosen initially and the slope of the function f is approximated using these two points. A negative aspect of these methods is that they assume the function is approximately linear in the region of interest. The two methods differ only in their choice of which point the new value will replace. The Secant method, while often the faster method, is not guaranteed to converge.

A schematic of the two methods can be seen in Figure 4.9. In plot b) the False Position Method is shown. Initially the points a and b where chosen such that they enclose the root. The next iterative point is found by the x-intercept of the line through $f(a)$ and $f(b)$. In this example b is then replaced by c such that the root can still be found in the interval $[a, b]$. With the Secant Method, as seen in graph c), this is not ensured and the next chosen point always replaces the iteratively older point of the previous two. Here the point a is replaced rather than b as in the False Position Method.

The application of these Newton based methods is usually faster than using the Bisection Search because the search can converge faster than in linear time. However it depends strongly on the shape of the function f and even linear convergence rates are not guaranteed.

A.3 Ridder's Method

In 1979 Ridder ([87]) developed a method that resolves the issues encountered by the Secant and False Position Method. In his approach Ridder takes the bent out of the function by using an exponential. Given a root lies in the interval $[a, b]$ the method first locates the midpoint $c = (a + b)/2$ and then searches for the exponential e^k that turns the residual function into a straight line, hence solving $f(a) - 2f(c)e^k + f(b)e^{2k} = 0$. The false position method is then applied to the resulting linear function to find the next point d. The algorithms convergence is supposed super linear and robust ([87]).

A.4 Brents Method

To combine fast convergence with the guaranty of at least linear convergence Brent developed an algorithm in 1970 on the basis of an approach previously taken by Dekker([88, 89]). With his method Brent ensures that the search converges at at least linear rate but often much faster. To achieve this the method uses a combination of Bisection Method, Secant Method and Inverse Quadratic Interpolation.

While we approximated the slope of the function f in the Secant Method with two points in this method three points are used. With quadratic interpolation the function f can be approximated by the polynomial $y_{app} = k_1x^2 + k_2x + k_3$ using the three known points. But when solving this function for zero we might get a complex value as a result. Brent's method therefore uses inverse quadratic interpolation to identify an approximate of the function $x_{app} = k_1y^2 + k_2y + k_3$.

Brent's method still uses two values a and b as inputs, assuming the root is in the interval $[a, b]$. In an initial step the Secant Method is used to compute the third parameter c. In the following iterative process the parameters a, b and c are arranged such that $f(a)$ and $f(b)$ are positive, $|f(b)| \leq |f(a)|$ and b is the

following value to c. Then the choice between inverse quadratic interpolation, Secant Method and Bisection method is done as follows: If $c \neq a$ an inverse quadratic interpolation step is taken, if $c = a$ a Secant step is taken, and if either of the two steps falls outside of the interval $[a, b]$ then a Bisection step is used instead. This approach ensures that the new interval will always keep the root enclosed.

Appendix B

Vehicle model

B.1 Steering and lateral vehicle model

To compute the vehicle's motion in the global X-Y plane a simple vehicle model was constructed. The model uses the bicycle representation of the vehicle, where the two front wheels and the two rear wheels are respectively represented by one central wheel. The so-called 'kinematic model' is based only on geometric relationships and therefore does not consider the forces that affect the motion.

In Figure B.1 the geometry of the bicycle model is presented. The vehicle's front wheels are represented by one centralized wheel at A with a steering angle of σ_f, while the rear wheels are represented by the wheel at B and, if necessary, a rear steering angle σ_r. The gravitational center of the vehicle is called C, which is found at distance l_r from the rear end and l_f from the front end of the vehicle. This point is also the rotational center, which is here assumed to be fixed. The major assumption made with this model is that the velocity at each wheel points in the direction of the wheel. We therefore assume that the slip angle at each wheel is zero. For small vehicle speeds this can be assumed since lateral tire forces are small. We will later discuss how we adapt this model to higher speeds. The vehicle's heading in the plane is defined by ϕ and the vehicle's slip angle is represented by the angle β.

A detailed outline of the model construction can be found in [103]. We define V to be the vehicle speed, which is computed as an output of the vehicle drive train

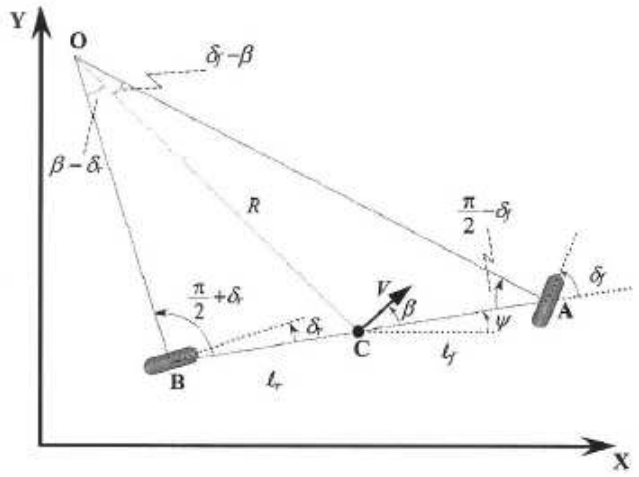

FIGURE B.1: Kinematic vehicle model

model. The vehicle position can now be calculated using geometric relationships by:

$$\dot{X}_{glob} = V cos(\Psi + \beta) \tag{B.1}$$

$$\dot{Y}_{glob} = V sin(\Psi + \beta) \tag{B.2}$$

$$\dot{\Psi} = \frac{V cos(\beta)}{l_f + l_r}(tan(\delta_f) - tan(\delta_r)) \tag{B.3}$$

$$\beta = tan^{-1}\frac{l_f tan(\delta_r) + l_r tan(\delta_f)}{l_f + l_r} \tag{B.4}$$

With this the vehicle longitudinal and lateral speed is defined as a function of vehicle speed and wheel angle. Given the steering wheel position the angle of the wheels can be computed with a steering ratio [104]. Measurements have shown that the ratio can be specified to a value around 16 for passenger vehicles. In our work the steering ratio is specified as a parameter, that is fixed to 16 for very small speeds, but grows proportionally with the vehicle speed. Due to increasing slip angles the vehicle usually turns less with increased speeds. Since the implemented lateral model does not consider tire slip angles, using a changing steering ratio can lead to more realistic vehicle operation.

Appendix C

Survey

Bonjour,

merci de remplir le questionnaire suivant après avoir fini le test préliminaire.

Il y a 19 questions dans ce questionnaire

Concernant la personne

1 [0]Votre numéro de test

Veuillez écrire votre réponse ici :

2 [1]Sexe

Veuillez sélectionner **une seule** des propositions suivantes :

- ◯ Féminin
- ◯ Masculin

Choissisez votre sexe.

3 [2]Votre Age

Veuillez écrire votre réponse ici :

4 [3]Avez-vous le permis B?

Veuillez sélectionner **une seule** des propositions suivantes :

- ◯ Oui
- ◯ Non

5 [4]Avez-vous des problèmes de vision non corrigés ou de santé pouvant gêner à la conduite?

Veuillez sélectionner **une seule** des propositions suivantes :

- ◯ Oui
- ◯ Non

6 [41]Si oui précisez:

Répondre à cette question seulement si les conditions suivantes sont réunies :
° La réponse était 'Oui' à la question '5 [4]' (Avez-vous des problèmes de vision non corrigés ou de santé pouvant gêner à la conduite?)

Veuillez écrire votre réponse ici :

7 [5]Presbytie

Veuillez sélectionner **une seule** des propositions suivantes :

- ○ Oui
- ○ Non

Expérience de conduite

8 [1]En quelle année avez-vous obtenue le permis de conduite?

Veuillez écrire votre réponse ici :

9 [2]Le nombre de kilomètres moyen vous conduisez pendant une année

Veuillez écrire votre réponse ici :

10 [3]Utilisation de la voiture

Choisissez la réponse appropriée pour chaque élément :

	Tous les jours	Plusieur fois par semaine	Plusieur fois par mois	Plusieur fois par an	Jamais
La fréquence à laquelle vou utilisez votre voiture	○	○	○	○	○
Fréquence d'utilisation d'autoroute	○	○	○	○	○
Fréquence d'utilisation des départementales, nationales	○	○	○	○	○
Fréquence d'utilisation en ville	○	○	○	○	○

11 [4]Connaissance du parcour

Choisissez la réponse appropriée pour chaque élément :

	Routiniers	Courant	Occasionnels	Inconnus
Les parcours que vous faîtes sur autoroute	○	○	○	○
Les parcours que vous faîtes sur RN ou départementales	○	○	○	○
Les parcours que vous faîtes en ville	○	○	○	○

12 [5]Quel modèle de voiture conduisez-vous?

Veuillez écrire votre réponse ici :

13 [6]Mettez des critères d'achat dans l'ordre

Numérotez chaque case dans l'ordre de vos préférences de 1 à 3

☐ Esthétique
☐ Performance
☐ Practicité

(1 critère le plus important, 3 le moins important)

14 [7]Effort perçu lors de certaines situations de conduite

Choisissez la réponse appropriée pour chaque élément :

	Effort extrême	Gros effort	Certains effort	Petit effort	Quasi pas d'effort	Aucun effort
Franchir un cédez le passage	○	○	○	○	○	○
Passer un rond-point	○	○	○	○	○	○
Franchir un feu	○	○	○	○	○	○
Suivre une voiture	○	○	○	○	○	○
Tourner dans une intersection	○	○	○	○	○	○

Technologie et Environnement

15 [1]Quel type de système embarqué utilisez-vous et quelle expérience en avez-vous?

Choisissez la réponse appropriée pour chaque élément :

	utilisé couramment	petite experièncе	déjà entendu parler, jamais utilisé	non, je ne connais pas
GPS	○	○	○	○
Limiteur de vitesse	○	○	○	○
Régulateur de vitesse	○	○	○	○
Radar de recul	○	○	○	○
Système d'information de la consommation	○	○	○	○
Avertisseur de radar	○	○	○	○

16 [2]Indiquez votre experièncе avec les technologies suivantes:

Choisissez la réponse appropriée pour chaque élément :

	Expérimenté	Intermédiaire	Débutant	Aucune expérience
Email	○	○	○	○
Internet	○	○	○	○
Ordinateur	○	○	○	○
Appareil photo numérique	○	○	○	○
Smartphone/tablette	○	○	○	○

17 [3]Vous sentez-vous concerné par les problèmes liés à l'environnement?

Choisissez la réponse appropriée pour chaque élément :

	Beaucoup	Assez	Un peu	Pas du tout
Concerné par l'environnement	○	○	○	○

18 [4]Quelle(s) action(s) individuelle(s) faites-vous pour participer à la proctection de l'environnement?

Choisissez **toutes** les réponses qui conviennent :

- ☐ Tri des déchets
- ☐ Eteindre les appareils électriques
- ☐ Compost (dans le jardin)
- ☐ Utiliser un vélo
- ☐ Conduite économique
- ☐ Utiliser les transports en commun
- ☐ Utiliser une chasse-d'eau économique
- ☐ Autre: ____

19 [5]Classer ces règles par ordre d'importance pour une conduit économique.

Numérotez chaque case dans l'ordre de vos préférences de 1 à 5

- ____ Vitesse
- ____ Accélération
- ____ Anticipation
- ____ Freinage
- ____ Régime moteur

Merci de répondre à quelques questions après avoir fini les tests avec le système d'assistance.

Il y a 9 questions dans ce questionnaire

Effort de conduite

1 [1]Effort perçu lors de certaines situations de conduite

Choisissez la réponse appropriée pour chaque élément :

	Effort extrême	Gros effort	Certain effort	Petit effort	Quasi pas d'effort	Aucun effort
Franchir un cédez le passage	○	○	○	○	○	○
Passer un rond-point	○	○	○	○	○	○
Franchir un feu	○	○	○	○	○	○
Suivre une voiture	○	○	○	○	○	○
Tourner dans une intersection	○	○	○	○	○	○

Evaluation du système d'assistance

2 [1]Connaissance mécanique:

Choisissez la réponse appropriée pour chaque élément :

	Beaucoup d'expérience	Intermédiaire	Débutant	Aucune expérience
Connaissance mécanique automobile	○	○	○	○

3 [2]Compréhension du système d'assistance

Choisissez la réponse appropriée pour chaque élément :

	Impossible	Difficilement	Facilement	Très facilement
Avez-vous compris le foncionnement du système?	○	○	○	○
Avez-vous compris la signification de chaque logo?	○	○	○	○
La jauge d'indication de vitesse optimale est-elle compréhensible?	○	○	○	○
Le conseil de rapport est-il compréhensible?	○	○	○	○
Les conseils d'accélération et de déceleration du segment sont-ils compréhensible?	○	○	○	○
Le conseil de vitesse stabilisée est-il compréhensible?	○	○	○	○
Les conseils du choix de rapport pour le segment est-il compréhensible?	○	○	○	○

4 [3]Quel(s) symbol(s) n'avez vous pas compris?

Veuillez écrire votre réponse ici :

5 [4]Efficacité, Confiance, Utilisation du système

Choisissez la réponse appropriée pour chaque élément :

	toujours	souvent	de temps en temps	pas du tout
Est-ce que les conseils divulgués vous semblent judicieux	○	○	○	○
Ressentez-vous que le système vous aide à conduire plus économiquement?	○	○	○	○
Pensez-vous qu'il pourrait changer vos habitudes de conduite après une utilisation de longue durée?	○	○	○	○
Pensez-vous que les conseils donnés sont fiables?	○	○	○	○
Pensez-vous avoir suivi les conseils donnés?	○	○	○	○
Pensez-vous avoir conduit économiquement?	○	○	○	○

6 [5]Evaluation subjective de l'interface du système

Choisissez la réponse appropriée pour chaque élément :

	d'accord	plutôt d'accord	pas d'avis	plutôt pas d'accord	pas du tout d'accord
Le design de l'interface est agréable	○	○	○	○	○
Les couleurs de l'interface sont adaptées	○	○	○	○	○
La visibilité générale est bonne	○	○	○	○	○
La visibilité des differents symboles est bonne	○	○	○	○	○
La disposition des différents symboles est bonne	○	○	○	○	○
La visibilité du cadran de compte-tours est bonne	○	○	○	○	○
Les consignes de changement de rapport sont visibles	○	○	○	○	○
Les consignes d'accélération et de décleration sont visibles	○	○	○	○	○
Les consignes de vitesse stabilisée sont visibles	○	○	○	○	○

7 [6]Intérêt d'un systèms d'éco-conduite

Choisissez la réponse appropriée pour chaque élément :

	Oui	Plutôt oui	Plutôt non	Non
Un système de ce type serrait utile afin d'aider à diminuer la consommation	○	○	○	○
Vous êtes prêt à acheter un tel système	○	○	○	○

8 [7]Evaluation finale du système (x sur 20)

Veuillez écrire votre(vos) réponse(s) ici :

Esthétique	
Facilité d'utilisation	
Utilité	
Fonctionnement	

x sur 20 (x/20)

9 [8]Avez vous des remarques?

Veuillez écrire votre réponse ici :

Merci pour votre participation.
01.01.1970 – 01:00

Envoyer votre questionnaire.
Merci d'avoir complété ce questionnaire.

Appendix D

Synthèse

D.1 Introduction

En 1885 Karl Benz développa le premier véhicule conventionnel [1]. Après la mise au point de voitures propulsées par vapeur et électricité, il fût le premier à construire une voiture dotée d'un moteur thermique à combustion. Depuis le 19ème siècle le nombre de véhicules a augmenté de façon spectaculaire et devrait atteindre 1200 million en 2030 [17]. S'il a représenté un facteur de progrès et de développement majeur pour l'humanité, le secteur des transports doit aujourd'hui faire face à de grandes problématiques.

L'atteinte du maximum de production mondial de pétrole (le pic pétrolier s'est produit en 2006 selon l'IEA (International Energy Agency) [3]) associé au nombre croissant de véhicule en circulation conduit à la raréfaction des sources d'énergie fossile et à une augmentation constante du prix des carburants. D'autre part les réactions prenant place dans les moteurs thermiques ne se limitent pas à la création d'énergie mais génèrent aussi des produits comme le dioxyde de carbone, le monoxyde de carbone (CO), les hydrocarbures (HC), les oxydes d'azote (NOx) et des matières particulières, indésirables pour leur impact environnemental. Pour résoudre ces problèmes, deux approches sont envisageables, l'une est technologique et vise à améliorer les composants du véhicule ou son architecture, l'autre est comportemental et cherche à changer la manière d'utiliser les véhicules.

De multiples solutions technologiques ont été développées visant l'amélioration des composants afin d'augmenter le rendement de la chaîne du véhicule. Une approche complémentaire est la création de nouvelles configurations de chaîne motopropulseur. En effet les voitures alternatives, comme les véhicules hybrides et électriques atteignent des niveaux de consommation inférieure à celui des véhicules conventionnels, grâce notamment à la récupération d'énergie au freinage. Les véhicules électriques permettent aussi au secteur des transports de réduire sa dépendance aux sources d'énergie fossile.

En parallèle l'utilisation efficace des ressources existantes doit être assurée. Par exemple des études sur des réseaux de véhicules ont montré qu'une communication entre véhicule et infrastructure peut aider à réduire la consommation d'énergie dans les transports. L'éco-conduite représente une méthode, réalisable immédiatement, permettant à chaque conducteur d'améliorer sa consommation. En effet, le rendement d'un véhicule dépend du taux d'accélération et des vitesses choisies. Une conduite qui minimise la consommation d'énergie en sélectionnant des accélérations et vitesses optimales d'un point de vue énergétique est nommée éco-conduite. Dans plusieurs pays des formations à l'éco-conduite sont proposés aux conducteurs et des études ont montré que ceux-ci réussissent à réduire leur consommation d'énergie de 10 à 15% [24]. D'autres projets tentant également de développer des systèmes d'assistance pour assurer une conduite économique.

Dans le cadre de cette thèse nous analyserons les gains potentiels de l'éco-conduite. Le fonctionnement optimal de différents types de véhicules sera examiné à l'aide d'algorithmes numériques. Enfin, les connaissances acquises à travers la détermination de profils de conduite optimaux seront appliquées à la conception d'un système d'assistance pour l'éco-conduite.

Souvent des règles d'éco-conduite sont définies généralement et indépendamment du châssis ou de la chaîne du véhicule. Pourtant, avec les nouvelles chaînes de véhicules alternatifs, il est important de prendre en compte des paramètres spécifiques pour atteindre des gains maximaux d'éco-conduite. Pour cette raison des modèles détaillés des différents types de véhicule ont été construit. Cette approche nous permet d'appliquer les algorithmes développés aux véhicules simples, mono-source, comme les véhicules conventionnels et électriques, mais aussi aux véhicules complexes, multi-source, comme le véhicule hybride.

Pour l'identification du fonctionnement optimal d'un véhicule des algorithmes d'optimisation de la trajectoire de vitesse ont été appliqués. Dans un premier temps nous avons mis en IJuvre la méthode de la programmation dynamique en trois dimensions [25] pour optimiser les trajectoires. Une deuxième approche a été développée afin de réduire le temps de calcul en introduisant un facteur de pondération dans la fonction de coût. Ainsi des méthodes de calcul du zéro ont été utilisées en combinaison avec la programmation dynamique en deux dimensions [26]. Le compromis entre durée du trajet et consommation d'énergie a également été étudié en calculant la frontière de Pareto avec une méthode d'optimisation multi-objectif [27].

Sur la base de cycles standards et de la définition d'un comportement de conduite de référence, les algorithmes d'optimisation nous on permit de calculer les cycles optimaux correspondant pour chaque type de véhicule (conventionnel, électrique, hybride). A l'aide de ces résultats nous avons pu spécifier les facteurs les plus importants de l'éco-conduite pour les véhicules conventionnels ainsi que les véhicules électrique [28] et hybrides [29].

Alors que la première partie s'est focalisée sur une étude théorique visant à calculer les gains potentiels de l'éco-conduite, la seconde partie consiste en une mise en situation plus réaliste et une intégration des algorithmes dans un système d'assistance pour le conducteur.

La prise en compte des contraintes de trafic et d'émission de polluants permet de se placer dans un contexte plus réaliste et de déterminer de manière plus précise les gains de consommation. Ainsi, nous avons introduit un modèle de suivi de véhicule pour simuler et étudier l'influence du trafic sur les gains potentiel de l'éco-conduite [30]. Alors que la plupart des études examinent seulement les gains de consommations, l'éco-conduite doit également être vue comme un comportement respectueux de l'environnement. Dans le cadre de cette thèse nous avons évalué dans le cas d'un véhicule thermique les aspects économiques et écologiques d'une conduite qui minimise la consommation. Pour rendre l'éco-conduite réellement écologique, nous proposons une méthode pour intégrer des contraintes sur les émissions dans l'algorithme d'optimisation [31].

Pour compléter ce travail nous présenterons enfin l'intégration du principe d'éco-conduite en temps réel dans un système d'assistance basé sur les algorithmes d'optimisation détaillés dans ce travail.

D.2 Etat de l'art

Les premières études visant à réduire la consommation de carburant dans le secteur des transports furent publiées en 1976 consécutivement au premier choc pétrolié. La motivation était alors purement économique. Aujourd'hui les restrictions environnementales obligent les pays et les constructeurs automobiles à investir dans un transport efficace et 'vert'. Dans cette optique certains pays proposent une formation à l'éco-conduite, par exemple dans le cadre de l'obtention du permis de conduire. Ces dix dernières années plusieurs études sur l'intérêt de l'instruction des règles d'éco-conduite ont été réalisées, révélant l'efficacité de ce dispositif. Toutefois, une étude sur les conséquences à long terme de ces formations [45] a démontré la limitation dans le temps de ses effets positifs, le conducteur reprenant instinctivement ses mauvaises habitudes de conduite. En conséquence, il est nécessaire d'utiliser des systèmes d'assistance pour l'éco-conduite afin d'assurer une conduite efficace sur le long terme.

La littérature est riche en option de multiples systèmes d'assistance pour l'éco-conduite et le tableau 2.1 en présente le comparatif détaillé. Il existe aujourd'hui des systèmes informatifs et des systèmes consultatifs. Les systèmes informatifs affichent des informations sur la consommation ou d'autres paramètres du véhicule au conducteur sans lui fournir de conseil sur les modifications à apporter pour réduire sa consommation. Par opposition les systèmes consultatifs conseillent le conducteur sur le comportement à adopter pour réduire sa consommation. Dans cette catégorie on distingue les systèmes d'assistance avancés (ADAS) qui utilisent des paramètres du véhicule pour identifier une conduite optimale pour ce véhicule. Les systèmes ADAS peuvent être classés en deux catégories:

- Système ADAS fournissant du conseil en continu pendant la conduite
- Système ADAS de rapport, proposant du conseil suite à un trajet

Le tableau 2.1 montre que les systèmes ADAS ont la capacité de fournir un conseil détaillé au conducteur, mais les algorithmes sont assez complexes et souvent de nombreuses données d'entrée sont nécessaires. Généralement les systèmes ADAS intègrent un algorithme d'évaluation, qui utilise les entrées du véhicule pour calculer et proposer une indication appropriée pour le conducteur. A notre connaissance la plupart des systèmes utilisent des algorithmes basés sur une machine

d'états appliquant un ensemble de règles expertes. Un tel algorithme ne peut identifier qu'un fonctionnement sous-optimal car il ne prend pas en compte la situation globale. Toutefois, en supposant que le trajet du véhicule est connu, le fonctionnement optimal peut être évalué en appliquant des algorithmes d'optimisation en combinaison avec un modèle de véhicule détaillé.

Afin d'identifier la trajectoire optimale d'un véhicule terrestre de nombreux travaux ont été réalisés depuis 1977. Le tableau 2.2 présente une synthèse des travaux et des méthodes appliquées, trouvés dans la littérature pour résoudre ce problème. Schwarzkopf fût le premier à montrer que la consommation d'énergie peut être minimisée en choisissant le meilleur profil de vitesse. Son travail était basé sur un modèle de véhicule très simple et se basait sur la méthode du principe minimal de Pontryagin. Ses travaux portèrent sur un problème d'accélération et une conduite à travers des montagnes.

Dans les études postérieures une grande variété de problèmes a été étudiée visant à optimiser la consommation de carburant mais aussi le temps de trajet. La trajectoire optimale a été évaluée pour des véhicules conventionnels, électriques, hybrides ainsi que pour des bus et des véhicules à pile à combustible. Néanmoins, nos études semblent montrer qu'un compromis entre le détail du modèle de véhicule considéré et la méthode d'optimisation existe. La plupart des travaux ont utilisé soit la méthode de la programmation dynamique soit le principe de Pontryagin. Les travaux qui ont appliqué le principe de Pontryagin employant généralement un modèle de véhicule simple. La programmation dynamique nous permet d'intégrer un modèle plus complexe et d'ajouter des contraintes facilement.

Cet état de l'art montre que l'éco-conduite représente une bonne façon à réduire la consommation des véhicules particuliers. Néanmoins, des systèmes d'assistance efficaces sont nécessaires pour indiquer au conducteur la conduite optimale. L'originalité de ces travaux de thèse se repose donc sur les points suivants:

- L'identification des gains potentiels de l'éco-conduite en calculant le fonctionnement optimal pour chaque type de véhicule
- L'évaluation des effets de contraintes sur la consommation optimale
- L'intégration des algorithmes d'optimisation dans un système d'assistance à l'éco-conduite

D.3 Modélisation

Afin d'identifier et de comparer le fonctionnement optimal des différents véhicule, nous avons modélisé trois véhicules représentatifs: conventionnel, électrique et hybrides. Afin de réduire les temps de calcul et intégrer de manière simple les modèles de véhicule dans les algorithmes d'optimisation nos travaux ce sont appuyés sur la modélisation inverse. Les avantages d'une telle modélisation sont expliqués par le schéma en figure 3.1.

La simulation directe d'un véhicule se base sur des entrées fournies par un conducteur pour calculer le fonctionnement du véhicule en direction du flux de puissance. La vitesse et l'accélération de la voiture sont déterminées à l'aide des entrées que sont les pédales. On parle de modèle inverse lorsque le fonctionnement des composants dans la chaîne du véhicule est calculé en utilisant la vitesse et l'accélération comme variables données. L'intérêt de cette approche est de retirer le conducteur du calcul. Dans la modélisation inverse le conducteur est supposé idéal, seules certaines hypothèses sur son comportement sont faites.

En général tous les véhicules peuvent être séparés en un châssis et un groupe motopropulseur (figure 3.2). Si la chaîne motopropulseur diffère suivant le type de véhicule modélisé ici, le modèle du châssis reste un élément commun à toutes les chaînes et il est seulement nécessaire de changer le paramétrage pour chacune des configurations étudiées. Afin de développer un modèle énergétique du véhicule nous avons spécifié deux hypothèses concernant le châssis:

- Seul le mouvement longitudinal est considéré
- Le contact pneu chaussée est parfait

En utilisant ces hypothèses le couple (T_{drive}) à fournir par la chaîne motopropulseur peut être calculé en fonction de vitesse (v) et de l'accélération (a) du véhicule avec :

$$T_{drive} = f(v,a) \tag{D.1}$$

$$= J_{veh}\frac{a}{R_{tire}} + F_{res}(v)R_{tire} \tag{D.2}$$

Les forces résistantes (F_{res}) se composent de la force de résistance au roulement entre le pneu et la chaussée, la force aérodynamique du châssis et la force due à la pente (figure 3.3). Les forces résistantes représentent les pertes du châssis, qui sont fortement liées à la vitesse du véhicule, mais elles varient aussi avec le poids et la géométrie du véhicule.

D.3.1 Véhicule thermique

La Peugeot 308 a été utilisée comme exemple de véhicule conventionnel (figure 3.5). La chaîne de transmission du véhicule se compose d'un différentiel, d'une boîte de vitesse, d'un embrayage et du moteur thermique. Afin de simplifier le modèle du véhicule la dynamique de la chaîne n'a pas été considérée. Pour une inversion du modèle de ce véhicule les hypothèses suivantes ont été appliquées :

- L'éco-conducteur choisi toujours le rapport optimal
- Les changements de rapports sont faits instantanément
- Le patinage d'embrayage ne se produit que lorsque la vitesse de la chaîne est plus basse que le ralenti du moteur thermique
- Une puissance constante est fournie aux auxiliaires.

Les rendements du différentiel et du rapport sélectionné sont spécifiés indépendamment de la vitesse et du couple. Tenant en compte la puissance fournie aux auxiliaires et des autres hypothèses le fonctionnement est évalué à partir du modèle inverse du châssis:

$$\omega_{eng} = max(\omega_{eng-idle}, \omega_{wheel} * R_{FD} * R_G(i_{gear})) \tag{D.3}$$

$$T_{eng} = T_{drive}\frac{\eta_{FD}^{\psi}\eta_G^{\psi}(i_{gear})}{R_{FD}R_G(i_{gear})} + \frac{P_{aux}}{\omega_{eng}} + J_{eng}\dot{\omega}_{eng} \tag{D.4}$$

Pour l'étude du véhicule thermique, le choix s'est porté sur un moteur essence de 1.6 L, peuvent fournir un couple maximal de 160 Nm à 4250 tr/m et une puissance maximale de 88 kW à 6000 tr/m. La figure 3.7 montre une cartographie de la

consommation en fonction de la vitesse et du couple fourni. Cette cartographie a été relevée expérimentalement et peut être utilisée pour calculer la consommation instantanée à un point de fonctionnement donné. Comme illustré dans la figure 3.7, la consommation d'un véhicule pour une vitesse et une accélération définie peut changer suivant le rapport de vitesse choisi. Le rendement maximum des moteurs thermiques se trouve généralement dans la partie haute du couple. Avec ce modèle la consommation instantanée de carburant peut être calculée en fonction de la vitesse et de l'accélération du véhicule.

D.3.2 Véhicule électrique

Le deuxième type de véhicule étudié est le véhicule électrique. Les véhicules électriques deviennent de plus en plus populaires, du fait de la flexibilité dans le choix de la source d'énergie. De plus, la chaîne de la traction permet de récupérer de l'énergie cinétique grâce à la réversibilité des composants électriques. Dans cette thèse la voiture électrique AIXAM Mega City, présentée en figure 3.8, a été choisie comme exemple d'étude. La chaîne de traction d'un véhicule électrique se compose d'un différentiel, d'un moteur électrique qui est couplé par un convertisseur à une batterie.

Dans la AIXAM Mega city l'énergie est fournie par 12 éléments de batterie au plomb. Le moteur installé dans le véhicule est un moteur à courant continu, qui peut produire une puissance maximale de 14 kW à 3000 tr/m et un couple maximal de 60 Nm peut être fourni à basse vitesse. Prenant en compte le rendement du différentiel et l'inertie du moteur électrique, le fonctionnement du moteur électrique se calcule par:

$$\omega_{EM} = \omega_{wheel} R_{FD} \tag{D.5}$$

$$T_{EM} = T_{wheel} \frac{\eta_{FD}^{\psi}}{R_{FD}} - J_{EM} \dot{\omega_{wheel}} R_{FD} \tag{D.6}$$

Le rendement de l'association convertisseur et moteur a été identifié expérimentalement (figure 3.10). Les pertes dans le moteur sont calculées en utilisant une

interpolation. La puissance totale à fournir par la batterie se compose de la puissance fournie au moteur électrique, des pertes dans le moteur et le convertisseur et la puissance des auxiliaires:

$$P_{battout} = T_{EM}\omega_{EM} + P_{lossEM} + P_{aux} \tag{D.7}$$

Pour modéliser les pertes dans la batterie, nous avons utilisé un modèle simple tenant compte uniquement du phénomène résistif (figure 3.11). Cette résistance change de valeur suivant le mode de la batterie, charge ou décharge. Il a été constaté que la dépendance des pertes par rapport à l'état de charge était faible pour une grande plage de l'état de charge. En conséquence nous avons utilisé un état de charge constant pour le calcul de la consommation d'énergie. Avec ce modèle la consommation d'énergie dans la batterie peut être calculée en fonction de la vitesse et de l'accélération du véhicule:

$$P_{batt} = f(v, a) \tag{D.8}$$

D.3.3 Véhicule hybride

Généralement les véhicules hybrides consomment moins de carburant que les véhicules conventionnels grâce à leur capacité de récupération d'énergie au freinage et à leur utilisation du moteur thermique dans les régions de haut rendement. Un véhicule hybride est, par définition, un véhicule avec plusieurs sources de puissance. Alors que la source primaire est souvent le moteur thermique, la deuxième source peut être de différente nature: une pile à combustible, un volant d'inertie, un accumulateur hydraulique ou une batterie électrique. Nous nous sommes concentrés ici sur les véhicules hybrides électriques qui utilisent une batterie et un moteur électrique pour assister le moteur thermique. Néanmoins, les algorithmes présentés sont applicables à tous les types de véhicules hybrides.

Dans les véhicules hybrides, la puissance fournie par la chaîne motopropulseur est repartie entre plusieurs sources en utilisant différentes configurations des composants de la chaîne. La figure 3.12 et la figure 3.13 illustrent les différentes architectures : l'hybride série, l'hybride parallèle et l'hybride de répartition de

puissance (série-parallèle). Pour illustrer une application des algorithmes d'éco-conduite à un véhicule hybride, la Toyota Prius II a été prise comme exemple. Ce véhicule correspond à la configuration hybride la plus complexe : la répartition de puissance.

La chaîne de la Prius (figure 3.13) se compose d'une réduction, de deux moteurs électriques, d'un moteur thermique, d'un train épicycloïdal et d'une batterie. La puissance fournie par le moteur thermique est répartie par le train épicycloïdal entre les chaînes mécanique et électrique. Dans une telle chaîne, l'identification du fonctionnement des composants en fonction de la vitesse et de l'accélération du véhicule est difficile. Une stratégie de gestion d'énergie est utilisée pour assurer le fonctionnement le plus efficace de la chaîne. La gestion d'énergie tient compte les entrées du conducteur ainsi que de l'état de charge de la batterie pour décider du fonctionnement de chaque composant. Dans une modélisation inverse de la chaîne du véhicule hybride nous avons supposé que l'état de charge est connu pour calculer le fonctionnement des composants avec la bonne répartition d'énergie. Tenant compte de cette hypothèse nous avons développé un modèle inverse de la Prius, qui est utilisé pour calculer la consommation de carburant et la consommation d'électricité de la batterie en fonction de la vitesse, de l'accélération et de l'état de charge de la batterie.

Afin de vérifier les résultats de la simulation, un modèle direct prenant en compte des phénomènes dynamiques plus détaillés, a été utilisé. Le logiciel VEHLIB est un logiciel de simulation énergétique de véhicule qui permet l'identification du fonctionnement des composants, le calcul de la consommation d'énergie pour une trajectoire de vitesse ainsi qu'à des applications en temps réel dans un cadre expérimental.

D.4 Optimisation

Dans le but d'identifier la trajectoire optimale pour un véhicule considéré, nous avons appliqué des méthodes d'optimisation de trajectoire pour un trajet connu. Le déplacement du véhicule peut être décrit par deux états, la distance et la vitesse du véhicule. La forme discrétisée des équations est donnée par :

$$d_{i+1} = d_i + v_i \Delta t + \frac{1}{2} a_i \Delta t^2 \tag{D.9}$$

$$v_{i+1} = v_i + a_i \Delta t \tag{D.10}$$

Afin de déterminer la trajectoire optimale pour l'éco-conduite, nous allons minimiser la consommation d'énergie globale pour un trajet. La fonction de coût est approximée par une somme des coûts énergétiques instantanés pour la durée du trajet :

$$\Gamma_1 = \int_t \gamma_{veh}(t) \approx \sum_{i=t_0}^{t_f} \gamma_{veh_i}(\Delta t_i) \tag{D.11}$$

Le coût énergétique d'un véhicule dépend de son architecture. Dans ce travail nous allons considérer trois véhicules représentatifs: le véhicule conventionnel, le véhicule électrique et le véhicule hybride.

$$\gamma_{veh}^{conv}(t) = \sum_{i=t_0}^{t_f} m_{fuel_i}(\Delta t_i) \tag{D.12}$$

$$\gamma_{veh}^{elec}(t) = \sum_{i=t_0}^{t_f} P_{batt_i}(\Delta t_i) \tag{D.13}$$

$$\gamma_{veh}^{hyb}(t) = \sum_{i=t_0}^{t_f} (m_{fuel_i}(\Delta t_i) + \alpha \Delta SOC(\Delta t_i)) \tag{D.14}$$

Contrairement aux véhicules mono-source pour lesquels on considère une seule source d'énergie, les véhicules hybrides nécessitent que l'on considère toute l'énergie consommée à chaque instant. C'est pourquoi le carburant (m_{fuel}) et la décharge (ΔSOC) sont inclus dans la fonction de coût de ce type de véhicule.

Pour évaluer le niveau d'éco-conduite d'une conduite particulière il est nécessaire de définir une référence. Pour cela nous avons utilisé des cycles standards et des cycles d'usage réels. Dans la figure 4.1 un cycle d'usage réel d'une conduite urbaine est représenté. A l'aide de ce cycle de conduite le trajet du véhicule peut être défini. Afin d'identifier une trajectoire de vitesse optimale correspondant à un trajet donné, des contraintes de trajet et de route doivent être spécifiées. Les contraintes de trajet précisent l'état initial et final de distance et de vitesse. De plus, la durée du trajet doit être définie. Cette contrainte est nécessaire pour assurer

l'acceptation des stratégies d'éco-conduite par les utilisateurs. Une comparaison équitable est possible seulement si les contraintes de route qui limitent les choix de vitesse d'un vrai conducteur, sont prises en compte. En conséquence les limitations de vitesse ont été spécifiées en fonction de la distance (figure 4.1). La pente est également prise en compte comme paramètre dépendant de la route en fonction de distance.

Dans une première approche nous avons étudié le problème d'optimisation mono-objectif. Il existe une grande variété de méthodes d'optimisation qui sont applicables à ce problème. La non-linéarité de la fonction de coût et le besoin d'intégrer facilement des contraintes nous ont poussés à choisir la méthode de la programmation dynamique. Cette méthode d'optimisation est basée sur le Principe d'optimalité de Bellman [86], qui permet de décomposer des problèmes complexes en des sous-problèmes simples, qui peuvent être résolus de manière récursive. Par la suite les problèmes peuvent être facilement résolus avec un calculateur de puissance limitée. Avec une discrétisation appropriée, la méthode identifie toujours la solution globalement optimale. L'inconvénient de cette méthode est le temps de calcul, qui peut être très élevé pour des problèmes à plusieurs dimensions.

Comme dans les travaux de Hooker [57], la méthode de programmation dynamique a été initialement appliquée en trois dimensions : temps, vitesse et distance. Cette approche facilite une intégration des contraintes en temps, vitesse et distance. Afin de réduire le temps de calcul la méthode a par la suite été réduite à deux dimensions. Pour respecter toutes les contraintes de trajet un facteur de pondération a été introduit dans la fonction de coût :

$$\Gamma_2 = \int_d \gamma_{veh}(d) + \beta \Delta T(d) = \sum_{i=d_0}^{d_f} \gamma_{veh_i}(d_i) + \beta \Delta t_i \tag{D.15}$$

Pour un trajet donné un facteur β peut maintenant être associé à une durée de trajet. Dans une application en temps-réel ce paramètre peut être spécifié par le conducteur pour définir un compromis entre le temps d'arrivée et l'énergie consommée. Cependant afin de pouvoir comparer les trajectoires de vitesse et identifier le gain potentiel d'éco-conduite, une contrainte de temps doit être respectée. Par la suite nous avons étudié les méthodes d'identification d'un facteur de pondération correspondant à une consommation minimale à iso-durée de trajet.

Dans un premier temps une méthode de cartographie a été utilisée. En calculant les temps d'arrivée en fonction de la distance à parcourir en fonction de β, un tableau peut être généré. Ensuite, une méthode d'interpolation peut être utilisée pour calculer le β correspondant à une distance et un temps de trajet désiré. Cette méthode d'identification conduite à de bons résultats si le trajet est définie seulement par sa distance. Si d'autres contraintes, comme la vitesse maximale ou la pente, doivent être prises en compte, une telle méthode ne permet pas d'identifier un facteur de pondération suffisamment précis.

En utilisant un β donné, la durée de trajet devient un résultat de l'optimisation. Par conséquent, la durée de trajet peut être définie en fonction du facteur de pondération. Pour déterminer les trajectoires à iso-durée, une fonction d'erreur, entre temps d'arrivée de la trajectoire de vitesse calculée et le temps désiré, est définie ainsi :

$$f_{error}(\beta) = T_f(\beta) - t_f^{des} \tag{D.16}$$

En utilisant l'équation D.16, l'identification de β est réduit à un problème de recherche de zéro. Plusieurs méthodes de recherche de zéro et leur application à ce problème ont été étudiées. Une étude comparative des méthodes de Dichotomie, de Secant, de False-Position, de Ridder et de Brent a permis d'identifier la méthode de Brent comme la plus adaptée à cette problématique d'optimisation. Par la suite nous avons donc choisit d'appliquer la méthode de programmation dynamique et de l'associé à la méthode de Brent pour le calcul d'une trajectoire optimale d'un parcourt donné avec contrainte de durée.

Pour conclure cette étude d'optimisation, un problème multi-objectif a été considéré pour évaluer le compromis entre la consommation d'énergie et la durée du trajet. En se basant sur l'algorithme de programmation dynamique, nous avons pu calculer la frontière de Pareto sans utiliser de facteur de pondération. Une méthode de troncation a été proposée pour réduire le nombre de trajectoires calculées et donc le temps de calcul et l'espace mémoire utilisée. La figure 4.12 représente la frontière de Pareto pour un trajet de 300 mètres, illustrant le compromis entre la durée du trajet et la consommation. La forme de la frontière montre qu'il est possible d'atteindre une réduction significative de la consommation avec un faible impact sur la durée du trajet.

D.5 Optimisation de trajectoire pour chaque type de véhicule

En se basant sur les algorithmes développés précédemment nous avons calculé les trajectoires optimales, pour des cycles de conduite donnés, réalisés avec les véhicules conventionnel, électrique et hybride retenus pour l'illustration de ce travail. La détermination des gains potentiels d'éco-conduite est obtenue en comparant les "éco" cycles aux cycles originaux, ainsi le fonctionnement optimal pour chaque type de véhicule peut être spécifié.

D.5.1 Véhicule thermique

Pour le véhicule conventionnel nous avons considéré quatre cycles de conduite : un cycle standard (NEDC), un cycle représentant une conduite urbaine (HYZURB), un cycle représentant une conduite routière (HYZROUT) et un cycle décrivant une conduite autoroutière (HYZAUTO). Les trajectoires optimales correspondantes ont été calculées en appliquant la méthode de programmation dynamique 2D couplé à la recherche de zéro pour le calcul du paramètre β optimale. La figure 5.2 présente les cycles originaux en bleu et les cycles éco en rouge. Pour chaque cycle la trajectoire de vitesse et les rapports de boite sont données.

Afin de vérifier les résultats les cycles originaux et éco ont été testés sur banc moteur. En s'appuyant sur un équipement 'hardware-in-the-loop testing', le véhicule a été simulé alors que le moteur thermique été piloté en temps réel (figure 5.3). Cette méthode nous a permis de mesurer les valeurs réelles de consommation de carburant pour chaque cycle. Le tableau D.1 présente les résultats pour les cycles originaux et éco. Suivant le cycle évalué, les gains potentiels d'éco-conduite se situent entre 7,9 et 27,2 %. Par ailleurs ces résultats montrent que les gains d'éco-conduite sont plus élevés pour une conduite urbaine et routière que pour une conduite autoroutière.

Deux facteurs ont été identifiés comme principales causes des gains d'eco-conduite :

- Un meilleur changement de rapport
- Un meilleur choix des vitesses et des taux d'accélération du véhicule.

cycle de conduite	original [L/100km]	éco [L/100km]	réduction [%]
NEDC	6.7	5.5	17.9
HYZURB	9.76	7.11	27.2
HYZROUT	7.22	5.41	25.1
HYZAUTO	6.92	6.37	7.9

TABLE D.1: Gains d'éco-conduite pour le cas du véhicule conventionnel

Grâce à une sélection de rapports élevés, le rendement du moteur thermique est augmenté, induisant une réduction de consommation. De plus la consommation d'énergie diminue avec un choix adéquat des vitesses et des taux d'accélération du véhicule. Pour minimiser la consommation de carburant du véhicule conventionnel une accélération forte pour atteindre une vitesse stabilisée le plus rapidement possible est recommandée. Dans les phases de décélération, il est préférable d'utiliser le frein moteur afin de réduire la vitesse du véhicule, puis d'appliquer un freinage mécanique pour minimiser la durée de la phase de décélération.

D.5.2 Véhicule électrique

La trajectoire optimale d'un véhicule électrique a été identifiée pour quatre cycles adaptés. Le véhicule électrique considéré ici est limité à une vitesse maximale de 65 km/h. Pour la comparaison d'une conduite originale et d'une conduite éco, deux cycles réels représentant une conduite urbaine ont été utilisés (AIXAM1, 3). En autre, un cycle standard (AXIAM2) avec une durée de moins de 200 s ainsi qu'un cycle routier adapté aux basses vitesses (AIXAM4) ont été optimisés. Dans la figure 5.11 les cycles originaux et les cycles éco sont illustrés.

Les cycles originaux et les cycles optimisés du véhicule électrique ont été testés expérimentalement sur un banc à rouleaux. Dans une telle configuration expérimentale le véhicule est stationnaire, les roues sont placées sur des rouleaux reliées à une machine électrique qui simule les forces résistant au véhicule. Les tests sur banc à rouleaux permettent de mesurer la consommation d'énergie du véhicule dans une situation contrôlée. Une comparaison de la consommation des différents cycles de conduite est détaillée dans le tableau D.2.

Grâce aux stratégies d'éco-conduite une réduction de 12 à 19 % est théoriquement possible pour les cycles d'usage réel. En comparant les cycles originaux

cycle	cycle original	cycle éco	gain
AIXAM1	872.2	705.56	19.3%
AIXAM2	89.4	85.56	4.5%
AIXAM3	283.3	248.89	12.1%
AIXAM4	427.78	386.11	9.4%

TABLE D.2: Consommation d'énergie en Wh

et les cycles d'éco, nous avons pu montrer que cette amélioration de consommation n'est pas due à une augmentation du rendement des composants dans la chaîne. La consommation de la trajectoire optimale a été diminuée en raison des choix de vitesse et des taux d'accélération. En utilisant des accélérations fortes, des vitesses stabilisées basses et des taux de décélération adaptés à la chaîne du véhicule, l'énergie nécessaire pour réaliser le cycle éco a été fortement diminuée. La figure 5.14 montre l'énergie dépensée lors de l'accélération du véhicule et celle utilisée pour vaincre les forces de résistance. Un second graphique représente le freinage pour un cycle original et un cycle éco. Alors que le cycle original perd beaucoup d'énergie cinétique par freinage mécanique, les taux de décélération du cycle optimisé permettent de récupérer plus d'énergie au niveau de la batterie.

D.5.3 Véhicule hybride

Afin d'analyser le fonctionnement optimal d'un véhicule hybride, la trajectoire de vitesse d'une Toyota Prius II a été optimisée pour un trajet donné. Il est à noter que dans cette thèse nous n'avons pas tenté d'optimiser ou de changer la gestion d'énergie du véhicule, mais c'est en modélisant l'ensemble du véhicule avec sa gestion énergie propre que nous avons identifié le profil de vitesse optimal.

Le fonctionnement du véhicule étant dépendant de l'état de charge de la batterie, une application de la méthode de programmation classique, qui consiste à rechercher la meilleure solution état par état en commençant par le dernier, n'est pas appropriée. Pour évaluer le cycle éco du véhicule hybride, l'algorithme de programmation dynamique a été appliqué en sens direct (chronologique) en commençant du premier état. Avec cette approche, l'évolution de l'état de charge de la batterie peut être surveillée et le coût de fonctionnement du véhicule peut être calculé en fonction de la vitesse, de l'accélération et de l'état de charge.

Un utilisateur de véhicule hybride peut penser contrôler sa consommation en surveillant la quantité de carburant utilisée. Mais cette approche est incorrecte, la consommation de carburant d'un véhicule hybride n'étant pas nécessairement proportionnelle à la consommation d'énergie du véhicule. Sur un trajet, le véhicule peut consommer une faible quantité de carburant mais entièrement décharger la batterie électrique. Cela induira une plus forte consommation de carburant sur les trajets suivants. Pour identifier le meilleur fonctionnement de façon globale nous avons donc pris en compte l'utilisation de la batterie en introduisant un facteur de pondération α dans l'optimisation (Equation D.14).

Nous avons utilisé la méthode d'évaluation de la consommation proposée par la SAE en 2002 [96] pour comparer la consommation des différents cycles. En calculant au minimum deux points de consommation et d'utilisation batterie, la méthode d'interpolation est utilisée pour identifier la consommation de carburant quand la variation de la batterie est nulle.

Une conduite originale a été définie à partir d'un cycle routier, puis optimisée pour plusieurs valeurs de pondération α et pour trois niveaux différents d'état de charge initiale de la batterie. Dans la figure 5.17 et 5.18 les résultats sont tracés en fonction du changement de l'état de charge de la batterie et en fonction de la valeur de pondération α. En choisissant la bonne valeur de α nous avons montré que le gain potentiel de l'éco-conduite peut atteindre 23 %. A noter que le choix de la valeur α est très important pour le calcul d'une trajectoire optimale.

Globalement nous pouvons conclure que pour une conduite économique le choix des vitesses et des accélérations appropriées est primordial. Il semble qu'une fort accélération et une vitesse stabilisée la plus basse possible est préférable pour minimiser la consommation d'énergie. De plus, dans la phase de décélération le freinage doit être adapté à la nature de la chaîne de traction du véhicule afin d'utiliser au maximum la capacité de récupération.

D.6 Intégration des contraintes

Nous nous sommes jusqu'ici intéressé aux gains potentiels de l'éco-conduite dans une situation idéale, nous allons par la suite décrire comment des contraintes de trafic et d'émission ont été intégrées afin de calculer des gains d'éco-conduite plus réalistes.

L'intégration de l'éco-conduite en temps réel doit prendre en compte le trafic à proximité du véhicule et ne doit pas influer sur la sécurité du conducteur. Afin d'évaluer l'impact de la prise en compte du trafic, les configurations dans lesquelles il existe potentiellement une voiture devançant le véhicule dont la trajectoire est optimisée ont été mises en place (figure 6.1). Dans une telle situation une distance de sécurité doit être conservée. Nous avons étudié trois paramètres différents de suivi d'un véhicule en toute sécurité:

- Distance de freinage sûr : distance nécessaire pour pouvoir freiner quand le conducteur précédant freine au maximum
- Time-inter-véhicular (TIV) : le temps séparant les deux véhicules
- Time-to-collision (TTC) : le temps avant qu'une collision se produise si les deux véhicules conservent leur vitesse courante

Le code de la route français conseille un TIV de 2 s pour les véhicules sur une autoroute. Le TIV est un critère facile à prendre en compte pour le conducteur, néanmoins, il ne prend pas en compte la vitesse du véhicule précédent. La forme de l'évolution des trois paramètres en fonction de la vitesse des deux véhicules est illustrée dans la figure 6.3. Afin d'étudier les effets du trafic sur les gains de l'éco-conduite, nous avons défini deux types de conducteur: un premier à haut risque et un autre à faible risque. Pour spécifier la distance de sécurité le critère de TTC a été utilisé, en prenant une valeur de 2 s pour une conduite à haut risque et de 4 s pour une conduite à faible risque.

La trajectoire de vitesse optimale correspondant à un trajet urbain a été identifiée pour les deux types de conducteur. La consommation de carburant pour chaque cycle est présentée dans le tableau D.3. La consommation de référence a été calculée sans contrainte de trafic, elle correspond à un gain potentiel d'éco-conduite de 34 % pour le trajet considéré. Cependant les limitations dues au trafic rendent cette trajectoire non réalisable. En prenant en compte le trafic un conducteur à haut risque peut réduire sa consommation de 28 % grâce à l'éco-conduite alors qu'un conducteur à faible risque obtient une réduction de 15 % seulement. Alors que la consommation optimale n'est pas accessible en présence de trafic, la stratégie d'éco-conduite entraîne toujours une réduction de consommation non négligeable.

Généralement l'éco-conduite est considérée comme un comportement respectueux de l'environnement. Toutefois, à notre connaissance, la plupart des études sur

cycle	contrainte	consommation [g]	gain [%]
cycle original	driver	97.36	-
cycle éco	-	64.10	34
cycle éco	TTC=2sec	69.62	28
cycle éco	TTC=4sec	82.30	15

TABLE D.3: Consommation de carburant pour les différentes trajectoires

le sujet se restreignent à la consommation d'énergie, sans prendre en compte les émissions de polluants. Dans cette partie de thèse nous nous sommes intéressés également aux aspects écologiques de l'éco-conduite.

La mesure expérimentale de la consommation d'un cycle de conduite est réalisée à l'aide d'un banc moteur. De plus, les équipements du laboratoire LTE de l'IFSTTAR permettent de déterminer les émissions de polluants pour un cycle complet ainsi qu'en instantané. La combustion dans le moteur thermique d'un véhicule conventionnel n'est jamais parfaite, les produits sont principalement la vapeur d'eau et le dioxyde de carbone, mais aussi le monoxyde de carbone (CO), les hydrocarbures (HC) et les oxydes d'azote (NOx). Ces polluants gazeux contribuent au phénomène d'effet de serre et ont des effets négatifs sur notre santé.

Les données présentées dans le tableau D.4 résultent de tests de parcours routiers réalisés sur banc moteur pour un cycle original et un cycle éco obtenu uniquement en minimisant la consommation d'énergie. Le moteur est celui de la Peugeot 308 (EP6) respectant la norme Euro IV, qui limite les valeurs d'émission de CO, HC et NOx pour le cycle de test (NEDC). Les résultats du cycle éco sont présentés en comparaison de ceux du cycle original et des valeurs d'émission de la norme Euro IV (tableau D.4).

Ces résultats montrent qu'en appliquant le cycle éco nous avons réussi à diminuer la consommation de carburant de 9.0 L/100km à 6.5 L/100km. Les émissions de CO2, qui sont généralement proportionnelles à la quantité de carburant consommé, ont effectivement diminués. Par contre les émissions de CO et de HC ont augmenté considérablement : alors que le niveau moyen d'émission de CO pour le cycle original est de 2,06 g/km, il est de 5,78 g/km pour le cycle éco. De même si les émissions de HC respectent les limites de la norme Euro IV pour le cycle de base, elles dépassent la valeur maximale admissible avec le cycle éco. Enfin la mesure des NOx donne des valeurs trop faibles pour être exploitables. Ces constatations

révèlent qu'une conduite économique n'est pas nécessairement écologique et qu'il faut donc ajouter la prise en compte des émissions à l'algorithme d'optimisation.

Nous avons étudié le fonctionnement du moteur thermique et ses émissions de polluants pour identifier la cause de l'augmentation des CO et HC dans le cycle optimisé. La figure 6.10 montre qu'une zone de haute densité des émissions existe pour un fonctionnement du moteur à un couple élevé. Pour déterminer la trajectoire de vitesse qui diminue l'impact environnemental du véhicule, une nouvelle fonction de coût a été définie[1]:

$$\Gamma_{veh_2} = \sum_i (\gamma_{fuel}(t_i) + \lambda_i) \tag{D.17}$$

avec

$$\lambda_i = \begin{cases} \lambda_0 & if\ T_{eng} > \chi T_{engmax}(\omega_{eng}) \\ 0 & if\ T_{eng} <= \chi T_{engmax}(\omega_{eng}) \end{cases} \tag{D.18}$$

En prenant en compte les résultats précédents, la valeur de χ a été fixée à 0,85. Cette nouvelle fonction de coût a comme résultat une restriction du couple du moteur. Nous nommerons le cycle, qui minimise cette fonction coût, cycle éco^2 par référence a son intérêt économique et écologique. Une comparaison entre les cycles originaux, éco et éco^2 est détaillée dans la figure 6.13. Les résultats montrent que les changements du profil de vitesse entre le cycle éco et éco^2 sont minimes à l'exception de la sélection des rapports qui a beaucoup évolué.

La sélection des rapports optimaux, étant calculée avec un modèle inverse sans considérer la dynamique de la boîte de vitesses, on observe sur le cycle éco des changements de rapport fréquents. En conséquence, dans une intégration du cycle éco^2 en simulation direct et en prenant en compte le temps de changement de rapport, le véhicule ne parvient pas à suivre la trajectoire donnée. Afin de simuler le cycle, une méthode de sélection des rapports optimale en ligne est proposée (figure 6.11). Dans cette approche le modèle inverse du véhicule conventionnel est utilisé pour calculer les rapports optimaux écologiques, le régime moteur et le couple moteur pour des vitesses et accélérations du véhicule donné. Ensuite, nous

[1] $\lambda_0 = 10000$; Une valeur très grande par rapport au coût normal des points de fonctionnement a été choisi

utiliserons les résultats pour évaluer le domaine de fonctionnement du moteur pour chaque rapport. Avec ces domaines le régime maximal et minimal pour chaque rapport est défini en fonction du couple. Dans la figure 6.12 les points de fonctionnement et les limitations du régime sont listés pour les rapports un à quatre.

Lors de la simulation directe d'un véhicule conventionnel, un changement de rapport peut maintenant être invoqué si le régime moteur dépasse la limitation du régime pour le couple fourni. La figure 6.13 illustre les rapports implémentés en simulation directe pour le cycle original, le cycle éco et le cycle éco^2 dans le second graphique.

émission g/km	CO2	CO	NOx	HC	consommation de carburant [l/100km]
cycle original	206.96	2.06	0.0055	0.068	9.0
cycle éco	140.96	5.78	0.0046	0.12	6.5
Euro IV	-	1	0.08	0.1	
cycle éco^2	151.51	2.18	0.0025	0.063	6.7

TABLE D.4: Résultats finales des mesures d'émissions

Les valeurs de consommation de carburant et d'émission de polluants sont présentées dans le tableau D.4. La figure 6.14 montre qu'en contrepartie d'une faible augmentation de la consommation nous avons réussi à réduire globalement les émissions de polluants. Nous pouvons conclure que l'éco-conduite représente des avantages économiques ainsi qu'écologiques si toutefois des contraintes d'émissions sont prises en compte.

D.7 Réalisation et test d'un système d'assistance pour l'éco-conduite

Pour compléter cette thèse, les algorithmes développés ont été intégrés dans un système d'assistance pour l'éco-conduite prenant en compte le trafic et les émissions. Afin de vérifier l'efficacité du système il a été testé expérimentalement sur un simulateur de conduite.

Le projet VERONESE est un projet interne à l'IFSTTAR. Il s'agit d'une collaboration de plusieurs laboratoires (LTE, LESCOT, LEPSIS) qui s'investissent dans

les moyens de réduire la consommation d'énergie dans le secteur des transports. Cette collaboration nous a aidé dans le développement d'un système d'assistance et dans la réalisation des évaluations du système sur un simulateur de conduite. Ce projet, comportait plusieurs volets:

- Adaptation du simulateur
- Développement de l'interface et de l'algorithme du système ADAS (advanced driver assist system)
- Intégration du système ADAS dans l'environnement du simulateur
- Réalisation des expérimentations

La figure 7.1 présente un schéma de la configuration expérimentale. Dans le simulateur de conduite le conducteur est assis dans un vrai véhicule qui est utilisé pour transmettre des entrées du conducteur à la simulation du véhicule et à l'environnement virtuel. Dans notre cas un modèle de véhicule physique a été intégré en utilisant une simulation du Peugeot 308 véhicule de la base de VEHLIB. Le modèle de véhicule utilise les entrées des pédales et du volant pour calculer le fonctionnement de chaque composant dans la chaîne du véhicule et détermine ainsi la consommation d'énergie, la position et la vitesse du véhicule. Avec un environnement virtuel pré-défini la position du véhicule peut être affichée au conducteur en utilisant les coordonnées données par le modèle du véhicule. Dans notre cas, l'environnement virtuel est projeté sur un écran de 220 cm de hauteur et 165 cm de longueur, résultant en une vue horizontal de 180 ° et une vue vertical de 47 °. Même s'il est difficile de rendre des sensations réelles avec un simulateur, il est possible de tester le système d'assistance dans des situations contrôlées et comparables.

Le système d'assistance est intégré dans le véhicule indépendamment du simulateur (figure 7.1). Néanmoins, le système ADAS prend en compte des entrées de l'environnement et du véhicule pour générer le conseil donné au conducteur. De plus il utilise les données de cartographie telles les rues, les intersections et les vitesses maximales. Le véhicule, qui est équipé d'un radar, transmet la vitesse, l'accélération et la position du véhicule précédant au système ADAS. Afin de transmettre des recommandation sur une meilleure conduite, au conducteur deux écrans sont utilisés (figure 7.7). Le premier écran affiche un conseil en continu sur

la vitesse optimale et la sélection des rapports. Sur un deuxième écran des informations pédagogiques sont affichées à chaque phase d'arrêt du véhicule. Cette information peut servir au conducteur pour évaluer sa conduite de la phase précédant.

L'algorithme du système ADAS se base sur une logique de segment de route. Un segment peut être défini comme une partie de route entre deux intersections. Une illustration de la logique du système ADAS est présenté dans la figure 7.9. Pendant que le conducteur se trouve sur un segment, la vitesse appropriée et le conseil du rapport sont affichés sur l'écran de conseil en continue. Tout au long d'un segment une détection identifie les situations de risque, par exemple dans le cas d'un véhicule précédant, pour lesquelles aucun conseil de vitesse optimale n'est donné au conducteur. Une jauge colorée est utilisée pour indiquer la bonne vitesse en fonction de la distance du véhicule sur l'odomètre de la vitesse. Une image de boîte de vitesse avec des flèches nous ont servi pour communiquer le rapport le plus efficace (figure 7.13, figure 7.14). Quand le véhicule s'approche de la fin d'un segment, la conduite tout au long du segment est évaluée. Afin de ne pas interférer avec la sécurité du conducteur, ces informations ne sont affichées que si le véhicule est à l'arrêt.

Trois algorithmes d'optimisation sont intégrés dans la logique du système (figure 7.9):

- Optimisation des rapports en continu
- Optimisation pré-segment
- Optimisation post-segment

Le conseil de sélection du rapport de vitesse est calculé en continu en utilisant le point de fonctionnement du moteur thermique et la méthode développée dans la section D.6. Une optimisation pré-segment prend en compte l'état initial du véhicule et un état final estimé avec les données du segment, pour calculer la trajectoire de vitesse optimale correspondant à ce segment. Cet algorithme d'optimisation applique la méthode de programmation dynamique en deux dimensions. Un facteur de pondération entre le coût du carburant et le temps peut être défini par le conducteur. Si la distance de sécurité ne nous permet pas de communiquer la vitesse optimale, le profil optimal est annulé et une nouvelle

	référence [L/100km]	assisté [L/100km]	gain [%]
urbain	8.31	7.58	8.74
routier	7.00	5.90	15.25

TABLE D.5: Gains de consommation dans un environnement urbain et routier

trajectoire optimale est calculée lorsque le véhicule précédant est parti. Un algorithme d'optimisation post-segment utilise les données enregistrée tout au long du segment, afin d'optimiser et d'évaluer la conduite sur le segment précédant. La méthode de programmation dynamique est utilisée prenant en compte les contraintes de trafic et le temps d'arrivée.

Pour évaluer l'efficacité d'un tel système ADAS, nous l'avons testé avec 12 sujets (conducteurs) sur le simulateur de conduite. Après un entrainement sur le simulateur, les sujets ont fait un premier parcours sans système d'assistance. Les mesures de ce test ont été utilisées comme référence pour définir une conduite normale pour chaque pilote. Un premier questionnaire est rempli lors d'une pause il permet d'identifier des paramètres décrivant la personne et son utilisation de son véhicule particulier. Après une initiation au système d'assistance, un second test a servi pour mesurer la consommation du conducteur sur un second parcours. Un deuxième questionnaire nous permet ensuite d'évaluer la compréhension et l'acceptabilité du système.

Une évaluation des résultats a montré que, en moyenne, la consommation de carburants a diminuée en utilisant le système ADAS. Le tableau D.5 présente la consommation de carburant pour des environnements urbain et routier. Les limitations dues au trafic nous ont permis d'identifier que les gains d'éco-conduite sont plus élevés dans une conduite routière que dans un environnement urbain. La consommation étant réduite par 8,7 % en ville alors que la réduction atteint 15,3 % pour un parcours routier.

Une analyse des paramètres personnels a montré que les sujets indiquant avoir des connaissances mécanique ont eu une consommation de base plus basse que les gens sans connaissances mécanique. Les résultats indiquent également que les conducteurs qui utilisent leur véhicule fréquemment ont développé une conduite plus économique à la base. Il a été identifié que les personnes avec la plus haute acceptabilité et compréhension du système ont atteints des gains maximaux avec le système.

Avec les résultats de cette étude nous pouvons conclure qu'un tel système ADAS présente un vrai intérêt.

D.8 Conclusion et perspectives

Le travail de cette thèse concerne l'optimisation énergétique de l'utilisation des véhicules conventionnels, électriques et hybrides. L'application des algorithmes d'optimisation au principe d'éco-conduite y est discutée.

Tout d'abord la méthode de modélisation inverse a été appliquée dans le développement d'une simulation de châssis et des trois chaînes de propulsion: conventionnelle, électrique et hybride. Prenant en compte des contraintes de trajet et de route, un problème d'optimisation a été défini pour minimiser la consommation d'énergie d'un véhicule pour un trajet donné. Des cycles standards et d'usage réel ont été utilisés afin de définir des contraintes de distance, vitesse et temps d'arrivée. La méthode de programmation dynamique a été appliquée à ce problème. L'algorithme développé peut être utilisé pour identifier un cycle éco correspondant à un cycle original.

Par la suite les gains d'éco-conduite ont été identifiés pour les trois types de véhicules en minimisant la consommation d'énergie pour différents cycles de conduite. En analysant le fonctionnement optimal, nous avons trouvé qu'une trajectoire optimale se compose d'une accélération forte, une vitesse stabilisée basse et une décélération adaptée à la chaîne et à la capacité de récupération du véhicule. En général un gain considérable de l'éco-conduite a été identifié pour chacun des trois types de véhicule.

D'autre part une étude sur l'intégration des contraintes de trafic et des émissions a été réalisée. Nous avons montré que le gain potentiel d'éco-conduite diminue avec le trafic mais représente toujours un moyen d'améliorer sa consommation. En intégrant des contraintes d'émissions nous avons montré que, en faisant un petit compromis de consommation, l'éco-conduite peut représenter des avantages économiques et écologiques.

Enfin, l'intégration des algorithmes d'optimisation dans un système d'assistance efficace et sécurisé a démontré que l'éco-conduite ne peut pas être négligée dans le développement du transport durable.

Dans des travaux futurs les aspects suivant semblent intéressants à aborder:

- Simplification des algorithmes en se basant sur les résultats d'optimisation
- Application des algorithmes développés ici à d'autres architectures de véhicule (véhicule hybride hydraulique, véhicule à pile à combustible), afin d'évaluer leur fonctionnement optimal
- Une intégration du système ADAS dans un scénario sur un véhicule réel

Bibliography

[1] Mercedes-Benz. When will there finally be a vehicle that no longer has to be pulled by horses, 2013. URL http://www2.mercedes-benz.com.au.

[2] ACEA. EU fleet by fuel type, 2010. URL http://www.acea.be.

[3] The Oil Drum. Oil production in the 21st century and peak oil, 2012. URL http://oilprice.com/Energy/Crude-Oil/Oil-Production-in-the-21st-Century-and-Peak-Oil.html.

[4] EEA. Total greenhouse gas emissions by sector in eu-27, 2007, 2007. URL www.eea.europa.eu.

[5] David Diamond. The impact of government incentives for hybrid-electric vehicles: Evidence from US states. *Energy Policy*, 37(3):972–983, March 2009.

[6] IEA. Eight countries join IEA electric vehicle initiative, 2010. URL evworld.com.

[7] James Jenness, Jeremiah Singer, Jeremie Walrath, and Elisha Lubar. NHTSA- fuel economy driver interfaces: Design range and driver opinions (report tasks 1 and 2), August 2009.

[8] Nissan. News releases - world first eco pedal helps reduce fuel consumption, 2008. URL http://www.nissan-global.com/EN/NEWS/2008/_STORY/080804-02-e.html.

[9] Mascha van der Voort. A prototype fuel-efficiency support tool. *Transportation Research Part C*, 9(4):279–296, 2001.

[10] Vexia. Vexia econav, 2013. URL http://www.vexia.co.uk/eco-tech.

[11] A. B. Schwarzkopf and R. B. Leipnik. Control of highway vehicles for minimum fuel consumption over varying terrain. *Transportation Research*, 11 (4):279–286, August 1977.

[12] J. N. Hooker, A. B. Rose, and G. F. Roberts. Optimal control of automobiles for fuel economy. *Transportation Science*, 17(2):146–167, May 1983.

[13] Ken-Jui Tsao, Si-Sheng Wan, Po-Ting Kuo, and Ran-Ren Chang. Trajectory generation for vehicle moving with constraints on a complex terrain. In *Proceedings of 2003 IEEE International Conference on Robotics and Automation*, 2003.

[14] Thijs van Keulen, Bram Jager, A. Serrarens, and M. Steinbuch. Optimal energy management in hybrid electric trucks using route information. *Oil and Gas Science and Technology*, 65(1):103–113, 2010.

[15] P.G. Howlett, P.J. Pudney, and Xuan Vu. Local energy minimization in optimal train control. *Automatica*, 45(11):2692–2698, November 2009.

[16] Masafumi Miyatake and Hideyoshi Ko. Optimization of train speed profile for minimum energy consumption. *IEEJ Transactions on Electrical and Electronic Engineering*, 5(3):263–269, 2010.

[17] Glenn Elert Marina Stasenko. The physics factbook: Number of cars, 2001. URL http://hypertextbook.com/facts/2001/MarinaStasenko.shtml.

[18] NationMaster. Transportation statistics, 2013. URL http://www.nationmaster.com/graph/tra_mot_veh-transportation-motor-vehicles.

[19] EEA. Car ownership rates projections, 2010. URL http://www.eea.europa.eu/data-and-maps/figures/car-ownership-rates-projections.

[20] IPCC. Climate change 2007: Working group ii: Mitigation of climate change; 5.3.1.2 improving drive train efficiency, 2007. URL http://www.ipcc.ch.

[21] Lino Figueiredo, Isabel Jesus, J.A. Tenreiro Machado, Jose Rui Ferreira, and J.L. Martins de Carvalho. Towards the development of intelligent transportation systems. *IEEE Intelligent Transportation Systems Conference Proceedings*, August 2001.

[22] Audi. Travolution, 2013. URL http://www.travolution-ingolstadt.de.

[23] NHTSA Public Affairs. Connected vehicles - vehicle-to-vehicle (v2v) communications for safety, 2011. URL http://www.safercar.gov.

[24] Hornung Wirtschafts und Sozialstudien. Evaluationen von eco-drive - Ausbildungen im Ueberblick, 2004.

[25] Felicitas Mensing, Rochdi Trigui, and Eric Bideaux. Vehicle trajectory optimization for application in ECO-driving. In *2011 IEEE Vehicle Power and Propulsion Conference (VPPC)*, pages 1–6. IEEE, September 2011. ISBN 978-1-61284-248-6.

[26] Felicitas Mensing, Eric Bideaux, Rochdi Trigui, and Bruno Jeanneret. Trajectory optimisation for eco-driving - an experimentally verified optimisation method. *Int. J. Vehicle Systems Modelling and Testing*, x(XX), accepted to be published 2013.

[27] Felicitas Mensing, Eric Bideaux, and Rochdi Trigui. Single- and multi-objective velocity trajectory optimization for application in eco-driving. *Journal of Dynamic Systems, Measurement and Control*, x(XX), submitted for review 2013.

[28] Felicitas Mensing, Rochdi Trigui, and Eric Bideaux. Vehicle trajectory optimization of electric vehicles for eco driving applications. In *2012 EEVC European Electric Vehicle Conference*. EEVC, November 2012.

[29] Felicitas Mensing, Rochdi Trigui, and Eric Bideaux. Vehicle trajectory optimization for hybrid vehicles taking into account battery state-of-charge. In *2012 IEEE Vehicle Power and Propulsion Conference (VPPC)*. IEEE, September 2012.

[30] Felicitas Mensing, Eric Bideaux, Rochdi Trigui, and Helene Tattegrain. Trajectory optimization for eco-driving taking into account traffic constraints. *Transportation Research Part D: Transport and Environment*, 18(1):55–61, January 2013.

[31] Felicitas Mensing, Eric Bideaux, Rochdi Trigui, Julien Ribet, and Bruno Jeanneret. Eco-driving: An economic or ecologic driving style? *Transportation Research Part C*, x(XX), submitted for review 2013.

[32] M.G. Hinton, L. Forrest, D.P. Duclos, T.H. Davey, R.R. Sheahan, and K.B. Swan. Survey of driver aided devices for improved fuel economy. Technical Report DOT-TSC-OST-76-45, Department of Transportation, 1976.

[33] M. Huntley, Jr. Stephen, and William Z. Leavitt. Effectiveness of miles-per-gallon meters as a means to conserve gasoline in automobiles. Technical Report DOT-TSC-OST-76-38, Department of Transportation, October 1976.

[34] Leonard Evans, Robert Herman, and Tenny Lam. Multivariate analysis of traffic factors related to fuel consumption in urban driving. *Transportation Science*, 10(2):205–215, January 1976.

[35] Leonard Evans. Driver behavior effects on fuel consumption in urban driving. *Human Factors: The Journal of the Human Factors and Ergonomics Society*, 21(4):389–398, August 1979.

[36] J. Nader. Measurement of the impact of driving technique on fuel consumption : Preliminary results. *Roads & Transportation*, pages 1–6, 1991.

[37] Alex Runnion, Jesse O Watson, and John McWhorter. Energy savings in interstate transportation through feedback and reinforcement. *Journal of Organizational Behavior Management*, 1(3):181–191, 1978.

[38] ACEA (European Automobile Manufacturers' Association). Reducing CO2 emissions: Working together to achieve better results, 2013.

[39] FIA Brussels. Ecodriving as a policy; highly cost-effective CO2 emission reductions, 2007. URL http://www.fiabrussels.com/download/projects/ecodriven/english_brochure_august_2007.pdf.

[40] R.G. Fairchild, J.F. Brake, N. Thorpe, S.A. Birrell, M.S. Young, T. Felstend, and M. Fowkes. Foot-LITE: using on-board driver feedback systems to encourage safe, ecological and efficient driving: The foot LITE project. *AISB 2009 Convention: Adaptive and Emergent Behaviour and Complex Systems*, 2009.

[41] Austrian Energy Agency. ECOWILL the project, 2013. URL http://www.ecodrive.org/.

[42] ERTICO ITS Europe. eCoMove cooperative mobility systems and services for energy efficiency, 2013. URL http://www.ecomove-project.eu.

[43] VITO Flemish Institute for Technological Research. FLEAT project, 2013. URL http://www.fleat-eu.org.

[44] Michael Masner, Michael Rakauskas, Justin Graving, and James Jenness. NHTSA-Fuel economy driver interfaces: Develop interface recommendations (report task 3), May 2010.

[45] Bart Beusen, Steven Broekx, Tobias Denys, and Carolien Beckx. Using on-board logging devices to study the longer-term impact of an eco- driving course. *Transportation Research Part D*, 14(7):514–520, 2009.

[46] A.E. af Wahlberg. Long-term effects of training in economical driving: Fuel consumption, accidents, driver acceleration behavior and technical feedback. *International Journal of Industrial Ergonomics*, 37(4):333–343, April 2007.

[47] P.J. Feenstra and A.R.A. van der Horst. TNO report - literature review of in-vehicle support for fuel-efficient driving related to pricing mechanisms, July 2006.

[48] Hanna Larsson and Eva Ericsson. The effects of an acceleration advisory tool in vehicles for reduced fuel consumption and emissions. *Transportation Research Part D: Transport and Environment*, 14(2), 2009.

[49] Institute of Advanced Motorists (ed). *How to Be A Better Driver: Advanced Driving the Essential Guide*. Motorbooks International, October 2007. ISBN 9780760333143.

[50] Porsche. Acc innodrive, 2013. URL http://www.porsche.com/middle-east/aboutporsche/responsibility/environment/technology/accinnodrive/.

[51] Fiat. Fiat EcoDrive, April 2012. URL http://www.fiat.co.uk/ecodrive/.

[52] ACEA (European Automobile Manufaacturers' Association). 'Eco-driving' is easy to apply and has significant, long-term effects, 2013.

[53] Ford Motor Company. 10 eco-driving tips for everyone, 2013. URL http://media.ford.com/article_display.cfm?article_id=28946.

[54] Ericsson Eva. Independent driving pattern factors and their influence on fuel-use and exhaust emission factors. *Transportation Research Part D: Transport and Environment*, 6(5):325–345, September 2001.

[55] Guillaume Saint Pierre and Cindie Andrieu. Caracterisation de l'eco-conduite et construction d'un indicateur dynamique pour vehicules thermiques. *PRAC 2010 Prevention des risques et aides a la conduite*, 2010.

[56] M. C. v.d. Voort. Design and evaluation of a new fuel-efficiency support tool. *Ph. D. thesis. Enschede: University of Twente*, 2001.

[57] J.N. Hooker. Optimal driving for single-vehicle fuel economy. *Transportation Research-A*, pages 183–201, 1988.

[58] V. V. Monastyrsky and I. M. Golownykh. Rapid computation of optimal control for vehicles. *Transportation Research Part B: Methodological*, 27(3): 219–227, June 1993.

[59] A.P. Stoicescu. On fuel-optimal velocity control of a motor vehicle. *International Journal of Vehicle Design*, pages 229–256, 1995.

[60] Antonio Sciarretta, Lino Guzzella, and van Janneke Baalen. Fuel optimal trajectories of a fuel cell vehicle. In *Proceedings of AVCS 2004*, 2004.

[61] E. Velenis and P. Tsiotras. Optimal velocity profile generation for given acceleration limits; the half-car model case. In *IEEE International Symposium on Industrial Electronics 2005*, pages 361–366, 2005.

[62] Efstathios Velenis and Panagiotis Tsiotras. Optimal velocity profile generation for given acceleration limits: Receding horizon implementation. In *2005 American Control Conference, ACC*, pages 2147–2152, 2005.

[63] Efstathios Velenis and Panagiotis Tsiotras. Optimal velocity profile generation for given acceleration limits: Theoretical analysis. In *2005 American Control Conference, ACC*, pages 1478–1483, 2005.

[64] L. Nouveliere and M. Braci. Fuel consumption optimization for a city bus. In *UKACC Control 2008*, 2008.

[65] Erik Hellstroem, Jan Aslund, and Lars Nielsen. Design of an efficient algorithm for fuel-optimal look-ahead control. *Control Engineering Practice*, 18 (11):1318–1327, 2010.

[66] Erik Hellstroem, Maria Ivarsson, Jan Aslund, and Lars Nielsen. Look-ahead control for heavy trucks to minimize trip time and fuel consumption. *Control Engineering Practice*, 17(2):245–254, 2009.

[67] Wei Huang, David M. Bevly, Xiaopeng Li, and Steve Schnick. 3D road geometry based optimal truck fuel economy. In *ASME Conference Proceedings*, volume 2007, pages 63–70, January 2007.

[68] Wei Huang and David M. Bevly. Evaluation of 3D road geometry based heavy truck fuel optimisation. *International Journal of Vehicle Autonomous Systems*, 8(1):39 – 55, 2010.

[69] Thijs van Keulen, Bram Jager, Darren Foster, and Maarten Steinbuch. Velocity trajectory optimization in hybrid electric trucks. In *Proceeding of American Control Conference*, Baltimore, MD, USA, July 2010.

[70] Kunihiko Ichikawa. Application of optimization theory of bounded state variable problems to the optimization of train. *The Japan Society of Mechanical Engineers*, 11(47), 1968.

[71] Rongfang (Rachel) Liu and Iakov M. Golovitcher. Energy-efficient operation of rail vehicles. *Transportation Research Part A: Policy and Practice*, 37(10): 917–932, December 2003.

[72] P Howlett. Optimal strategies for the control of a train. *Automatica*, 32(4): 519–532, April 1996.

[73] H. Ko, T. Koseki, and M. Miyatake. Application of dynamic programming to the optimization of the running profile of a train. In *Advances in Transport*, volume 15, pages 103–112. WITPress, 2004.

[74] Robert Bosch GmbH. *Bosch Automotive Handbook*. Bentley Publishers, 7th edition, 2007. ISBN 9780837615400.

[75] Wikipedia-The free encyclopedia. Automobile drag coefficient, 2013. URL http://en.wikipedia.org/wiki/Automobile_drag_coefficient.

[76] Renault. Renault zoe the electric supermini for everyday use, 2013. URL www.renault-ze.com.

[77] Williams F1. Williams hybrid power, 2013. URL www.williamshybridpower.com.

[78] M.C. Gannon. Hydraulic hybrid fleets hit the streets, 2013. URL http://hydraulicspneumatics.com/200/IndZone/RecyclingWasteM/Article/Fa%lse/86501/IndZone-RecyclingWasteM.

[79] EPA. Clean automotive technology; world's first full hydraulic hybrid in a delivery truck, 2006. URL http://www.epa.gov/midwestcleandiesel/publications/mcdi-factsheets/hydraulichybrid5.pdf.

[80] PSA Peugeot Citroen. Hybrid air, une solution innovante full hybrid essence, 2013. URL http://www.psa-peugeot-citroen.com.

[81] U.S. Departement of Energy. Evaluation of 2004 toyota prius hybrid electric drive system, 2006.

[82] Emmanuel Vinot, Julien Scordia, Rochdi Trigui, Bruno Jeanneret, and Francois Badin. Model simulation, validation and case study of the 2004 THS of toyota prius. *International Journal of Vehicle Systems Modelling and Testing*, 3(3):139–167, January 2008.

[83] Lianfang Tian and Curtis Collins. An effective robot trajectory planning method using a genetic algorithm. *Mechatronics*, 14(5):455–470, June 2004.

[84] Erik Hellstroem, Jan Aslund, and Lars Nielsen. Horizon length and fuel equivalents for fuel-optimal look-ahead control. In *Proceedings 6th IFAC Symposium on Advances in Automotive Control*, Munich, 2010.

[85] B. A. Conway. A survey of methods for the numerical optimization of continuous dynamic systems. *Journal of Optimization Theory and Applications*, 152(2):271–306, 2012.

[86] Donald E. Kirk. *Optimal Control Theory: An Introduction*. Dover Publications, April 2004. ISBN 0486434842.

[87] C. Ridders. A new algorithm for computing a single root of a real continuous function. *Circuits and Systems, IEEE Transactions on*, 26(11):979–980, 1979.

[88] R. P. Brent. An algorithm with guaranteed convergence for finding a zero of a function. *The Computer Journal*, 14(4):422 –425, January 1971.

[89] Richard P. Brent. *Algorithms for Minimization Without Derivatives*. Dover Publications, January 2002. ISBN 0486419983.

[90] A. Guigue, M. Ahmadi, R. Langlois, and M. J. Hayes. Pareto optimality and multiobjective trajectory planning for a 7-DOF redundant manipulator. *IEEE Transactions on Robotics*, 26(6):1094–1099, 2010.

[91] Hai-Lin Liu and Yu-Ping Wang. Solving constrained optimization problem by a specific-design multiobjective genetic algorithm. In *Fifth International Conference on Computational Intelligence and Multimedia Applications, 2003. ICCIMA 2003*, pages 200– 205. IEEE, September 2003.

[92] Eckart Zitzler, Marco Laumanns, and Lothar Thiele. SPEA2: improving the strength pareto evolutionary algorithm. Technical report, Eidgenoessische Technische Hochschule Zuerich, 2001.

[93] Michel Andre. Artemis european driving cycles for measuring car pollutant emissions. *Science of the Total Environment*, pages 73–84, 2004.

[94] Rochdi Trigui, Bruno Jeanneret, Bertrand Malaquin, and Cedric Plasse. Performance comparison of three storage systems for mild-HEVs using PHIL simulation. *IEEE Transactions on Vehicular Technology*, pages 3959–3969, 2009.

[95] Truck And Bus Advanced And Hybrid Powertrain Steering Committee. Recommended practice for measuring the exhaust emissions and fuel economy of hybrid-electric vehicles, 4.4.2. *SAE J 1711*, 1999.

[96] Truck And Bus Advanced And Hybrid Powertrain Steering Committee. Recommended practice for measuring fuel economy and emissions of hybrid-electric and conventional heavy duty vehicles, 4.4.2. *SAE J 2711*, 2002.

[97] A. Kanaris, P. Ioannou, and Fu-Sheng Ho. Spacing and capacity evaluations for different AHS concepts. In *American Control Conference, 1997*, volume 3, pages 2036 –2040 vol.3, June 1997.

[98] M. Brackstone and M. McDonald. Driver headway: How close is too close on a motorway? *Ergonomics*, pages 1183–1197, August 2007.

[99] Valentina E. Balas and Marius M. Balas. Constant time to collision platoons. *Int. J. of Computers, Communications and Control*, 2008.

[100] Hakan Johansson, Paer Gustafsson, Magnus Henke, and Mattias Rosengren. Impact of eco driving on emissions. In *Transportation and Air Pollution, Proceeding from the 12th Symposium*, June 2003.

[101] U.S.Environmental Protection Agency. Automobile emissions: An overview EPA 400-f-92-007, August 1994.

[102] Lino Guzzella and Christopher Onder. *Introduction to Modeling and Control of Internal Combustion Engine Systems*. Springer Verlag, 2010. ISBN 978-3-642-10774-0.

[103] Rajamani Rajesh. *Vehicle Dynamics and Control*. Springer Verlag, 2006. ISBN 978-0-387-26396-0.

[104] Thomas D. Gillespie. *Fundamentals of Vehicle Dynamics*. Society of Automotive Engineers, February 1992. ISBN 9781560911999.

.

Folio Administratif
Thèse soutenue devant l'Institut National des Sciences Appliquées de Lyon

Nom : MENSING **Date de soutenance** : 03/10/13
Prénoms : Felicitas

Titre :Optimal Energy Utilization in Conventional, Electric and Hybrid Vehicles and its Application to Eco Driving

Nature : Doctorat **Numéro d'ordre** :
Ecole doctorale : Electronique, Electrotechnique, Automatique
Spécialité : Energie et Systèmes

Résumé Pour résoudre les problèmes environnementaux et énergétiques liés au nombre croissant de véhicules en circulation, deux approches sont envisageables : l'une est technologique et vise à améliorer les composants du véhicule ou son architecture, l'autre est comportementale et cherche à changer la manière d'utiliser les véhicules. Dans ce contexte, l'éco-conduite représente une méthode, applicable immédiatement, permettant à chaque conducteur de réduire sa consommation.

L'objectif de cette thèse est donc l'analyse des gains potentiels de l'éco-conduite pour les différents types de véhicules existant : thermique, électrique et hybride. Ainsi, la première partie de ce travail se focalise sur une étude théorique visant à calculer les gains potentiels et à déterminer les règles d'éco-conduite, avant d'aborder dans un second temps une mise en situation plus réaliste et une intégration des algorithmes dans un système d'assistance pour le conducteur.

En s'appuyant sur une modélisation énergétique des différents types de véhicules, la détermination et la comparaison du fonctionnement optimal se base sur l'optimisation du profil de vitesse pour des trajets connus. La programmation dynamique a été mise enoeuvre pour calculer la trajectoire optimale énergétique en tenant compte de la contrainte temporelle afin de ne pas pénaliser l'intérêt d'une conduite économe. Evidemment, l'intégration de l'éco-conduite doit, d'une part, tenir compte du trafic à proximité du véhicule et d'autre part, ne pas aboutir à une augmentation des émissions de polluants. Ainsi, en nous appuyant sur des modèles de suivi de véhicules (trafic), nous avons montré que les principes d'éco-conduite restent valables et conduisent de toute façon à des gains énergétiques. Concernant les contraintes d'émissions, des résultats expérimentaux nous ont conduit à adapter nos algorithmes pour répondre simultanément aux aspects écologiques et économiques. Enfin, les connaissances acquises ont été appliquées à la conception d'un système d'assistance testé sur un simulateur de conduite.

Mots-clés : Eco Driving, Energetic Trajectory Optimization, Dynamic Programming, Emissions, Electric Vehicle, Hybrid Vehicle, Advanced Driver Assist System (ADAS)

Laboratoire de Recherches : AMPERE, UMR CNRS 5005

Directeur de Thèse : Eric BIDEAUX

Président du Jury : XXXXXXXXXXXXX

Composition du Jury :Xavier ROBOAM, Michel BASSET, Roger Fotsu NGWOMPO, Bo EGARDT, Xavier MOREAU, Sebastien DELPRAT, Eric BIDEAUX, Rochdi TRIGUI, Helene TATTEGRAIN, Maxime PASQUIER